

1986

Photophysics and Photochemical Studies of Polypyridine Ruthenium (II) Complexes.

Mario Alberto Ollino

Louisiana State University and Agricultural & Mechanical College

Follow this and additional works at: https://digitalcommons.lsu.edu/gradschool_disstheses

Recommended Citation

Ollino, Mario Alberto, "Photophysics and Photochemical Studies of Polypyridine Ruthenium (II) Complexes." (1986). *LSU Historical Dissertations and Theses*. 4317.

https://digitalcommons.lsu.edu/gradschool_disstheses/4317

This Dissertation is brought to you for free and open access by the Graduate School at LSU Digital Commons. It has been accepted for inclusion in LSU Historical Dissertations and Theses by an authorized administrator of LSU Digital Commons. For more information, please contact gradetd@lsu.edu.

INFORMATION TO USERS

While the most advanced technology has been used to photograph and reproduce this manuscript, the quality of the reproduction is heavily dependent upon the quality of the material submitted. For example:

- Manuscript pages may have indistinct print. In such cases, the best available copy has been filmed.
- Manuscripts may not always be complete. In such cases, a note will indicate that it is not possible to obtain missing pages.
- Copyrighted material may have been removed from the manuscript. In such cases, a note will indicate the deletion.

Oversize materials (e.g., maps, drawings, and charts) are photographed by sectioning the original, beginning at the upper left-hand corner and continuing from left to right in equal sections with small overlaps. Each oversize page is also filmed as one exposure and is available, for an additional charge, as a standard 35mm slide or as a 17"x 23" black and white photographic print.

Most photographs reproduce acceptably on positive microfilm or microfiche but lack the clarity on xerographic copies made from the microfilm. For an additional charge, 35mm slides of 6"x 9" black and white photographic prints are available for any photographs or illustrations that cannot be reproduced satisfactorily by xerography.

8710580

Ollino, Mario Alberto

PHOTOPHYSICS AND PHOTOCHEMICAL STUDIES OF POLYPYRIDINE
RUTHENIUM (II) COMPLEXES

The Louisiana State University and Agricultural and Mechanical Col.

Ph.D. 1986

University
Microfilms
International 300 N. Zeeb Road, Ann Arbor, MI 48106

PLEASE NOTE:

In all cases this material has been filmed in the best possible way from the available copy.
Problems encountered with this document have been identified here with a check mark ✓.

1. Glossy photographs or pages _____
2. Colored illustrations, paper or print _____
3. Photographs with dark background _____
4. Illustrations are poor copy _____
5. Pages with black marks, not original copy _____
6. Print shows through as there is text on both sides of page _____
7. Indistinct, broken or small print on several pages ✓ _____
8. Print exceeds margin requirements _____
9. Tightly bound copy with print lost in spine _____
10. Computer printout pages with indistinct print _____
11. Page(s) _____ lacking when material received, and not available from school or author.
12. Page(s) _____ seem to be missing in numbering only as text follows.
13. Two pages numbered _____. Text follows.
14. Curling and wrinkled pages _____
15. Dissertation contains pages with print at a slant, filmed as received ✓ _____
16. Other _____

University
Microfilms
International

PHOTOPHYSICS AND PHOTOCHEMICAL STUDIES OF
POLYPYRIDINE RUTHENIUM (II) COMPLEXES

A Dissertation

Submitted to the Graduate Faculty of the
Louisiana State University and
Agricultural and Mechanical College
in partial fulfillment of the
requirements for the degree of
Doctor in Philosophy
in
The Department of Chemistry

by

Mario A. Ollino

Ch.E. Universidad Santa Maria, Valparaiso,

Chile, 1981

December 1986

To my wife, Laura Edith.

ACKNOWLEDGEMENT

The author wishes to express his sincere thanks to his major professor Dr. William Cherry for his assistance, advice, and guidance given during the main stages of the experimental work carried out in the present research, as well as for his interest and useful suggestions during the publication of the present dissertation.

Sincere thanks are given also to Professor Robert Nauman for his interest and assistance in my enrollment in this graduate program, as well as for his continuous assistance and friendship freely given during my stay at LSU. His help is greatly appreciated and it is with a profound sense of gratitude that the author also wants to emphasize the highly esteemed advice, scientific guidance, criticism, support, and encouragement received from Professor Robert Nauman during the writing of this work.

Dr. Russell Schmehl of the Department of Chemistry of Tulane University is acknowledged for obtaining luminescence lifetimes and electrochemical measurements of some of the complexes studied in this work.

The technical assistance of Robert Zinn in the curve - fitting procedure is gratefully acknowledged.

I also want to thank Dr. Jerry Lewis for his interest and advice in many aspects of this dissertation. The continuous support and aid of many fellow graduate students and also the special support of some friends with whom I had interaction during my permanence at the LSU Chemistry Department are sincerely thanked. In particular, the friendship and comradeship of the members of the research group : Mr. Leslie Henderson Jr. and Mr. Reeves Huie are gratefully appreciated. The assistance of the LSU Chemistry Department Staff is sincerely acknowledged.

The receipt of a graduate assistantship from the Department of Chemistry at LSU and the study fellowship granted by the Oficina de Planificacion Nacional, Chile are acknowledged. The study leave from Universidad Tecnica Federico Santa Maria , Valparaiso, Chile, is also gratefully acknowledged.

The financial assistance in support of this work by Louisiana State University and in the publication of this dissertation by Dr. Charles E. Coates Memorial Fund of Louisiana State University is gratefully acknowledged.

TABLE OF CONTENTS

	Page
DEDICATION.....	ii
ACKNOWLEDGEMENT.....	iii
TABLE OF CONTENTS.....	v
LIST OF ABBREVIATIONS.....	xiii
LIST OF TABLES.....	xvii
LIST OF FIGURES.....	xxiv
ABSTRACT.....	xxxiv
CHAPTER I. INTRODUCTION.....	1
A. GENERAL BACKGROUND.....	4
1. Photophysics of Tris - bipyridineruthenium(II).....	4
2. Photosubstitution model.....	23
3. The effect of ring size on photophysical and photochemical properties.....	26
B. AIMS AND SCOPE OF THIS RESEARCH.....	35
CHAPTER II. EXPERIMENTAL.....	41
A. MATERIALS.....	41
1. Solvents.....	41
2. Inorganic Reagents.....	41
3. Organic Reagents.....	43
B. PREPARATION OF COMPLEXES.....	47
C. ANALYTICAL PROCEDURES, TECHNIQUES, AND PHYSICAL MEASUREMENTS.....	56

CHAPTER III. EXPERIMENTAL RESULTS.....	68
A. QUENCHING OF $[\text{Ru}(\text{bipy})_3]\text{X}_2$ ($\text{X} = \text{Cl}^-, \text{Br}^-$) EMISSION AND PHOTOSUBSTITUTION BY FERROCENE AND OXYGEN.....	68
1. Quenching of $[\text{Ru}(\text{bipy})_3]\text{Cl}_2$ at 298 K in a 0.10 M solution of TBACl in DMF by Ferrocene.....	68
2. Quenching of $[\text{Ru}(\text{bipy})_3]\text{Cl}_2$ at 298 K in a 0.10 M solution of TBACl in CH_3CN by Oxygen.....	70
3. Quenching of $[\text{Ru}(\text{bipy})_3]\text{Br}_2$ at 298 K in a 0.10 M solution of TBABr in DMF by Ferrocene.....	72
4. Quenching of $[\text{Ru}(\text{bipy})_3]\text{Br}_2$ at 298 K in a 0.10 M solution of TBABr in DMF by Oxygen.....	73
5. Quenching of $[\text{Ru}(\text{bipy})_3]\text{Br}_2$ at 298 K in a 0.10 M solution of TBABr in CH_2Cl_2 by Ferrocene.....	75
6. Quenching of $[\text{Ru}(\text{bipy})_3]\text{Br}_2$ at 298 K in a 0.10 M solution of TBABr in CH_2Cl_2 by Oxygen.....	76
B. CORRELATION OF LIGAND FIELD EXCITED STATE ENERGIES WITH LIGAND FIELD STRENGTH IN (POLYPYRIDINE) RUTHENIUM (II) COMPLEXES.....	85
1. Luminescence measurements.....	85
1.a. Emission intensities of EtOH/MeOH (4:1, v/v) solutions as a function of temperature.....	85
1.a.1. Complex : $[\text{Ru}(\text{bipy})_3]^{+2}$	85
1.a.2. Complex : $[\text{Ru}(\text{bipy})_2(\text{diaz})]^{+2}$	87
1.a.3. Complex : $[\text{Ru}(\text{bipy})_2(\text{py})_2]^{+2}$	88
1.b. Emission quantum yields of EtOH/MeOH (4:1, v/v)	

solutions as a function of temperature.....	88
1.b.1. Complex : $[\text{Ru}(\text{bipy})_3]^{+2}$	89
1.b.2. Complex : $[\text{Ru}(\text{bipy})_2(\text{diaz})]^{+2}$	90
1.b.3. Complex : $[\text{Ru}(\text{bipy})_2(\text{py})_2]^{+2}$	91
2. Temperature dependence of the lifetime of complexes $[\text{Ru}(\text{bipy})_2\text{L}]^{+2}$ in EtOH/MeOH (4:1,v/v).....	92
2.a.1. Complex : $[\text{Ru}(\text{bipy})_3]^{+2}$	92
2.a.2. Complex : $[\text{Ru}(\text{bipy})_2(\text{diaz})]^{+2}$	93
2.a.3. Complex : $[\text{Ru}(\text{bipy})_2(\text{py})_2]^{+2}$	94
3. Intersystem crossing determinations.....	97
C. ION PAIRING EFFECT ON THE PHOTOSUBSTITUTION QUANTUM YIELD OF cis - bispyridyl bis - 2,2'-bipyridylruthenium(II)hexafluorophosphate tetrahydrate AT 298 K IN 0.01 M TBAX (X = Cl^- , ClO_4^-) IN MIXTURES OF DIOXANE AND WATER.....	110
1. Determination of molar absorption coefficients....	110
2. Photolysis of $[\text{Ru}(\text{bipy})_2(\text{py})_2]^{+2}$ at 298 K in 0.01 M TBACl (mixtures of dioxane and water).....	114
3. Photolysis of $[\text{Ru}(\text{bipy})_2(\text{py})_2]^{+2}$ at 298 K in 0.01 M in TBACl (mixture of dioxane and water, 90/10, v:v), with excess free pyridine ligand present.....	115
4. Photolysis of $[\text{Ru}(\text{bipy})_2(\text{py})_2]^{+2}$ at 298 K in 0.01 M in TBAClO_4 (mixtures of dioxane and water).....	116
D. EFFECT OF CHELATE RING SIZE ON THE PHOTOSUBSTITUTION REACTION OF POLYPYRIDINE RUTHENIUM (II) COMPLEXES..	119

1. Complexes $[\text{Ru}(\text{bipy})_2\text{L}]^{+2}$ where the L's are methylene - linked pyridine ligands.....	119
1.a. Photophysical properties.....	119
1.a.1. Emission properties at 77 K.....	119
1.a.2. Temperature dependence of the emission quantum yield of complexes $[\text{Ru}(\text{bipy})_2\text{L}]^{+2}$ in EtOH/MeOH (4:1,v/v).....	120
1.a.3. Temperature dependence of the emission quantum yield of complexes $[\text{Ru}(\text{bipy})_2\text{L}]^{+2}$ in CH_3CN	124
1.a.4. Temperature dependence of the emission quantum yield of complexes $[\text{Ru}(\text{bipy})_2\text{L}]^{+2}$ in CH_2Cl_2 and in H_2O	125
1.b. Photochemical studies.....	127
1.b.1. Complex : $[\text{Ru}(\text{bipy})_3]^{+2}$	129
1.b.2. Complex : $[\text{Ru}(\text{bipy})_2(\text{pic})_2]^{+2}$	130
1.b.3. Complex : $[\text{Ru}(\text{bipy})_2\text{DPM}]^{+2}$	132
1.b.4. Complex : $[\text{Ru}(\text{bipy})_2\text{DPE}]^{+2}$	134
2. Complexes $[\text{Ru}(\text{bipy})_2\text{L}]^{+2}$ in which the L's are methylene - linked amine ligands.....	145
2.a. Photophysical properties.....	145
2.a.1. Emission properties at 77 K.....	145
2.a.2. Emission quantum yields at 298 K.....	146
2.a.2.1. Solvent : EtOH/MeOH (4:1,v/v).....	146
2.a.2.2. Solvent : H_2O	147

2.a.3. Temperature dependence of the emission quantum yield of complexes $[\text{Ru}(\text{bipy})_2\text{L}]^{+2}$ in EtOH/MeOH (4:1,v/v).....	148
2.a.3.1. L = 2,2' - bipyridine (bipy).....	148
2.a.3.2. L = ethylenediamine (en).....	148
2.a.3.3. L = trimethylenediamine (tn).....	148
2.a.4. Determination of lifetimes of complexes at 298 K.....	149
2.a.5. Quenching of emission of $[\text{Ru}(\text{bipy})_2(\text{en})]^{+2}$ at 298 K.....	150
2.a.5.1. In CH_2Cl_2 by Ferrocene	150
2.a.5.2. In a 0.01 M solution of TEACl in CH_2Cl_2 by Ferrocene.....	151
2.a.5.3. In CH_2Cl_2 by Anthracene.....	152
2.a.5.4. In a 0.01 M solution of TEACl in CH_2Cl_2 by Anthracene.....	153
2.a.5.5. In CH_2Cl_2 by 1,1' Dimethyl 4,4' bipyridinium dichloride	154
2.a.5.6. In a 0.01 M solution of TEACl in CH_2Cl_2 by 1,1' Dimethyl 4,4' bipyridinium dichloride	155
2.a.5.7. In CH_2Cl_2 by 1,2,4,5 - Tetracyanobenzene (TCNB).....	155
2.a.5.8. In a 0.01 M solution of TEACl in CH_2Cl_2 by 1,2,4,5 - Tetracyanobenzene (TCNB)	155
2.b. Photochemical studies at 298 K.....	160

2.b.1. Complex :[Ru(bipy) ₂ (en)] ⁺²	160
2.b.2. Complex :[Ru(bipy) ₂ (tn)] ⁺²	163
2.c. O ₂ role in the photochemistry of [Ru(bipy) ₂ (en)] ⁺² in a 0.01 M solution of TEACl in CH ₂ Cl ₂	166
2.c.3. Photolysis of the O ₂ saturated sample.....	168
2.c.4. Quenching of the emission by O ₂	168
2.c.5. Photolysis of [Ru(bipy) ₂ (en)] ⁺² in 0.50 M H ₂ SO ₄	169
2.d. Cation - assisted ligand photosubstitution in the photoreaction of [Ru(bipy) ₂ (en)] ⁺² with Ag ⁺ in CH ₃ CN at 298 K.....	170
2.d.1. Quenching of emission in CH ₃ CN at 298 K by AgNO ₃	171
2.d.4. Photolysis in a 0.40 M solution of AgNO ₃ in CH ₃ CN in the presence of methyl viologen concentration sufficient to quench > 90 % of the [Ru(bipy) ₂ (en)] ⁺² excited luminescent state...	174
3. Temperature dependence of the photosubstitution quantum yields of the complexes [Ru(bipy) ₂ L] ⁺² in a 0.01 M solution of TEACl in CH ₂ Cl ₂	175
3.a. L = 2,2' bipyridine (bipy).....	176
3.b. L = ethylenediamine (en).....	176
3.c. L = trimethylenediamine (tn).....	176
CHAPTER IV. DISCUSSION OF THE EXPERIMENTAL RESULTS.....	195
A. QUENCHING OF [Ru(bipy) ₃]X ₂ (X = Cl ⁻ , Br ⁻) EMISSION	

AND PHOTOSUBSTITUTION BY FERROCENE AND OXYGEN.....	195
1. Introduction.....	195
2. Discussion.....	201
3. Conclusions.....	208
B. CORRELATION OF LIGAND FIELD EXCITED STATE ENERGIES WITH LIGAND FIELD STRENGTH IN (POLYPYRIDINE)RUTHENIUM(II) COMPLEXES.....	210
1. Introduction.....	210
2. Discussion.....	213
3. Conclusions.....	225
C. EXPLORATORY ANALYSIS OF THE EFFECT OF ION - PAIRING UPON PHOTOSUBSTITUTION QUANTUM YIELDS.....	226
1. Introduction.....	226
2. Discussion.....	227
3. Conclusions.....	230
D. EFFECT OF CHELATE RING SIZE ON THE PHOTOSUBSTITUTION REACTION OF POLYPYRIDINE RUTHENIUM(II) COMPLEXES, WITH THE GENERAL FORMULATION, $[\text{Ru}(\text{bipy})_2\text{L}]^{+2}$	232
1. Introduction.....	232
2. Discussion.....	234
2.1. Effect of chelate ring size on the photosubstitution reaction of polypyridine ruthenium(II) complexes, $[\text{Ru}(\text{bipy})_2\text{L}]^{+2}$, in which L indicates ligand that has two pyridine rings linked by methylene bridges of	

different lengths.....	234
2.1.1. Conclusions.....	235
2.2. Effect of chelate ring size on the photosubstitution reaction of polypyridine ruthenium(II) complexes, $[\text{Ru}(\text{bipy})_2\text{L}]^{+2}$, in which L indicates ligand that has two amine groups linked by methylene bridges of different lengths.....	259
2.2.1. Conclusions.....	290
CHAPTER V. GENERAL CONCLUSIONS AND SUGGESTIONS FOR FUTURE RESEARCH.....	293
APPENDIX A.1. Removal of inner filter effect produced by quencher absorption from apparent quenching emission measurements.....	301
APPENDIX A.2. Dependency of the quantum yield of photosubstitution upon Cl^- concentration...	302
REFERENCES.....	304
VITA.....	318

LIST OF ABBREVIATIONS.

I. ORGANIC GROUPS.

An	anthracene
EtOH	ethanol
CH ₃ CN	acetonitrile
CH ₂ Cl ₂	dichloromethane
DMSO	dimethyl sulphoxide
DMF	N, N - dimethylformamide
Ferr	ferrocene
MV ⁺²	methyl viologen
MeOH	methanol
phen	1, 10 - phenanthroline
TMS	tetramethylsilane
TBACl	tetra (n - butyl) ammonium chloride
TBABr	tetra (n - buytyl) ammonium bromide
TBAClO ₄	tetra (n - butyl) ammonium perchlorate
TEACl	tetra ethyl ammonium chloride
TCNB	1, 2, 4, 5 - tetracyanobenzene

II.COMMON LIGANDS.

bipy	2,2' - bipyridine
DPE	1,2 - di (2 - pyridyl) ethane
DPM	di (2 - pyridyl) methane
en	ethylenediamine
diaz	4, 5 diazafluorene
py	pyridine
pic	4 - picoline
tn	1, 3 - propylenediamine

III. THEORIES, CONCEPTS, OTHER.

A	absorbance
b.p.	boiling point
CT	charge transfer state
D	static dielectric constant
10Dq	ligand field parameter
E	energy
$E_{1/2}$	half - wave potential
E_a	activation energy
GS	ground state
I	luminescent intensity
I_{abs}	absorbed light intensity of irradiation
I_0	luminescent intensity when a quencher is absent

K	equilibrium constant
k	rate constant
k_r	radiative rate constant
$k_{i.s.c.}$	rate constant for intersystem crossing
k_{nr}	non - radiative rate constant
k_q	quenching rate constant
k_p	photoproduct generation rate constant
k_o	non - radiative rate constant from LF excited state
K_{sv}	Stern - Volmer constant
L	a two electron ligand
LF	ligand field excited state
LMCT	ligand to metal charge transfer
M	molarity
MLCT	metal to ligand charge transfer
MSCT	metal to solvent charge transfer
m. p.	melting point
m. w.	molecular weight
NMR	nuclear magnetic resonance
	quencher
SCE	standard calomelelectrode
sh	shoulder

SHE	standard hydrogen electrode
SSCE	saturated sodium chloride electrode
T	temperature
t	time
x	mole fraction
E_o	molar absorption coefficient
E_{ph}	molar absorption coefficient of photosubstitution product.
ΔE	energy separation
λ	wavelength
λ_{irr}	irradiation wavelength
λ_{exc}	excitation wavelength
λ_{em}	emission wavelength
T_o	excited - state lifetime
T_{oo}	excited - state lifetime when a quencher is absent
Q_o	quantum yield of emission
$Q_{i.s.c.}$	quantum yield of intersystem crossing
Q_{oo}	quantum yield of emission when a quencher is absent
Q_{ph}	quantum yield of photosubstitution

LIST OF TABLES.

	Page
I. Calibration curve of the emission intensity at 298 K as a function of the emission bandpass.....	64
II. Calibration curve of the emission intensity at 77 K as a function of the emission bandpass.....	65
III. Quenching of the emission lifetime and of the photosubstitution : $[\text{Ru}(\text{bipy})_3]\text{Cl}_2$ at 298 K in a 0.10 M solution of TBACl in DMF by Ferrocene	69
IV. Quenching of the emission lifetime and of the photosubstitution : $[\text{Ru}(\text{bipy})_3]\text{Cl}_2$ at 298 K in a 0.10 M solution of TBACl in CH_3CN by Oxygen	71
V. Quenching of the emission lifetime and of the photosubstitution : $[\text{Ru}(\text{bipy})_3]\text{Br}_2$ at 298 K in a 0.10 M solution of TBABr in DMF by Ferrocene.....	72
VI. Quenching of the emission lifetime and of the photosubstitution : $[\text{Ru}(\text{bipy})_3]\text{Br}_2$ at 298 K in a 0.10 M solution of TBABr in DMF by Oxygen.....	74

VII. Quenching of the emission lifetime and of the photosubstitution : $[\text{Ru}(\text{bipy})_3]\text{Br}_2$ at 298 K in a 0.10 M solution of TBABr in CH_2Cl_2 by Ferrocene.....	75
VIII. Quenching of the emission lifetime and of the photosubstitution : $[\text{Ru}(\text{bipy})_3]\text{Br}_2$ at 298 K in a 0.10 M solution of TBABr in CH_2Cl_2 by Oxygen.....	77
IX. Relative emission intensity of $[\text{Ru}(\text{bipy})_3]^{+2}$ in EtOH/MeOH(4:1, v/v) as a function of temperature.....	86
X. Relative emission intensity of $[\text{Ru}(\text{bipy})_2(\text{diaz})]^{+2}$ in EtOH/MeOH(4:1, v/v) as a function of temperature.....	87
XI. Relative emission intensity of $[\text{Ru}(\text{bipy})_2(\text{py})_2]^{+2}$ in EtOH/MeOH(4:1, v/v) as a function of temperature....	88
XII. Emission quantum yield dependency of $[\text{Ru}(\text{bipy})_3]^{+2}$ in EtOH/MeOH(4:1, v/v) as a function of temperature.....	89
XIII. Emission quantum yield dependency of $[\text{Ru}(\text{bipy})_2(\text{diaz})]^{+2}$ in EtOH/MeOH(4:1, v/v) as a function of temperature.....	90
XIV. Emission quantum yield dependency of	

[Ru(bipy) ₂ (py) ₂] ⁺² in EtOH/MeOH(4:1, v/v) as a function of temperature	91
XV. Lifetime temperature dependency of [Ru(bipy) ₃] ⁺² in EtOH/MeOH (4:1, v/v)	92
XVI. Lifetime temperature dependency of [Ru(bipy) ₂ (diaz)] ⁺² in EtOH/MeOH (4:1,v/v).....	93
XVII. Lifetime temperature dependency of [Ru(bipy) ₂ (py) ₂] ⁺² in EtOH/MeOH (4:1, v/v).....	94
XVIII. Curve fitting parameters obtained for the polypyridine complexes based upon emission intensities and lifetimes.....	96
XIX. Observed dependence of the reciprocal quantum yield of oxidation of [Ru(bipy) ₃] ⁺² to [Ru(bipy) ₃] ⁺³ upon 1/[S ₂ O ₈ ⁻²].....	99
XX. Electrochemical data of some polypyridine ruthenium (II) complexes.....	100
XXI. Absorption characteristics of the complexes [Ru(bipy) ₂ DPE] ⁺² and [Ru(bipy) ₂ (py) ₂] ⁺² in a 95/5,	

v:v dioxane/water mixture.....	111
XXII. Molar absorption coefficients (E_o) at 450 nm of the complexes $[Ru(bipy)_2DPE]^{+2}$ and $[Ru(bipy)_2(py)_2]^{+2}$ in a 95/5, v:v dioxane/water mixture as well as of their respective monochloro (E_{ph1}) and dichloro (E_{ph2}) photosubstitution products.....	111
XXIII. Dependence of the photosubstitution quantum yield as a function of the polarity of the medium (mixtures of dioxane and water, 0.01 M in TBACl).....	114
XXIV. Dependence of the photosubstitution quantum yield as a function of the pyridine concentration.....	116
XXV. Dependence of the photosubstitution quantum yield as a function of the polarity of the medium (mixtures of dioxane and water, 0.01 M in $TBAClO_4$).....	117
XXVI. Emission properties of the bis (bipy), methylene - linked pyridine ruthenium complexes at 77 K.....	120
XXVII. Temperature dependence of the emission quantum yield of $[Ru(bipy)_2(pic)_2]^{+2}$	121
XXVIII. Temperature dependence of the emission quantum	

yield of $[\text{Ru}(\text{bipy})_2\text{DPM}]^{+2}$122

XXIX. Parameters of the photophysical properties of polypyridine complexes with a methylene - linked pyridine ligand in EtOH/MeOH (4:1,v/v), based upon emission intensities123

XXX. Parameters of the photophysical properties of polypyridine complexes with a methylene - linked pyridine ligand in CH_3CN , based upon emission intensities.....124

XXXI. Emission properties of $[\text{Ru}(\text{bipy})_2\text{L}]^{+2}$ complexes in CH_3CN at 298 K.....126

XXXII. Emission properties of $[\text{Ru}(\text{bipy})_2\text{L}]^{+2}$ complexes in CH_2Cl_2 at 298 K.....126

XXXIII. Quantum yields of photosubstitution and of production of the higher LF state for bis(bipy), methylene - linked pyridine ruthenium complexes at 298 K.....136

XXXIV. Emission properties of the bis (bipy) - methylene - linked amine ruthenium complexes at 77 K.....145

XXXV. Emission quantum yields of bis (bipy) - methylene

- linked amine ruthenium complexes in EtOH/MeOH (4:1,v/v) at 298 K.....	146
XXXVI. Emission quantum yields of bis (bipy) - methylene - linked amine ruthenium complexes in H ₂ O at 298 K.....	147
XXXVII. Parameters of the photophysical properties of polypyridine complexes with a methylene - linked amine ligand based upon emission intensities.....	149
XXXVIII. Lifetimes of polypyridine complexes with a methylene - linked amine ligand at 298 K.....	149
XXXIX. Quenching of the emission of [Ru(bipy) ₂ (en)] ⁺² in CH ₂ Cl ₂ at 298 K by Ferrocene.....	150
XXXX. Quenching of the emission of [Ru(bipy) ₂ (en)] ⁺² in a 0.01 M solution of TEACl in CH ₂ Cl ₂ at 298 K by Ferrocene.....	151
XXXXI. Quenching of the emission of [Ru(bipy) ₂ (en)] ⁺² in CH ₂ Cl ₂ at 298 K by Anthracene.....	153
XXXXII. Quenching of the emission of [Ru(bipy) ₂ (en)] ⁺² in a 0.01 M solution of TEACl in CH ₂ Cl ₂ at 298 K by Anthracene.....	153

XXXXIII. Quenching of the emission of [Ru(bipy) ₂ (en)] ⁺² in CH ₃ CN at 298 K by AgNO ₃	171
XXXXIV. Quantum yields of photosubstitution and of the production of the higher lying LF state for bis (bipy) - methylene - linked amine ruthenium complexes at 298 K..	177
XXXXV. Quantum yields of observed photoreactions of [Ru(bipy) ₂ (en)] ⁺² , in different media.....	179

LIST OF FIGURES.

	Page
1. Metal to Ligand Charge Tranfer in a d^6 low spin complex.....	15
2. A) Electronic absorption spectrum of an aqueous solution of $[Ru(bipy)_3]^{+2}$. Emission spectra of $[Ru(bipy)_3]^{+2}$: B) at 77 K. C) at 273 K.....	16
3. Absorption and emission spectra of $[Ru(bipy)_3]^{+2}$ in H_2O at 298 K.....	17
4. Empirical splitting of the excited state of $[Ru(bipy)_3]^{+2}$ arising from an MLCT excitation.....	18
5. Variation with temperature of the luminescence lifetime of $[Ru(bipy)_3]^{+2}$ at low temperatures.....	19
6. Photophysical processes of $[Ru(bipy)_3]^{+2}$	20
7. Modified Jablonski diagram of the photophysics of polypyridine ruthenium complexes.....	21
8. Energy difference between the 3MLCT and LF excited state.....	22

9. Model of the photosubstitution of polypyridine ruthenium (II) complexes. The $^3\text{MLCT}$ is formed with unit efficiency upon excitation.....	32
10. Perturbation of the energy of LF state due to 4,5 - diazafluorene in a complex of the type $[\text{Ru}(\text{bipy})_2\text{L}]^{+2}$...	33
11. Emission spectra of complexes A and B.....	34
12. Schematic representation of complexes (a) $[\text{Ru}(\text{bipy})_2(\text{diaz})]^{+2}$, (b) $[\text{Ru}(\text{bipy})_2(\text{py})_2]^{+2}$, (c) $[\text{Ru}(\text{bipy})_3]^{+2}$, (d) $[\text{Ru}(\text{bipy})_2(\text{en})]^{+2}$, (e) $[\text{Ru}(\text{bipy})_2(\text{tn})]^{+2}$	54
13. Schematic representation of complexes (f) $[\text{Ru}(\text{bipy})_2(\text{pic})_2]^{+2}$, (g) $[\text{Ru}(\text{bipy})_2\text{DPE}]^{+2}$, (h) $[\text{Ru}(\text{bipy})_2\text{DPM}]^{+2}$, (i) $[\text{Ru}(\text{bipy})_2(\text{pic})(\text{H}_2\text{O})]^{+2}$, (j) $[\text{Ru}(\text{bipy})_2(\text{pic})(\text{Cl})]^{+1}$	55
14. Stern - Volmer plot for the quenching of $[\text{Ru}(\text{bipy})_3]\text{Cl}_2$ emission lifetime (τ) and photosubstitution (θ) at 298 K in a 0.10 M solution of TBACl in DMF by Ferrocene.....	79
15. Stern - Volmer plot for the quenching of	

[Ru(bipy)₃]Cl₂ emission lifetime (■) and
 photosubstitution (○) at 298 K in a 0.10 M solution of
 TBACl in CH₃CN by Oxygen.....80

16. Stern - Volmer plot for the quenching of
 [Ru(bipy)₃]Br₂ emission lifetime (■) and
 photosubstitution (○ and ●) at 298 K in a 0.10 M solution
 of TBABr in DMF by Ferrocene.....81

17. Stern - Volmer plot for the quenching of
 [Ru(bipy)₃]Br₂ emission lifetime (■) and
 photosubstitution (○ and ●) at 298 K in a 0.10 M solution
 of TBABr in DMF by Oxygen.....82

18 . Stern - Volmer plot for the quenching of
 [Ru(bipy)₃]Br₂ emission lifetime (■) and
 photosubstitution (○) at 298 K in a 0.10 M solution of
 TBABr in CH₂Cl₂ by Ferrocene.....83

19 . Stern - Volmer plot for the quenching of
 [Ru(bipy)₃]Br₂ emission lifetime (■) and
 photosubstitution (○) at 298 K in a 0.10 M solution of
 TBABr in CH₂Cl₂ by Oxygen.....84

20 . Emission intensity of [Ru(bipy)₃]²⁺,

[Ru(bipy)₂(diaz)]²⁺ and [Ru(bipy)₂(py)₂]²⁺
as a function of temperature. The solvent is EtOH/MeOH
(4:1, v/v).....101

21. Temperature dependence of the relative emission
intensities of [Ru(bipy)₃]²⁺ in EtOH/MeOH (4:1, v/v).
The solid curve is the computer fit generated from the
parameters given in Table XVIII.....102

22 . Temperature dependence of the relative emission
intensities of [Ru(bipy)₂(diaz)]²⁺ in EtOH/MeOH (4:1, v/v).
The solid curve is the computer fit generated from the
parameters given in Table XVIII.....103

23 . Temperature dependence of the relative emission
intensities of [Ru(bipy)₂(py)₂]²⁺ in EtOH/MeOH (4:1, v/v).
The solid curve is the computer fit generated from the
parameters given in Table XVIII.....104

24. Temperature dependence of the emission lifetime
of [Ru(bipy)₃]²⁺ in EtOH/MeOH (4:1, v/v). The solid
curve is the computer fit generated from the parameters
given in Table XVIII.....105

25. Temperature dependence of the relative emission

lifetimes of $[\text{Ru}(\text{bipy})_2(\text{diaz})]^{+2}$ in EtOH/MeOH (4:1,v/v).
 The solid curve is the computer fit generated from the
 parameters given in Table XVIII.....106

26 . Temperature dependence of the relative emission
 intensities of $[\text{Ru}(\text{bipy})_2(\text{py})_2]^{+2}$ in EtOH/MeOH (4:1,v/v).
 The solid curve is the computer fit generated from the
 parameters given in Table XVIII.....107

27. Reaction scheme for the photooxidation of
 $[\text{Ru}(\text{bipy})_3]^{+2}$ and $[\text{Ru}(\text{phen})_3]^{+2}$ by $\text{S}_2\text{O}_8^{2-}$
 ions.....108

28 . Dependence of the reciprocal quantum yield of
 oxidation of $[\text{Ru}(\text{bipy})_3]^{+2}$ to $[\text{Ru}(\text{bipy})_3]^{+3}$ upon
 $1 / [\text{S}_2\text{O}_8^{2-}]$109

29. Methylene - linked pyridine ligands.....138

30 . Temperature dependence of the relative emission
 intensities of $[\text{Ru}(\text{bipy})_2(\text{pic})_2]^{+2}$ in EtOH/MeOH (4:1,v/v).
 The solid curve is the computer fit generated using
 the parameters given in Table XXIX.....139

31 . Temperature dependence of the relative emission

intensities of $[\text{Ru}(\text{bipy})_2\text{DPM}]^{+2}$ in EtOH/MeOH (4:1, v/v).
 The solid curve is the computer fit generated from the
 parameters given in Table XXIX.....140

32 . Absorption spectra during the photolysis of
 $[\text{Ru}(\text{bipy})_3]^{+2}$ in 0.01 M TBACl in CH_2Cl_2 . The
 photolysis times (in seconds) are: curve a,0; curve b,15;
 curve c,30; curve d,45; curve e,60; curve f,180; curve g,
 300; curve h,600; curve i,1,200.....141

33 . Absorption spectra during the photolysis of
 $[\text{Ru}(\text{bipy})_2(\text{pic})_2]^{+2}$ in 0.01 M TBACl in CH_2Cl_2 . The
 photolysis times (in seconds) are: curve a,0; curve b,15;
 curve c,30; curve d,45; curve e,60; curve f,180; curve g,
 300; curve h,600; curve i,1,200.....142

34 . Absorption spectra during the photolysis of
 $[\text{Ru}(\text{bipy})_2\text{DPM}]^{+2}$ in 0.01 M TBACl in CH_2Cl_2 . The
 photolysis times (in seconds) are: curve a,0; curve b,15;
 curve c,30; curve d,45; curve e,60; curve f,180; curve g,
 300; curve h,600; curve i,1,200.....143

35 . Absorption spectra during the photolysis of
 $[\text{Ru}(\text{bipy})_2\text{Cl}(\text{py}'-\text{CH}_2\text{CH}_2-\text{py})]^{+1}$ in 0.01 M TBACl in
 CH_2Cl_2 . The photolysis times (in seconds) are : curve

a,0; curve b,15; curve c,30; curve d,45; curve e,60;
 curve f,180; curve g,300; curve h,600; curve i,1,200...144

36 . Methylene - linked amine ligands.....156

37 . Temperature dependence of the relative emission
 intensities of $[\text{Ru}(\text{bipy})_2(\text{en})]^{+2}$ in EtOH/MeOH (4:1,v/v).
 The solid curve is the computer fit generated from the
 parameters given in Table XXXVII.....157

38 . Temperature dependence of the relative emission
 intensities of $[\text{Ru}(\text{bipy})_2(\text{tn})]^{+2}$ in EtOH/MeOH (4:1,v/v).
 The solid curve is the computer fit generated from the
 parameters given in Table XXXVII.....158

39 . Stern - Volmer plot of the quenching of the
 emission of $[\text{Ru}(\text{bipy})_2(\text{en})]^{+2}$ in a 0.01 M solution of
 TEACl in CH_2Cl_2 at 298 K by Ferrocene.....159

40 . Extensive photolysis of $[\text{Ru}(\text{bipy})_2(\text{en})]^{+2}$ in
 CH_3CN (no Cl^-). Curve A : before irradiation. Curve B :
 final spectrum.....181

41 . Extensive photolysis of $[\text{Ru}(\text{bipy})_2(\text{en})]^{+2}$ in
 H_2O (no Cl^-). Curve A : before irradiation. Curve B :

final spectrum.....	182
42 . Extensive photolysis of $[\text{Ru}(\text{bipy})_2(\text{en})]^{+2}$ in CH_2Cl_2 (no Cl^-). Curve A :before irradiation.	
Curve B :final spectrum.....	183
43 . Extensive photolysis of $[\text{Ru}(\text{bipy})_2(\text{tn})]^{+2}$ in CH_3CN (no Cl^-). Curve A :before irradiation.	
Curve B :final spectrum.....	184
44 . Extensive photolysis of $[\text{Ru}(\text{bipy})_2(\text{tn})]^{+2}$ in H_2O (no Cl^-). Curve A :before irradiation.	
Curve B :final spectrum.....	185
45 . Extensive photolysis of $[\text{Ru}(\text{bipy})_2(\text{tn})]^{+2}$ in CH_2Cl_2 (no Cl^-). Curve A :before irradiation.	
Curve B :final spectrum.....	186
46 . Quenching of the emission of $[\text{Ru}(\text{bipy})_2(\text{en})]^{+2}$ in CH_3CN at 298 K by AgNO_3	187
47 . Temperature dependence of the photosubstitution quantum yields of : (A) , $[\text{Ru}(\text{bipy})_3]^{+2}$; (B) , $[\text{Ru}(\text{bipy})_2(\text{tn})]^{+2}$; (C), $[\text{Ru}(\text{bipy})_2(\text{en})]^{+2}$ in a 0.01 M solution of TEACl in CH_2Cl_2	188

48 . Absorption spectra during the photolysis of
 $[\text{Ru}(\text{bipy})_2(\text{en})]^{+2}$ in 0.01 M TEACl in CH_3CN . The
 photolysis times (in min) are : curve a, 0; curve b, 10;
 curve c, 20; curve d, 30; curve e, 40. Curve F, 10 hours
 of full irradiation.....189

49 . Absorption spectra during the photolysis of
 $[\text{Ru}(\text{bipy})_2(\text{en})]^{+2}$ in 0.01 M TEACl in H_2O . The
 photolysis times (in min) are : curve a, 0; curve b, 20;
 curve c, 40; curve d, 60; curve e, 80; curve f, 100.
 Curve F, 10 hours of full irradiation.....190

50 . Absorption spectra during the photolysis of
 $[\text{Ru}(\text{bipy})_2(\text{en})]^{+2}$ in 0.01 M TEACl in CH_2Cl_2 . The
 photolysis times (in min) are : curve a, 0; curve b, 10;
 curve c, 20; curve d, 30; curve e, 40; curve f, 50;
 curve g, 60; Curve F, 10 hours of full irradiation.....191

51 . Absorption spectra during the photolysis of
 $[\text{Ru}(\text{bipy})_2(\text{tn})]^{+2}$ in 0.01 M TEACl in CH_3CN . The
 photolysis times (in min) are : curve a, 0; curve b, 10;
 curve c, 20; curve d, 30; curve e, 40. Curve F, 10 hours
 of full irradiation.....192

52 . Absorption spectra during the photolysis of

[Ru(bipy)₂(tn)]²⁺ in 0.01 M TEACl in H₂O . The
 photolysis times (in min) are : curve a, 0; curve b, 20;
 curve c, 40; curve d, 60; curve e, 80 . Curve F, 10 hours
 of full irradiation.....193

53 . Absorption spectra during the photolysis of
 [Ru(bipy)₂(tn)]²⁺ in 0.01 M TEACl in CH₂Cl₂. The
 photolysis times (in min) are : curve a, 0; curve b, 10;
 curve c, 20; curve d, 30; curve e, 40. Curve F, 10 hours
 of full irradiation.....194

ABSTRACT

Stern - Volmer plots for the quenching of luminescence and for the photosubstitution reaction of tris - bipyridylruthenium(II) at 298 K were obtained. The two Stern - Volmer plots were found to be similar; this result is different from that of a previous report, but it agrees well with a general model postulated to represent the photophysical processes of the excited states of polypyridine ruthenium(II) complexes. The temperature dependence of the emission intensities and of the lifetimes of tris - bipyridylruthenium(II), cis - bispyridyl bis - 2,2'bipyridylruthenium(II), and 4, 5 - diazafluorenyl - bis - 2,2'bipyridylruthenium(II) were reinvestigated in order to evaluate the difference in energy between the triplet metal to ligand charge transfer and ligand field excited states. The activation energies of these complexes were found to be well correlated with the respective ligand field strengths.

The 77 K emission properties and the temperature dependence of the emission intensities of two series of polypyridine ruthenium(II) complexes $[\text{Ru}(\text{bipy})_2\text{L}]^{+2}$ were examined. Their photochemistries at 298 K were also investigated. The main goal was to determine the effect of chelate ring size on their photosubstitution reactions in different

solvents. The first series included methylene - linked pyridine ligands, and the second involved methylene - linked diamine ligands.

In the case of the pyridine series there was an increase in quantum yield of the photosubstitution reactions as the chelate ring size increased. In contrast, significantly lower quantum yields were observed for complexes of the diamine series in which the two chelating N atoms of the bidentate ligands do not belong to an aromatic ring.

It was also established that the Ag^+ cation has a catalytic effect on the photosubstitution reaction of the complex ethylenediamine bis - 2,2'-bipyridylruthenium(II) dissolved in CH_3CN . Results of the photolyses of this complex and of 1,3 - propylenediamine bis - 2,2'-bipyridylruthenium(II) suggested that under certain conditions oxidation of the methylene - linked ligand occurs. The temperature dependence of the quantum yields of the photosubstitution reactions of these complexes in 0.01 M tetraethylammoniumchloride solutions in CH_2Cl_2 showed small apparent activation energies.

CHAPTER I. INTRODUCTION.

In recent years, the photophysical and photochemical behavior of polypyridine ruthenium complexes has been extensively examined. Since the literature in this field is rich with many more contributions than those that can be listed here, only a representative set of some of the most comprehensive reviews is offered to the reader¹.

The photophysics and the photochemistry of $[\text{Ru}(\text{bipy})_3]^{+2}$ and related complexes are sufficiently important to have aroused the attention of many research groups in many parts of the world; literally hundreds of articles have been published. Nevertheless, much of the subject matter is not well defined and is still controversial. Despite all the work that has been done numerous questions are still unanswered. For example, there still does not exist an unambiguous assignment of either the electronic absorption spectrum or the luminescence spectrum of $[\text{Ru}(\text{bipy})_3]^{+2}$; the assignment of the transitions of similar but more complicated molecules are even less well understood.

Interest in these complexes arises from

consideration of several properties. First, even in fluid solution at ambient temperature these complexes often exhibit intense emission from long - lived excited states; this emission greatly facilitates their investigation and permits the evaluation of rate constants for fundamental photophysical and photochemical processes. Furthermore, this usefulness extends into the realm of bimolecular processes since these excited states readily participate in both energy and electron transfer reactions². Certainly, $[\text{Ru}(\text{bipy})_3]^{+2}$ and related complexes constitute one of the preeminent paradigms of organometallic photochemistry. Hence, many of the currently emerging concepts of organometallic and inorganic photochemistry have been quantitatively verified by studying these complexes. For example, Ford and co - workers³ have utilized a series of $[\text{Ru}(\text{NH}_3)_5\text{L}]^{+2}$ and $[\text{Ru}(\text{NH}_3)_4\text{L}_2]^{+2}$ complexes (L = para - substituted pyridine or pyrazine) in order to demonstrate that photosubstitution reactions occur from a ligand field (LF) excited state. If the pyridine ligand is a good acceptor, the lowest excited state has mainly metal - to - ligand charge transfer (MLCT) character and the photosubstitution is an inefficient process. In contrast, when the pyridine ligand is a poor acceptor,

the lowest excited state has mainly LF character and the photosubstitution occurs very efficiently. A MLCT transition in a d^6 low spin complex is shown in the energy diagram in Figure 1.

These long - lived excited states readily participate in electron transfer reactions with both organic and inorganic quenchers. Consequently, these complexes have often been utilized in experiments designed to scrutinize theories of electron transfer⁴. As just one of many examples, Bock et al. investigated both the oxidative and the reductive quenching of tris - bipyridineruthenium(II) by a series of structurally related quenchers that had different redox potentials⁵. In both cases the quenching rate constants could be successfully treated by means of the Marcus - Hush theory⁶.

Finally, these complexes have been extensively investigated for their use as potential components in systems capable of producing hydrogen photochemically from water. In fact, with $[\text{Ru}(\text{bipy})_3]^{+2}$ as a photoactive catalyst, the efficiency of hydrogen production has been reported to be as high as 13% ⁷.

A. GENERAL BACKGROUND.

1. Photophysics of Tris -bipyridineruthenium(II).

The solution phase ultraviolet - visible absorption spectrum of $[\text{Ru}(\text{bipy})_3]^{+2}$ consists of three major absorption bands, centered at 244, 285, and 438 nm (see Figure 2)⁸. The first and third bands exhibit fine structure and have been assigned to MLCT transitions^{9 - 10}. The second band occurs in the same region as the $\pi \rightarrow \pi^*$ transition of the diprotonated form of bipyridine and has consequently been assigned to an intraligand transition (Figure 3).

The $[\text{Ru}(\text{bipy})_3]^{+2}$ complex displays a relatively intense emission (Figure 2), the quantum efficiency of which is independent of the excitation wavelength and of the nature of the exciting transition (i. e., the same result is obtained from a $\pi \rightarrow \pi^*$ excitation as from a $d \rightarrow \pi^*$ initial excitation). Therefore, $Q_{\text{f.f.}}$ is unity regardless of the nature of the pumping state¹¹. Excitation at any wavelength below approximately 550 nm results in rapid quantitative formation of the lowest excited state MLCT. It has been suggested that this initially formed

state contains largely singlet character and undergoes intersystem crossing with unit efficiency to the corresponding triplet MLCT state²⁰. The emission is then assigned to phosphorescence from this ³MLCT state. Since rather large spin - orbit coupling occurs in $[\text{Ru}(\text{bipy})_3]^{+2}$, the use of pure spin labels may not be justified²¹. However, most photophysical features of $[\text{Ru}(\text{bipy})_3]^{+2}$ can be rationalized in terms of a model for which D_3 symmetry is assumed and spin - orbit coupling for the d^5 $[\text{Ru}(\text{bipy})_3]^{+2}(\text{III})$ core is incorporated²². Since the exact multiplicity of the emitting state will not affect most of the arguments presented in this work, these spin labels will be maintained, merely as a formalism, throughout the remainder of the text with the understanding that singlet/triplet mixing does occur to some extent; the terms fluorescence and phosphorescence are virtually meaningless for this model.

Since emission is readily observed, this lowest excited ³MLCT state has been extensively investigated. After measuring the lifetimes of $[\text{Ru}(\text{bipy})_3]^{+2}$ complex at low temperature, Crosby and co-workers concluded that this transition

actually consists of three closely spaced transitions from states that have widely different lifetimes¹². However, at 298 K, all three states are populated and hence the luminescence can be considered to be an "average state". The representation which best accomodates the experimental data is shown in Figures 4 and 5 .

The assumptions in the model are : (i) The luminescence observed experimentally for D_3 complexes (as $Ru(II)$, d^6 , low - spin), originates from three closely spaced electronic states (in the case of C_2 complexes, four levels must be assumed) (ii) Each of these states is capable of undergoing both radiative and non - radiative decay to the ground state. These pathways are controlled by first order kinetics, with rate constants k_r and k_{nr} which are temperature independent (iii) A Boltzman equilibrium between these states is stablised and maintained upon a time scale much shorter than the characteristic lifetimes of the state (iv) The manifold of these states is populated from higher excited states with unit efficiency.

The symmetry of the excited state molecule also appears to be temperature dependent ; it is D_3

at low temperatures²³ and changes to C_{2v} as the temperature increases²⁴. Thus, at 298 K this 3MLCT state can best be described as $[Ru(III)(bipy)_2(bipy^-)]$; that is, the excitation is not delocalized over all three bipy ligands but rather is localized on a single ligand.

The conclusion that the excitation is apparently localized in a single ligand²⁵ at least in solution phase²⁶, was initially based upon polarized absorption and photoselection spectra of $[Ru(bipy)_3]^{+2}$ ^{27,28,29}. More recently, time - resolved resonance Raman (TR^3) has indicated that the lowest excited 3MLCT state is best described by the formula $[Ru(III)(bipy)_2(bipy^-)]^{+2}$ ^{30,31,32,33}. This assignment was accomplished by a comparison of the observed shifts of vibrational bands in the ground and lowest excited states with those of bipy and bipy⁻. This assignment implies that the electron is localized on a single bipy ligand. Analogously, Caspar et al.³⁴ have examined the TR^3 of $[Os(bipy)_n(P_2)_3]^{+2}$ ($P_2 = cis - (C_6H_5)_2P - CH = CH - P(C_6H_5)_2$; $n = 1 - 3$) and found that the observed spectral shifts are nearly identical for all complexes and quite similar to the shift observed for the

comparison of bipy/bipy⁻ .

Further indication that the transferred electron is best described as residing on a single ligand comes from flash photolysis experiments. The initial studies of the lowest excited state of [Ru(bipy)₃]⁺² were not self - consistent but all of them gave absorption bands very similar to those of bipy⁻³⁵ . A more recent study extended the results throughout the visible region and resulted in a more resolved spectrum³⁶. In total, five bands were observed and each could be assigned after consideration of suitable model compounds. Again, the absorption spectrum was consistent with charge localization on a single ligand in the excited state.

The ³MLCT excited state of the [Ru(bipy)₃]⁺² complex in water at 298 K is reasonably longlived (~ 0.6/ μ sec) and is thought to be deactivated by the three processes shown in Figure 6. Also the photophysics of tris - bipyridineruthenium(II) and related complexes can be represented by means of a modified Jablonsky diagram (Figure 7) . One process is the radiative decay to the ground state, with emission occurring around 600 nm. For a large number of polypyridine ruthenium complexes the values for the

radiative rate constant are found to lie between 10^{+4} and 10^{+5} sec^{-1} ³⁵. Demas and Crosby have developed a semiempirical spin - orbit coupling model which gives semiquantitative predictions of radiative lifetimes ($= 1 / k_r$) for numerous ruthenium, osmium, and iridium complexes³⁷. This agreement supports the assignment of the emission to a spin forbidden charge transfer process.

A radiationless deactivation pathway is also available to this excited state. In fact, this pathway is generally responsible for dissipating the majority of the excitation energy. The rate constant for this process is theoretically predicted to depend exponentially on the energy difference between the initial state (³MLCT) and the ground state (GS)³⁸. Meyer and co - workers have indeed verified this expected dependence for numerous ruthenium and osmium complexes^{39,40}.

The radiationless rate constant is subject to a large solvent isotope effect, which is 1.8 for $\text{H}_2\text{O} / \text{D}_2\text{O}$ at 298 K^{41} . This large isotope effect has led Van Houten and Watts to suggest that the luminescent state contains some metal - to - solvent charge

transfer (MSCT) character⁴¹. In fact, by evaluating k_{nr} for $[Ru(bipy)_3]^{+2}$ in different solvents, Nakamura estimated the relative ratio of MLCT and MSCT for $[Ru(bipy)_3]^{+2}$ in water to be nearly unity⁴².

However, a series of complexes that have systematically decreasing 3MLCT excited state energies has been investigated⁴³. The stabilization of the 3MLCT state should increase the contribution of this configuration to the overall wavefunction of the emitting state. This stabilization necessarily decreases the magnitude of the MSCT configuration in the emitting state and should decrease the observed isotope effect. This prediction is not borne out since the isotope effects for all complexes studied were similar. These results suggest that the quenching mechanism does not involve electron transfer which would be predicted for the MSCT model, but rather a specific quenching involving the OH(D) bond.

The final process that deactivates the 3MLCT state is population of a higher excited state that can then undergo efficient radiationless decay to the ground state (Figure 6). Population of this higher excited state also results in a low yield

photosubstitution reaction which implies that this state be identified as an LF state⁴⁴. By studying the temperature dependences of the phosphorescence lifetime and of the emission intensity of $[\text{Ru}(\text{bipy})_3]^{+2}$ in water, Van Houten and Watts were able to evaluate the energy difference between the $^3\text{MLCT}$ and LF excited state as $3,600 \text{ cm}^{-1}$ ⁴¹ (Figure 8). In order to substantiate these conclusions further, the activation energy for LF population, E , in a number of complexes that have different $^3\text{MLCT}$ energies has been investigated ⁴⁵. As shown in Figure 6, if only the $^3\text{MLCT}$ energy decreases, the activation energy should increase proportionately. Such a correlation has indeed been observed and clearly suggests that there is a thermal equilibrium between these two excited states.

Similarly, Caspar and Meyer have recently reported a study of $[\text{Ru}(\text{bipy})_2\text{L}_2]^{+2}$ complexes (L= mono - and bidentate ligands with N, P, or As donor atoms)³⁹. There was a dramatic effect of the ligand upon the excited state properties of the complexes. Unfortunately, no clear correlation between the $^3\text{MLCT}$ energy and activation energy for LF population was apparent. This observation results from a substantial variation of both the $^3\text{MLCT}$ and LF energies. The

former is easily evaluated by means of emission spectroscopy of these complexes while the latter is difficult, if not impossible, to evaluate. On the other hand, a study of solvent effects on the excited state behavior of $[\text{Ru}(\text{bipy})_3]^{+2}$ has clearly indicated a relationship between the $^3\text{MLCT}$ energy and the activation energy for LF population⁴⁵.

From the above discussion, it is clear that the model presented in Figures 6 and 7 is substantiated by numerous experimental data. Nevertheless, despite the vast literature supporting that model, which is generally accepted to explain the observed behavior of other polypyridine ruthenium complexes, recent studies have presented experimental evidence that was not in agreement.

For instance, Fasano and Hoggard have recently reported results which seem to suggest that the $^3\text{MLCT}$ and LF excited states are not in thermal equilibrium⁴⁶. They investigated the quenching of both the emission intensity (from $^3\text{MLCT}$), and the photosubstitution reaction (from LF) of $[\text{Ru}(\text{bipy})_3]^{+2}$ in DMF with 0.1 M TBABr present. The effective, uncharged quencher selected was ferrocene, which actively interacted in the emission and

photosubstitution processes. However, the resulting two linear Stern - Volmer plots were found to have substantially different slopes. In fact, the slope for the quenching of the photosubstitution was determined to be 3 - fold larger than the slope for the luminescence quenching. These results suggest that the $^3\text{MLCT}$ and LF excited states are not in thermal equilibrium, and produce evidence against the postulated model which involves the suggested equilibrium. Furthermore, the lifetime of the LF state appears to be much larger than that of the $^3\text{MLCT}$ state.

As an additional example of disagreement with the currently accepted model, some published photophysical studies seem to indicate that there is not a clear correlation of the ligand field excited state energies of some polypyridine ruthenium(II) complexes with the corresponding ligand field strengths. Thus, as was previously stated, the difference between the $^3\text{MLCT}$ and LF excited state of $[\text{Ru}(\text{bipy})_3]^{+2}$ in H_2O has been evaluated to be $3,600 \text{ cm}^{-1}$ ⁴¹; the 4,5 - diazafluorene ligand has been shown to cause little change in the energy of any MLCT state⁴⁷. Nevertheless, in the case of

$[\text{Ru}(\text{bipy})_2(\text{diaz})]^{+2}$ over the temperature range of 250 - 350 K, the observed temperature dependence of the emission intensity yielded a value of $3,450 \text{ cm}^{-1}$, which is a value quite similar to that observed for $[\text{Ru}(\text{bipy})_3]^{+2}$ ⁴⁸. This determination was in sharp contrast with results expected on the basis of the accepted model since the energy of this presumed LF excited state did not seem to depend on the ligand field strength in the expected manner. Likewise, in the case of $[\text{Ru}(\text{bipy})_2(\text{py})_2]^{+2}$, although pyridine is lower in the spectrochemical series than bipyridine, the value of ΔE has been evaluated over the 250 - 350 K temperature range and found to be $3,410 \text{ cm}^{-1}$ ^{39,49}. Once more, this value of ΔE suggests little change in the energy of the presumed LF state, and gives the impression that the ligand field trends which are very apparent in studies of other metal complexes were absent in the behavior of these complexes.

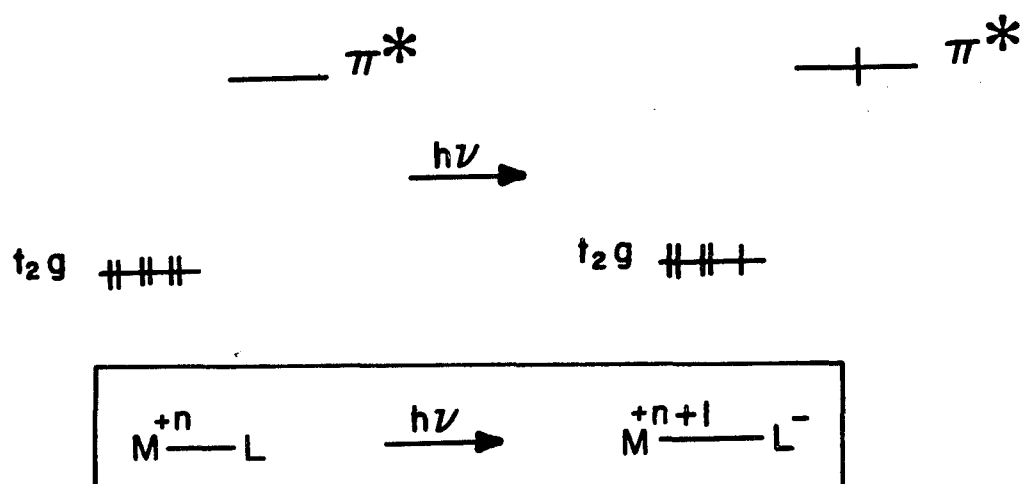


Figure 1. Metal to Ligand Charge Transfer in a d^6 low spin complex.

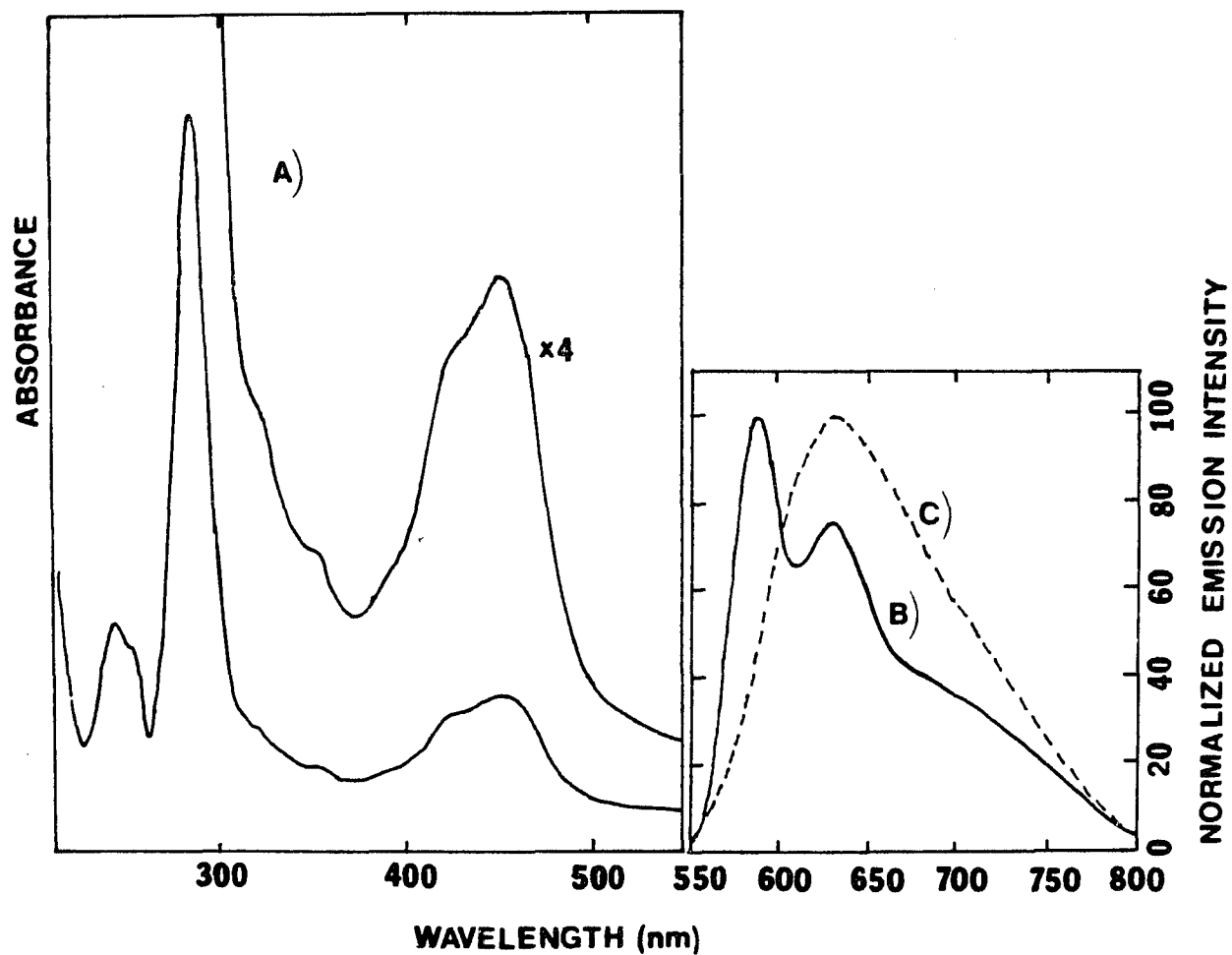


Figure 2. A) Electronic absorption spectrum of an aqueous solution of $[\text{Ru}(\text{bipy})_3]^{2+}$. Emission spectra of $[\text{Ru}(\text{bipy})_3]^{2+}$: B) at 77 K. C) at 273 K.

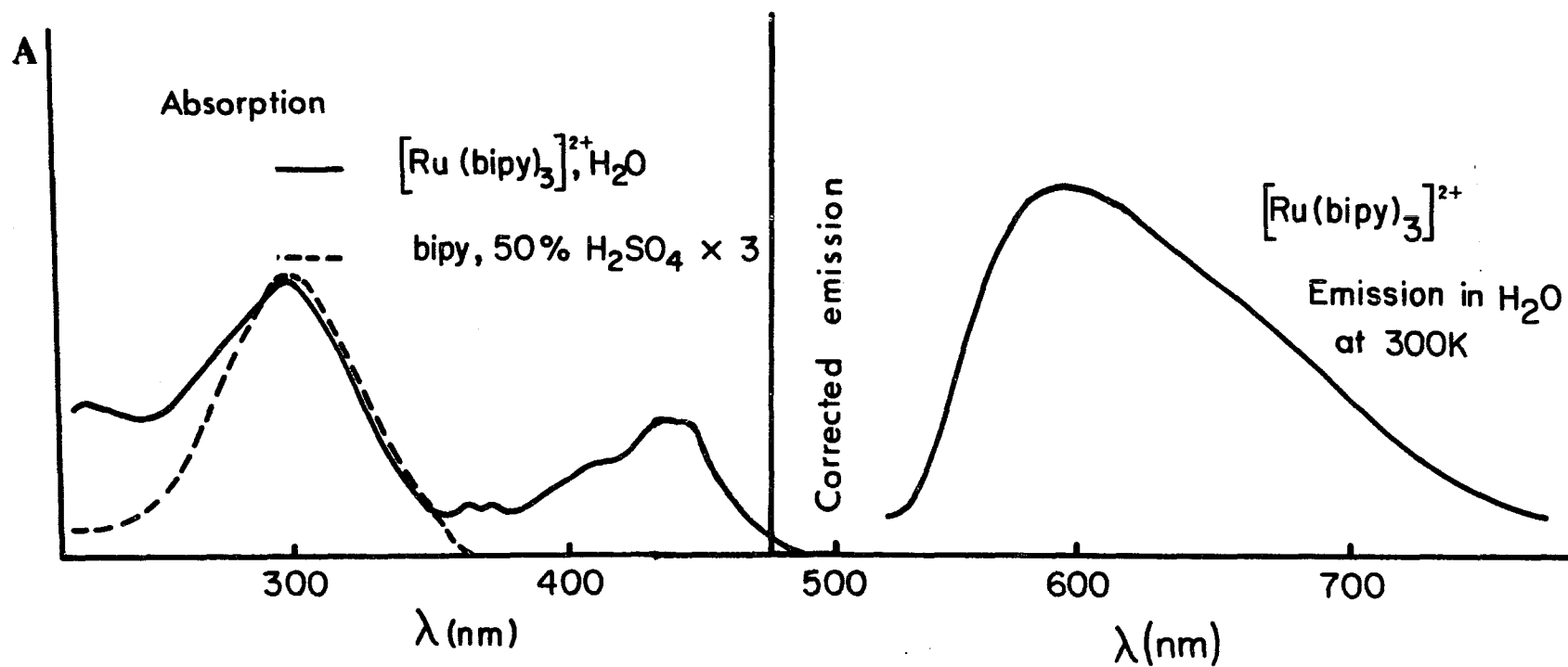


Figure 3. Absorption and emission spectra of $[\text{Ru}(\text{bipy})_3]^{2+}$ in H_2O at 298 K.

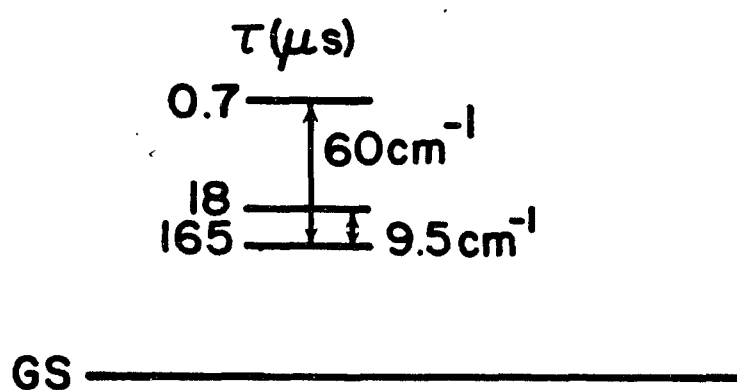


Figure 4. Empirical splitting of the excited state of $[\text{Ru}(\text{bipy})_3]^{2+}$ arising from an MLCT excitation.

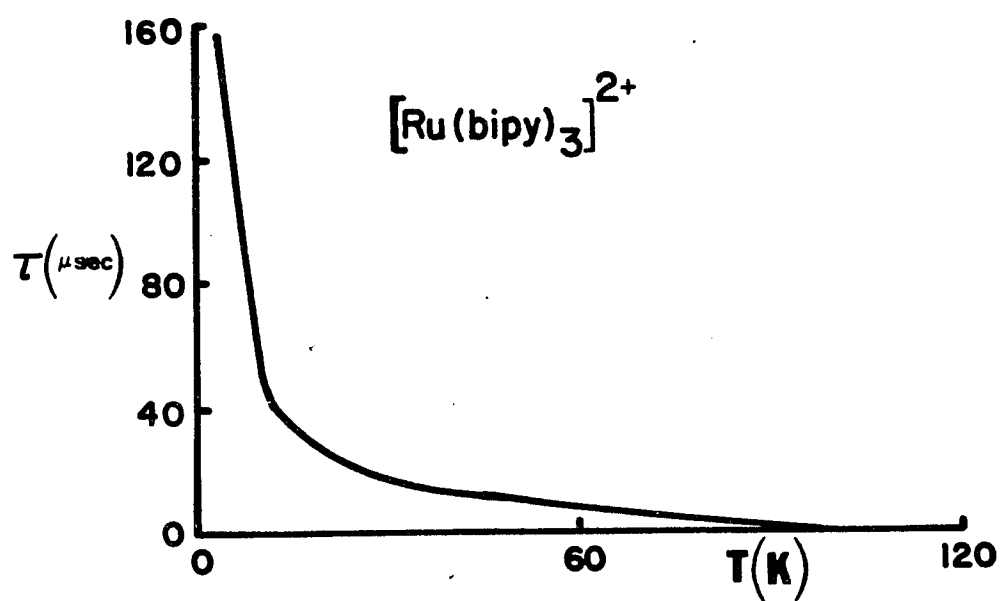


Figure 5. Variation with temperature of the luminescence lifetime of $[\text{Ru}(\text{bipy})_3]^{2+}$ at low temperatures.

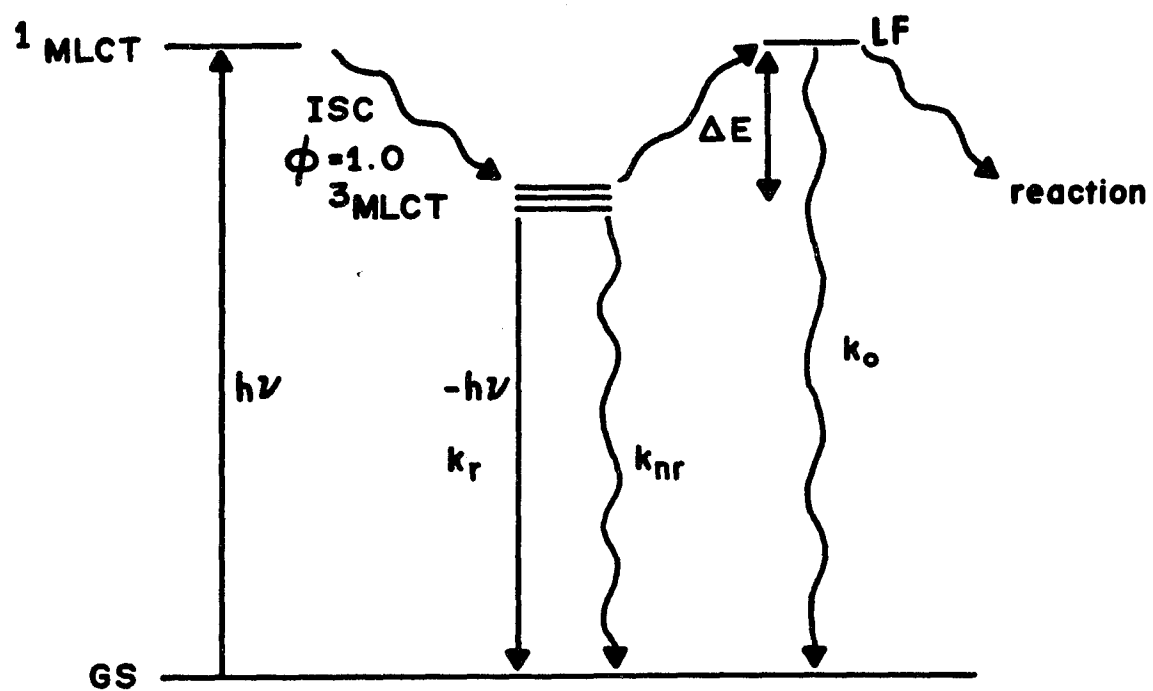


Figure 6. Photophysical processes of $[\text{Ru}(\text{bipy})_3]^{2+}$.

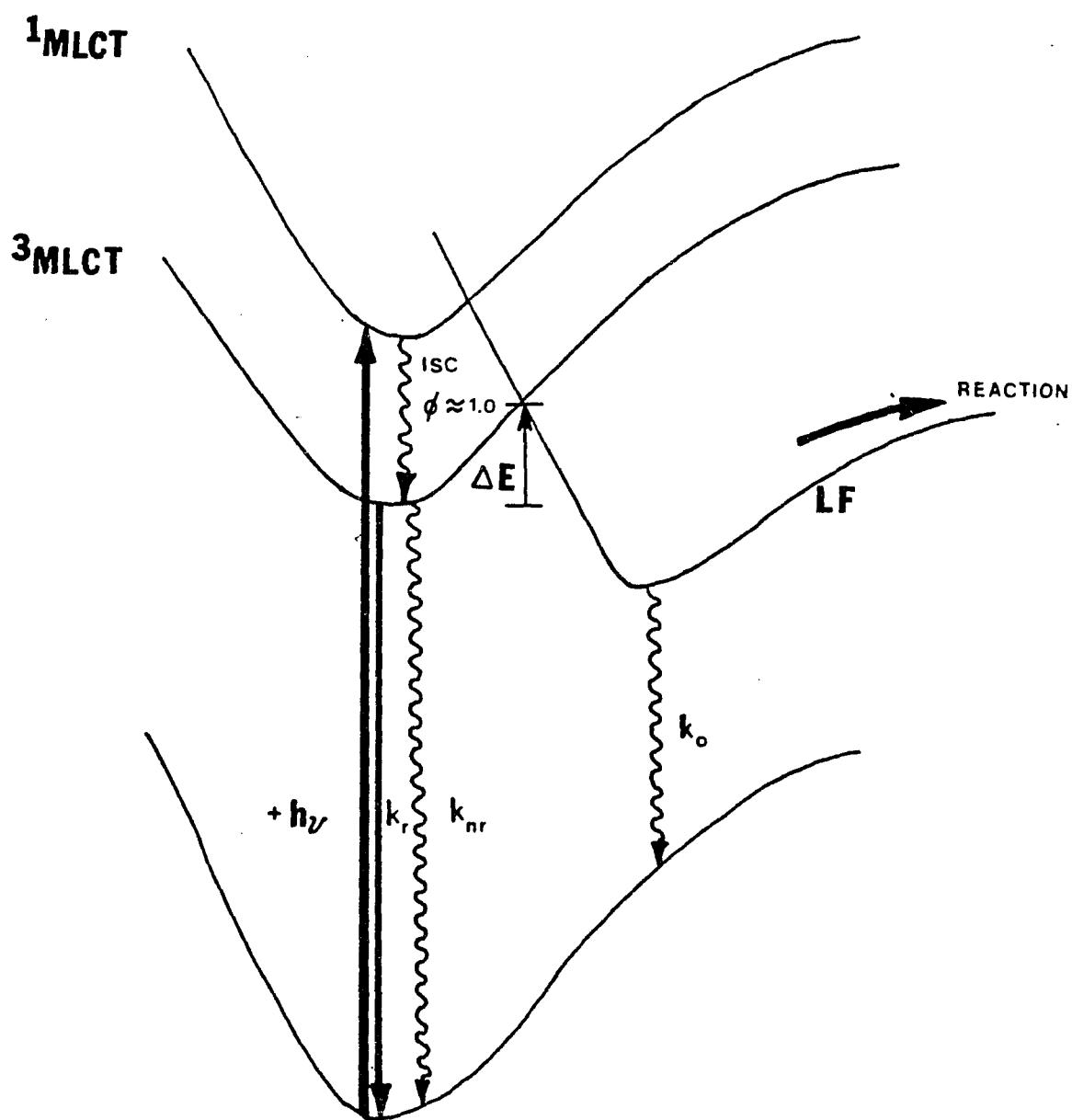
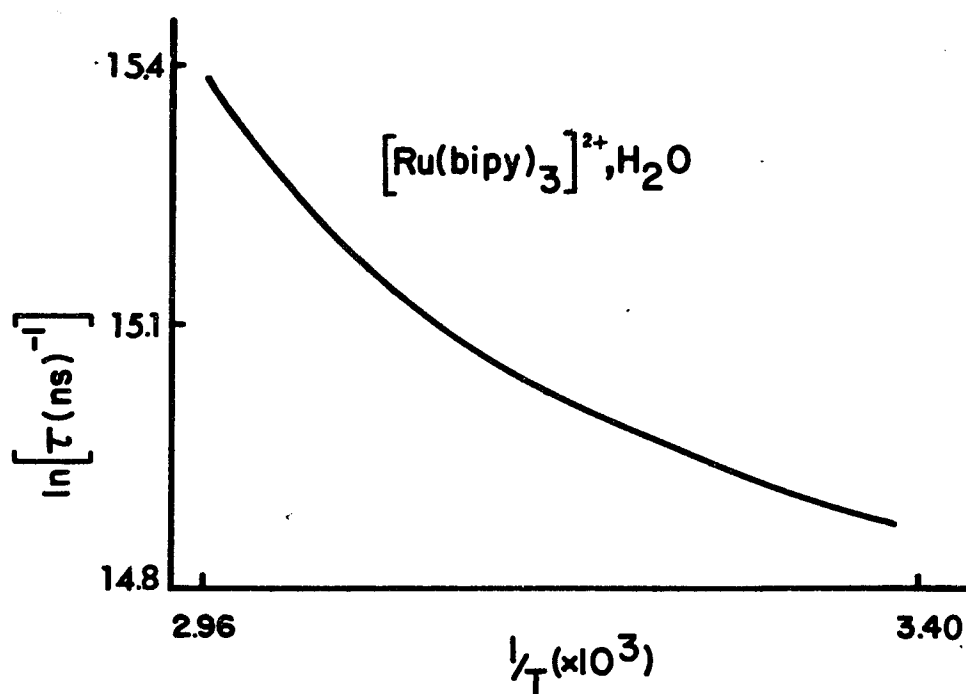


Figure 7. Modified Jablonski diagram of the photophysics of polypyridine ruthenium complexes.



$$\tau^{-1} = k_{\text{exp}} = k + k_0 e^{-\Delta E/RT}$$

$$\Delta E = 3600 \text{ cm}^{-1}$$

Figure 8. Energy difference between the $^3\text{MLCT}$ and LF excited state.

2. Photosubstitution Model.

The photosubstitution quantum yield of $[\text{Ru}(\text{bipy})_3]^{+2}$ in aqueous solution is pH dependent. There is no detectable photoreaction of the complex at neutral pH, while the efficiency of the photoreaction of the complex in either acidic or basic media rises to a detectable, albeit low, value⁴⁴. On the other hand, a marked increase in the efficiency of this process can be observed when the complex is dissolved in organic solvents such as CH_2Cl_2 and DMF⁵⁰. An elegant investigation of this process has been reported by Meyer and co-workers^{45,49}. Several polypyridine ruthenium complexes were investigated and the most enlightening contrast was provided by $[\text{Ru}(\text{bipy})_3]^{+2}$ and cis - $[\text{Ru}(\text{bipy})_2(\text{py})_2]^{+2}$. The emission intensities and lifetimes of both complexes were found to be comparable. In contrast, their photochemical behavior was found to be quite different. In the case of $[\text{Ru}(\text{bipy})_2(\text{py})_2]^{+2}$, the photosubstitution of a pyridine ligand is very efficient and essentially independent of either solvent (water versus CH_2Cl_2) or counterion. In the case of $[\text{Ru}(\text{bipy})_3]^{+2}$ in organic solvents, the

photoreaction has a low efficiency and the reaction occurs only in the presence of a good entering ligand such as isothiocyanate, NCS^- .

This dramatic difference in the photochemical behavior of these complexes cannot result from a difference in their $^3\text{MLCT}$ states. Indeed, the various rate constants of both species for deactivation of this state are comparable. Consequently, the dramatic photochemical difference must depend on a state formed after this excited $^3\text{MLCT}$ state is deactivated. Meyer and co-workers have suggested that the key intermediate which dictates the photochemical efficiency is a pentacoordinated species obtained by photoextrusion of a pyridine ligand. In the case of $[\text{Ru}(\text{bipy})_2(\text{py})_2]^+{}^2$, this intermediate is trapped by any nearby ligand and the product distribution will depend solely only on relative concentrations. In the case of $[\text{Ru}(\text{bipy})_3]^+{}^2$, this coordinately unsaturated species is also formed. However, the extruded pyridine is prevented from diffusing away and, in fact, is held in a position that facilitates rapid recoordination. The only possible method of competing with this rapid collapse to the starting complex is to have a strongly complexing ligand nearby. This nearby ligand is surely present in the formation

of $[\text{Ru}(\text{bipy})_3]^{+2}$ $[\text{NCS}^-]_2$ in organic solvents (e.g., CH_2Cl_2), where these species must certainly exist as ion pairs.

These observations^{49, 51} have been rationalized within the framework of the postulated model which, at present, is generally accepted at least as a first approximation for studies of photosubstitution processes involving polypyridine ruthenium (II) complexes. The essential features of this model are presented in Figure 9. Excitation results in the quantitative production of a triplet MLCT state. Besides radiative and radiationless decay, this $^3\text{MLCT}$ excited state may undergo a thermally induced internal conversion to a higher - lying LF excited state. Once this LF state has been populated, it may be deactivated by either decay back to the ground state or by photochemical pathways. In the later process, a pentacoordinated intermediate (I) is produced. The intermediate may in turn decay to the ground state by undergoing a reclosure to the starting complex or may be trapped by another external ligand (L) to produce a net photosubstitution. The key to understanding the photoanation efficiency is to follow the partitioning of the intermediate (I) between products and starting

material.

3. The effect of ring size on photophysical and photochemical properties.

From another perspective, it has been determined that any change in the Ru - N bond overlap has an important effect on the excited state of polypyridine ruthenium(II) complexes. Cherry and co-workers⁴⁷ reported a convenient method for selectively perturbing the energy of LF state while leaving the MLCT state nearly unchanged. This method was based upon the 4, 5 - diazafluorene (diaz) ligand in which the methylene bridge distorts the bipyridine portion of the molecule so that the N - metal overlap is reduced. Hence, diaz is effectively lower than bipy in the spectrochemical series and consequently the energy of any LF state is lowered (Figure 10). On the other hand, the reduction potentials of both diaz and bipy should be similar so that any change in the energy of the MLCT state is expected to be modest. The 77 K temperature emission spectra for $\text{Ru}[(\text{bipy})_3]^{+2}$ and $[\text{Ru}(\text{bipy})_2(\text{diaz})]^{+2}$ (Figure 11) demonstrates that the intensities are comparable and very few differences in the band shapes of these spectra were apparent. A

small 4 nm bathocromic shift noted for $[\text{Ru}(\text{bipy})_3]^{+2}$ supported the contention that any MLCT's are only slightly affected by substitution of diaz for bipy. Both spectra of the compounds at 298 K undergo a substantial bathocromic shift and a loss of fine structure. However, the most spectacular change was in their relative intensities. The emission intensity of $[\text{Ru}(\text{bipy})_3]^{+2}$ at 298 K is almost fifty - fold larger than that of $[\text{Ru}(\text{bipy})_2(\text{diaz})]^{+2}$ at the same temperature. The results summarized above could be readily rationalized by the previously described model of Figure 6. At 77 K only the radiative and non - radiative processes to the ground state are operational and both complexes have similar emission intensities. When the temperature is raised, thermal population of the LF excited state becomes important. Since the LF state of $[\text{Ru}(\text{bipy})_2(\text{diaz})]^{+2}$ is energetically lower than that of $[\text{Ru}(\text{bipy})_3]^{+2}$, the population of the former is much greater at 298 K, and thus the observed drastic reduction of the emission intensity occurs.

From the previous discussion, it is clear that changes introduced in the Ru - N bond overlap can exert a profound effect on the excited state processes of

polypyridine ruthenium(II) complexes, and these observations are directly related to the photochemical behavior associated with the LF state.

A related perturbation, which also modifies the geometry and therefore the characteristics of the Ru - N bonds, can be achieved by varying the ring size of a series of complexes with the general formulation $[Ru(bipy)_2L]^{+2}$ in which the complexes contain ligands, L, that have two pyridines linked by methylene bridges of varying lengths. This series of ligands is shown in Figure 29.

Of course, several effects can be visualized to operate when this series is studied. As n increases, not only does the size of the chelating ring increase, but also the N - Ru - N chelation angle should increase. A careful study of the photophysics of these related complexes would be valuable in order to delineate changes in the energies of any LF state. In addition, the adequate investigation of the photoextrusion process could provide valuable information about the dynamics of reclosure of the chelating ring, one of the processes involved in the photosubstitution model presented in the previous section (Figure 9).

A complementary study, also related to the variation of the ring size of complexes, has been designed to add more useful information with which to rationalize the photochemical behavior of polypyridine ruthenium(II) complexes. This series of complexes in which the general formulation is as given above but prepared with ligands, L, that have two amine groups linked by methylene bridges of different lengths is shown in Figure 36.

Under ideal conditions, the temperature dependence of the emission intensity and/or lifetimes for both series of complexes should be evaluated. These studies would allow the energetic mapping of both the $^3\text{MLCT}$ and LF state. The dependence of both upon the chelate ring size and chelation angle should be evaluated for the two series of complexes. Then, the photochemistry of these complexes in different solvents should be evaluated at known Cl^- concentrations. The initial counter ion should be PF_6^- which does not participate in trapping the pentacoordinate intermediate. The quantum yield of photoextrusion should be evaluated at various Cl^- concentrations. As shown in Appendix A.2, the quantum yield of

photosubstitution is related to the $[Cl^-]$ by Eq. (1),

$$\frac{1}{Q(P)} = \frac{1}{[T_e Q(I) k_{LF}]} + \left\{ \frac{1}{[T_e Q(I) k_{LF}]} \right\} \left\{ \frac{k_{rc}}{k_p} \right\} \left\{ \frac{1}{[Cl^-]} \right\} \quad (1)$$

in which $Q(P)$ and $Q(I)$ are the quantum yields of photosubstitution and formation of the pentacoordinate intermediate from the LF state, T_e is the luminescent lifetime, k_{LF} , k_{rc} and k_p are the rate constants for production of LF from 3MLCT , ring closure, and Cl^- ion trapping of the pentacoordinate intermediate. Clearly, the graph of $Q(P)^{-1}$ versus $[Cl^-]^{-1}$ should be linear. The intercept would allow direct evaluation of the efficiency of the formation of the pentacoordinated intermediate from the LF state. The relative importance of ring closure can be established by evaluating the ratio of slope / intercept which is k_{rc} / k_p . If one assumes that the bimolecular rate constant for Cl^- trapping is similar for all the complexes, the relative importance of ring reclosure would be directly related to the slope / intercept ratio. Evaluation of this parameter would be a crucial

test for the photosubstitution model proposed by Meyer and co-workers^{45,47}.

The photosubstitution quantum yield of $[\text{Ru}(\text{bipy})_3]^{+2}$ has been shown to be catalyzed by the presence of metal ions⁵². Specifically, Ag^+ greatly increases the photosubstitution of $[\text{Ru}(\text{bipy})_3]^{+2}$ to $[\text{Ru}(\text{bipy})_2(\text{CH}_3\text{CN})_2]^{+2}$ in CH_3CN solution upon photolytic irradiation. There is a continuous efficiency increase as $[\text{Ag}^+]$ increases until a limiting value at 0.8 M is reached. Whitten and co-workers have attributed this increase to the trapping of the pentacoordinate intermediate by Ag^+ ⁵². Presumably, the silver ion complexes the liberated ligand and thus reduces the efficiency of ring closure. The vacant initial site is eventually filled by a solvent molecule. An excellent method of verifying this hypothesis would be to determine the catalytic effect of Ag^+ on series of pyridine complexes outlined above that have increasingly larger chelating rings.

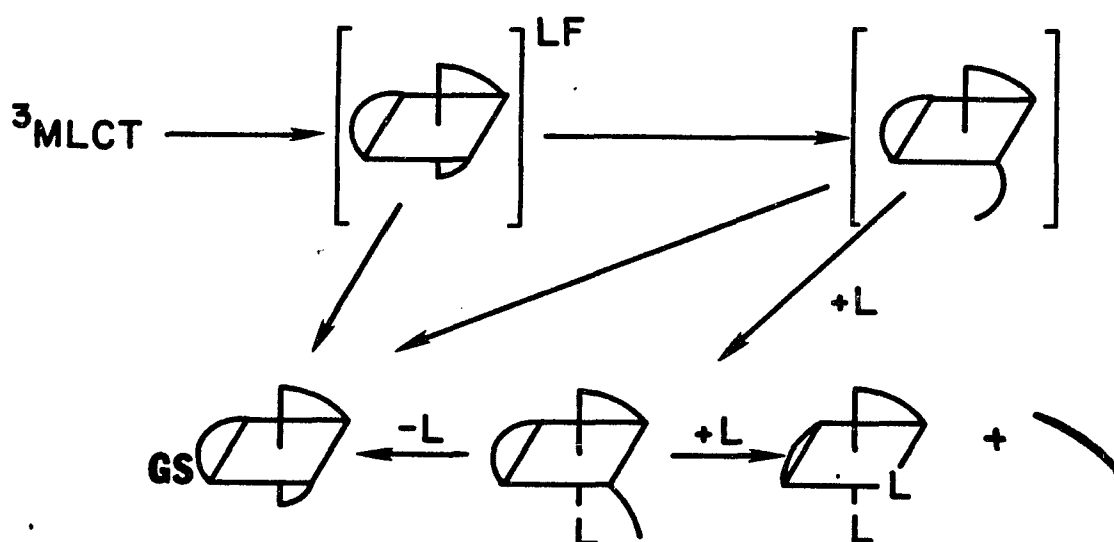
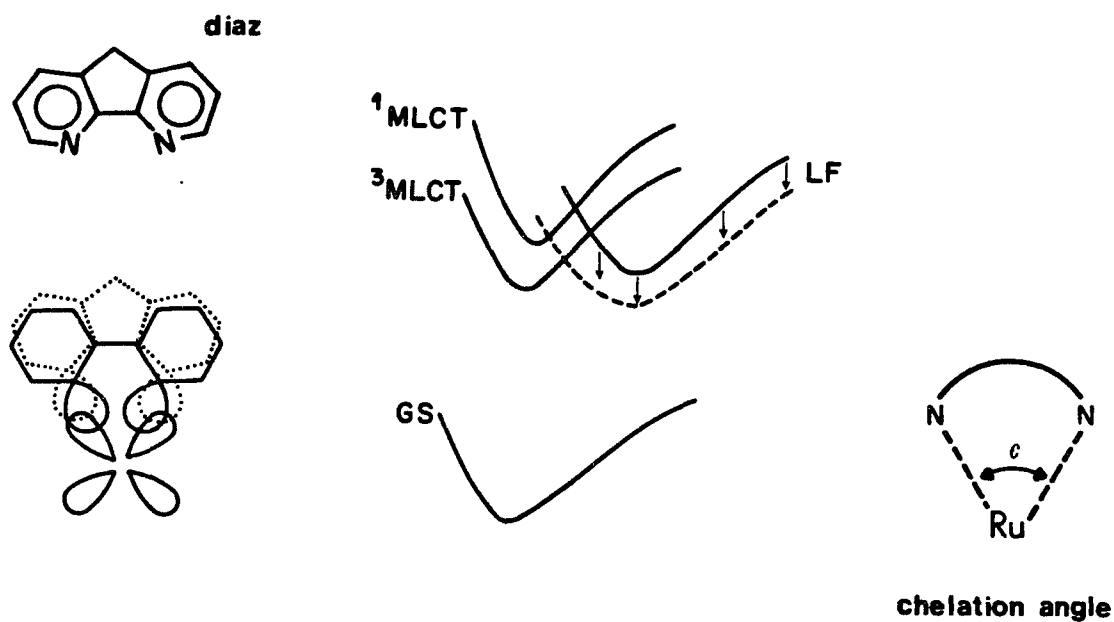


Figure 9. Model of the photosubstitution of polypyridine ruthenium (II) complexes. The $^3\text{MLCT}$ is formed with unit efficiency upon excitation.



- CH_2 bridge distorts $\text{N}\sigma\text{-Md}$ overlap
- little change in π system

Result: diaz lowers LF energy but no change in MLCT or IL energy

Figure 10. Perturbation of the energy of LF state due to 4,5 - diazafluorene in a complex of the type $[\text{Ru}(\text{bipy})_2\text{L}]^{+2}$.

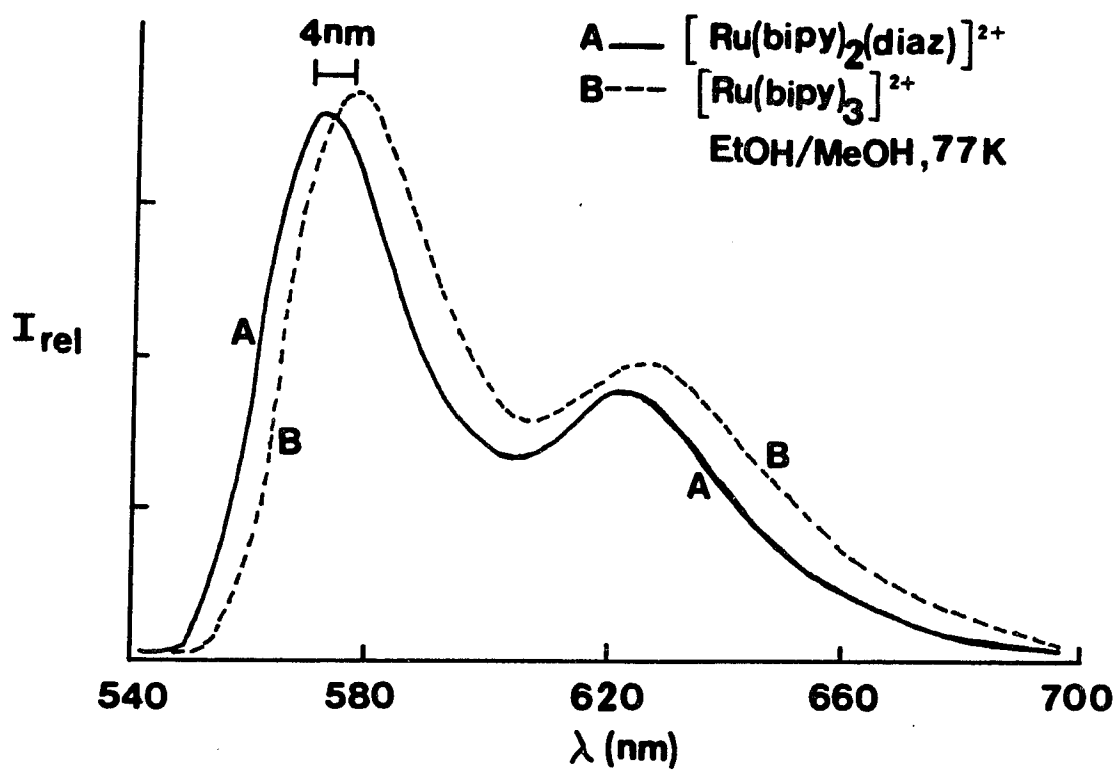


Figure 11. Emission spectra of complexes A and B.

B. AIMS AND SCOPE OF THIS RESEARCH.

Elucidation of the comprehensive photochemistry of polypyridine ruthenium(II) complexes was the general goal of the investigation reported herein. In contrast to the extensive photophysical studies of polypyridine ruthenium(II) complexes, there have been relatively few investigations of the photochemistry of these complexes. As a result, large gaps in the understanding of these processes exist. While two intermediates, a ligand field (LF) excited state and a pentacoordinated intermediate (I), are postulated to be associated with the observed photosubstitution reactions of different polypyridine ruthenium(II) complexes, they have not been directly observed. Little is known about the kinetics of the processes that originate from the LF excited state or the pentacoordinate intermediate. Some pertinent questions that should be addressed are :

a) Are the $^3\text{MLCT}$ and LF excited states in thermal equilibrium, or is there some undeniable experimental evidence that suggests that the photophysical processes follow well defined paths?

b) If the thermal equilibrium between those two excited states cannot be ruled out, what are the kinetic parameters for both the forward and the reverse reactions ?

c) What are the decay processes available to the LF excited state and what are their associated kinetic parameters ?

d) What are the kinetic parameters associated with a possible pentacoordinated intermediate and the process of chelate ring reformation ?

e) How do these parameters depend upon the size and aromaticity of the chelate ring that is assumed to be involved in the photosubstitution process?

f) Is the photosubstitution quantum yield dictated primarily by the dynamics of the LF or by that of the pentacoordinated intermediate ? Obtaining definitive answers to all these questions would be a very ambitious, long - range goal.

The real goals of this research are, in comparison to the general goal, much more modest. In order to gain further insight into the photophysical and photochemical processes of polypyridine ruthenium(II) complexes, and to collect new data to be

used in future complementary studies, reinvestigation of the photophysical and photochemical behavior of some systems was carried out. The behavior of these systems had been reported to be different from that predicted by consideration of the generally accepted models that are used to rationalize photophysical processes of polypyridine ruthenium(II) complexes. This reinvestigation was an important step that could not be overlooked, because any understanding of the observed photochemical behavior depends primarily on a correct understanding of the photophysics.

Thus, in the present work the quenchings of both the luminescent lifetimes, and the photosubstitution reactions of $[\text{Ru}(\text{bipy})_3]^{+2}$ under different conditions were studied in order to determine the relationship between the $^3\text{MLCT}$ and LF excited states, the populations of which are generally assumed to be thermally equilibrated. In addition, the temperature dependence of the emission intensities and luminescent lifetimes of the complexes $[\text{Ru}(\text{bipy})_3]^{+2}$, $[\text{Ru}(\text{bipy})_2(\text{py})_2]^{+2}$, and $[\text{Ru}(\text{bipy})_2(\text{diaz})]^{+2}$ were evaluated. The goal of the temperature dependence studies was to determine the values of ΔE between the $^3\text{MLCT}$ and LF excited

states. It was hoped that the ΔE values could be rationalized by use of the ideas associated with ligand field theory.

A qualitative determination of the effect of solvents, with different dielectric constants, and which therefore support distinct degrees of ion - pairing association, on the observed quantum yields was judged to be necessary. Thus, photosubstitution quantum yields of the complex $[\text{Ru}(\text{bipy})_2(\text{py})_2]^{+2}$ in different dioxane - water mixtures were determined.

Several new polypyridine ligands that have two pyridine rings linked by methylene bridges of different lengths were synthesized, and the corresponding $[\text{Ru}(\text{bipy})_2\text{L}]^{+2}$ complexes were prepared. The photophysical and photochemical properties of these complexes were then examined. Investigation of the photoextrusion processes should provide valuable information about the dynamics of reclosure of the chelating ring. The photosubstitution quantum yield is determined by the competition between the reclosure of the pentacoordinate intermediate and an effective process of chelation of a new entering ligand.

As the ring size increases, the efficiency of ring reclosure is predicted to decrease and the

behavior of the pentacoordinated intermediate is expected to converge to that of the complex $[\text{Ru}(\text{bipy})_2(\text{py})_2]^{+2}$. This study should permit the semiquantitative evaluation of the importance of ring closure in the observed photochemical behavior of polypyridine ruthenium(II) complexes in different solvents.

Complexes of the type, $[\text{Ru}(\text{bipy})_2\text{L}]^{+2}$ were prepared in which L represents ligands that have two amine groups linked by methylene bridges of different lengths. Again, the photophysical and photochemical properties of the complexes in different solvents were examined. Although different ring sizes are again involved in the photosubstitution processes, a new effect can be expected because in this last series, aromatic rings are not involved and interaction with the ruthenium is very different. Therefore, it should be possible to study the effect that this kind of ligand replacement has in the polypyridine ruthenium(II) complexes, and to infer the alteration of the photosubstitution processes when the properties of the excited states are modified in this way.

The catalytic effect of Ag^+ on the

photosubstitution quantum yield of the complex $[\text{Ru}(\text{bipy})_2(\text{en})]^{+2}$ was also studied. Additionally, the temperature dependence of the photosubstitution quantum yields of the complexes $[\text{Ru}(\text{bipy})_2(\text{en})]^{+2}$ and $[\text{Ru}(\text{bipy})_2(\text{tn})]^{+2}$ was investigated.

CHAPTER II. EXPERIMENTAL

A. MATERIALS.

Unless noted, reagent grade chemicals were not subjected to further purification. The preparations of the reagents employed in this work or their sources are summarized below.

1. Solvents.

Acetic acid, acetone, acetonitrile, benzene, chloroform, cyclohexane, dichloromethane, diethylether, dimethylformamide, dimethylsulfoxide, ethanol, ethylacetate, methanol, and para - dioxane were purified by standard procedures⁵³ and were stored under N₂ in amber bottles.

Water was distilled three times from alkaline potassium permanganate in an all - glass apparatus.

2. Inorganic Reagents.

Tetra - N - butylammonium chloride and tetra - N butylammonium perchlorate were purchased from

Aldrich, purified by crystallization from ethanol, and dried in vacuum at ambient temperature.

Potassium persulfate, lithium chloride, and potassium permanganate (reagent grade) were purchased from J. T. Baker Chemical Co. and were not further purified.

Silver nitrate and potassium carbonate (anhydrous) were purchased from Mallinckrodt Chemical Works and were not further purified.

Tetra - N - butylammonium bromide, tetra - ethylammonium chloride, ammonium hexafluorophosphate, and phosphorous pentoxide were all purchased from Aldrich Chemical Co. (reagent grade) and were not further purified.

Tris - 2,2' bipyridyl ruthenium (II) dichloride hexahydrate was obtained from G. Frederick Smith Inc. and recrystallized from acetone/water. Absorption spectroscopy : in H_2O , (298 K), λ_{max} , nm (E_o) 451 (14,500), 343 (6,400), 285 (86,000); literature values 452 (14,600), 345 (6,400), 285 (87,000)⁵⁴. Corrected emission spectrum : in H_2O , (298 K), λ_{max} , nm, 627; literature value 628⁵⁵. In EtOH / MeOH glass (4:1, v/v), (77 K), 581, 628 ; literature values 584, and 630 ⁵⁵.

Cis - dichloro bis - 2,2'bipyridyl
ruthenium(II) dihydrate : was synthesized by means of
 the procedure of Sullivan, Salmon , and Meyer⁵⁶.
 Based on starting ruthenium a yield of 60% was
 obtained. The same compound had been previously
 prepared in accord with the method of Sprintschnik,
 Sprintschnik, Kirsch and Whitten⁵⁷ and lower yields
 were obtained. Absorption spectroscopy : in CH₂Cl₂,
 (298 K), λ_{max} , nm (E₀), 554 (9,300), 381 (9,300)
 ; literature values 556 (9,400), 380 (9,400) ⁵⁴.

3. Organic Reagents.

4 - picoline was purchased from Eastman
 Organic Chemicals and was not further purified.

Azafluorene, ethylenediamine, 1, 3 -
 diaminopropane, hydrazine hydrate (85%), 1,1 dimethyl
 4,4'bipyridiniumdichloride , di (2 - pyridyl)ketone,
 and 2 - pyridine carboxaldehyde were all reagent grade
 chemicals, obtained from Aldrich, and were not further
 purified.

Acetic anhydride (Aldrich) was purified by
 fractional distillation, b.p., 138 - 141 °C ; literature
 b.p. 139 °C ⁵⁸.

Pyridine was purchased from Baker and was distilled prior to use⁵⁸, b.p., 115 - 118 °C ; literature b.p. 115.3 °C ⁵³.

2,2' bipyridine was purchased from Aldrich and was recrystallized from ethylacetate. Absorption spectroscopy : in 50 % H₂SO₄, (298 K), λ_{max} , nm (E₀) 288 (15,800) ; literature value 289 (16,100)⁵⁷. In 0.1 M NaOH , (298 K), λ_{max} , nm (E₀) 279 (12,500) ; literature value 280 (12,900)⁵⁷.

1, 2, 4, 5 - tetracyanobenzene (TCNB) was obtained from Eastman Organic Chemicals and was recrystallized from ethanol⁶⁰, m.p., 257 - 259 °C ; literature m. p. 258 °C ⁶¹.

Anthracene was also purchased from Eastman and purified by recrystallization⁵⁸, m.p., 213 - 215 °C ; literature m.p. 214 °C ⁵⁸.

Ferrocene (reagent grade) was purchased from Baker and twice sublimed ⁵⁸. Absorption spectroscopy : in EtOH, (298 K), λ_{max} , nm (E₀) 230 (sh, 4,550), 261 (sh, 2,200), 323 (60), 442 (100), 530 (sh, 8) ; literature values 230 (sh, 4,600), 260 (sh, 2,190), 324

(54.8), 440 (95.7), 528 (sh, 7.5)⁶².

Di(2 - pyridyl) methane⁶³ : was prepared by a Wolff - Kishner reduction of di - pyridyl ketone with hydrazine and base in a steel bomb at 150 °C ⁶⁴ ; colorless oil. the nature of the product was satisfactorily confirmed by ¹ H NMR in CDCl₃ ⁶³.
 Anal. Calcd for C₁₁H₁₀N₂ : C, 77,62% ; H, 5.92% ; N,16.46%. Found : C,77.51% ; H,6.03% ; N,16.28%.

Di(2 - pyridyl)ethene⁶⁵ : A mixture of 2 - pyridine carboxaldehyde (50 g), redistilled pyridine (150 ml), and acetic anhydride (60 ml) was refluxed for four hours. The volatile unreacted starting materials were removed in vacuo and the residue was vacuum distilled; the crude olefin was obtained. Recrystallization from benzene - cyclohexane gave the colorless, crystalline olefin : m.p. 117 - 119 °C ; lit. m.p. 118 - 119 °C ⁶⁵.

Di(2 - pyridyl)ethane⁶³ : was prepared by the hydrogenation of the corresponding ethene⁶⁵ in absolute ethanol at 25 °C over 5 % Pd/C catalyst : colorless oil. The nature of the product was satisfactorily confirmed by ¹H NMR in CDCl₃ ⁶³.

Anal. Calcd for $C_{12}H_{12}N_2$: C, 78.23 % ; H, 6.56 %
; N, 15.20 %. Found C, 78.10 %; H, 6.73 %; N, 15.01 %.

4,5 diazafluorene : was prepared by L. J. Henderson Jr. of this laboratory⁴⁷ via a modification of the method of Kloc and al.⁴⁴ : m.p., 171 - 173 °C ; lit. m.p. 172 °C ⁴⁴. The nature of the product was satisfactorily confirmed by ¹H NMR in CD₃CN ⁴⁷.

B. PREPARATION OF COMPLEXES.

1. 4,5 - Diazafluorenyl - bis - 2,2'bipyridyl ruthenium(II) hexafluorophosphate⁴⁷: was prepared by L. J. Henderson Jr. of this laboratory. Cis - dichlorobis - 2,2'bipyridyl ruthenium(II) dihydrate (0.5 g) and 4,5 - diazafluorene (0.2 g) were refluxed in 30 ml of ethanol for 4 hours. The hot solution was filtered and ammonium hexafluorophosphate (2 g) was added. Upon standing overnight, crystals of $[\text{Ru}(\text{bipy})_2(\text{diaz})][\text{PF}_6]_2$ precipitated. These crystals were twice recrystallized from acetone - water and twice from ethanol - water. Yield : 12%. The nature of the product was satisfactorily confirmed by ^1H NMR in CD_3CN . Anal. Calcd. for $\text{C}_{31}\text{H}_{24}\text{N}_6\text{P}_2\text{F}_{12}\text{Ru}$:
C, 42.39 % ; H, 2.78 % ; N, 9.64 % . Found : C, 43.09 % ;
H, 2.89 % ; N, 9.59 %.

2. cis - Bispyridyl bis - 2,2'bipyridyl ruthenium(II) hexafluorophosphate tetrahydrate⁴⁸:
Pyridine (0.2 ml) was added to a solution of $[\text{Ru}(\text{bipy})_2\text{Cl}_2] \cdot 2\text{H}_2\text{O}$ (0.25 g) in methanol (10 ml) and water (10 ml). The mixture was refluxed for 2

hours. The bright orange hot solution was filtered, and ammonium hexafluorophosphate was added. Upon standing overnight, crystals of $[\text{Ru}(\text{bipy})_2(\text{py})_2][(\text{PF}_6)_2]$ formed. This product was recrystallized from water - acetone mixtures three times. Next, the product was further purified by column chromatography (Sephadex LH - 20 - 100, Lipophilic, MeOH eluent). Yield : 22 %. Absorption spectroscopy : in CH_2Cl_2 , (298 K), λ_{max} , nm (E_o) 462 (9,150) ; literature value 460 (9,200)^{51,54}. In CH_3CN , (298 K), λ_{max} , nm (E_o), 457 (8,400), 337 (15,100), 287 (48,500), 240 (23,000) ; literature values 455 (8,200), 338 (15,900), 289 (50,000), 243 (24,000)⁶⁷. The absorption located at 473 nm (8,600) for trans - $[\text{Ru}(\text{bipy})_2(\text{py})_2]^{+2}$ was absent⁶⁸.

3. Tris - 2,2'-bipyridyl ruthenium(II) dibromide dihydrate: This complex was obtained from the available chloride complex by ion exchange (Dowex 1-X8, 50 -100 Mesh). The collected product was twice passed through fresh exchange resin columns, the solvent was evaporated, and the final orange compound was dried in vacuo at ambient temperature. Yield : 9%. Absorption spectroscopy : in CH_2Cl_2 , (298 K), λ_{max} , nm (E_o) 450 (13,300), 347 (8,560), 285 (79,000). In DMF,

(298 K), λ_{max} , nm (E_o), 453 (14,100) ; literature values 454 (14,600)⁶⁷.

4. Ethylenediamine bis - 2,2' bipyridyl
ruthenium(II) hexafluorophosphate dihydrate⁶⁸:

[Ru(bipy)₂Cl₂]. 2H₂O (0.50 g) was suspended in a 1:1 (by volume) water - methanol solution (20 ml) of the ligand ethylenediamine (3 g). The mixture was heated and refluxed for 2 hours. The condenser was removed and the methanol was evaporated under a stream of nitrogen. Next ammonium hexafluorophosphate (3 g) was added. The crystals which formed were collected by suction filtration and dried. The deep red - brown crystals were thrice recrystallized from water. Yield : 31 % . A modification of this procedure for the preparation of [Ru(bipy)₂(en)][ClO₄]₂ reports a yield of 70 % ⁷⁰. Absorption spectroscopy : in CH₃CN, (298 K), λ_{max} , nm (E_o) 487 (9,800), 343 (7,650), 295 (58,600), 242 (20,100) ; literature values 485 (9,900), 344 (7,600), 291 (60,000), 243 (21,000)⁷⁰. Corrected emission spectrum : in EtOH / MeOH glass (4:1, v/v), (77 K), λ_{em} 668 ; literature value 660 ⁷¹.

5. 1,3 - propylenediamine bis - 2,2' bipyridyl

ruthenium(II) hexafluorophosphate dihydrate: This complex was prepared by means of the method described above. In this case, the mixture of 1,3 - diaminopropane (3 g) and $[\text{Ru}(\text{bipy})_2\text{Cl}_2] \cdot 2\text{H}_2\text{O}$ (0.5 g) in the 1:1 (by volume) water - methanol solution (20 ml) was refluxed for 24 hours, the solvent was evaporated, and the dark solid was recrystallized three times from acetone - water. Yield : 14 % . Absorption spectroscopy : in CH_3CN , (298 K), λ_{max} , nm (ϵ) 490 (8,910), 350 (6,700), 293 (53,000), 245 (18,100) ; literature values 492 (8,500), 348 (6,600), 292 (52,000), 244 (18,000)⁷⁰. Corrected emission spectrum in EtOH / MeOH glass (4:1, v/v), (77 K), λ_{em} 675.

6. bis 4 - picoline bis - 2,2'-bipyridyl
ruthenium(II) hexafluorophosphate dihydrate: 4 - Picoline (0.5 ml) was mixed with $[\text{Ru}(\text{bipy})_2\text{Cl}_2] \cdot 2\text{H}_2\text{O}$ (0.50 g) in a 1:1 water - methanol solution (20 ml). This mixture was refluxed for 4 hours. After filtration, ammonium hexafluorophosphate was added. Upon standing overnight crystals of $[\text{Ru}(\text{bipy})_2(\text{pic})_2][(\text{PF}_6)_2]$ formed. This product was recrystallized from water - acetone mixtures and then was further purified by column chromatography, in

which Sephadex LH - 20 - 100, and MeOH as eluent were used. Yield : 17 % . Anal. Calcd for

$C_{32}H_{34}N_6O_2P_2F_{12}Ru$: C, 41.52 % ; H, 3.70 %;

N, 9.08 %. Found : C, 40.9 % ; H, 3.6 % ; N, 10.4 %.

7. 1, 2 - di(2 - pyridyl) ethane bis - 2,2'bipyridyl ruthenium(II) hexafluorophosphate

hexahydrate : This compound was prepared from a solution of cis - dichlorobis - 2,2'bipyridyl ruthenium(II) dihydrate (0.5 g) in a 1:1 (by volume) water - methanol mixture (20 ml) and dipyridylethane (1 g, 10 % excess) by the general procedure given above; the mixture was refluxed for 2 hours. Yield : 37 %.

Anal. Calcd for $C_{32}H_{42}N_6O_6P_2F_{12}Ru$: C, 38.52

% ; H, 4.21 % ; N, 8.43 %. Found: C, 37.62 % ; H, 3.89% ;

N, 8.97 % .

8. di(2 - pyridyl) methane bis - 2,2'bipyridyl ruthenium(II) hexafluorophosphate hexahydrate: A freshly

prepared solution of cis - dichlorobis - 2,2'bipyridyl ruthenium (II) dihydrate (0.5 g) in 1:1 (by volume) water - methanol mixture (20 ml) was reacted with the ligand dipyridylmethane (1 g, 10% excess) by means of the general procedure given above. In this case it was necessary to reflux the mixture for three days. Anal.

Calcd. for $C_{31}H_{40}N_6O_6P_2F_{12}Ru$: C, 37.84 %
 ;H, 4.07 % ;N, 8.54 %. Found : C, 38.61 % ; H, 4.22 % ;N,
 8.87 %.

9. Aquo 4 - picoline bis(2,2'bipyridyl)
ruthenium(II) hexafluorophosphate dihydrate
 : $[Ru(bipy)_2(pic)_2]^{+2}$ (0.5 g) in water (20 ml) was
 heated on a water - bath for 1 hour. The solution
 gradually became brown. On adding ammonium
 hexafluorophosphate, dark brown crystals of the
 product deposited. These were recrystallized from
 ethanol/ether mixture, and air dried. Anal. Calcd for
 $C_{26}H_{29}N_5O_3P_2F_{12}Ru$: C, 36.70 % ;H, 3.40 %;
 N, 8.20 %. Found : C, 37.13 % ;H, 2.91% ;N 8.42 %.

10. Chloro 4 - picoline bis(2,2'bipyridyl)
ruthenium(II) hexafluorophosphate dihydrate :
 $[Ru(bipy)_2(pic)_2]^{+2}$ (0.2 g) in water (10 ml) was
 heated under reflux for 15 min in the presence of excess
 LiCl. The product crystallized after ammonium
 hexafluorophosphate was added and the solution was
 cooled. It was washed with cold water and
 recrystallized from ethanol/ether. Anal. Calcd for
 $C_{26}H_{27}N_5O_2P_2F_{12}ClRu$: C, 36.01 % ;H, 3.12 %;
 N, 8.08 %. Found : C, 35.6 % ;H, 3.17 % ;N 8.12 %.

A schematic representation of the prepared complexes is given in Figures 12 and 13 .

Note : Complexes of the type $[M(bipy)_2L_2]^{+2}$, both for Ru and for other metals, have been widely accepted to exist only in the cis geometry. This notion has been rationalized by considering the severe steric crowding which exists between the hydrogen atoms at the positions in the bipyridine rings when the geometry is trans¹³⁹. Krause reported⁴⁰ the synthesis of trans - $[Ru(bipy)_2(py)_2]^{+2}$ and a series of related complexes. However, the proposed trans - structures have not been confirmed crystallographically and the spectral evidence has not been considered convincing¹³⁴. Meyer and co - workers reported a novel and surprising result in the photochemistry of cis - $[Ru(bipy)_2(H_2O)_2]^{+2}$ in acidic aqueous solutions: a cis \rightleftharpoons trans photoisomerization was observed and the trans stereochemistry was confirmed by X - ray crystallography¹³⁶.

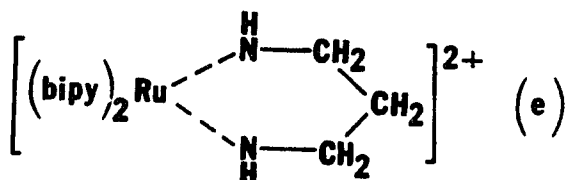
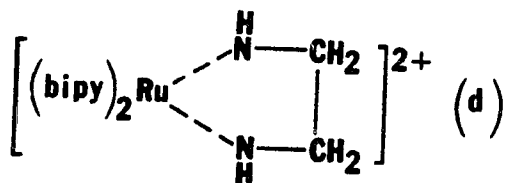
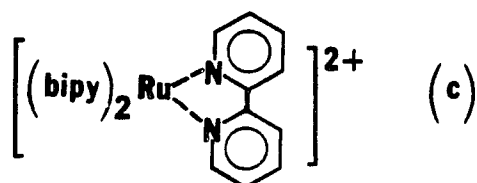
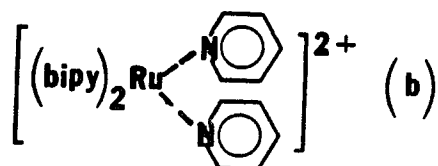
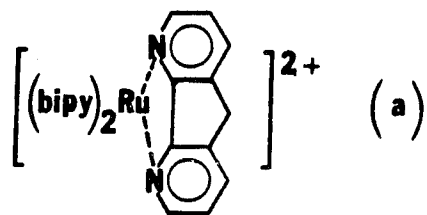


Figure 12. Schematic representation of complexes (a) $[\text{Ru}(\text{bipy})_2(\text{diaz})]^{2+}$, (b) $[\text{Ru}(\text{bipy})_2(\text{py})_2]^{2+}$, (c) $[\text{Ru}(\text{bipy})_3]^{2+}$, (d) $[\text{Ru}(\text{bipy})_2(\text{en})]^{2+}$, (e) $[\text{Ru}(\text{bipy})_2(\text{tn})]^{2+}$.

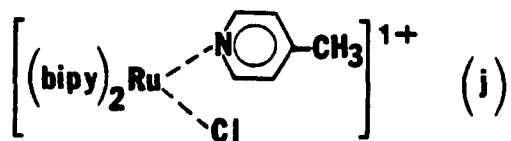
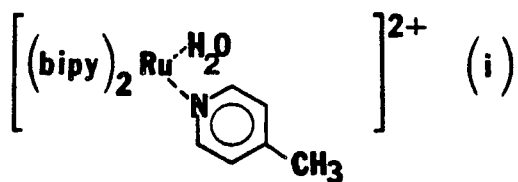
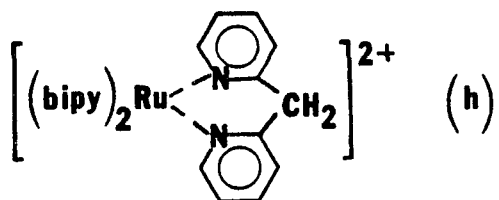
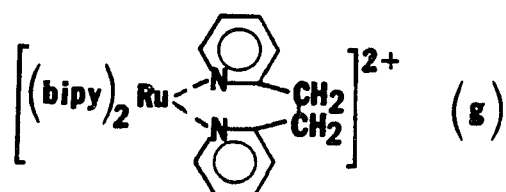
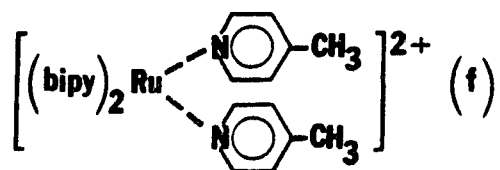


Figure 13. Schematic representation of complexes (f) $[\text{Ru}(\text{bipy})_2(\text{pic})_2]^{+2}$, (g) $[\text{Ru}(\text{bipy})_2\text{DPE}]^{+2}$, (h) $[\text{Ru}(\text{bipy})_2\text{DPM}]^{+2}$, (i) $[\text{Ru}(\text{bipy})_2(\text{pic})(\text{H}_2\text{O})]^{+2}$, (j) $[\text{Ru}(\text{bipy})_2(\text{pic})(\text{Cl})]^{+1}$.

C. EXPERIMENTAL PROCEDURES, TECHNIQUES, AND PHYSICAL MEASUREMENTS.

Melting points were determined by means of a Mel - Temp melting point apparatus and were uncorrected.

Carbon, hydrogen, and nitrogen analyses were carried out by either Galbraith Laboratories, Knoxville, Tennessee or by Micro - Anal Co., Tucson, Arizona.

The ^1H NMR spectra were recorded by means of either a Bruker WP 200 or a Varian Associates 60 A spectrometer, operating at 300 K. Spectra of the compounds dissolved in either deuterated acetonitrile - d_3 , or deuterated chloroform - d_1 , were obtained; the choice of solvent depended on solubility considerations. Tetramethylsilane was used as the internal standard.

Ultraviolet - visible absorption spectra were recorded by means of a Cary Model 14 Spectrophotometer. Molar absorption coefficients were obtained from absorbance measurements of at least three solutions of

different concentrations. Coleman matched quartz 1.00 cm cells were used.

When photosubstitution reactions were spectrally monitored at various temperatures, a locally constructed cell holder - in which the sample could be stirred, the temperature could be controlled, and right angle irradiation was possible - was used. The sample temperature was maintained to ± 0.5 by circulating a water/ethylene glycol mixture through the cell holder. A copper/constantan thermocouple was used for temperature determinations; ice/water was the reference. An Omega Digital Temperature Controller, Model 4002, was used for temperature monitoring.

The modified Cary 14 was used to monitor all the photolysis experiments; the modification permitted excitation at right angles to the absorption beam. Usually, solutions containing ruthenium(II) complexes with or without quencher were excited at or close to the absorption maximum of the complex. The absorption spectra of the solutions containing the complex and various amounts of quenchers were equal, within experimental error, to the combined spectra of the complex and quencher.

Typically, samples (3.0 ml) of the solvent, having the desired concentration of salt, were degassed by Ar bubbling (20 min) while the cuvette was kept in a bath of ice/water in order to minimize losses of solvent by evaporation. Just prior to the experiment, the complex under study (concentrated stock solution in convenient solvent) was added by means of a microsyringe. Similarly, when the effect of different quenchers on the efficiency of photosubstitution was studied, the desired amounts of quencher were added. Care was exercised in order to prevent the introduction of oxygen and to maintain the sample in the dark as much as possible.

When the quenching of emission and photosubstitution by oxygen were studied, the solvents used in the preparation of the samples were degassed by means of several freeze/pump/thaw cycles and then were equilibrated at the desired O_2 pressure. After equilibration for at least 1 hour, the solvent was drained into a cuvette that contained the appropriate amount of solid complex (the proper volume of the stock solution of the complex was previously discharged from a microsyringe and the solvent was evaporated by exposure to a stream of Ar). The sample was then

sealed. After sealing, the emission intensity and lifetime were evaluated ; finally, the photosubstitution quantum yield was determined.

The excitation source for the photolysis experiments was a 150 W Xe/Hg lamp from Shoeffel Instruments Corp. and the desired band was isolated by means of Corning glass filters. In some cases, an interference filter ($\lambda = 436$ nm) was used.

Determinations of light intensity were performed by potassium ferrioxalate actinometry; the method of Hatchard and Parker⁷² was followed. Standard mixtures of the aqueous actinometric solution ($[K_3Fe(C_2O_4)_3]$), buffer (sodium acetate and sulfuric acid), and 0.2 % by weight 1,10 phenanthroline in water were prepared⁷³. The actinometric determinations were made by pipetting 3.0 ml of the actinometer solution in the cuvettes used for photolysis studies. Then, under the experimental conditions identical with those of the photolysis, each cuvette was irradiated for an appropriate period of time. Next, 1.0 ml of each of the irradiated solutions was put into separate 10.0 ml volumetric flasks, to which were then added 2.0 ml of 0.2 % phenanthroline

solution and 0.5 ml of buffer, and the solution was diluted to the mark with water. Additionally, the same method was used to study a reference solution prepared with 1.0 ml of non - irradiated actinometric solution. Finally, the absorptions of the irradiated solutions were taken at 510 nm when the reference solution was in the reference light beam. All these manipulations were performed in the dark. The appropriate irradiation period was experimentally determined in order to give an absorption of about 0.30. The average of the three independent determinations was used to calculate the light intensity. Light intensity determinations were made from time to time for each set of experimental conditions in order to check for possible changes in lamp performance.

Quantum yields of photosubstitution reactions were determined with the aid of a computer program designed to analyze the decrease in absorption of the starting complex. Necessary input data were the respective molar absorption coefficients of the initial complex and the photoproduct at both monitoring and excitation wavelengths, the light intensity, and the volume of the sample.

In all cases , corrections for dark reactions proved to be unnecessary. Nevertheless, corrections due to small absorptions of some of the quenchers in the region of interest, were made.

The emission spectra were recorded by means of an SLM 4800 spectrophotofluorimeter and were properly corrected for the response of the Hamamatsu R928 photomultiplier tube. Additional emission spectra were recorded by means of an SLM 8000 Photon - Counting spectrofluorimeter; again, correction factors for the Thorn EMI Gencom Inc., WCT S - 1016 photomultiplier tube were used to correct the recorded spectra. In both cases MC320 monochromators for excitation and emission were used. A 450 Watt Xenon arc lamp was the excitation source. The spectra were integrated in wavenumbers.

All recorded spectra were obtained with Glan - Thompson polarizers set for horizontally polarized excitation and vertically polarized emission. This was necessary in order to avoid an artifact of the grating spectrometers at 605 nm.

Low temperature (77 K) emission spectra were recorded for each sample in a 6 mm i. d. pyrex tube

after several freeze/pump/thaw degassing cycles. The solution was then immersed in a Dewar containing liquid nitrogen. During recording of the spectrum a dry atmosphere of N_2 was maintained in the sample chamber in order to avoid condensation of moisture on cell windows.

The emission spectra of the compounds in degassed solvents at higher temperatures (120 - 273 K) were recorded; at least five freeze/pump/thaw cycles were used. The variable temperatures were maintained by flowing precooled nitrogen gas through the sample holder; the sample temperature was determined by means of a copper/constantan thermocouple; a bath of ice/water was used as a reference. Readings of potentials were made with a Millivolt Potentiometer, Leeds & Northrup Co. Cat. Num. 8690. Conversion to temperatures was accomplished by use of standard tables⁷⁴. These results were compared with similar determinations made by using data taken from National Bureau of Standards, Circular 561⁷⁵. No significant deviation was detected.

All relative quantum yields obtained in this work were converted into absolute quantum yields by

using $[\text{Ru}(\text{bipy})_3]^{+2}$ as the standard. The following standard procedure⁷⁶ was used. Dilute solutions of the standard luminescent complex and of the complex under study that had the same optical density at the excitation wavelength were prepared. Next, the apparent emission spectra of both solutions were determined under identical experimental conditions. The spectra were corrected for solvent background and for photomultiplier response, and were then integrated. The luminescence quantum efficiency of the studied complex, Q_x , was then evaluated by means of the simplified expression : $Q_x = Q_s (I_x/I_s)$, where both I_x and I_s refer to the respective area under the emission curves of the corrected spectra of the sample and standard, respectively, and Q_s is the emission quantum yield of $[\text{Ru}(\text{bipy})_3]^{+2}$ under the experimental conditions. Corrections to the luminescence related to the average refractive indexes of the solutions were disregarded⁷⁷.

Due to the large variations of emission intensity of some of the complexes relative to the intense emission of $[\text{Ru}(\text{bipy})_3]^{+2}$, it was necessary to calibrate the response of emission intensity to changes in the monochromater slit widths. The following

procedure was done at 77 K and 298 K. Conditions of the spectrometer were adjusted in order to yield a reasonable emission intensity for a standard sample of $[\text{Ru}(\text{bipy})_3]^{+2}$ in EtOH/MeOH (4:1, v/v) solvent, when the emission monochromator was adjusted to have the slitwidth at the maximum setting. The intensity was then monitored while the emission slitwidth was decreased. The slitwidth of the excitation monochromator was kept at the original setting. In this manner, the effect of slitwidth upon emission intensity could be calibrated and the results are shown below.

Table I . Calibration curve of the emission intensity at 298 K as a function of the emission bandpass.

emission slitwidth (bandpass in nm)	relative intensity(a)
0.5	.27
1.0(b)	1.00
2.0	3.83
4.0	15.92
8.0	54.88
16.0	169.31

(a) : The areas of the corrected emission

spectra were integrated; wavenumbers were used for the energy axis. With $\lambda_{exc} = 475$, the 530 - 830 nm range was scanned. Reported tabulated values represent an average of three independent determinations.

(b) : Taken as the reference.

Table II . Calibration curve of the emission intensity at 77 K as a function of the emission bandpass.

emission slitwidth (bandpass in nm)	relative intensity(a)
0.5	0.26
1.0(b)	1.00
2.0	3.47
4.0	14.00
8.0	37.63
16.0	102.42

(a) : Same conditions as those of (a) in the previous Table I.

(b) : Chosen as the reference.

These values vary somewhat from the theoretical squared dependence^{7e}. It could be

observed that the deviations from this expected dependence were systematically more significant in the extent that the emission slitwidth was adjusted at the larger settings.

For samples that were extremely weak emitters, the slitwidth was increased from that of the standard and the above factors were used to correct for this increase.

The procedure for ambient temperature quenching studies typically included the degassing of the sample by means of Ar bubbling (20 min), measuring the emission spectrum in the absence of quencher, and further recording the emission spectra after sequential addition of quencher from a microsyringe. Care was taken to avoid introduction of oxygen.

Excited - state lifetimes were determined by the single - photon counting method⁷⁹. Due to the long lifetimes, no correction for the lamp pulse (~ 3 ns width) was deemed necessary. A locally - constructed apparatus was used. The data were collected on 256 channels of a multichannel analyzer. Given the time/channel, a linear least squares computer program

was used to fit the first - order luminiscence decay curves⁸⁰.

Electrochemical measurements for some of the complexes were made by R. H. Schmehl of Tulane University. Redox potentials for some of the complexes in acetonitrile containing 0.10 M tetrabutylammonium perchlorate as supporting electrolyte were measured by means of cyclic voltammetry. The apparatus consists of a E66/ Princeton Applied Research model 173 potentiostat and a model 175 Universal programmer. The reference electrode for all measurements was the calomel electrode; a saturated aqueous sodium chloride salt bridge was used. Reported potentials are not corrected for the liquid junction potential.

CHAPTER III. EXPERIMENTAL RESULTS.

A. QUENCHING OF $[\text{Ru}(\text{bipy})_3]\text{X}_2$ ($\text{X} = \text{Cl}^-, \text{Br}^-$) EMISSION AND PHOTOSUBSTITUTION BY FERROCENE AND OXYGEN.

Reported results⁴⁶ were in clear disagreement with the postulated model describing the photophysical processes of $[\text{Ru}(\text{bipy})_3]^{+2}$. In order to determine whether emission and photosubstitution occurred from excited states that were thermally equilibrated, their quenching by ferrocene and O_2 were investigated. The general procedures described in the experimental section were followed; specific conditions are indicated.

1. Quenching of $[\text{Ru}(\text{bipy})_3]\text{Cl}_2$ at 298 K
in a 0.10 M solution of TBACl in DMF by Ferrocene.

General experimental conditions :

$[\text{Ru}(\text{bipy})_3]\text{Cl}_2 \cong 3 \cdot 10^{-5} \text{ M}$.

Light intensity = $1.53 \cdot 10^{-9}$ einstein/sec .

Total irradiation time = 20 min .

Molar absorption coefficient (450 nm) of the
starting complex = $15,000 \text{ M}^{-1}\text{cm}^{-1}$.

Molar absorption coefficient (450 nm) of the photoproduct = $7,700 \text{ M}^{-1}\text{cm}^{-1}$. (a)

(a): In this experiment only the photoreaction leading to the first photoproduct was followed.

Table III . Quenching of the emission lifetime and of the photosubstitution : $[\text{Ru}(\text{bipy})_3]\text{Cl}_2$ at 298 K in a 0.10 M solution of TBACl in DMF by Ferrocene.

$[\text{Ferrocene}] \cdot 10^{+5}, \text{M}$	$(T_{oe}/T_e)(a)$	$(Q_{pho}/Q_{ph})(b)$
0.00	1.00	1.00
12.4	1.38	1.22
24.8	1.76	1.44
37.2	2.14	1.66
49.6	2.52	1.88
62.0	2.90	2.10

slopes(M^{-1}) (c) $3,070 \pm 600$ $1,780 \pm 700$

(a): T_{oe}/T_e is the quenching of the emission lifetime.

(b): Q_{pho}/Q_{ph} is the quenching of the photosubstitution.

(c): The slopes were evaluated by means of linear regression analysis; they are an average of three independent experiments.

For the determination of photosubstitution quantum yields when ferrocene was the quencher, the measured absorption spectra were corrected for partial absorption of the incident light by ferrocene. ($E_0 = 100 \text{ M}^{-1}\text{cm}^{-1}$ at 450 nm). These corrections became more serious as the ferrocene concentration increased but never amounted to more than 10 % of absorption of the incident light.

2. Quenching of $[\text{Ru}(\text{bipy})_3]\text{Cl}_2$ at 298 K in a 0.10 M solution of TBACl in CH_3CN by Oxygen.

General experimental conditions :

$[\text{Ru}(\text{bipy})_3]\text{Cl}_2 \cong 5 \cdot 10^{-5} \text{ M}$.

Light intensity = $1.53 \cdot 10^{-9}$ einstein/sec.

Total irradiation time = 10 min.

Molar absorption coefficient (450 nm) of the starting complex = $13,600 \text{ M}^{-1}\text{cm}^{-1}$.

Molar absorption coefficient (450 nm) of the photoproduct = $3,800 \text{ M}^{-1}\text{cm}^{-1}$. (a)

(a): In this case, the generation of the second

photoproduct was monitored .

Table IV . Quenching of the emission lifetime and of the photosubstitution : $[\text{Ru}(\text{bipy})_3]\text{Cl}_2$ at 298 K in a 0.10 M solution of TBACl in CH_3CN by Oxygen.

$p\text{O}_2$ (Torr)	$[\text{O}_2], \text{M} \cdot 10^{+3}$ (a)	(T_{oe}/T_e) (b)	(Q_{pho}/Q_{ph}) (c)
0	0.0	1.00	1.00
152	2.0	2.10	2.02
400	5.3	4.80	3.93
593	7.9	5.20	5.03
760	10.0	5.93	5.66
slopes (M^{-1}) (d)		506 ± 40	470 ± 60

(a): O_2 concentrations were evaluated in terms of molarity ; an estimated value of Henry's constant of 1,900 atm/mole fraction²¹ and the approximation $x\text{O}_2 = [n(\text{O}_2) / n(\text{solvent})]$ were used (n represents the number of moles).

(b): Quenching of emission excited lifetimes.

(c): Quenching of photosubstitution.

(d): The slopes were evaluated by means of a linear regression analysis; they are an average of three

independent experiments.

The formation of just one final photoproduct, $[\text{Ru}(\text{bipy})_2\text{X}_2]^{+2}$, was always preferentially monitored except in the case of the photolysis carried out in DMF ; then two photoproducts, $[\text{Ru}(\text{bipy})_2\text{DMFX}]^{+1}$, and $[\text{Ru}(\text{bipy})_2\text{X}_2]$ were assumed⁶⁹.

3. Quenching of $[\text{Ru}(\text{bipy})_3]\text{Br}_2$ at 298 K in a 0.10 M solution of TBABr in DMF by Ferrocene.

General experimental conditions :

$[\text{Ru}(\text{bipy})_3]^{+2} \cong 5 \cdot 10^{-5} \text{ M}$.

Light intensity = $3.6 \cdot 10^{-9}$ einstein/sec .

Total irradiation time = 10 min .

Molar absorption coefficient (450 nm) of the starting complex = $14,100 \text{ M}^{-1}\text{cm}^{-1}$.

Molar absorption coefficient (450 nm) of the the first photoproduct = $7,700 \text{ M}^{-1}\text{cm}^{-1}$.

Molar absorption coefficient (450 nm) of the the second photoproduct) = $3,900 \text{ M}^{-1}\text{cm}^{-1}$.

Table V . Quenching of the emission lifetime and of the photosubstitution : $[\text{Ru}(\text{bipy})_3]\text{Br}_2$ at

298 K in a 0.10 M solution of TBABr in DMF by Ferrocene.

[Ferr].10⁺⁵, M (T_{oe}/T_e) (a) (Q_{pho1}/Q_{ph1}) (b) (Q_{pho2}/Q_{ph2}) (c)

0	1.00	1.00	1.00
12	1.36	1.21	1.18
24	1.37	1.34	1.33
36	1.53	1.53	1.51
48	1.67	1.56	1.53
60	1.72	1.75	1.70
84	2.00	-	-

slopes (M⁻¹) (d) 1,210 ± 200 1,170 ± 300 1,126 ± 200

(a): Quenching of luminescence lifetimes.

(b): Quenching of the first photoproduct substitution.

(c): Quenching of the second photoproduct substitution.

(d): Slopes were evaluated by means of linear regression analysis ; average of three runs.

4. Quenching of [Ru(bipy)₃]Br₂ at 298 K in a 0.10 M solution of TBABr in DMF by Oxygen.

General experimental conditions :

$[\text{Ru}(\text{bipy})_3\text{Br}_2] \cong 6.07 \cdot 10^{-5} \text{ M}$.

Light intensity = $3.6 \cdot 10^{-8}$ einstein/sec .

Total irradiation time = 12 min.

Molar absorption coefficient (450 nm) of the starting complex = $14,100 \text{ M}^{-1}\text{cm}^{-1}$.

Molar absorption coefficient (450 nm) of the first photoproduct = $7,700 \text{ M}^{-1}\text{cm}^{-1}$.

Molar absorption coefficient (450 nm) of the second photoproduct = $3,900 \text{ M}^{-1}\text{cm}^{-1}$.

Table VI . Quenching of the emission lifetime and of the photosubstitution : $[\text{Ru}(\text{bipy})_3]\text{Br}_2$ at 298 K in a 0.10 M solution of TBABr in DMF by Oxygen.

$p\text{O}_2$ (Torr) $[\text{O}_2], \text{M} \cdot 10^{+3} (T_{oe}/T_e)$	(a) (Q_{o1}/Q_1)	(b) (Q_{o2}/Q_2)	(c)
0	0.00	1.00	1.00
252(d)	1.00	1.56	1.22
760(e)	5.2	2.57	2.48
slopes (M^{-1}) (f)	283 ± 22	272 ± 30	289 ± 25

(a), (b), and (c), respectively, have the same meanings as those of the previous table presented above.

(d): Air saturated.

(e): O₂ saturated.

(f): Slopes were evaluated by means of linear regression analysis; they are an average of three independent experiments.

(g): The concentrations of O₂ were estimated with the use of a value for Henry's constant of 2,500 atm/mole fraction²¹ and the approximation $x_{O_2} = [n(O_2)/n(\text{solvent})]$.

5. Quenching of [Ru(bipy)₃]Br₂ at 298 K in a 0.10 M solution of TBABr in CH₂Cl₂ by Ferrocene.

General experimental conditions :

[Ru(bipy)₃]Br₂ \cong 6.0 . 10⁻⁵ M .

Light intensity = 3.9 . 10⁻⁷ einstein/sec .

Total irradiation time = 4 min .

Molar absorption coefficient (450 nm) of the starting material = 13,300 M⁻¹cm⁻¹ .

Molar absorption coefficient (450 nm) of the final photoproduct = 4,000 M⁻¹cm⁻¹.

Table VII. Quenching of the emission lifetime and of the photosubstitution : [Ru(bipy)₃]Br₂ at

298 K in a 0.10 M solution of TBABr in CH_2Cl_2 by Ferrocene.

[Ferr]. 10^{-5} , M	(T_{0e}/T_e) (a)	($Q_{\text{phoz}}/Q_{\text{phz}}$) (b)
0	1.00	1.00
12	1.71	1.61
24	2.27	2.21
36	3.04	2.83
48	3.31	3.43
60	3.95	4.04

slopes (M^{-1}) (c) $4,840 \pm 500$ $5,070 \pm 1,200$

(a): Quenching of luminescence lifetimes.

(b): Quenching of final photosubstitution product.

(c): The slopes are the average of three runs; they were evaluated by means of a linear regression analysis.

6. Quenching of $[\text{Ru}(\text{bipy})_3]\text{Br}_2$ at 298 K in a 0.10 M solution of TBABr in CH_2Cl_2 by Oxygen.

General experimental conditions :

$[\text{Ru}(\text{bipy})_3\text{Br}_2] \cong 5.5 \cdot 10^{-5} \text{ M}$.

Light intensity = $3.6 \cdot 10^{-8} \text{ einstein/sec}$.

Total irradiation time = 8 min .

Molar absorption coefficient (450 nm) of the starting material = $13,300 \text{ M}^{-1}\text{cm}^{-1}$.

Molar absorption coefficient (450 nm) of the final photoproduct = $4,000 \text{ M}^{-1}\text{cm}^{-1}$.

Table VIII. Quenching of the emission lifetime and of the photosubstitution : $[\text{Ru}(\text{bipy})_3]\text{Br}_2$ at 298 K in a 0.10 M solution of TBABr in CH_2Cl_2 by Oxygen.

$[\text{O}_2] \cdot 10^{18}, \text{M}$ (T_{00}/T_{∞}) (a) ($Q_{\text{pho2}}/Q_{\text{ph2}}$) (b)

0(c)	1.00	1.00
1.6(d)	1.47	1.48
8.0(e)	2.40	2.26

slopes (M^{-1}) (f) 166 ± 30 147 ± 40

(a): Quenching of luminescence lifetimes.

(b): Quenching of photoproduct generation.

(c): Sample Ar - degassed (20 min bubbling).

(d): Sample air - saturated (20 min bubbling).

(e): Sample O_2 - bubbled (20 min).

(f): Slopes were evaluated by means of linear regression analysis; they represent an average of

three independent experiments.

For (c), (d), and (e), the O_2 concentrations were estimated with the use of a value of Henry's constant of 1,950 atm/mole fraction²¹ and the approximation $x(O_2) = [n(O_2) / n(\text{solvent})]$.

The quenching plots for experiments 1 - 6 are shown in Figures 14 to 19 . In these plots, the photosubstitution quenching is shown with circles (o and ●) and the lifetime quenching with squares (■).

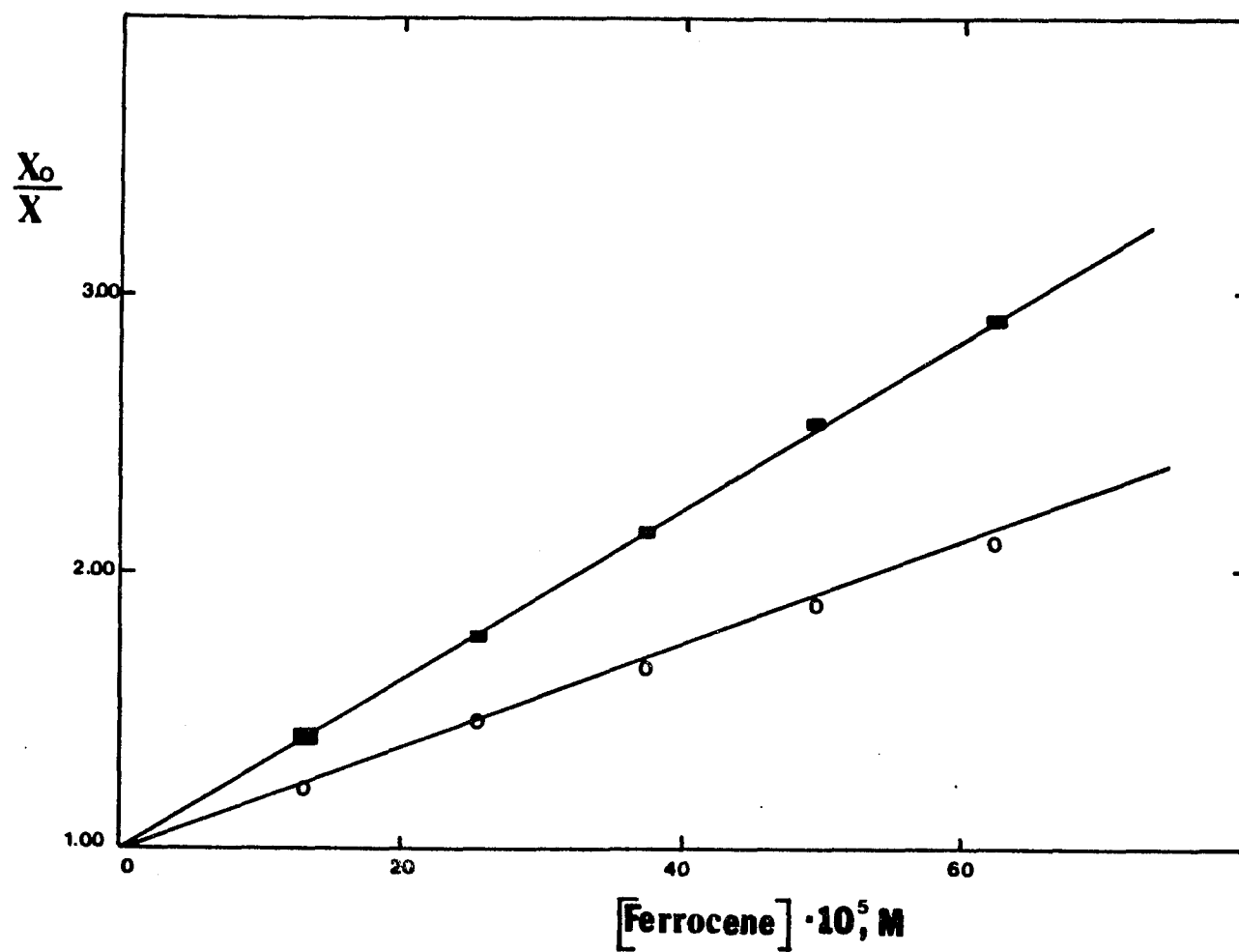


Figure 14. Stern - Volmer plot for the quenching of $[\text{Ru}(\text{bipy})_3]\text{Cl}_2$ emission lifetime (■) and photosubstitution (○) at 298 K in a 0.10 M solution of TBACl in DMF by Ferrocene.

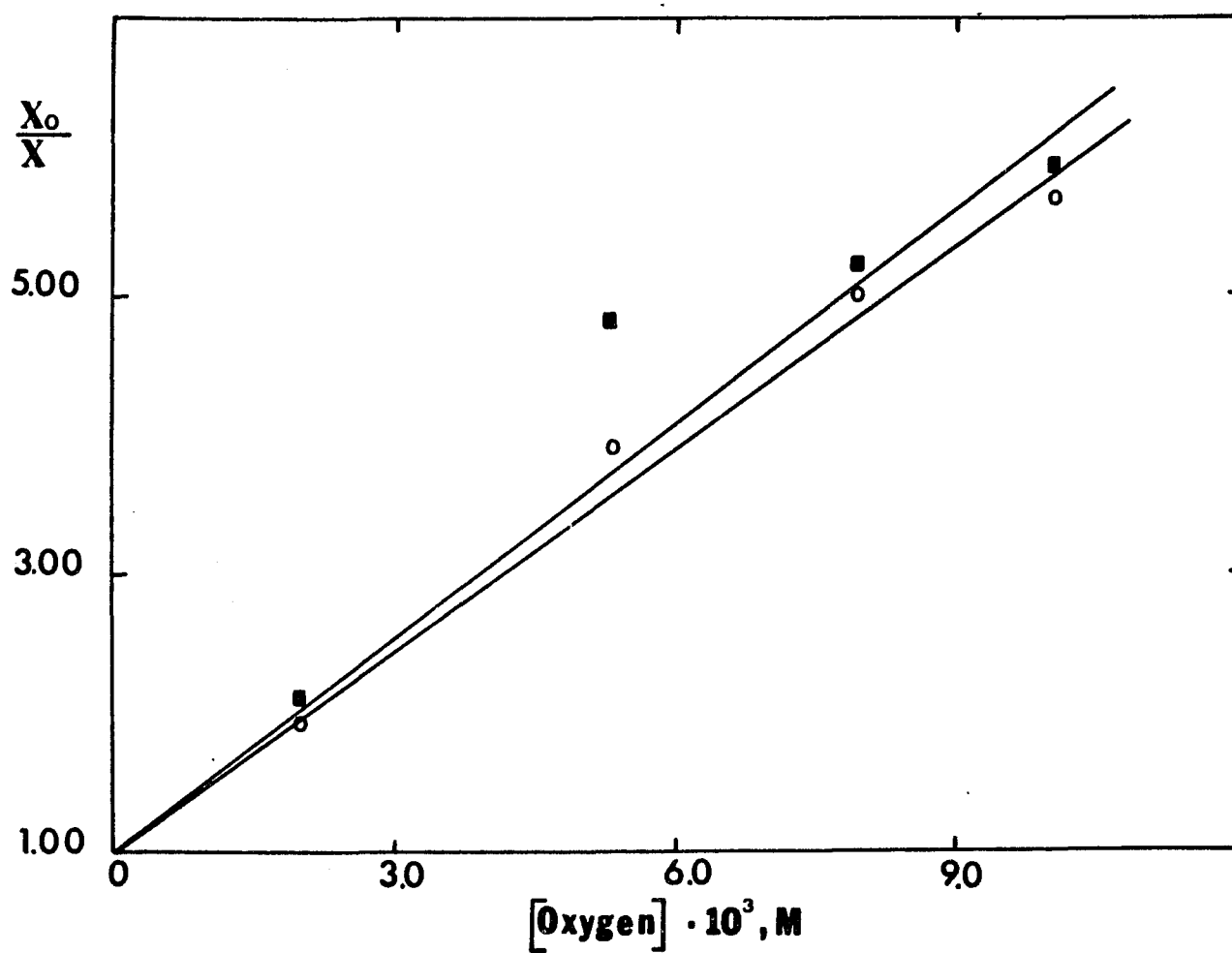


Figure 15. Stern - Volmer plot for the quenching of $[\text{Ru}(\text{bipy})_3]\text{Cl}_2$ emission lifetime (■) and photosubstitution (○) at 298 K in a 0.10 M solution of TBACl in CH_3CN by Oxygen.

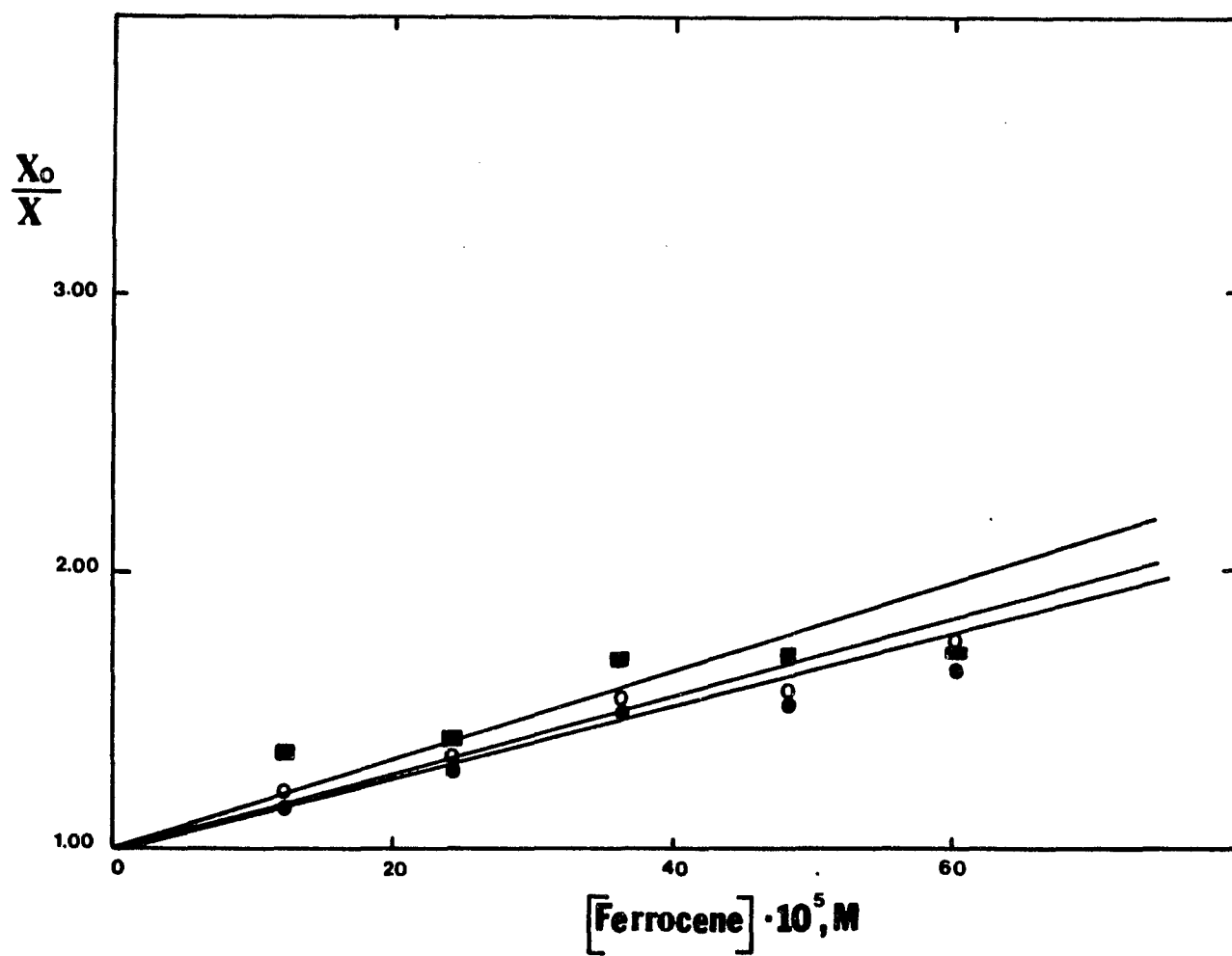


Figure 16. Stern - Volmer plot for the quenching of $[\text{Ru}(\text{bipy})_3]\text{Br}_2$ emission lifetime (■) and photosubstitution (○ and ●) at 298 K in a 0.10 M solution of TBABr in DMF by Ferrocene .

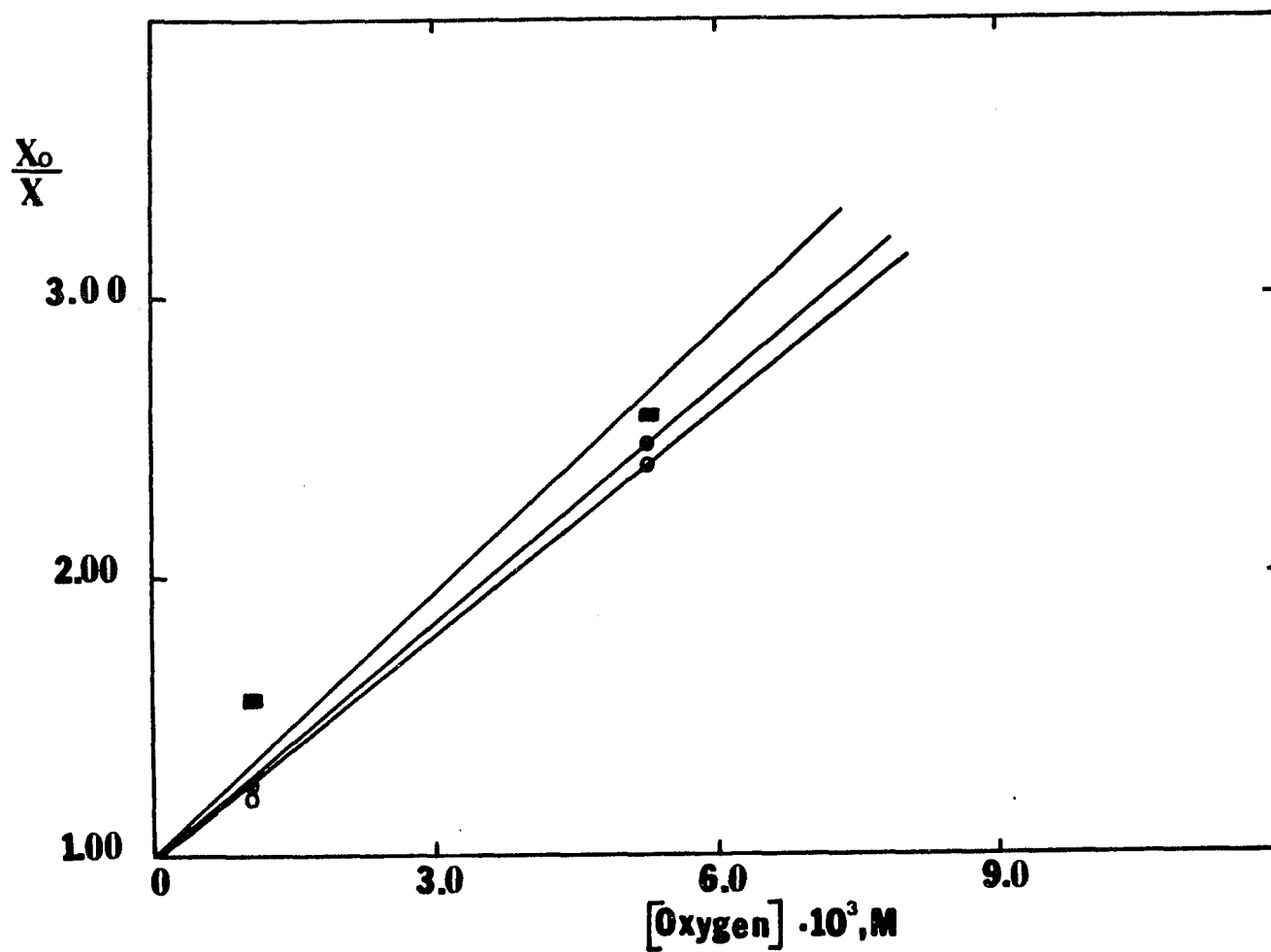


Figure 17. Stern - Volmer plot for the quenching of $[\text{Ru}(\text{bipy})_3]\text{Br}_2$ emission lifetime (■) and photosubstitution (○ and ●) at 298 K in a 0.10 M solution of TBABr in DMF by Oxygen .

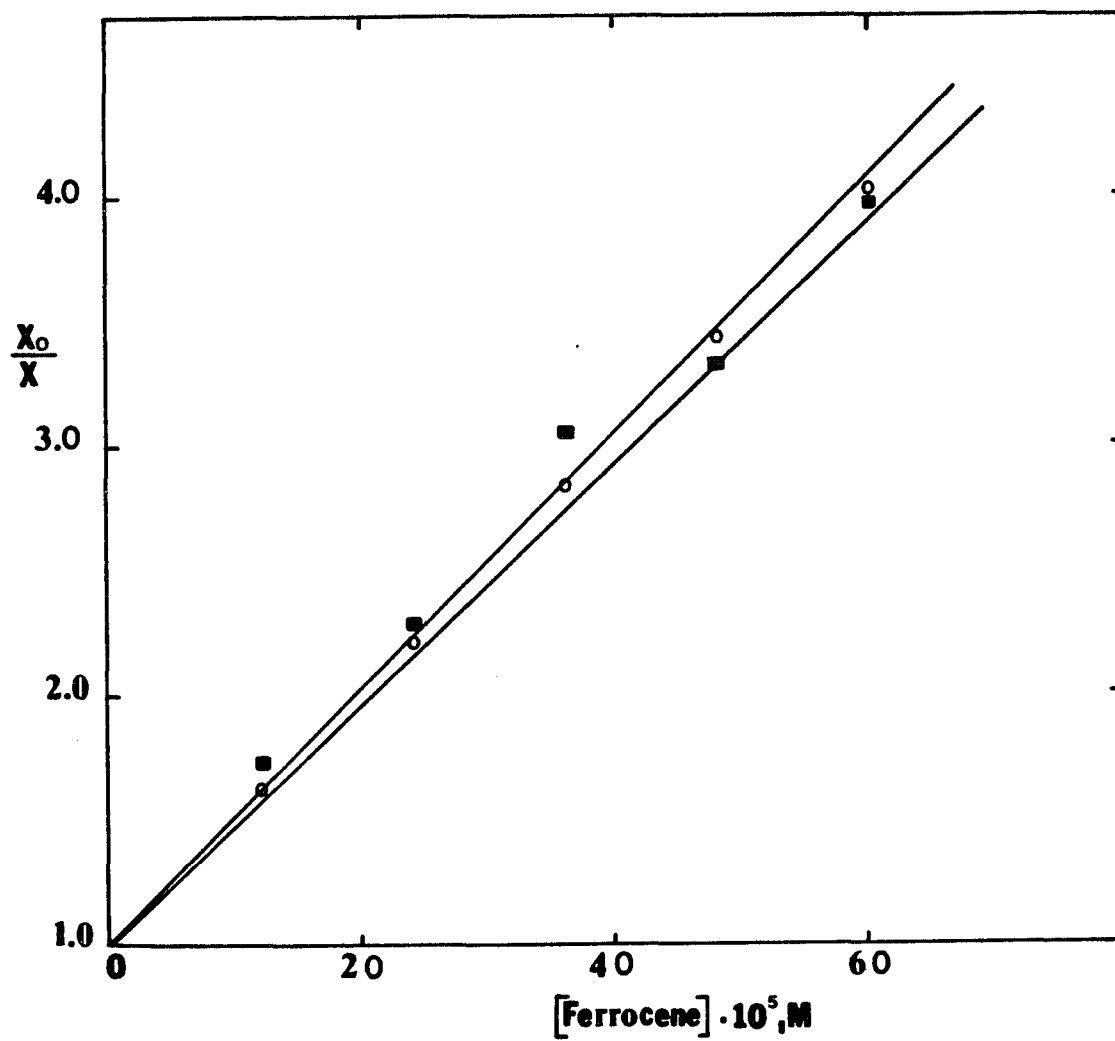


Figure 18 . Stern - Volmer plot for the quenching of $[\text{Ru}(\text{bipy})_3]\text{Br}_2$ emission lifetime (■) and photosubstitution (○) at 298 K in a 0.10 M solution of TBABr in CH_2Cl_2 by Ferrocene..75

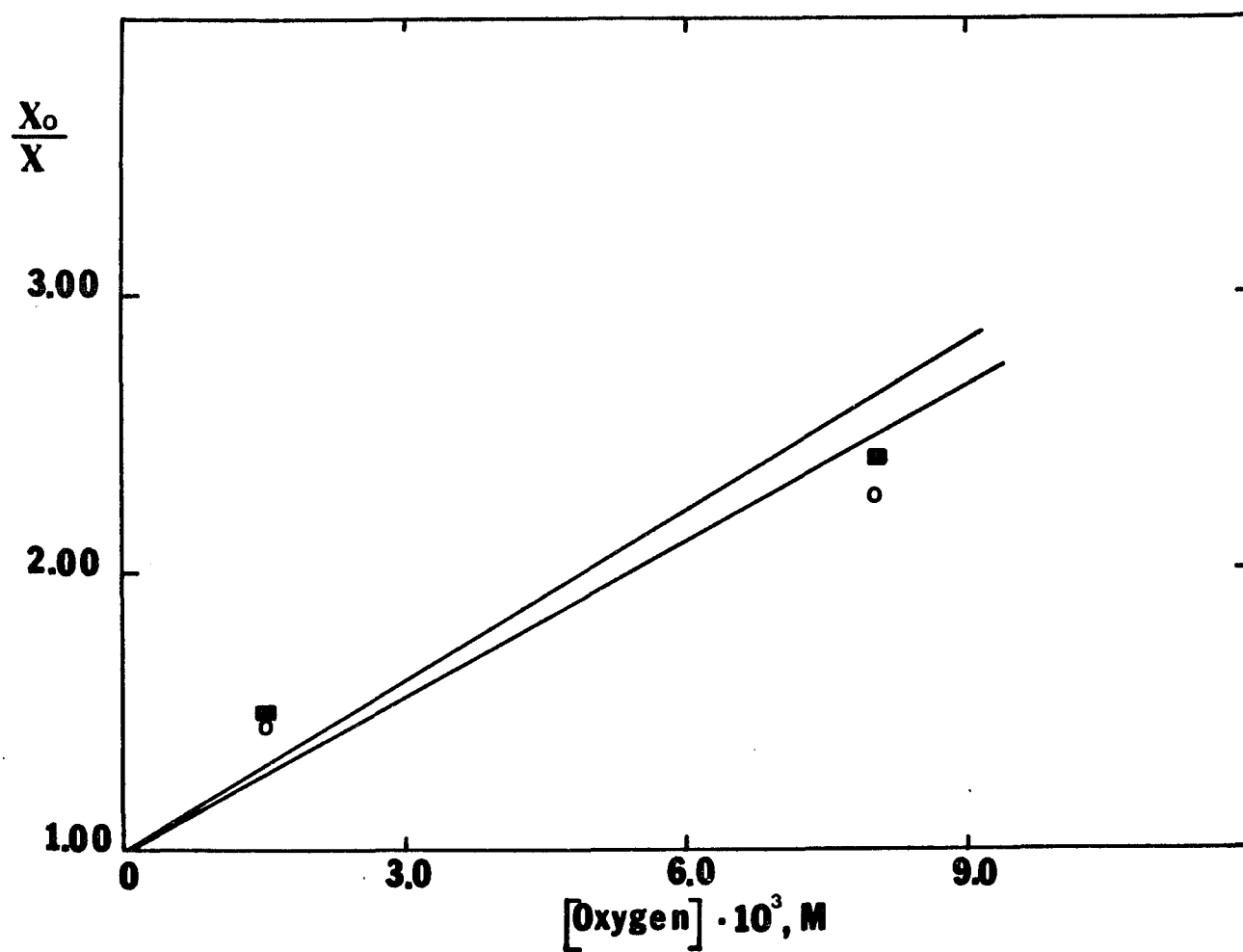


Figure 19 . Stern - Volmer plot for the quenching of $[\text{Ru}(\text{bipy})_3]\text{Br}_2$ emission lifetime (■) and photosubstitution (○) at 298 K in a 0.10 M solution of TBAEr in CH_2Cl_2 by Oxygen.

B. CORRELATION OF LIGAND FIELD EXCITED STATE ENERGIES WITH LIGAND FIELD STRENGTHS IN (POLYPYRIDINE) RUTHENIUM(II) COMPLEXES.

An analysis of reported experimental data concerning the energy difference between the $^3\text{MLCT}$ and LF excited states of the complexes $[\text{Ru}(\text{bipy})_3]^{+2}$ 41 , $[\text{Ru}(\text{bipy})_2(\text{diaz})]^{+2}$ 46 , and $[\text{Ru}(\text{bipy})_2(\text{py})_2]^{+2}$ 39,49 leads to the conclusion that the generally observed ligand field trends were absent in these complexes.

In order to further investigate changes in the energy of these LF states, the emission properties of $[\text{Ru}(\text{bipy})_2\text{L}]^{+2}$ complexes over an extended temperature range ($\text{L} = \text{diaz}, (\text{py})_2$) were reevaluated in this work and a new view of the energy changes of the LF state and their rationalization by means of ligand field theory were made possible.

1. Luminescence measurements.

1.a. Emission intensities of EtOH/MeOH (4:1, v/v) solutions as a function of temperature.

1.a.1. Complex : $[\text{Ru}(\text{bipy})_3]^{+2}$.

Table IX . Relative emission intensity of $[\text{Ru}(\text{bipy})_3]^{+2}$ in EtOH/MeOH(4:1,v/v) as a function of temperature.

T(K)	I_{rel} (a)
303	0.65
295	0.77
291	0.83
287	0.90
285	0.97
282	1.00
280	1.05
273	1.18
269	1.29
267	1.29
261	1.37
251	1.43
236	1.58
219	1.64
198	1.75
191	1.80
179	1.86
163	1.97
153	2.07

(a): Relative emission intensities, $\lambda_{exc} = 450$ nm and the range 500 - 750 nm was scanned. Integrals of the corrected emission spectra presented in wavenumbers were taken. These results are plotted in Figure 20. The general procedure described in the experimental section was followed.

1.a.2. Complex : $[\text{Ru}(\text{bipy})_2(\text{diaz})]^{+2}$.

Table X . Relative emission intensity of $[\text{Ru}(\text{bipy})_2(\text{diaz})]^{+2}$ in EtOH/MeOH(4:1,v/v) as a function of temperature.

T(K)	$I_{rel}(a)$
177	0.05
161	0.22
155	0.36
152	0.61
151	0.56
147	0.82
145	1.30
143	1.40
141	1.55
140	1.97
137	2.24
135	2.27

(a): The observations regarding the

experimental conditions used are the same as those of (a) in the previous Table IX.

1.a.3. Complex : $[\text{Ru}(\text{bipy})_2(\text{py})_2]^{+2}$.

Table XI . Relative emission intensity of $[\text{Ru}(\text{bipy})_2(\text{py})_2]^{+2}$ in EtOH/MeOH(4:1,v/v) as a function of temperature.

T(K)	$I_{r=1}$ (a)
250	0.05
228	0.10
213	0.16
200	0.30
186	0.43
171	0.63
161	0.88
153	1.15
147	1.34
141	1.58
135	1.96
129	2.20

(a): The meaning is the same as that in the previous Table X.

1.b. Emission quantum yields of EtOH/MeOH (4:1, v/v) solutions as a function of temperature.

1.b.1. Complex : $[\text{Ru}(\text{bipy})_3]^{+2}$.

Table XII . Emission quantum yield dependency of $[\text{Ru}(\text{bipy})_3]^{+2}$ in EtOH/MeOH(4:1,v/v) as a function of temperature .

T (K)	$Q_e \cdot 10^{+3}$	$1/Q_e$ (a)	$1/T(K) \cdot 10^{-3}$ (b)
327	15.24	65.6	3.06
321	22.73	44.0	3.12
315	30.49	32.8	3.18
309	47.17	21.20	3.24
305	53.19	18.80	3.28
300	62.5	16.0	3.38
292	69.44	14.4	3.42
287	75.76	13.20	3.48
286	80.64	12.40	3.50
283	86.21	11.60	3.54
279	92.59	10.80	3.58
273	100	10.0	3.66
267	108.7	9.20	3.76
263	125.0	8.00	3.80
260	138.9	7.60	3.84
251	147.1	6.80	3.99
235	156.1	6.40	4.25
219	166.7	6.00	4.56

198	178.6	5.60	5.04
192	192.3	5.20	5.20
181	208.0	4.80	5.52

(a): is plotted vs. (b) in Figure 21 .

1.b.2. Complex : $[\text{Ru}(\text{bipy})_2(\text{diaz})]^{+2}$.

Table XIII . Emission quantum yield dependency of $[\text{Ru}(\text{bipy})_2(\text{diaz})]^{+2}$ in EtOH/MeOH (4:1, v/v) as a function of temperature.

T (K)	$Q_e \cdot 10^{-3} (c)$	$1/Q_e (a)$	$1/T (K) \cdot 10^{-3} (b)$
177	2.00	500	5.65
160	8.80	113.6	6.25
155	14.88	67.2	6.45
151	26.04	38.4	6.62
150	20.83	48.0	6.67
149	28.41	35.2	6.71
148	31.25	32.0	6.76
142	41.67	24.0	7.04
141	62.50	16.0	7.09
137	78.13	12.8	7.30
136	104.17	9.6	7.35
133	125.00	8.0	7.52
132	112.87	8.9	7.58

(a) is plotted vs. (b) in Figure 22.

(c) : Absolute emission quantum yield;

$[\text{Ru}(\text{bipy})_3]^{+2}$ was the reference. The emission quantum yield for this complex was determined at 140 K; the evaluated lifetime and its radiative rate constant were used. The lifetime of $[\text{Ru}(\text{bipy})_3]^{+2}$ over the temperature range of 84 - 330 K has been evaluated²².

1.b.3. Complex : $[\text{Ru}(\text{bipy})_2(\text{py})_2]^{+2}$.

Table XIV . Emission quantum yield dependency of $[\text{Ru}(\text{bipy})_2(\text{py})_2]^{+2}$ in EtOH/MeOH (4:1, v/v) as a function of temperature.

T (K)	$\Phi_e \cdot 10^{+3} (c)$	$(1/\Phi_e) \cdot 10^{+1} (a)$	$1/T (K) \cdot 10^{-3} (b)$
250	1.00	100	4.00
227	2.98	33.6	4.40
212	6.25	16.0	4.70
199	12.50	8.0	5.02
196	15.63	6.4	5.10
185	25.00	4.0	5.41
169	35.71	2.8	5.92
158	59.52	1.7	6.33
149	62.50	1.6	6.70

143	65.79	1.5	6.99
132	114	0.88	7.58
126	125	0.80	7.94

(a) is plotted vs. (b) in Figure 23 .

(c): Absolute quantum yield; $[\text{Ru}(\text{bipy})_3]^{+2}$ was the reference.

2. Temperature dependence of the lifetime of complexes $[\text{Ru}(\text{bipy})_2\text{L}]^{+2}$ in EtOH/MeOH (4:1, v/v) .

Luminescence lifetimes were obtained in collaboration with R.H. Schmehl, from Tulane University, by pulsed nitrogen laser excitation with pulses at 337 nm and a 350 ps width. Emission was observed at right angles by means of a Hamamatsu R777 photomultiplier tube through a conventional monochromator system. Time resolved detection was accomplished by computerized scanning on a gated integrator.

2.a.1. Complex : $[\text{Ru}(\text{bipy})_3]^{+2}$.

Table XV . Lifetime temperature dependency of $[\text{Ru}(\text{bipy})_3]^{+2}$ in EtOH/MeOH (4:1, v/v).

T(K)	$T_e(\text{nsec})$	$(1/T_e) \cdot 10^{+4}$ (a)	$1/T(\text{K}) \cdot 10^{-3}$ (b)
------	--------------------	-----------------------------	-----------------------------------

298	575	174.00	3.36
284	966	103.60	3.52
273	1429	70.00	3.66
265	1701	58.80	3.78
254	1938	51.60	3.94
240	2212	45.20	4.16
234	2336	42.80	4.27
225	2475	40.40	4.45
216	2427	41.20	4.62

(a) is plotted vs. (b) in Figure 24 .

2.a.2. Complex : $[\text{Ru}(\text{bipy})_2(\text{diaz})]^{+2}$.

Table XVI . Lifetime temperature dependency
of $[\text{Ru}(\text{bipy})_2(\text{diaz})]^{+2}$ in EtOH/MeOH (4:1, v/v).

T (K)	T_e (nsec)	$(1/T_e) \cdot 10^{+5}$ (a)	$1/T(K) \cdot 10^{-3}$ (b)
175	129	77.60	5.72
173	168	59.60	5.79
165	379	26.40	6.05
163	617	16.20	6.14
154	1136	8.80	6.50
148	1471	6.80	6.77

139	1613	6.20	7.18
132	1923	5.20	7.58
124	2273	8.06	4.40
116	3125	8.62	3.20

(a) is plotted vs. (b) in Figure 25 .

2.a.3. Complex : $[\text{Ru}(\text{bipy})_2(\text{py})_2]^{+2}$.

Table XVII . Lifetime temperature dependency of $[\text{Ru}(\text{bipy})_2(\text{py})_2]^{+2}$ in EtOH/MeOH (4:1, v/v).

T(K)	$T_e(\text{nsec})$	$(1/T_e) \cdot 10^{+5} \text{ (a)}$	$1/T(\text{K}) \cdot 10^{-3} \text{ (b)}$
235	93	107.60	4.26
230	116	86.40	4.34
227	145	69.20	4.40
222	288	34.80	4.51
219	347	28.80	4.57
205	992	10.08	4.88
199	1388	7.20	5.03
193	1404	7.12	5.18
191	1437	6.96	5.24
186	1453	6.88	5.38
174	1462	6.84	5.76
168	1471	6.80	5.96
161	2083	4.80	6.22
156	2500	4.00	6.42
145	3049	3.28	6.90

136	3289	3.04	7.36
-----	------	------	------

(a) is plotted vs. (b) in Figure 26.

Table XVIII . Curve fitting parameters obtained for the polypyridine complexes based upon emission intensities and lifetimes.

complex	method(a)	A(b)	B(c)	$\Delta E(\text{cm}^{-1})$
[Ru(bipy) ₃] ²⁺	(L)	$3.9 \cdot 10^5$	$1.9 \cdot 10^{14}$	3,859
	(I)	7.86	$1.56 \cdot 10^9$	3,951
[Ru(bipy) ₂ (diaz)] ²⁺	(L)	$3.1 \cdot 10^5$	$8.5 \cdot 10^{14}$	2,271
	(I)	5.5	$1.7 \cdot 10^9$	1,846
[Ru(bipy) ₂ (py) ₂] ²⁺	(L)	$4.23 \cdot 10^5$	$2.34 \cdot 10^{14}$	2,758
	(I)	21.0	$1.35 \cdot 10^9$	1,957

(a) : Based upon lifetimes (L) or intensity

(I) measurements.

(b) : $A = k_r + k_{nr}$ (sec⁻¹) (for L).

$A = (k_r + k_{nr}) / k_r$ (unitless) (for I).

(c) : $B = k_o$ (sec⁻¹) (for L).

$B = k_o / k_r$ (unitless) (for I).

3. Intersystem crossing determinations.

In order to check further the quantum yield of LF production, from the $^3\text{MLCT}$ state, the efficiency of sensitized persulfate decomposition was examined. The method proposed by Bolleta et.al.⁶³ was followed. The technique is essentially based on electron transfer involving the $^3\text{MLCT}$ excited states of the complexes in the presence of $\text{S}_2\text{O}_8^{2-}$ ions, which act as the oxidizing agent. The proposed mechanism is shown in Figure 27. According to this model, a plot of $1/Q_{\text{Ru(II)}}$ vs. $1/[\text{S}_2\text{O}_8^{2-}]$ should be linear and should have a theoretical intercept of 0.5. ($Q_{\text{Ru(II)}}$ = disappearance of the Ru(II) complex). A steady state treatment of this reaction scheme indicates that, under sufficiently high concentrations of $\text{S}_2\text{O}_8^{2-}$, the photooxidation is the only deactivation path of the triplet. Furthermore, the quantum yield of $^1\text{MLCT}$ formation from the corresponding triplet state should be unity. For the bis - pyridine and diazafluorene complexes, the previous emission lifetime and quantum yield results suggest that the rate of LF formation will be too rapid for any bimolecular quenching process to compete at ambient temperature.

A stock acid solution of $1.0 \cdot 10^{-2}$ M $K_2S_2O_8$ in 0.50 M H_2SO_4 was prepared. Adequate dilutions were made in 25.0 ml volumetric flasks in order to obtain additional persulfate solutions of $5.0 \cdot 10^{-3}$ M, $3.3 \cdot 10^{-3}$ M, $2.5 \cdot 10^{-3}$ M, and $2.0 \cdot 10^{-3}$ M. After degassing with argon for twenty minutes $[Ru(bipy)_3]^{+2}$ was discharged from a microsyringe into each of these solutions in order to get an initial concentration of about $4.5 \cdot 10^{-5}$ M. Since these solutions were spectrophotometrically stable only in the dark, care was exercised in order to avoid exposure to light. Then, in each case, the course of the photolysis by irradiation was followed and was monitored at 446 nm.

General photolysis conditions :

$[Ru(bipy)_3]^{+2} \cong 5 \cdot 10^{-5}$ M.

Light intensity = $4.74 \cdot 10^{-7}$ einstein/sec.

Total irradiation time = 15 sec.

Molar absorption coefficient (446 nm) of the starting material = $13,185 \text{ M}^{-1}\text{cm}^{-1}$.

Molar absorption coefficient (446 nm) of the final photoproduct = $1,420 \text{ M}^{-1}\text{cm}^{-1}$.

Table XIX . Observed dependence of the reciprocal quantum yield of oxidation of $[\text{Ru}(\text{bipy})_3]^{+2}$ to $[\text{Ru}(\text{bipy})_3]^{+3}$ upon $1/[\text{S}_2\text{O}_8^{-2}]$ in 0.50 M H_2SO_4 .

$1/[\text{S}_2\text{O}_8^{-2}]$	$1/Q_{\text{Ru(II)}}$
100	0.74
200	0.92
300	1.17
400	1.34
500	1.60

These results are plotted in Figure 28. They represent an average of four experimental runs.

Similar experiments carried out with $[\text{Ru}(\text{bipy})_2(\text{diaz})]^{+2}$ indicated that there was no reactivity even when the samples were irradiated in the presence of high concentrations of $\text{S}_2\text{O}_8^{-2}$.

For $[\text{Ru}(\text{bipy})_2(\text{py})_2]^{+2}$, the persulfate appeared not to oxidize the complex; however, this experiment was complicated by the fact that the complex undergoes a photosubstitution reaction under these experimental conditions. This photosubstitution was unaffected by the presence of $\text{S}_2\text{O}_8^{-2}$. Hence, the $^3\text{MLCT}$ must be very short - lived .

Table XX . Electrochemical Data of some Polypyridine Ruthenium (II) Complexes.

Complex	λ_{\max} (a)	A(b)	B(c)	C(d)	D(e)
[Ru(bipy) ₃] ²⁺	452	1.29	-1.34	-1.53	2.63
[Ru(bipy) ₂ (py) ₂] ²⁺	460	1.27(f)	-1.43	-1.60(f)	2.70(f)
[Ru(bipy) ₂ (diaz)] ²⁺	450	1.30	-1.37	-1.51	2.67

(a) : Absorption maximum for MLCT transition.

(b) : A = E°(+3/+2) ; volts vs. SCE, CH₃CN
(0.01 M tetrabutyl ammonium hexafluorophosphate).

(c) : B = E°(+2/+1) ; volts vs. SCE, CH₃CN
(0.01 M tetrabutyl ammonium hexafluorophosphate).

(d) : C = E°(+1/0) ; volts vs. SCE, CH₃CN
(0.01 M tetrabutyl ammonium hexafluorophosphate).

(e) : D = E_{1/2} ; volts vs. SCE, CH₃CN
(0.01 M tetrabutyl ammonium hexafluorophosphate) .

(f) : volts vs. SCE, (0.10 M tetrabutyl ammonium perchlorate).

These electrochemical measurements were obtained by R. H. Schmehl of Tulane University.

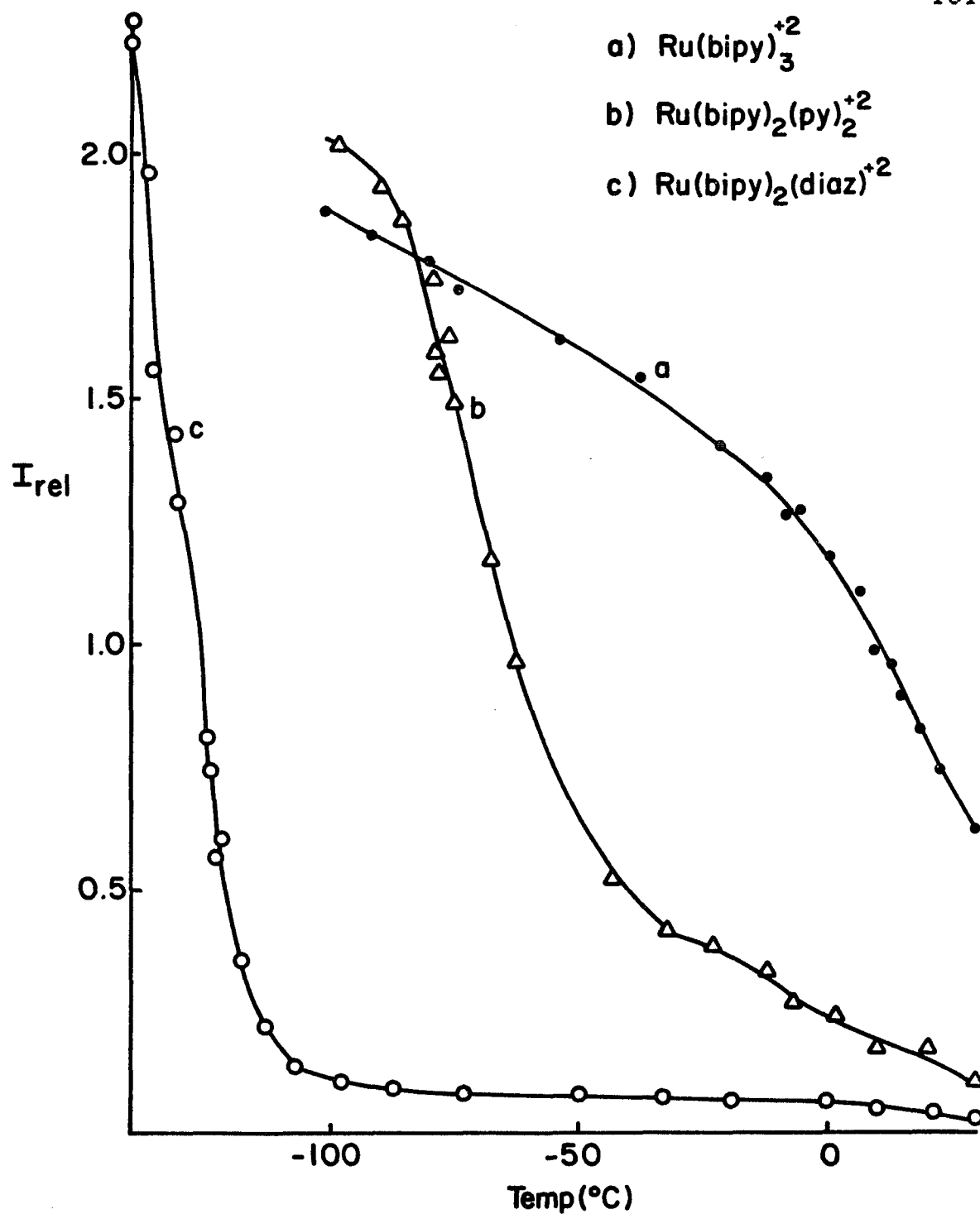


Figure 20 . Emission intensity of $[\text{Ru}(\text{bipy})_3]^{+2}$,
 $[\text{Ru}(\text{bipy})_2(\text{diaz})]^{+2}$ and $[\text{Ru}(\text{bipy})_2(\text{py})_2]^{+2}$ as a
 function of temperature. The solvent is EtOH/MeOH (4:1, v/v).

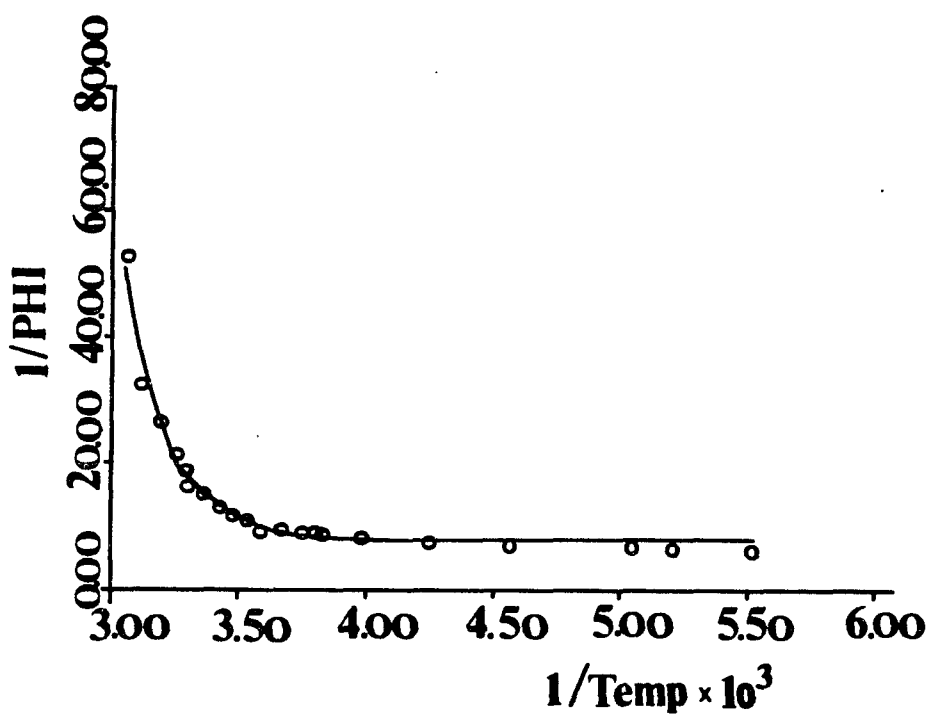


Figure 21. Temperature dependence of the relative emission intensities of $[\text{Ru}(\text{bipy})_3]^{2+}$ in EtOH/MeOH (4:1, v/v). The solid curve is the computer fit generated from the parameters given in Table XVIII.

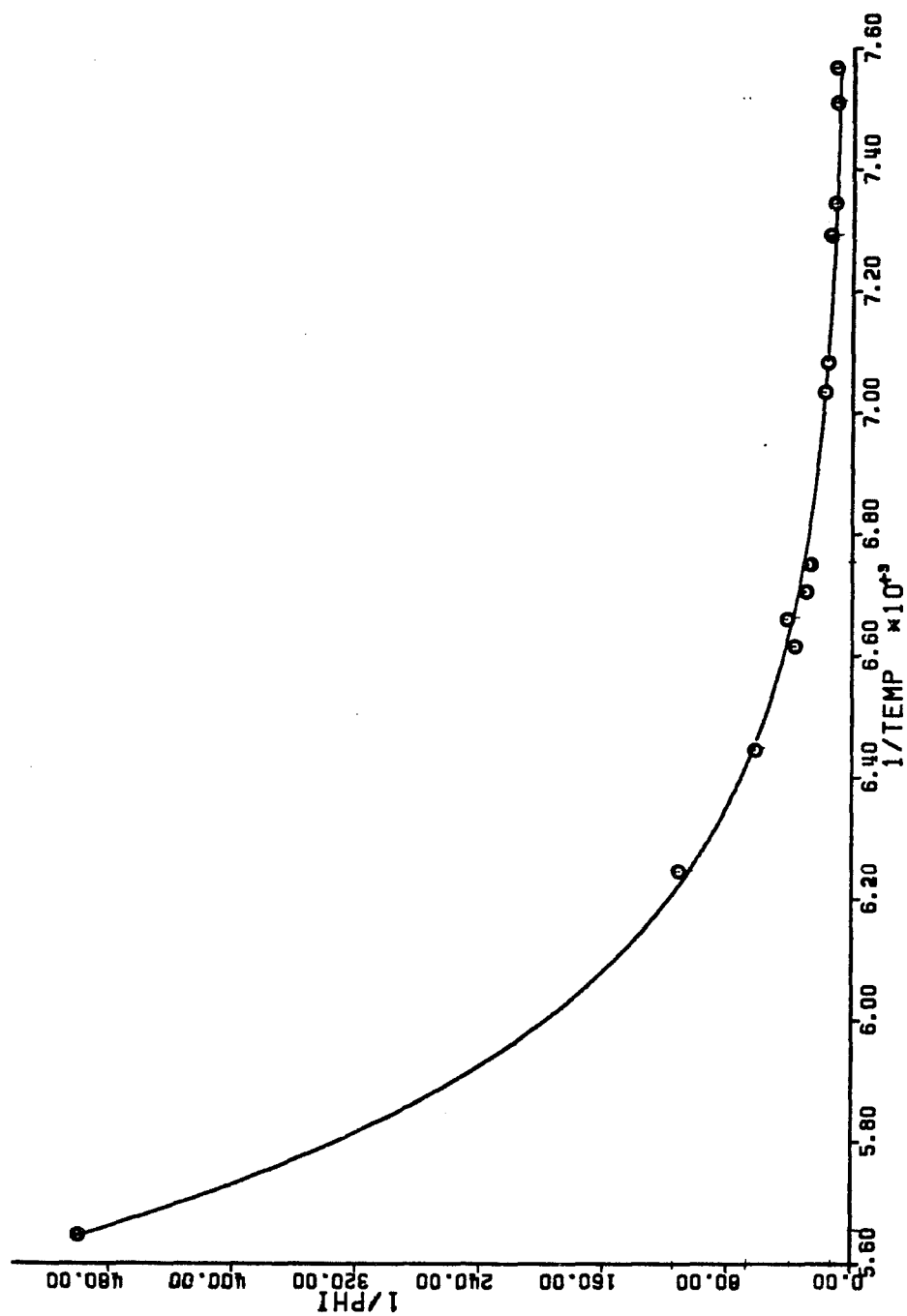


Figure 22 . Temperature dependence of the relative emission intensities of $[Ru(bipy)_2(diaz)]^{+2}$ in EtOH/MeOH (4:1,v/v). The solid curve is the computer fit generated from the parameters given in Table XVIII.

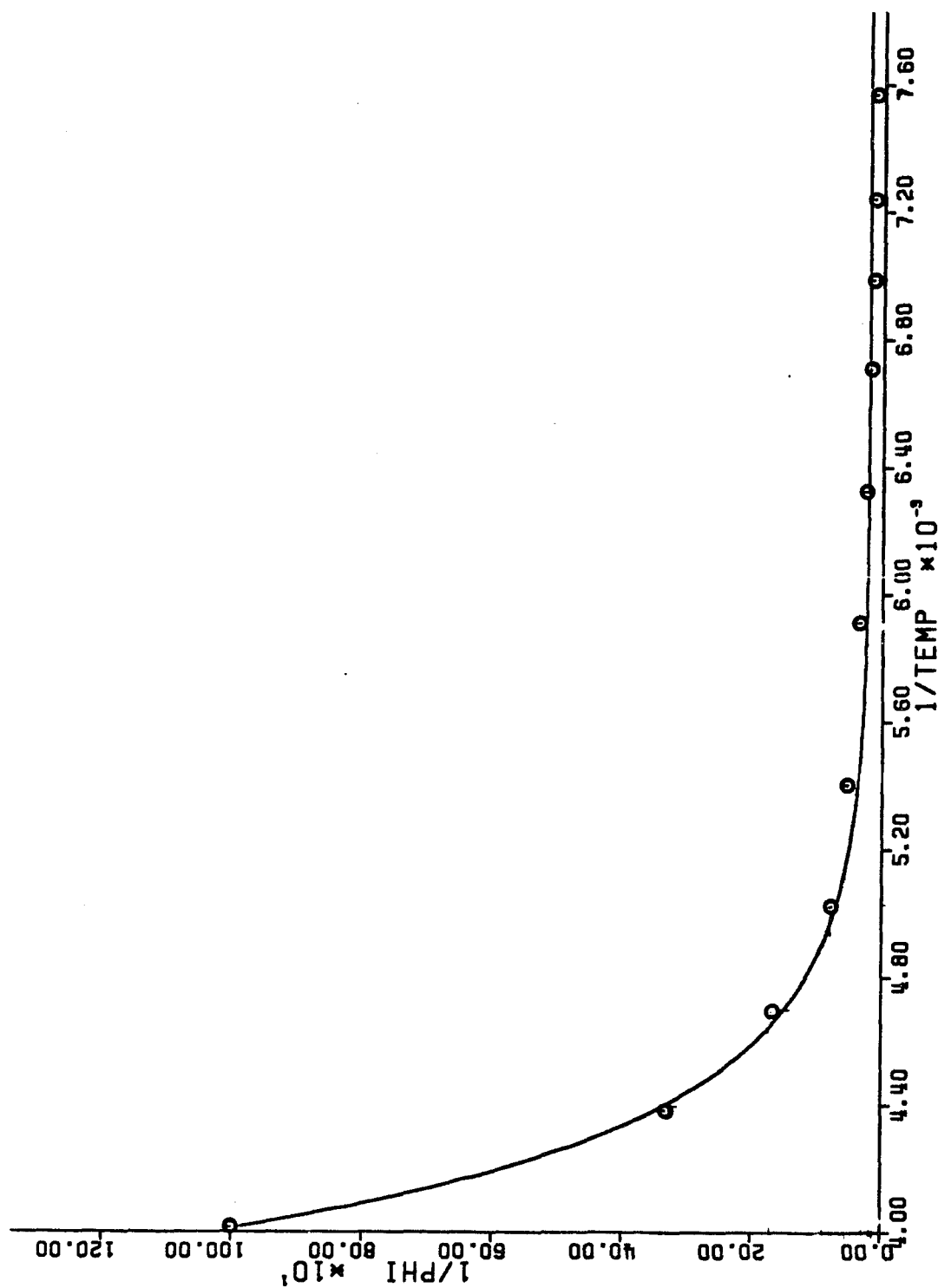


Figure 23 . Temperature dependence of the relative emission intensities of $[Ru(bipy)_2(py)_2]^{+2}$ in EtOH/MeOH (4:1, v/v). The solid curve is the computer fit generated from the parameters given in Table XVIII.

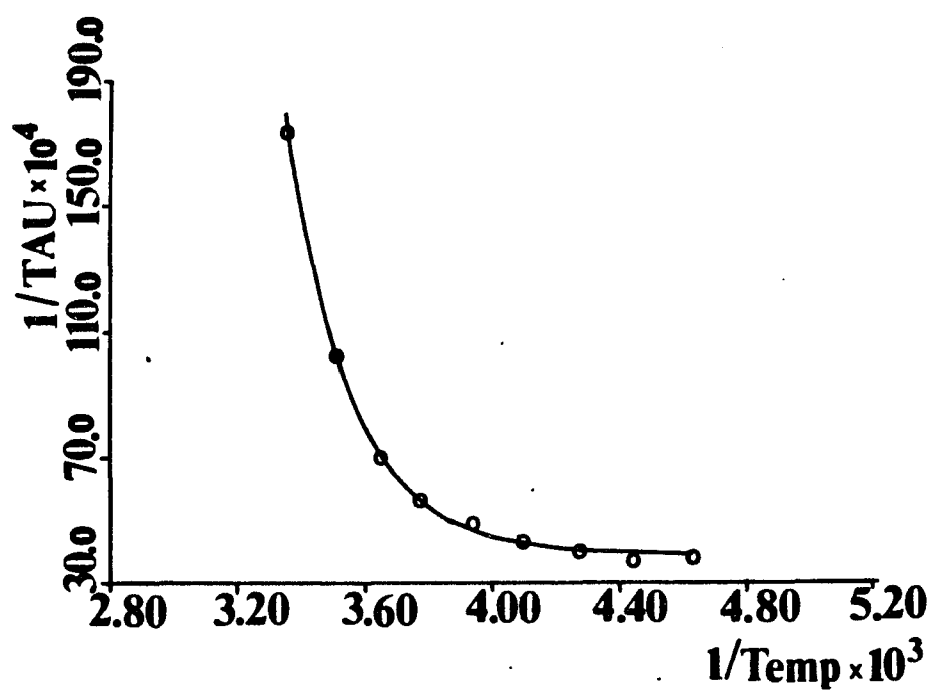


Figure 24. Temperature dependence of the emission lifetime of $[\text{Ru}(\text{bipy})_3]^{+2}$ in EtOH/MeOH (4:1, v/v). The solid curve is the computer fit generated from the parameters given in Table XVIII.

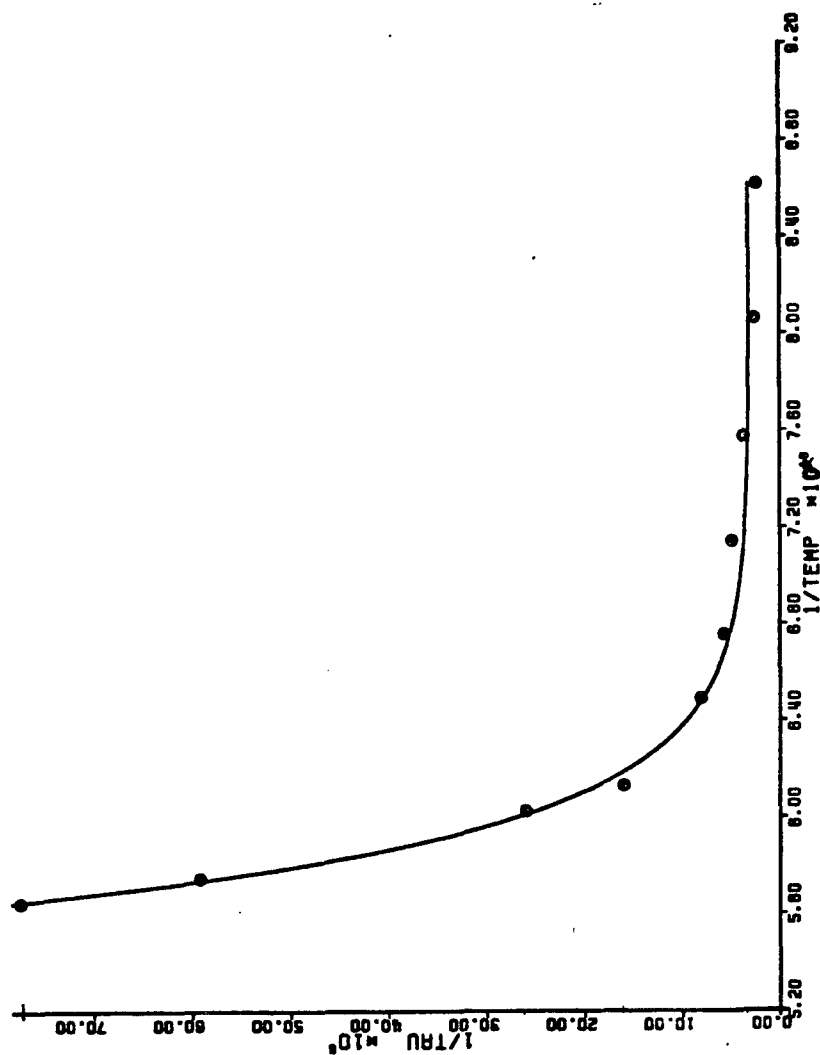


Figure 25. Temperature dependence of the relative emission lifetimes of $[Ru(bipy)_2(diaz)]^{+2}$ in EtOH/MeOH (4:1, v/v). The solid curve is the computer fit generated from the parameters given in Table XVIII.

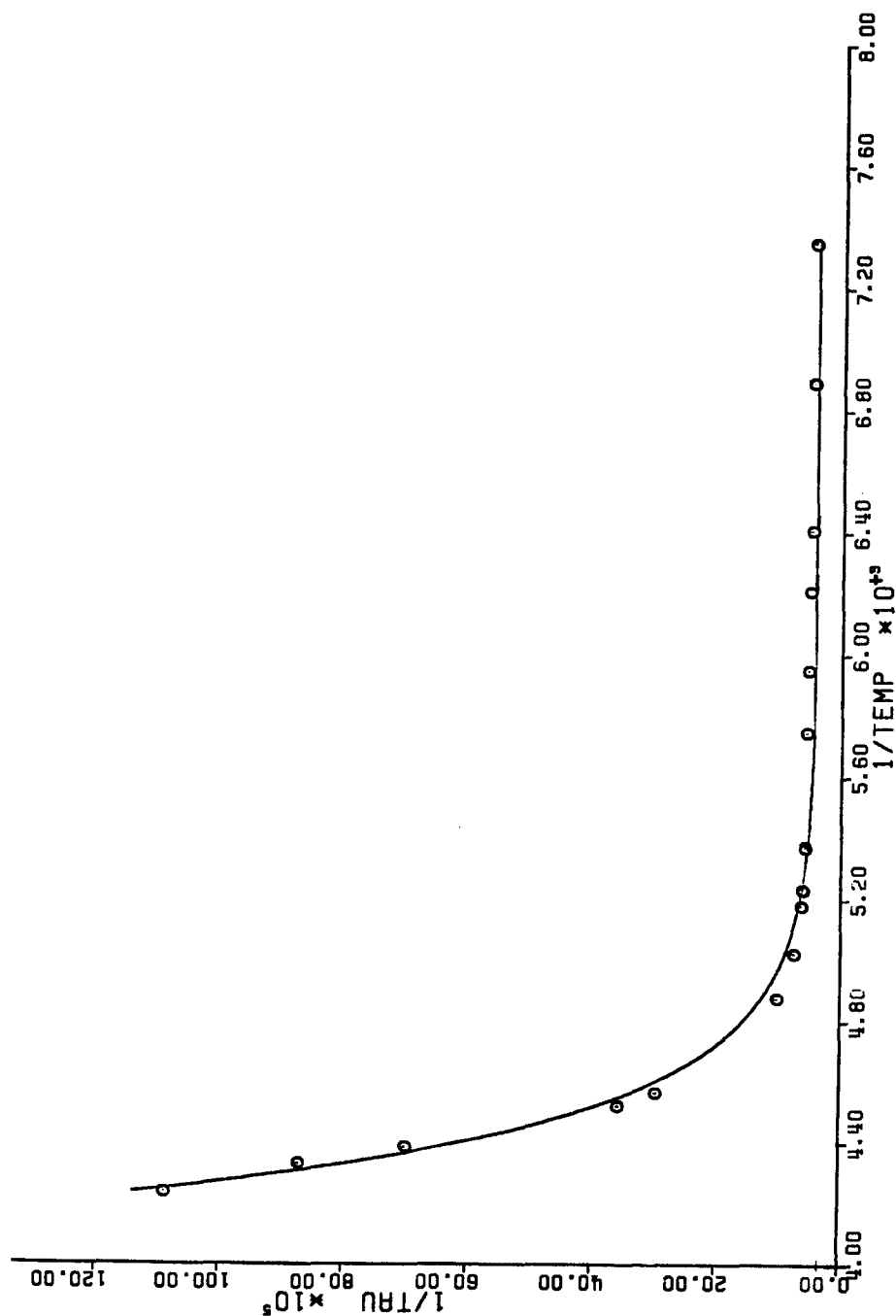


Figure 26 . Temperature dependence of the relative emission intensities of $[Ru(bipy)_2(py)_2]^{+2}$ in EtOH/MeOH (4:1,v/v). The solid curve is the computer fit generated from the parameters given in Table XVIII.

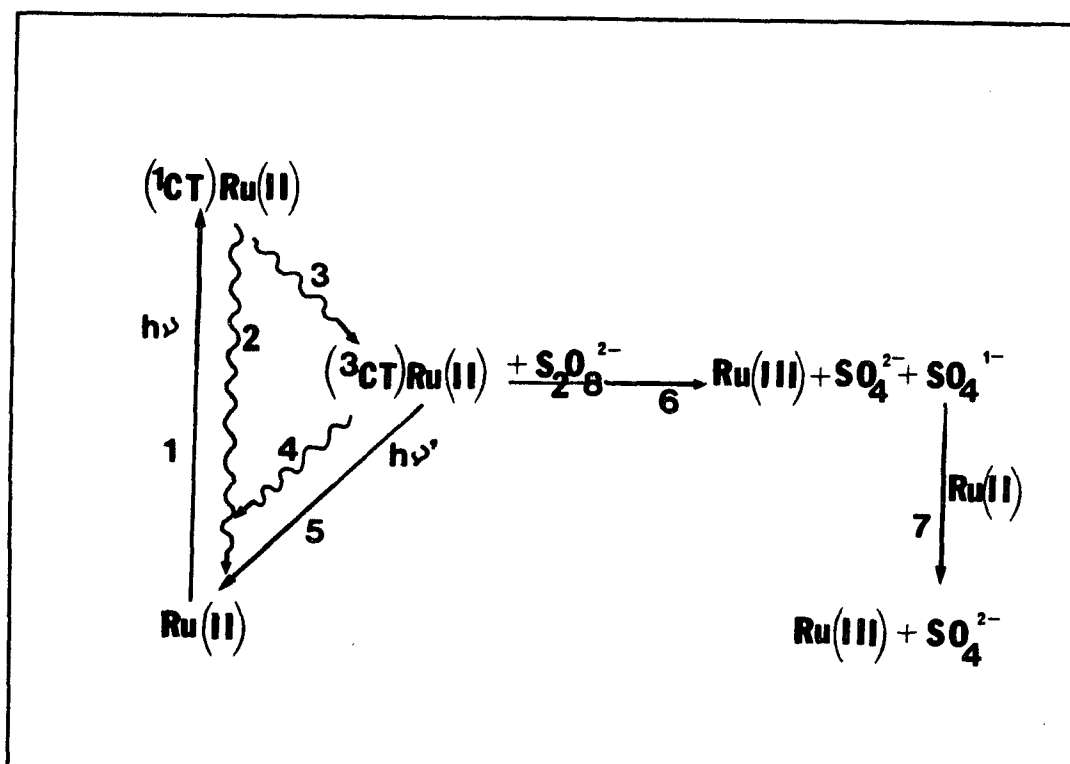


Figure 27. Reaction scheme for the photooxidation of $[\text{Ru}(\text{bipy})_3]^{2+}$ and $[\text{Ru}(\text{phen})_3]^{2+}$ by $\text{S}_2\text{O}_8^{2-}$ ions.

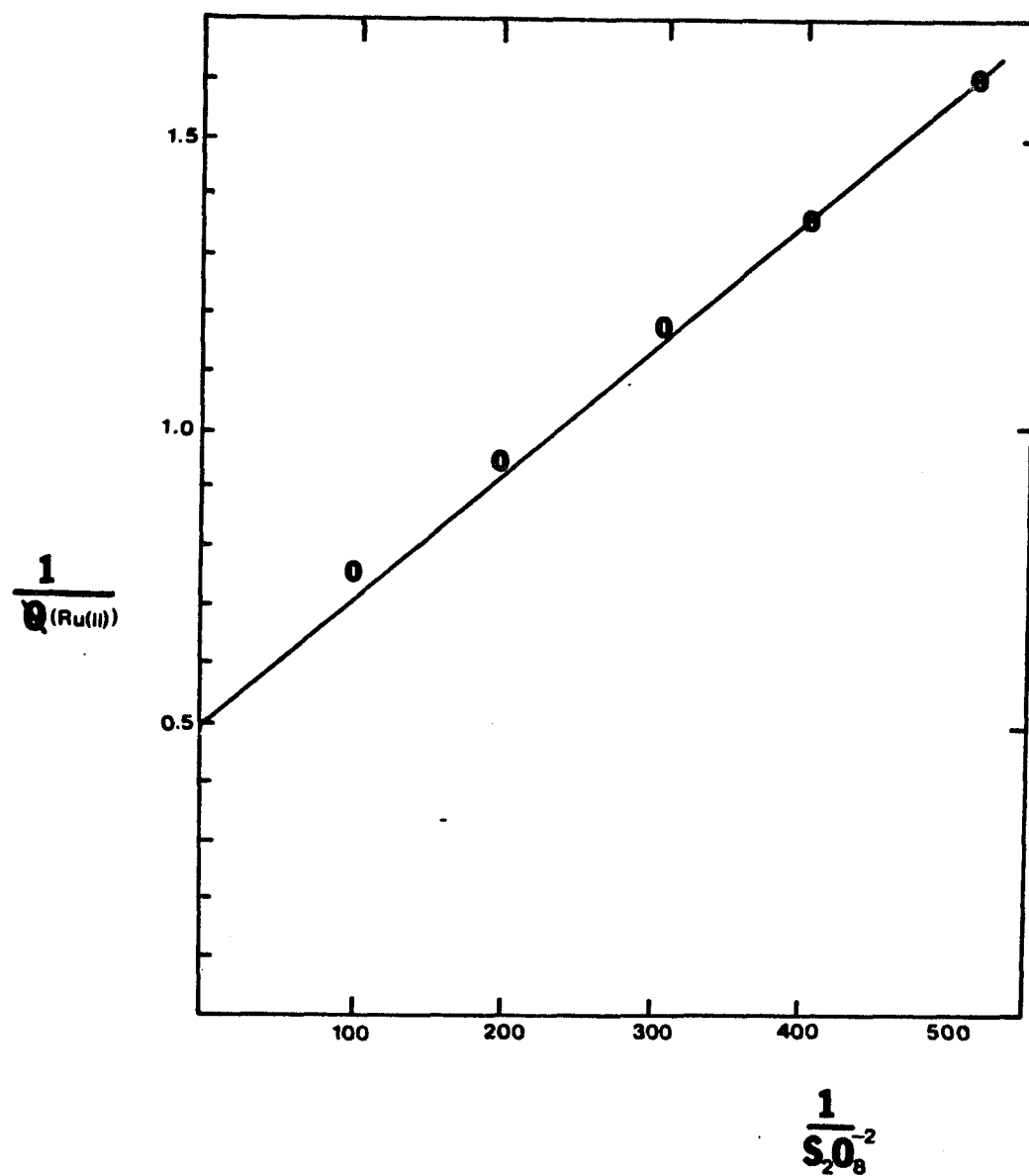


Figure 28 . Dependence of the reciprocal quantum yield of oxidation of $[Ru(bipy)_3]^{+2}$ to $[Ru(bipy)_3]^{+3}$ upon $1 / [S_2O_8^{2-}]$.

C. ION PAIRING EFFECT UPON PHOTOSUBSTITUTION
QUANTUM YIELDS of cis - bispyridyl bis - 2,2'bipyridyl
ruthenium(II) hexafluorophosphate tetrahydrate AT 298
K IN 0.01 M TBAX ($X = Cl^-$, ClO_4^-) IN MIXTURES OF
DIOXANE AND WATER .

1. Determination of molar absorption
coefficients.

The absorption spectrum of the complex
 $[Ru(bipy)_2DPE]^{+2}$ exhibits features similar to those
of $[Ru(bipy)_2(py)_2]^{+2}$ during each stage of the
photolysis. For this reason, $[Ru(bipy)_2DPE]^{+2}$ was
used to estimate the molar absorption coefficient
(E_{ph1}) for the first intermediate in the photolysis
of $[Ru(bipy)_2(py)_2]^{+2}$.

A known concentration of the complex was
prepared in 95/5, v:v dioxane/water - mixture, and the
molar absorption coefficient at 450 nm was determined.
Next, solid TBACl was added and the
 $[Ru(bipy)_2DPE]^{+2}$ was quantitatively converted by a
dark reaction to the monochloro - complex and the
respective molar absorption coefficient was evaluated.
Finally, the sample was photolyzed to
 $[Ru(bipy)_2Cl_2]$.

The respective molar absorption coefficients

at 450 nm were evaluated to be as 9,217, 6,452, and 5,300 $M^{-1}cm^{-1}$, respectively. The same ratio of the molar absorption coefficients was assumed to be valid for all the different dioxane/water solutions of $[Ru(bipy)_2(py)_2]^{+2}$ that were studied.

Table XXI. Absorption characteristics of the complexes $[Ru(bipy)_2DPE]^{+2}$ and $[Ru(bipy)_2(py)_2]^{+2}$ in a 95/5, v:v dioxane/water mixture .

Complex	(a)	(b)	(c)
$[Ru(bipy)_2DPE]^{+2}$	450 (9,217)	504 (8,300)	543 (9,200)
$[Ru(bipy)_2(py)_2]^{+2}$	452 (9,000)	502 (-----)	542 (9,230)

(a) : λ_{max} , nm(E_o), starting complex.

(b) : λ_{max} , nm(E_{ph1}), monochloro complex⁵¹.

(c) : λ_{max} , nm(E_{ph2}), $[Ru(bipy)_2Cl_2]$

Table XXII. Molar absorption coefficients (E_o) at 450 nm, of the complexes $[Ru(bipy)_2DPE]^{+2}$ and $[Ru(bipy)_2(py)_2]^{+2}$ in a 95/5, v:v dioxane/water mixture as well as of their respective monochloro (E_{ph1}) and dichloro (E_{ph2})

photosubstitution products.

	[Ru(bipy) ₂ DPE] ⁺²	[Ru(bipy) ₂ (py) ₂] ⁺²
E ₀	9,217	9,000
E _{ph1}	6,452	6,630 (a)
E _{ph2}	5,300	3,900
E ₀ /E _{ph2} (b)	1.7	2.3
E _{ph1} /E _{ph2} (c)	1.2	1.7
E ₀ /E _{ph1}	1.4	1.4 (d)

(a) : Molar absorption coefficient evaluated by assuming that the same ratio of the quotients between the known molar absorption coefficients (E₀/E_{ph2}) (b) of the [Ru(bipy)₂(py)₂]⁺² and [Ru(bipy)₂DPE]⁺² complexes is also valid for the quotients (E_{ph1}/E_{ph2}) (c) for the same compounds.

Below are shown the calculations made with use of the previous assumptions.

(E₀/E_{ph2}), for [Ru(bipy)₂(py)₂]⁺² : (E₀/E_{ph2}),
for [Ru(bipy)₂DPE]⁺² =

$$2.3 \quad : \quad 1.7 \quad = \quad 1.4$$

From this result and the assumption that the same ratio holds for the following expression :

$$(E_{ph1}/E_{ph2}) : (E_{ph1}/E_{ph2}) = 1.4$$

Then, (E_{ph1}/E_{ph2}) for $[Ru(bipy)_2(py)_2]^{+2} = (1.4).(1.2)$
 $= 1.7$

$E_{ph1} = (1.7).(3,900) = 6,630$ (value estimated and tabulated in (a) of the previous Table XXI).

The reported value of the absorption molar coefficient at λ_{max} located at 505 nm of the complex, $[Ru(bipy)_2(py)Cl]^{+1}$, in CH_2Cl_2 solution ($D = 9$) 105 is $8,200 \text{ M}^{-1}\text{cm}^{-1} \text{ }^{51}$. Meyer and co - workers have recognized the common difficulty in getting good measurements of the molar absorption coefficients of the intermediates being generated during photolysis experiments because of the large number of species generally present, all of which very often absorb at nearly the same wavelength 51 ; besides, the photogenerated intermediates cannot always be conveniently prepared by independent means.

As a final result, included in (d) of the

previous table, the ratio E_0/E_{ph1} of $[Ru(bipy)_2(py)_2]^{+2}$ becomes $9,000/6,630 = 1.4$

2. Photolysis of $[Ru(bipy)_2(py)_2]^{+2}$ at 298 K in 0.01 M in TBACl (mixtures of dioxane and water).

General experimental conditions.

$[Ru(bipy)_2(py)_2]^{+2} \approx 3.8 \cdot 10^{-5} M$.

Light intensity = $3.9 \cdot 10^{-7}$ einstein/sec

Total irradiation time = 80 sec.

Molar absorption coefficient of the starting complex (450 nm) = $9,000 M^{-1}cm^{-1}$.

Molar absorption coefficient of the first photoproduct (450 nm) = $6,630 M^{-1}cm^{-1}$.

Note : For each mixture, 20.0 ml were prepared.

Table XXIII. Dependence of the photosubstitution quantum yield as a function of the polarity of the medium (mixtures of dioxane and water, 0.01 M in TBACl).

mixture

(dioxane/water, v:v) D(a) M(H₂O) (b) $Q_{ph1} \cdot 10^{+2}$ (c)

50/50	32.5	27.78	2.36
-------	------	-------	------

60/40	26.5	22.22	2.43
70/30	20.1	16.67	4.89
80/20	12.5	11.11	6.82
90/10	5.6	5.56	8.37
95/5	3.9	2.78	14.37

(a) : Dielectric constant of the mixture; the values were estimated from data reported²⁴, where the conductance of sodium chloride at 298 K was measured in dioxane - water mixtures covering the range of dielectric constant $12.24 < D < 78.54$ (respectively corresponding to 79.9 % in weight, and 0 %, in dioxane). Also were considered data reported²⁵ where the solubility of KIO_3 and $Zn(IO_3)_2$ was studied in different dioxane - water mixtures covering the range of dielectric constant $2.10 < D < 78.5$ (respectively corresponding to pure dioxane, and pure water).

Density of water was considered to be 1 g/L, and that of dioxane, 0.98 g/L.

(b) : $[(d_{H_2O})(V_{H_2O}) / 18.0] / 20.0 \cdot 10^{-3} = M(H_2O)$

(c) : Evaluated with available program; verage of three runs.

3. Photolysis of $[Ru(bipy)_2(py)_2]^{+2}$ at

298 K in 0.01 M in TBACl (mixture of dioxane and water, 90/10 (v:v)), with excess free pyridine ligand present.

Table XXIV. Dependence of the photosubstitution quantum yield as a function of the pyridine concentration.

free [py], M	$Q_{ph1} \cdot 10^{+2} (a)$
0.00	10.4
$4.0 \cdot 10^{-4}$	8.2
$7.7 \cdot 10^{-4}$	7.4
$26.1 \cdot 10^{-4}$	7.3

(a) : Average of two runs. The presence of free pyridine ligand does not significantly change the course of the photolysis. The same bands are observed and no important deviations in the values calculated for Q_{ph1} are detected.

4. Photolysis of $[Ru(bipy)_2(py)_2]^{+2}$ at 298 K in 0.01 M in $TBAClO_4$ (mixtures of dioxane and water).

General experimental conditions.

$[Ru(bipy)_2(py)_2]^{+2} \approx 5.2 \cdot 10^{-5} \text{ M}$.

Ligth intensity = $3.9 \cdot 10^{-7}$ einstein/sec

Total irradiation time = 30 sec .

Molar absorption coefficient of the starting complex (450 nm) = $9,000 \text{ M}^{-1}\text{cm}^{-1}$.

Molar absorption coefficient of the first photosubstitution product(450 nm) = $6,630 \text{ M}^{-1}\text{cm}^{-1}$.

Table XXV. Dependence of the photosubstitution quantum yield as a function of the polarity of the medium (mixtures of dioxane and water , 0.01 M in TBAClO_4).

mixture

(dioxane/water)	D	M(H_2O)	$Q_{ph} \cdot 10^{+2} (a)$
50/50	32.5	27.28	6.43
70/30	20.1	16.67	7.43
90/10	5.6	5.56	7.72

(a) : Average of two runs. The same parameters that were used previously were used even though the detected photoproducts were different.

In this regard, after extensive photolysis, the final irradiated solution had a clearly dark - green color instead of the typical purple color of

[Ru(bipy)₂Cl₂] solutions. An absorption spectrum taken after 3 hours of full irradiation shows maxima located at 470 and 640 nm.

The initial [Ru(bipy)₂(py)₂]²⁺ solution had an initial maximum located at about 450 nm , and a photoproduct absorbing at 470 was detected after 10 sec of photolytic irradiation.

Therefore, the photoreactivity in mixtures 0.01 M in TBAClO₄ seems to be very different from the observed behavior of 0.01 M TBACl in dioxane/water mixtures.

D. EFFECT OF CHELATE RING SIZE ON THE
PHOTOSUBSTITUTION REACTION OF POLYPYRIDINE RUTHENIUM
(II) COMPLEXES.

Several new polypyridine ligands (L) with two pyridine rings linked by methylene bridges of different lengths were synthesized. The corresponding $[\text{Ru}(\text{bipy})_2\text{L}]^{+2}$ complexes were prepared and their photophysical and photochemical properties were examined.

A similar series of complexes, also having the previously mentioned formulation, but in this case prepared with ligands, L, that have two amine groups linked by methylene bridges of different lengths, were also investigated.

1. Complexes $[\text{Ru}(\text{bipy})_2\text{L}]^{+2}$ where the L's are methylene - linked pyridine ligands.

1.a. Photophysical Properties.

1.a.1. Emission properties at 77 K.

The emission properties of the complexes

$[\text{Ru}(\text{bipy})_2\text{L}]^{+2}$, in which the ligands, L, are those shown in Figure 29, were determined at 77 K, in EtOH/MeOH (4:1, v/v). These determinations were made by means of the procedures described in the experimental section. The results are shown in Table XXVI.

Table XXVI. Emission properties of the bis(bipy), methylene - linked pyridine ruthenium complexes at 77 K.

Complex	λ_{max} (nm)	Q_e (a)	T_e (μsec) (a)	A (b)	B (c)
$[\text{Ru}(\text{bipy})_3]^{+2}$	578	0.376	5.2(d)	7.2	1.2
$[\text{Ru}(\text{bipy})_2(\text{pic})_2]^{+2}$	592	0.41	5.6	7.3	1.1
$[\text{Ru}(\text{bipy})_2\text{DPM}]^{+2}$	584	0.56	7.2	7.7	0.6
$[\text{Ru}(\text{bipy})_2\text{DPE}]^{+2}$	605	0.11	7.5	1.5	1.2

(a) : At 77 K in EtOH/MeOH (4:1, v/v).

(b) : $A = k_r \cdot 10^{+4}$; calculated from $k_r = Q_e / T_e$.

(c) : $B = k_{nr} \cdot 10^{+5}$; calculated from $k_{nr} = 1/T_e - k_r$.

(d) : Reference⁸⁶.

1.a.2. Temperature dependence of the emission quantum yield of complexes $[\text{Ru}(\text{bipy})_2\text{L}]^{+2}$ in EtOH/MeOH (4:1, v/v).

1.a.2.1. L = 2,2' - bipyridine (bipy).

Emission parameters reported in Table XXIX were taken from data previously published⁸⁴.

1.a.2.2. L = bis - picoline (pic) .

Table XXVII. Temperature dependence of the emission quantum yield of $[\text{Ru}(\text{bipy})_2(\text{pic})_2]^{+2}$.

T (K)	$Q_e \cdot 10^{+3}$	$1/Q_e$	$1/T \text{ (K)} \cdot 10^{+3}$
127	400.0	2.5	7.87
143	384.6	2.6	6.99
171	322.6	3.1	5.85
180	185.2	5.4	5.56
191	129.9	7.7	5.24
197	97.1	10.3	5.08
207	45.2	22.1	4.83
213	27.8	36.0	4.69
222	15.0	66.8	4.50
241	4.2	240.1	4.15

Data obtained in this work are displayed as $1/Q_e$ vs. $1/T_e$ (K) in Figure 30.

1.a.2.3. L = dipyridylmethane (DPM).

Table XXVIII . Temperature dependence of the emission quantum yield of $[\text{Ru}(\text{bipy})_2\text{DPM}]^{+2}$.

T (K)	$Q_e \cdot 10^{+3}$	$1/Q_e$	$1/T \text{ (K)} \cdot 10^{+3}$
117	434.8	2.3	8.55
132	416.7	2.4	7.58
146	232.6	4.3	6.85
152	144.9	6.9	6.58
160	71.9	13.9	6.25
168	31.2	32.1	5.95
179	11.6	86.1	5.59
183	8.2	121.8	5.46
191	3.8	261.6	5.24
209	1.1	909.0	4.78

Data obtained in this work are presented as $1/Q_e$ vs. $1/T_e \text{ (K)}$ and are shown in Figure 31.

1.a.2.4. L = dipyridylethane (DPE).

For $[\text{Ru}(\text{bipy})_2\text{DPE}]^{+2}$, the emission intensity above the glass transition temperature ($\sim 95\text{K}$)

was too low for accurate evaluation of quantum yields.

Table XXIX. Parameters of the photophysical properties of polypyridine complexes with a methylene - linked pyridine ligand in EtOH/MeOH (4:1, v/v) , based upon emission intensities.

complex	A	B	$\Delta E(\text{cm}^{-1})$ (a)
$[\text{Ru}(\text{bipy})_3]^{+2}$	7.86	$1.56 \cdot 10^{-9}$	3,951
$[\text{Ru}(\text{bipy})_2(\text{pic})_2]^{+2}$	30.54	$6.67 \cdot 10^{-9}$	3,194
$[\text{Ru}(\text{bipy})_2\text{DPM}]^{+2}$	5.12	$1.80 \cdot 10^{-9}$	3,072

$$A = (k_r + k_{nr}) / k_r$$

$$B = k_o / k_r$$

(a): Energy difference between the LF and the $^3\text{MLCT}$ excited states.

The Figures 30 and 31 are representative of the procedure in which the experimental emission intensities at different temperatures data were analyzed in order to fit the Equation (2) with the purpose of further evaluation of the quantum yield of LF production at 298 K .

$$1 / Q_e = [k_r + k_{nr}] / k_r + [k_o/k_r]e^{-\Delta E/RT}$$

$$1 / Q_e = k + k'e^{-\Delta E/RT} \quad (2)$$

1.a.3. Temperature dependence of the emission quantum yield of complexes $[\text{Ru}(\text{bipy})_2\text{L}]^{+2}$ in CH_3CN .

The temperature dependence of the emission intensity was determined for all these complexes in CH_3CN over the range 273 K - 333 K. The nonlinear Arrhenius plot was fit to Eq. (2) in order to evaluate the probability of population of the LF state at 298 K. Again, the emission of $[\text{Ru}(\text{bipy})_2\text{DPE}]^{+2}$ was so weak that a similar study was not attempted. The collected data are presented in Table XXX.

Table XXX. Parameters of the photophysical properties of polypyridine complexes with a methylene-linked pyridine ligand, in CH_3CN , based upon emission intensities.

Complex	A	B	$\Delta E(\text{cm}^{-1})(a)$	P(a)
$[\text{Ru}(\text{bipy})_3]^{+2}$	11.9	8.4	3,424	0.30
$[\text{Ru}(\text{bipy})_2(\text{pic})_2]^{+2}$	2,548	2,350	3,064	0.64

[Ru(bipy) ₂ DPM] ⁺²	694	3,700	3,578	0.61
---	-----	-------	-------	------

$$A = (k_r + k_{nr}) / k_r$$

$$B = k_o / k_r$$

P = fraction of MLCT excited states that decay via population of the LF state.

(a) : in CH₃CN

1.a.4. Temperature dependence of the emission quantum yield of [Ru(bipy)₂L]⁺² complexes, in CH₂Cl₂, and in H₂O.

Unfortunately, the LF production in these solvents could not be evaluated. Ideally, the emission lifetime should be examined as a function of temperature. However, except for the case of [Ru(bipy)₃]⁺², the emission intensities were so low that the lifetime determinations at 298 K were unfeasable with the available apparatus. Consequently, only the emission intensities were determined as a function of temperature. Nevertheless, in the temperature range 273 - 308 K, the observed variations in intensities could not be fit to Eq.(2) with reasonable coefficients, in contrast to the results obtained in CH₃CN which were comparatively well

behaved. In short, the information gathered about the temperature dependency of these complexes in CH_2Cl_2 and H_2O , had to be disregarded for the present study.

In Tables XXXI and XXXII are presented the respective emission quantum yields of these complexes in CH_3CN and in CH_2Cl_2 .

Table XXXI. Emission properties of $[\text{Ru}(\text{bipy})_2\text{L}]^{+2}$ complexes, in CH_3CN , at 298 K.

Complex	λ_{max}	$\Phi_{\text{e}} \cdot 10^{+2}$
$[\text{Ru}(\text{bipy})_3]^{+2}$	621	6.2(b)
$[\text{Ru}(\text{bipy})_2(\text{pic})_2]^{+2}$	635	0.093
$[\text{Ru}(\text{bipy})_2\text{DPM}]^{+2}$	624	0.190

(b) : Reference⁴⁹.

Table XXXII. Emission properties of $[\text{Ru}(\text{bipy})_2\text{L}]^{+2}$ complexes, in CH_2Cl_2 , at 298 K.

Complex	λ_{max}	$\Phi_{\text{e}} \cdot 10^{+2}$
$[\text{Ru}(\text{bipy})_3]^{+2}$	624	2.9(b)
$[\text{Ru}(\text{bipy})_2(\text{pic})_2]^{+2}$	631	0.04
$[\text{Ru}(\text{bipy})_2\text{DPM}]^{+2}$	626	0.08

(b) : Reference⁴⁹.

1.b. Photochemical Studies.

The photosubstitution quantum yields were determined by means of the procedures described in the experimental section. The disappearance of the starting material was followed by absorption spectroscopy during the reaction's initial stages while an isosbestic point (IP) was still maintained.

The molar absorption coefficients of the $[\text{Ru}(\text{bipy})_2(\text{pic})_2]^{+2}$, $[\text{Ru}(\text{bipy})_2(\text{pic})(\text{H}_2\text{O})]^{+2}$, $[\text{Ru}(\text{bipy})_2(\text{pic})\text{Cl}]^{+1}$, and $\text{cis}-[\text{Ru}(\text{bipy})_2(\text{H}_2\text{O})_2]^{+2}$ complexes, in the appropriate solvents, were evaluated.

For $[\text{Ru}(\text{bipy})_2\text{DPM}]^{+2}$, the intermediate complexes could not be prepared by the usual methods. Consequently, the required molar absorption coefficients of the photoproducts were estimated by examining $[\text{Ru}(\text{bipy})_2\text{DPE}]^{+2}$; this complex was found to be thermally unstable in both a solution 0.01 M

TBACl in CH_2Cl_2 and in 0.50 M H_2SO_4 . Known concentrations of $[\text{Ru}(\text{bipy})_2\text{DPE}]^{+2}$ in CH_2Cl_2 and H_2O were prepared in CH_2Cl_2 and H_2O and the molar absorption coefficients at 450 nm were determined. Next, either TBACl or H_2SO_4 was added, and the $[\text{Ru}(\text{bipy})_2\text{DPE}]^{+2}$ was quantitatively converted to either the monochloro or the monoaquo complex and the molar absorption coefficients were evaluated. For $[\text{Ru}(\text{bipy})_2\text{DPM}]^{+2}$, the same ratio of the molar absorption coefficients of the initial complex and the monosubstituted photoproduct as that found for $[\text{Ru}(\text{bipy})_2\text{DPE}]^{+2}$ was assumed.

The intermediate complex generated in the photolysis of $[\text{Ru}(\text{bipy})_3]^{+2}$ cannot be detected; apparently, this complex reverts to the original compound or proceeds to $[\text{Ru}(\text{bipy})_2\text{Cl}_2]$. The IP maintained throughout the photoreaction seems to indicate that these decay pathways are thermally rapid. Molar absorption coefficients of the disubstituted photoproducts were used in the quantum yield evaluations of $[\text{Ru}(\text{bipy})_3]^{+2}$.

The absorption spectra of all four complexes after extensive photolysis were identical and matched

the absorption spectrum of $[\text{Ru}(\text{bipy})_2\text{Cl}_2]$.

1.b.1. Complex : $[\text{Ru}(\text{bipy})_3]^{+2}$.

1.b.1.1. Photolysis of $[\text{Ru}(\text{bipy})_3]^{+2}$ in a
0.01 M solution of TBACl in CH_2Cl_2 at 298 K .

General experimental conditions :

$[\text{Ru}(\text{bipy})_3]^{+2} \approx 5 \cdot 10^{-5} \text{ M}$.

Light Intensity = $1.53 \cdot 10^{-8}$ einstein/sec .

Total irradiation time = 120 sec .

Molar absorption coefficient of the starting
complex (450 nm) = $15,300 \text{ M}^{-1}\text{cm}^{-1}$.

Molar absorption coefficient of the
photoproduct (450 nm) = $3,900 \text{ M}^{-1}\text{cm}^{-1}$.

A typical series of spectra showing the
photolytic changes in the absorption spectrum for a
total irradiation time of 1,200 sec is shown in Figure
32 .

1.b.1.2. Photolysis of $[\text{Ru}(\text{bipy})_3]^{+2}$ in a
0.01 M solution of TBACl in CH_3CN at 298 K.

General experimental conditions :

$[\text{Ru}(\text{bipy})_3]^{+2} \cong 5 \cdot 10^{-5} \text{ M.}$

Light intensity = $2.75 \cdot 10^{-8} \text{ einstein/sec.}$

Total irradiation time = 120 sec.

Molar absorption coefficient of the starting complex (450 nm) = $14,900 \text{ M}^{-1}\text{cm}^{-1}$.

Molar absorption coefficient of the photoproduct (450 nm) = $3,870 \text{ M}^{-1}\text{cm}^{-1}$.

1.b.1.3. Photolysis of $[\text{Ru}(\text{bipy})_3]^{+2}$ in 0.50 M H_2SO_4 at 298 K.

General experimental conditions :

$[\text{Ru}(\text{bipy})_3]^{+2} \cong 5 \cdot 10^{-5} \text{ M.}$

Light intensity = $3.31 \cdot 10^{-8} \text{ einstein/sec.}$

Total irradiation time = 120 sec.

Molar absorption coefficient of the starting complex (450 nm) = $14,180 \text{ M}^{-1}\text{cm}^{-1}$.

Molar absorption coefficient of the photoproduct (450 nm) = $3,140 \text{ M}^{-1}\text{cm}^{-1}$.

Under these conditions, $[\text{Ru}(\text{bipy})_3]^{+2}$ was photostable, and practically no photoaquation was observed even after very long irradiation times.

1.b.2. Complex : $[\text{Ru}(\text{bipy})_2(\text{pic})_2]^{+2}$.

1.b.2.1. Photolysis of $[\text{Ru}(\text{bipy})_2(\text{pic})_2]^{+2}$
in a 0.01 M solution of TBACl in CH_2Cl_2 at 298 K.

General experimental conditions :

$[\text{Ru}(\text{bipy})_2(\text{pic})_2]^{+2} \cong 5 \cdot 10^{-5} \text{ M.}$

Light intensity = $1.53 \cdot 10^{-8} \text{ einstein/sec.}$

Total irradiation time = 50 sec.

Molar absorption coefficient of the starting complex (450 nm) = $10,385 \text{ M}^{-1}\text{cm}^{-1}$.

Molar absorption coefficient of the photoproduct (450 nm) = $6,178 \text{ M}^{-1}\text{cm}^{-1}$.

The changes in the absorption spectrum that occur during a typical photolysis during a total irradiation time of 1,200 sec are shown in Figure 33 .

1.b.2.2. Photolysis of $[\text{Ru}(\text{bipy})_2(\text{pic})_2]^{+2}$
in a 0.01 M solution of TBACl in CH_3CN at 298 K.

General experimental conditions ;

$[\text{Ru}(\text{bipy})_2(\text{pic})_2]^{+2} \cong 8 \cdot 10^{-5} \text{ M.}$

Light intensity = $2.75 \cdot 10^{-8} \text{ einstein/sec.}$

Total irradiation time = 90 sec.

Molar absorption coefficient of the starting

complex (450 nm) = $9,130 \text{ M}^{-1}\text{cm}^{-1}$.

Molar absorption coefficient of the photoproduct (450 nm) = $6,461 \text{ M}^{-1}\text{cm}^{-1}$.

1.b.2.3. Photolysis of $[\text{Ru}(\text{bipy})_2(\text{pic})_2]^{+2}$
in $0.50 \text{ M H}_2\text{SO}_4$ at 298 K .

General experimental conditions :

$[\text{Ru}(\text{bipy})_2(\text{pic})_2]^{+2} \cong 6 \cdot 10^{-5} \text{ M}$.

Light intensity = $3.31 \cdot 10^{-8} \text{ einstein/sec}$.

Total irradiation time = 30 sec .

Molar absorption coefficient of the starting complex (450 nm) = $9,830 \text{ M}^{-1}\text{cm}^{-1}$.

Molar absorption coefficient of the photoproduct (450 nm) = $7,720 \text{ M}^{-1}\text{cm}^{-1}$.

1.b.3. Complex : $[\text{Ru}(\text{bipy})_2\text{DPM}]^{+2}$.

1.b.3.1. Photolysis of $[\text{Ru}(\text{bipy})_2\text{DPM}]^{+2}$
in a 0.01 M solution of TBACl in CH_2Cl_2 at 298 K .

General experimental conditions :

$[\text{Ru}(\text{bipy})_2\text{DPM}]^{+2} \cong 7 \cdot 10^{-5} \text{ M}$.

Light intensity = $1.53 \cdot 10^{-8} \text{ einstein/sec}$.

Total irradiation time = 50 sec .

Molar absorption coefficient of the starting complex (450 nm) = $9,994 \text{ M}^{-1}\text{cm}^{-1}$.

Molar absorption coefficient of the photoproduct (450 nm) = $5,014 \text{ M}^{-1}\text{cm}^{-1}$.

The changes in the absorption spectrum that occur during a typical photolysis during a total irradiation time of 1,200 sec are shown in Figure 34.

1.b.3.2. Photolysis of $[\text{Ru}(\text{bipy})_2\text{DPM}]^{+2}$ in a 0.01 M solution of TBACl in CH_3CN at 298 K.

General experimental conditions ;

$[\text{Ru}(\text{bipy})_2\text{DPM}]^{+2} \cong 5 \cdot 10^{-5} \text{ M}$.

Light intensity = $2.75 \cdot 10^{-8} \text{ einstein/sec}$.

Total irradiation time = 90 sec.

Molar absorption coefficient of the starting complex (450 nm) = $8,963 \text{ M}^{-1}\text{cm}^{-1}$.

Molar absorption coefficient of the photoproduct (450 nm) = $6,132 \text{ M}^{-1}\text{cm}^{-1}$.

1.b.3.3. Photolysis of $[\text{Ru}(\text{bipy})_2\text{DPM}]^{+2}$ in 0.50 M H_2SO_4 at 298 K.

General experimental conditions :

$[\text{Ru}(\text{bipy})_2\text{DPM}]^{+2} \cong 7 \cdot 10^{-5} \text{ M.}$

Light intensity = $3.31 \cdot 10^{-8} \text{ einstein/sec.}$

Total irradiation time = 60 sec.

Molar absorption coefficient of the starting complex (450 nm) = $10,440 \text{ M}^{-1}\text{cm}^{-1}.$

Molar absorption coefficient of the photoproduct (450 nm) = $8,240 \text{ M}^{-1}\text{cm}^{-1}.$

1.b.4. Complex : $[\text{Ru}(\text{bipy})_2\text{DPE}]^{+2}.$

1.b.4.1. Photolysis of $[\text{Ru}(\text{bipy})_2\text{DPE}]^{+2}$ in CH_2Cl_2 0.01 M TBACl at 298 K.

This complex was thermally unstable when TBACl was added to the CH_2Cl_2 solution. The initial spectrum had an absorption maximum located at 450 nm and after the addition of the chloride salt, a new maximum became evident at 504 nm. It was determined that this monochloro intermediate (vide infra) was stable in the dark for at least one hour. A sample of the intermediate complex, was photolyzed after it was stored 30 min in the dark .

General experimental conditions :

" $[\text{Ru}(\text{bipy})_2\text{Cl}(\text{py}' - \text{CH}_2\text{CH}_2 - \text{py})]^{+1}$ "

$\approx 9.1 \cdot 10^{-5} \text{ M.}$

Light intensity = $1.53 \cdot 10^{-9} \text{ einstein/sec.}$

Total irradiation time = 30 sec.

Molar absorption coefficient of the monochloro intermediate (510 nm) = $8,794 \text{ M}^{-1}\text{cm}^{-1}$.

Molar absorption coefficient of the photoproduct (510 nm) = $5,013 \text{ M}^{-1}\text{cm}^{-1}$.

The changes in the absorption spectrum that occur during a typical photolysis during a total irradiation time of 1,200 sec are shown in Figure 35.

1.b.4.2. Photolysis of $[\text{Ru}(\text{bipy})_2\text{DPE}]^{+2}$ in a 0.01 M solution of TBACl in CH_3CN at 298 K .

General experimental conditions :

$[\text{Ru}(\text{bipy})_2\text{DPE}]^{+2} \approx 6 \cdot 10^{-5} \text{ M.}$

Light intensity = $2.75 \cdot 10^{-9} \text{ einstein/sec.}$

Total irradiation time = 90 sec.

Molar absorption coefficient of the starting complex (450 nm) = $10,442 \text{ M}^{-1}\text{cm}^{-1}$.

Molar absorption coefficient of the photoproduct (450 nm) = $6,871 \text{ M}^{-1}\text{cm}^{-1}$.

1.b.4.3. Photolysis of $[\text{Ru}(\text{bipy})_2\text{DPE}]^{+2}$ in

0.50 M H_2SO_4 at 298 K.

As in a 0.01 M solution of TBACl in CH_2Cl_2 , where the starting complex was thermally unstable, $[\text{Ru}(\text{bipy})_2\text{DPE}]^{+2}$ was also unstable in this medium, 0.50 M H_2SO_4 ; solvolysis produced the monoaquo complex. The intermediate in aqueous acidic solutions was also thermally stable, but upon photolytic irradiation underwent photosubstitution readily.

Unfortunately, the photolysis experiments, designed to determine quantum yields, led to widely varying results ($Q_{ph} = 0.35$ to 1.0) and showed little reproducibility. At least, a value of 0.3 could be clearly established as a lower limit.

The collected values of the quantum yields of photosubstitution for these complexes at 298 K along with those of $[\text{Ru}(\text{bipy})_3]^{+2}$ reported previously⁴⁹ are shown in Table XXXIII. Also reported in the same Table XXXIII are the calculated quantum yields for LF formation .

Table XXXIII. Quantum yields of photosubstitution and of production of the higher lying

LF state for bis(bipy) , methylene - linked pyridine ruthenium complexes at 298 K .

Complex	CH ₂ Cl ₂ (a)		CH ₃ CN (a)		0.50 M H ₂ SO ₄	
	(b)	(c)	(b)	(c)	(b)	(c)
[Ru(bipy) ₃] ²⁺	0.04	0.93(d)	0.003	0.54(d)	<1.10 ⁻⁴	0.22(d)
[Ru(bipy) ₂ (pic) ₂] ²⁺	0.17	1.0	0.21	1.0	0.24	1.0
[Ru(bipy) ₂ DPM] ²⁺	0.21	1.0	0.24	1.0	0.04	1.0
[Ru(bipy) ₂ DPE] ²⁺	0.58(e)	---	0.18	---	<0.3(e)	---

(a) : Solution 0.01 M in TBACl.

(b) : Q_{ph} : Photosubstitution quantum yield;
average of value obtained for at least three photolysis carried out under the general conditions previously tabulated. Data were analyzed with available program described in experimental section.

(c) : Q_{LF} : Quantum yield of LF production.

(d) : Reference⁴⁹.

(e) : Photolysis of intermediate complex , since the starting material was thermally unstable.

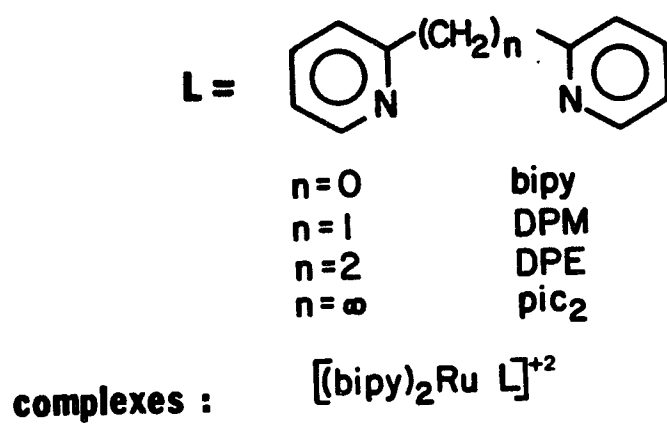


Figure 29. Methylene - linked pyridine ligands.

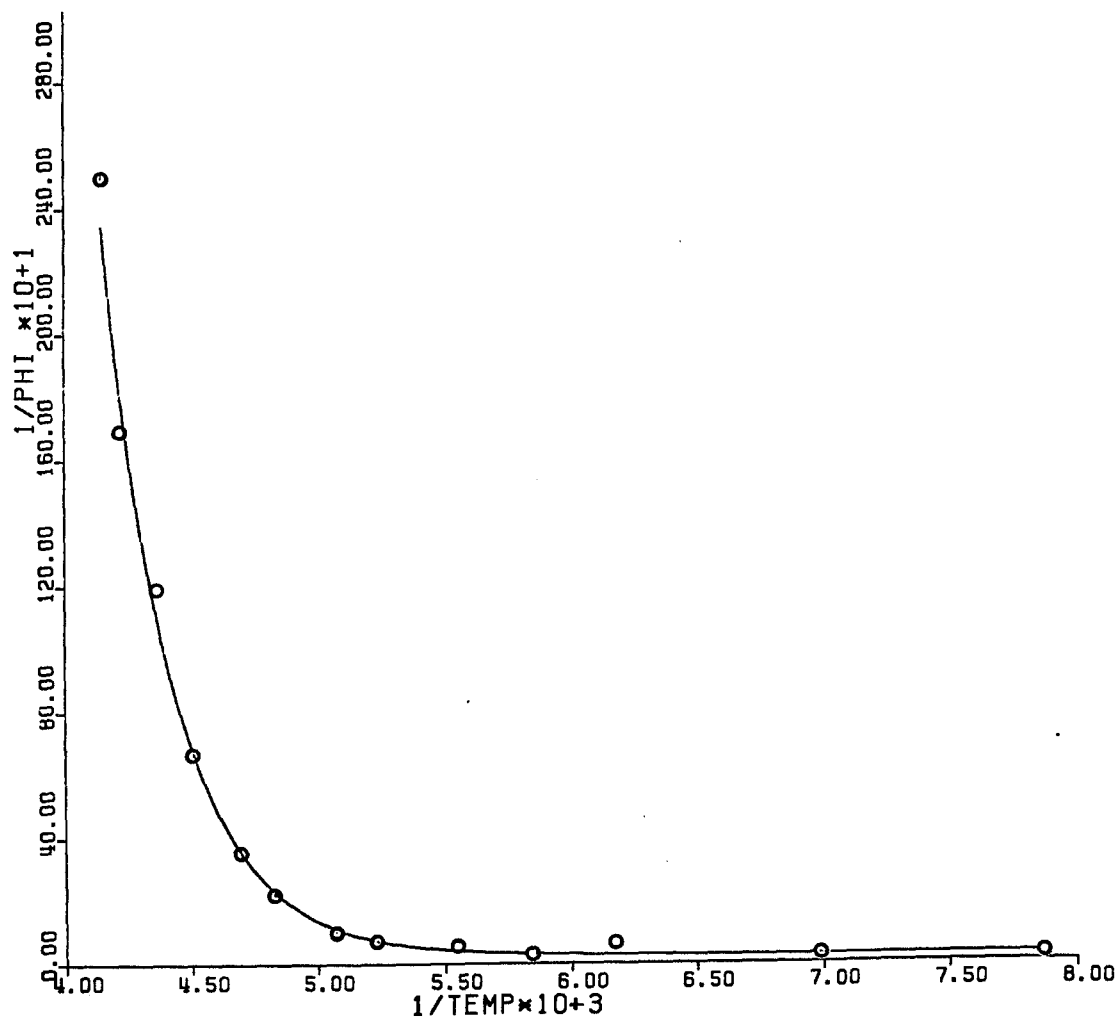


Figure 30 . Temperature dependence of the relative emission intensities of $[\text{Ru}(\text{bipy})_2(\text{pic})_2]^{+2}$ in EtOH/MeOH (4:1,v/v). The solid curve is the computer fit generated using the parameters given in Table XXIX.

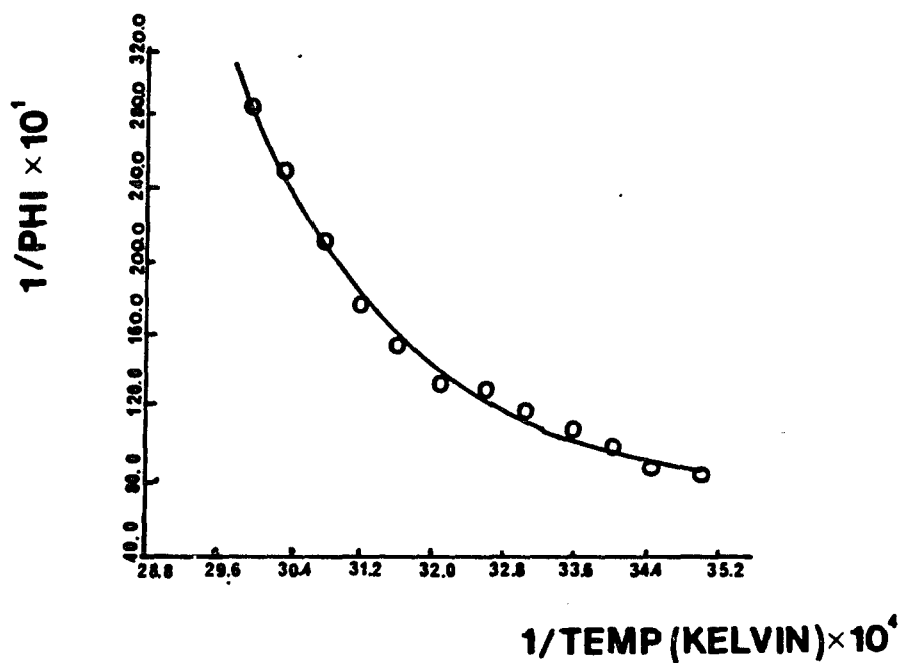


Figure 31 . Temperature dependence of the relative emission intensities of $[\text{Ru}(\text{bipy})_2\text{DPM}]^{2+}$ in EtOH/MeOH (4:1, v/v). The solid curve is the computer fit generated from the parameters given in Table XXIX.

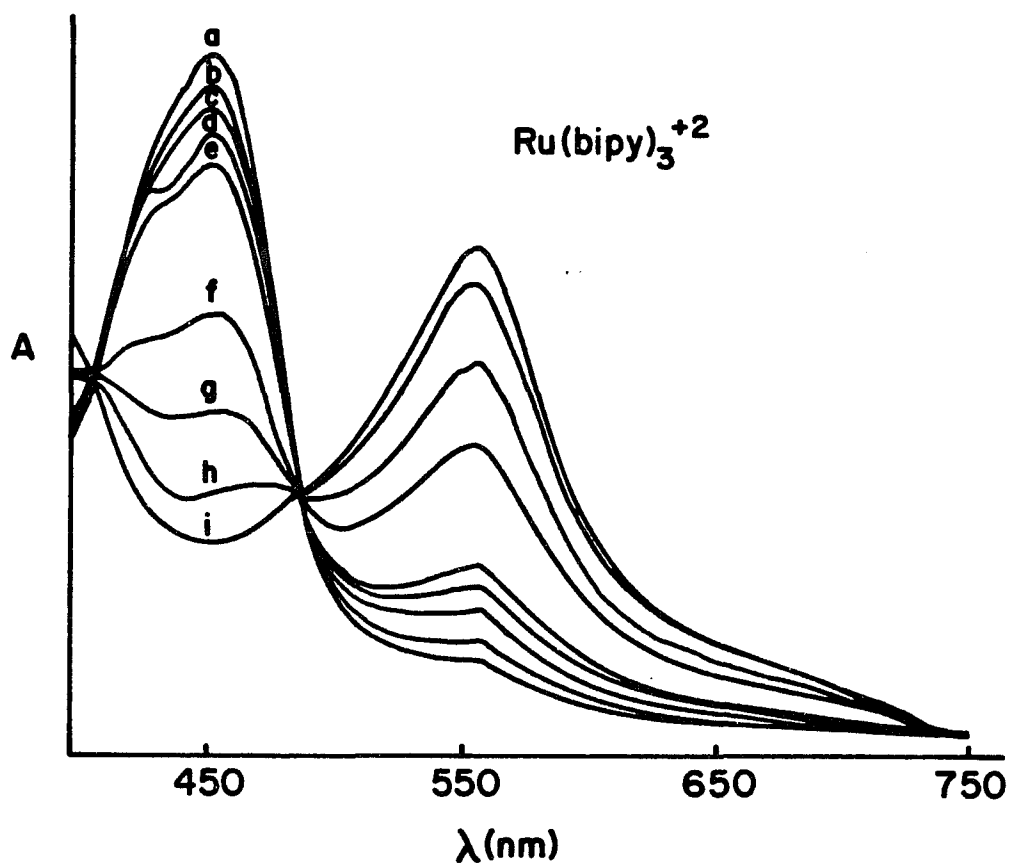


Figure 32 . Absorption spectra during the photolysis of $[\text{Ru}(\text{bipy})_3]^{+2}$ in 0.01 M TBACl in CH_2Cl_2 . The photolysis times (in seconds) are : curve a, 0; curve b, 15; curve c, 30; curve d, 45; curve e, 60; curve f, 180; curve g, 300; curve h, 600; curve i, 1,200.

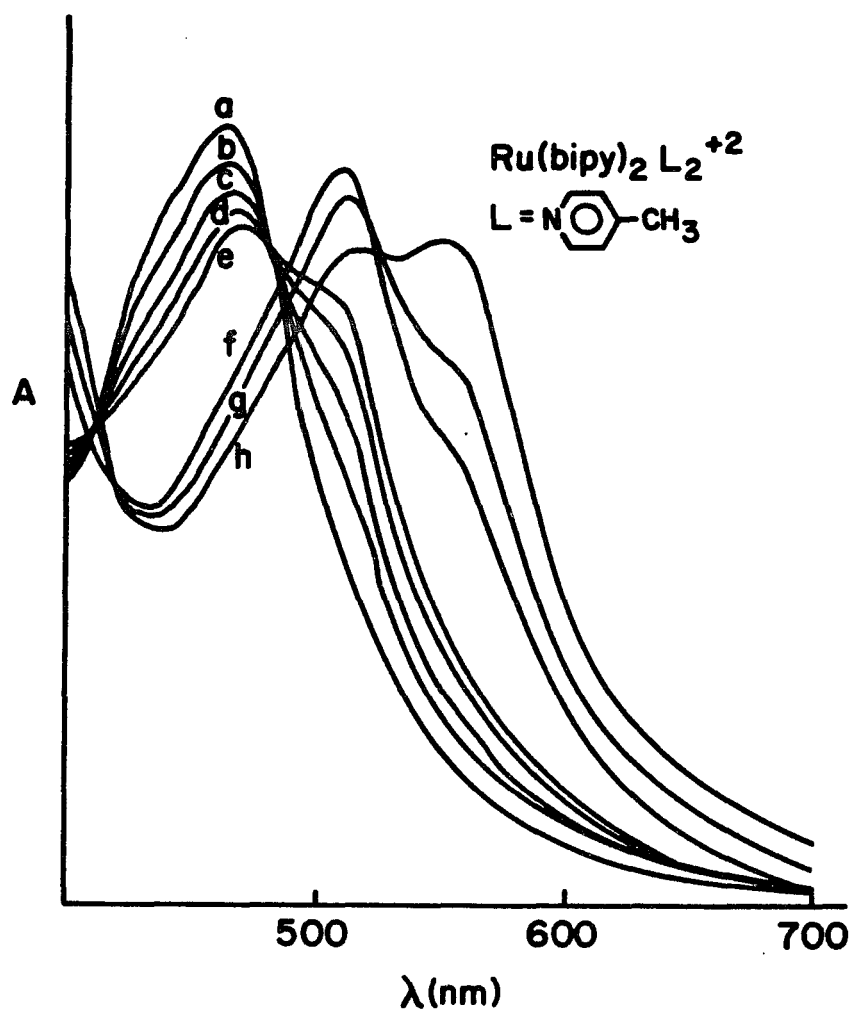


Figure 33 . Absorption spectra during the photolysis of $[\text{Ru(bipy)}_2(\text{pic})_2]^{+2}$ in 0.01 M TBACl in CH_2Cl_2 . The photolysis times (in seconds) are : curve a, 0; curve b, 15; curve c, 30; curve d, 45; curve e, 60; curve f, 180; curve g, 300; curve h, 600; curve i, 1,200.

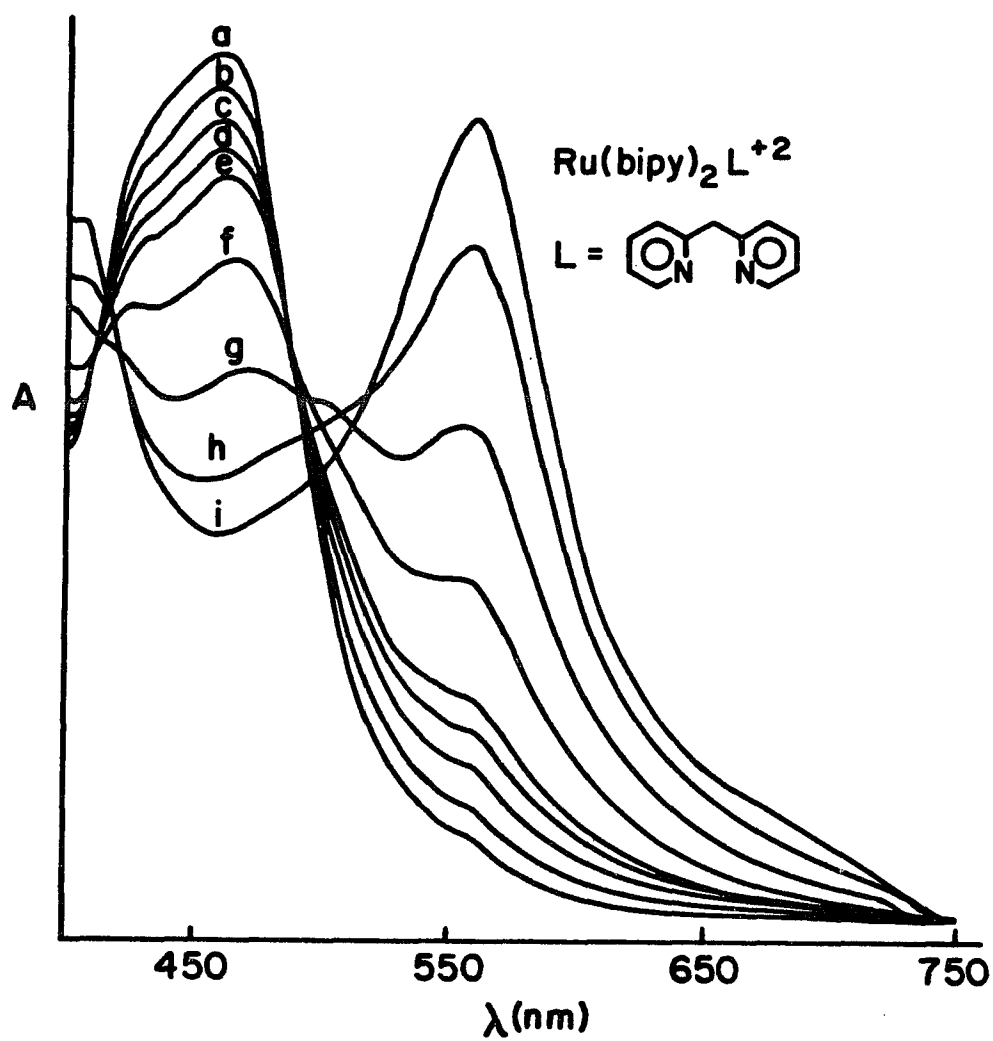


Figure 34 . Absorption spectra during the photolysis of $[\text{Ru}(\text{bipy})_2\text{DPM}]^{+2}$ in 0.01 M TBACl in CH_2Cl_2 . The photolysis times (in seconds) are : curve a, 0; curve b, 15; curve c, 30; curve d, 45; curve e, 60; curve f, 180; curve g, 300; curve h, 600; curve i, 1,200.

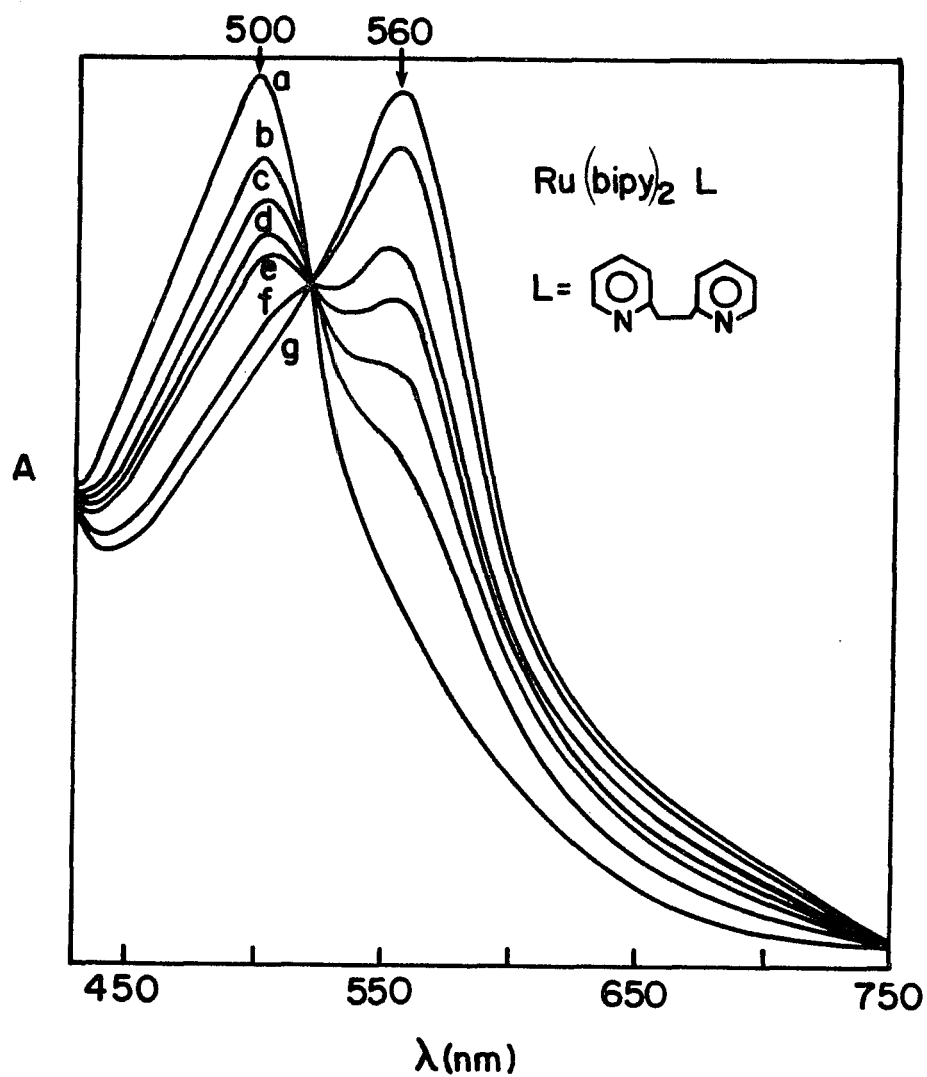


Figure 35 . Absorption spectra during the photolysis of $[\text{Ru}(\text{bipy})_2\text{Cl}(\text{py}' - \text{CH}_2\text{CH}_2 - \text{py})]^{+1}$ in 0.01 M TBACl in CH_2Cl_2 . The photolysis times (in seconds) are : curve a, 0; curve b, 15; curve c, 30; curve d, 45; curve e, 60; curve f, 180; curve g, 300; curve h, 600; curve i, 1,200.

2. Complexes $[\text{Ru}(\text{bipy})_2\text{L}]^{+2}$ in which the L's are methylene - linked diamine ligands .

2.a.Photophysical properties.

2.a.1. Emission properties at 77 K .

The 77 K emission quantum yields of the complexes $[\text{Ru}(\text{bipy})_2\text{L}]^{+2}$, in which the ligands, L , are those shown in Figure 36, were determined in EtOH/MeOH (4:1, v/v). The results are shown in Table XXXIV.

Table XXXIV. Emission properties of the bis (bipy) - methylene - linked diamine ruthenium complexes at 77 K.

Complex	λ_{max} (nm)	Q_e	T_e (μsec) (a)	A(b)	B(c)
$[\text{Ru}(\text{bipy})_3]^{+2}$	578	0.376(d)	5.21	7.2	1.2
$[\text{Ru}(\text{bipy})_2(\text{en})]^{+2}$	670	0.034	0.96(d)	3.5	10.1
$[\text{Ru}(\text{bipy})_2(\text{tn})]^{+2}$	675	0.023	----	---	---

(a): At 77 K in EtOH/MeOH (4:1, v/v).

(b): $A = k_r \cdot 10^{+4}$; calculated from $k_r = Q_e / T_e$

(c): $B = k_{nr} \cdot 10^{+5}$;calculated from $k_{nr} = 1/T_e - k_r$

(d) Reference⁸⁶.

Note : The emission quantum yields of $[\text{Ru}(\text{bipy})_2(\text{en})]^{+2}$, and $[\text{Ru}(\text{bipy})_2(\text{tn})]^{+2}$ were evaluated by means of the standard procedure described in the experimental section. λ_{exc} was 475 nm for all three complexes and the 530 - 830 nm emission range was scanned. Integrals of the corrected emission spectra presented in wavenumbers were evaluated. The excitation slitwidth was permanently set at 16.0. For the standard, $[\text{Ru}(\text{bipy})_3]^{+2}$, the emission slitwidth was set at 1.0, and in order to obtain a sufficiently high intensity for the other complexes a setting of 8.0 was necessary. Consequently, a correction factor of 37.63 previously presented in the calibration curve at 77 K in the experimental section (Table II) was used by means of the simplified expression :

$$Q_x = [Q_s(I_x/I_s)] / 37.63$$

2.a.2. Emission quantum yields at 298 K.

2.a.2.1. Solvent : EtOH/MeOH (4:1,v/v).

Table XXXV. Emission quantum yields of bis(bipy) - methylene - linked diamine ruthenium

complexes in EtOH/MeOH (4:1, v/v) at 298 K.

complex	λ_{max}	Q_e
$[Ru(bipy)_3]^{+2}$	610	0.029 ⁸⁷
$[Ru(bipy)_2(en)]^{+2}$	672	0.0017
$[Ru(bipy)_2(tn)]^{+2}$	681	0.0013

2.a.2.2. Solvent : H₂O.

Table XXXVI. Emission quantum yields of bis(bipy) - methylene - linked diamine ruthenium complexes in H₂O at 298 K .

complex	λ_{max}	Q_e
$[Ru(bipy)_3]^{+2}$	614	0.042 ⁴¹
$[Ru(bipy)_2(en)]^{+2}$	691	0.0015
$[Ru(bipy)_2(tn)]^{+2}$	702	0.0012

Note : Again, λ_{exc} was 475 nm for the three complexes and the 530 - 830 nm range was scanned. The excitation slitwidth was set at 16.0. In this case, for $[Ru(bipy)_3]^{+2}$, the emission slitwidth was set at 2.0 while for the other complexes a setting of 16.0 was necessary.

Therefore, a correction factor of 169.31/3.83

= 44.21 , obtained by means of the values presented in the calibration curve for 298 K, (Table I), was used in the following simplified expression :

$$Q_x = [Q_{\infty} (I_x / I_{\infty})] / 44.21 .$$

2.a.3. Temperature dependence of the emission quantum yield of complexes $[Ru(bipy)_2L]^{+2}$ in EtOH/MeOH (4:1, v/v).

2.a.3.1. L = 2,2' - bipyridine (bipy).

The emission parameters are reported in Table XXXVII. They were taken from the literature³⁶.

2.a.3.2. L = ethylenediamine (en) .

Data obtained in this work were plotted as $1/Q_{\infty}$ vs. $1/T$ (K) and are presented in Fig. 37.

2.a.3.3. L = trimethylenediamine (tn) .

Data obtained in this work were plotted as $1/Q_{\infty}$ vs. $1/T$ (K) and are presented in Fig.38.

The parameters obtained for these polypyridine complexes when the non - linear Arrhenius plot was fitted to Eq. (2) are displayed in Table XXXVII.

Table XXXVII. Parameters of the photophysical properties of polypyridine complexes with a methylene - linked diamine ligand based upon emission intensities.

complex	A(a)	B(b)	$\Delta E(\text{cm}^{-1})$ (c)
$[\text{Ru}(\text{bipy})_3]^{+2}$	7.86	$1.56 \cdot 10^{-9}$	3,951
$[\text{Ru}(\text{bipy})_2(\text{en})]^{+2}$	8.51	$1.72 \cdot 10^{-9}$	3,114
$[\text{Ru}(\text{bipy})_2(\text{tn})]^{+2}$	7.14	$1.48 \cdot 10^{-9}$	2,814

(a) : $A = (k_f + k_{nr}) / k_f$

(b) : $B = k_e / k_f$

(c) : Energy difference between the LF and the $^3\text{MLCT}$ excited states.

2.a.4. Determination of lifetimes of complexes at 298 K.

Table XXXVIII. Lifetimes of polypyridine complexes with a methylene - linked diamine ligand at 298 K.

complex	CH_2Cl_2 (a)	CH_2Cl_2 0.01 M TEACl (b)
$[\text{Ru}(\text{bipy})_2(\text{en})]^{+2}$	227	119

$[\text{Ru}(\text{bipy})_2(\text{tn})]^{+2}$ 168 113

(a) Average of two measurements ; units are nsec.

(b) One measurement only.

2.a.5. Quenching of emission of
 $[\text{Ru}(\text{bipy})_2(\text{en})]^{+2}$ at 298 K.

2.a.5.1. In CH_2Cl_2 by Ferrocene.

Table XXXIX. Quenching of the emission of
 $[\text{Ru}(\text{bipy})_2(\text{en})]^{+2}$ in CH_2Cl_2 at 298 K by
 Ferrocene.

[Ferr] $\cdot 10^{-4}$, M	I_0/I (a)
0.00	1.00
1.69	1.19
3.37	1.47
5.05	1.73
6.73	1.91
8.41	2.17
11.19	2.49
slope (Ksv), M^{-1}	1360 ± 30

(a) : The emission spectra were corrected and integrated over the range 550 - 820 nm. Three runs were averaged. $\lambda_{exc} = 490$ nm. The slitwidths of both the excitation and emission monochromators were set at 16.0.

(b): $k_q = 1360 / T_{oe} = 6.0 \cdot 10^9 \text{ M}^{-1}\text{sec}^{-1}$.

(c): $[\text{Quencher}] = [Q] = (M(Q) \cdot v) / (3,000 + v)$

where $M(Q)$ = molarity of stock solution of quencher and v = volume of quencher solution added from microsyringe (μl)

2.a.5.2. In a 0.01 M solution of TEACl in CH_2Cl_2 by Ferrocene.

Table XXXX. Quenching of the emission of $[\text{Ru}(\text{bipy})_2(\text{en})]^{+2}$ in a 0.01 M solution of TEACl in CH_2Cl_2 at 298 K by Ferrocene.

$[\text{Ferr}] \cdot 10^4, \text{ M}$	$(I_0/I)_{app} (a)$	$(I_0/I)_{corr} (b)$
0.00	1.00	1.00
5.62	1.21	1.16
11.19	1.43	1.32

22.24	1.87	1.61
33.14	2.46	1.97
43.90	3.04	2.27
slope(Ksv), M ⁻¹	-----	290 ±10

(a): The experimental conditions are the same as those reported in (a) of the previous Table XXXIX.

$$(b): \quad (I_0/I)_{\text{corr}} = (I_0/I)_{\text{app}} \{ [1 - 10^{-(AD + AQ)}] / [1 - 10^{-AD}] \} \{ AD / [AD + AQ] \}.$$

This correction was made in order to remove a detected curvature in the Stern - Volmer plot due to an inner filter effect produced by high concentrations of the quencher (Fig. 39).

$$(c): \quad k_q \text{ (Cl}^-) = 290 / T_{0.1} \text{ (Cl}^-) = 2.44 \cdot 10^{+9} \text{ M}^{-1}\text{sec}^{-1}.$$

2.a.5.3. In CH₂Cl₂ by Anthracene.

Table XXXXI. Quenching of the emission of
 $[\text{Ru}(\text{bipy})_2(\text{en})]^{+2}$ in CH_2Cl_2 at 298 K by Anthracene.

$[\text{An}] \cdot 10^{+5}, \text{M}$	$I_0/I(a)$
0.00	1.00
3.78	1.05
7.54	1.17
15.03	1.28
22.48	1.38

slope (Ksv), M^{-1} 1729 ± 20

(a) : The experimental conditions are the same as those reported in (a) of the Table XXXIX.

(b) : $k_q = 1729 / T_{0e} = 7.62$
 $\cdot 10^{+9} \text{M}^{-1} \text{sec}^{-1}$.

2.a.5.4. In a 0.01 M solution of TEACl in CH_2Cl_2 by Anthracene.

Table XXXXII. Quenching of the emission of
 $[\text{Ru}(\text{bipy})_2(\text{en})]^{+2}$ in a 0.01 M solution of TEACl in

CH_2Cl_2 at 298 K by Anthracene.

$[\text{An}] \cdot 10^4, \text{ M}$	$I_0/I \text{ (a)}$
0.00	1.00
1.86	1.07
3.70	1.14
5.51	1.27
7.30	1.34
10.80	1.59
13.38	1.73

slope (Ksv), M^{-1} 562 ± 10

(a) : The experimental conditions are the same as those reported in (a) of the Table XXXIX.

(b) : $k_a (\text{Cl}^-) = 562 / T_{0\infty} (\text{Cl}^-) = 4.72 \cdot 10^{10} \text{ M}^{-1}\text{sec}^{-1}$.

2.a.5.5. In CH_2Cl_2 by 1,1' Dimethyl 4,4' bipyridinium dichloride.

Although a perfectly linear Stern - Volmer plot was obtained, the determined value of k_a reached $1.6 \cdot 10^{10} \text{ M}^{-1}\text{sec}^{-1}$, which exceeds the diffusional limit of the rate constant, value estimated as $1.45 \cdot 10^{10} \text{ M}^{-1}\text{sec}^{-1}$ \approx .

2.a.5.6. In a 0.01 M solution of TEACl in CH_2Cl_2 by 1,1' Dimethyl 4,4' bipyridinium dichloride .

Again, there were problems ; $k_q (\text{Cl}^-)$ became $1.35 \cdot 10^{+10} \text{ M}^{-1}\text{sec}^{-1}$, a value extremely close to the previously estimated diffusional limit.

2.a.5.7. In CH_2Cl_2 by 1,2,4,5 - Tetracyanobenzene (TCNB).

2.a.5.8. In a 0.01 M solution of TEACl in CH_2Cl_2 by 1,2,4,5 - Tetracyanobenzene .

The last couple of experiments, 2.a.5.7. and 2.a.5.8. did not work well because no noticeable quenching of the emission intensity could be observed even when the TCNB concentrations were high. No further attempt to use this quencher was made.

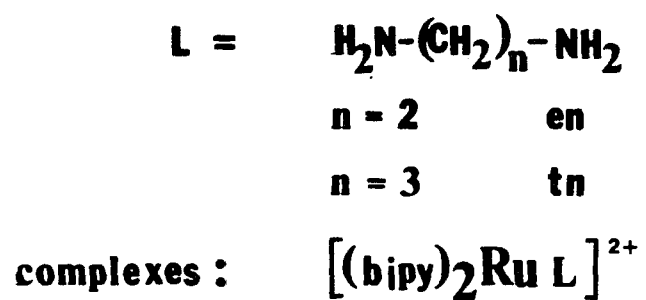


Figure 36 . Methylene - linked amine ligands.

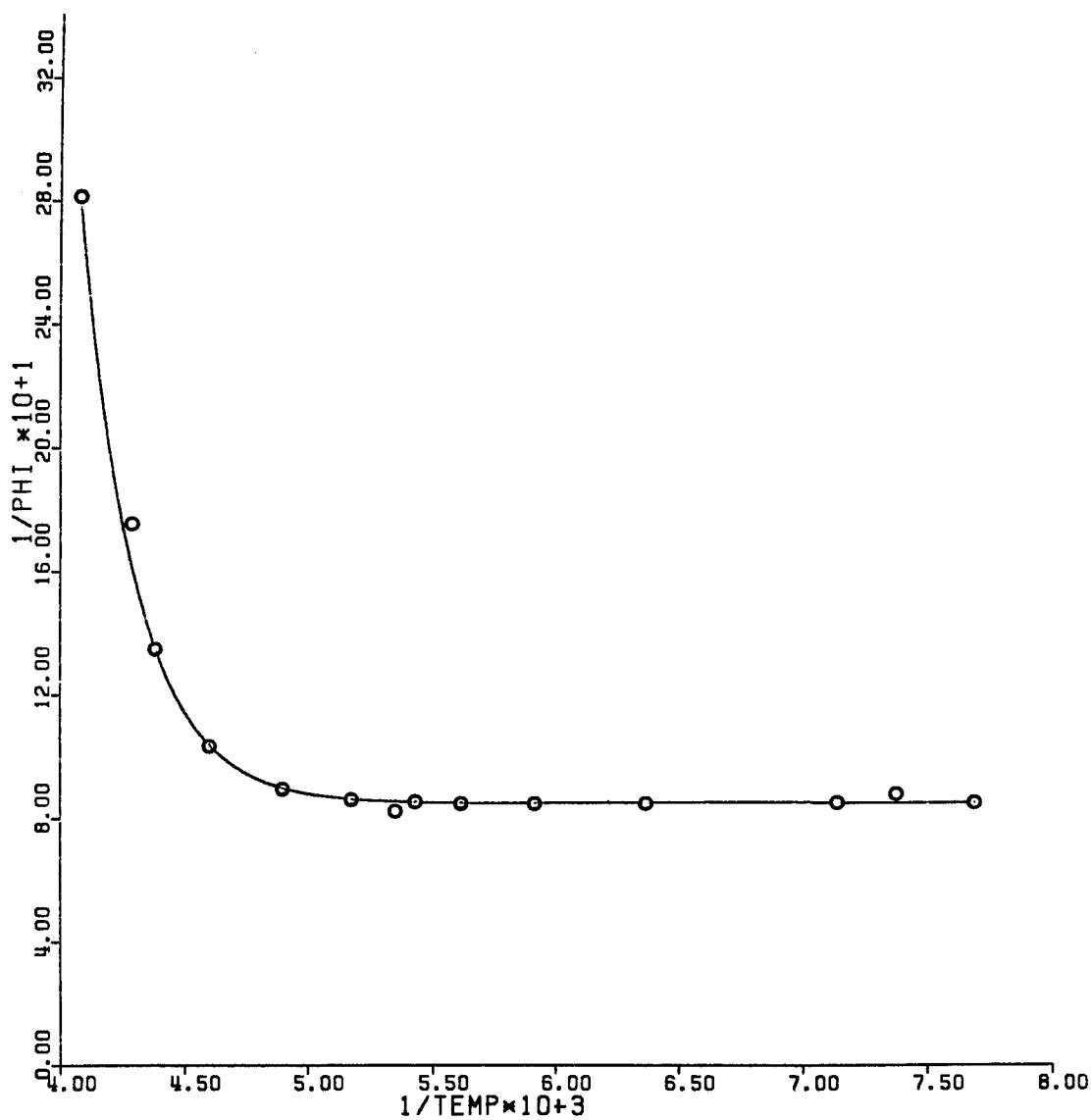


Figure 37 . Temperature dependence of the relative emission intensities of $[\text{Ru}(\text{bipy})_2(\text{en})]^{+2}$ in EtOH/MeOH (4:1,v/v). The solid curve is the computer fit generated from the parameters given in Table XXXVII.

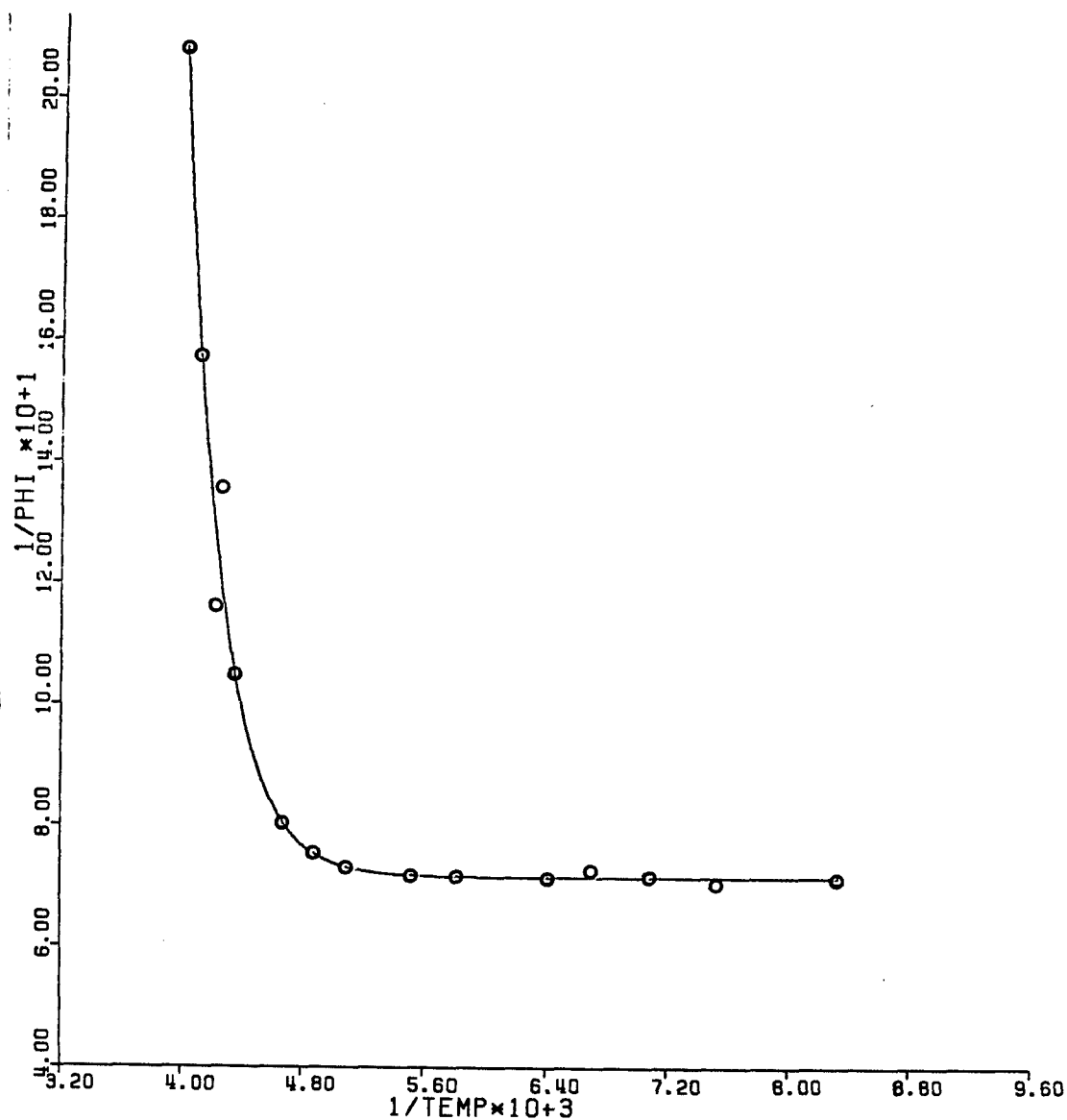


Figure 38 . Temperature dependence of the relative emission intensities of $[\text{Ru}(\text{bipy})_2(\text{tn})]^{+2}$ in EtOH/MeOH (4:1,v/v). The solid curve is the computer fit generated from the parameters given in Table XXXVII.

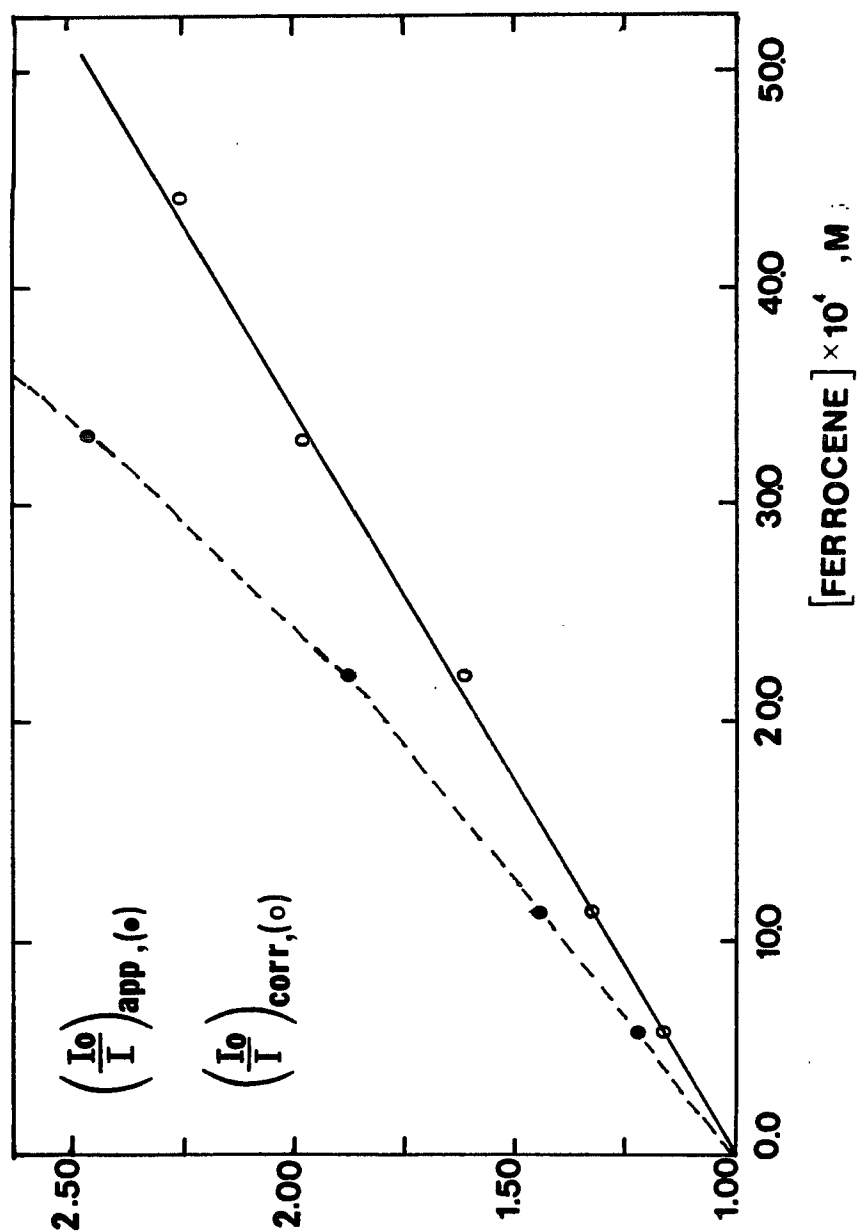


Figure 39 . Stern - Volmer plot of the quenching of the emission of $[Ru(bipy)_2(en)]^{+2}$ in a 0.01 M solution of TEACl in CH_2Cl_2 at 298 K by Ferrocene.

2.b. Photochemical Studies carried out at 298 K.

In these photolysis experiments the desired MLCT excitation band (500 nm) was isolated by means of a combination of two Corning glass filters (CS 4 - 74 and CS 3 - 70).

The observed photosubstitution reactions were very slow. The intermediate complexes generated during the photolysis could not be prepared by the usual methods. The quantum yields were determined by means of monitoring both the disappearance of the starting material and the generation of the final photoproduct that was detected.

2.b.1. Complex : $[\text{Ru}(\text{bipy})_2(\text{en})]^{+2}$.

2.b.1.1. Extensive photolysis in CH_3CN (no Cl^-).

A shift in the absorption λ_{max} from 490 to 455 nm was observed.

2.b.1.2. Extensive photolysis in H_2O (no Cl^-).

A shift in the absorption λ_{max} from 490 to 445 nm was observed .

2.b.1.3. Extensive photolysis in CH_2Cl_2
(no Cl^-).

A shift in the absorption λ_{max} from 490 to 472 nm was observed .

The spectral changes produced when $[\text{Ru}(\text{bipy})_2(\text{en})]^{+2}$ was irradiated under the extensive photolytic conditions described in these experiments, above, are shown in Figures 40 to 42. In each case, the dissolved complex was irradiated for about 10 hours, without using any kind of filter to isolate a specific irradiation band in order to accelerate the rate of photoreaction; it was only intended to observe the characteristics of the final absorption spectrum after prolonged irradiation.

2.b.1.4. Photolysis in a 0.01 M solution of TEACl in CH_3CN .

General experimental conditions :

$[\text{Ru}(\text{bipy})_2(\text{en})]^{+2} \cong 8.2 \cdot 10^{-3}$ M.

Light intensity = $5.68 \cdot 10^{-9}$ einstein/sec.

Total irradiation time = 40 min.

Molar absorption coefficient of the starting complex (490 nm) = $9,700 \text{ M}^{-1}\text{cm}^{-1}$

Molar absorption coefficient of the photoproduct (490 nm) = $4,700 \text{ M}^{-1}\text{cm}^{-1}$.

There was extensive photolytic irradiation until no further absorption spectral changes were detected; a shift in λ_{max} from 490 to 556 nm occurred (Fig 48).

2.b.1.5. Photolysis in a 0.01 M solution of TEACl in H_2O .

General experimental conditions :

$[\text{Ru}(\text{bipy})_2(\text{en})]^{+2} \approx 8.5 \cdot 10^{-5} \text{ M}$.

Light intensity = $3.62 \cdot 10^{-9} \text{ einstein/sec}$.

Total irradiation time = 100 min.

Molar absorption coefficient of the starting complex (490 nm) = $9,400 \text{ M}^{-1}\text{cm}^{-1}$.

Molar absorption coefficient of the photoproduct (490 nm) = $7,800 \text{ M}^{-1}\text{cm}^{-1}$.

Photolysis showed that there was a very slow reaction, the course of which was difficult to follow because of a masking of its absorption by that of the starting complex. Nevertheless, a final photoproduct with an absorption maximum located at 472 nm was

detected (Figure 49).

2.b.1.6. Photolysis in a 0.01 M solution of TEACl in CH_2Cl_2 .

General experimental conditions :

$[\text{Ru}(\text{bipy})_2(\text{en})]^{+2} \approx 7.97 \cdot 10^{-5} \text{ M.}$

Light intensity = $5.68 \cdot 10^{-8} \text{ einstein/sec.}$

Total irradiation time = 60 min.

Molar absorption coefficient of the starting complex (490 nm) = $10,100 \text{ M}^{-1}\text{cm}^{-1}$

Molar absorption coefficient of the photoproduct (490 nm) = $4,700 \text{ M}^{-1}\text{cm}^{-1}$.

There was extensive photolytic irradiation until no further absorption spectral changes were detected; the major observation was that a shift in the λ_{max} from 490 to 548 nm occurred (Figure 50) ; also a small bump was noted at 470 nm.

2.b.2. Complex : $[\text{Ru}(\text{bipy})_2(\text{tn})]^{+2}$.

2.b.2.1. Extensive photolysis in CH_3CN (no Cl^-).

A shift in the absorption maximum from 490 to

430 nm was observed.

2.b.2.2. Extensive photolysis in H_2O (no Cl^-).

A shift in the absorption maximum from 490 to 480 nm was observed .

2.b.2.3. Extensive photolysis in CH_2Cl_2 (no Cl^-).

A shift in the absorption maximum from 490 to 481 nm was observed.

The spectral changes produced when $[Ru(bipy)_2(tn)]^{+2}$ was irradiated under the extensive photolytic conditions described in these experiments, above, are shown in Figures 43 to 45.

2.b.2.4. Photolysis in a 0.01 M solution of TEACl in CH_3CN .

General experimental conditions :

$[Ru(bipy)_2(tn)]^{+2} \cong 9.1 \cdot 10^{-5} M$.

Light intensity = $5.68 \cdot 10^{-2}$ einstein/sec.

Total irradiation time = 40 min.

Molar absorption coefficient of the starting complex (490 nm) = $8,900 M^{-1}cm^{-1}$.

Molar absorption coefficient of the

photoproduct (490 nm) = $4,900 \text{ M}^{-1}\text{cm}^{-1}$.

Extensive photolytic irradiation led to a final absorption spectrum that had λ_{max} at 550 relative to 490 for the original material (Figure 51) .

2.b.2.5. Photolysis in a 0.01 M solution of TEACl in H_2O .

General experimental conditions :

$[\text{Ru}(\text{bipy})_2(\text{tn})]^{+2} \cong 9.0 \cdot 10^{-5} \text{ M}$.

Light intensity = $3.62 \cdot 10^{-8} \text{ einstein/sec}$.

Total irradiation time = 80 min.

Molar absorption coefficient of the starting complex (490 nm) = $9,090 \text{ M}^{-1}\text{cm}^{-1}$.

Molar absorption coefficient of the photoproduct (490 nm) = $7,800 \text{ M}^{-1}\text{cm}^{-1}$.

Photolysis showed the occurrence of a very slow reaction. The reaction was difficult to follow because the absorbance of the photoproduct was masked by that of the starting complex. However, extensive photolytic irradiation produced a species with an absorption spectrum that had a maximum located at 470 nm (Figure 52).

2.b.2.6. Photolysis in a 0.01 M solution of TEACl in CH_2Cl_2 .

General experimental conditions :

$[\text{Ru}(\text{bipy})_2(\text{tn})]^{+2} \cong 9.0 \cdot 10^{-5} \text{ M}$.

Light intensity = $5.68 \cdot 10^{-9}$ einstein/sec.

Total irradiation time = 40 min.

Molar absorption coefficient of the starting complex (490 nm) = $9,020 \text{ M}^{-1}\text{cm}^{-1}$.

Molar absorption coefficient of the photoproduct (490 nm) = $4,900 \text{ M}^{-1}\text{cm}^{-1}$.

Extensive photolytic irradiation led to a final absorption spectrum in which λ_{max} occurred at 548 nm relative to 490 nm for λ_{max} of the original material (Figure 53). Again was also noted a small bump, in this case located at 480 nm.

2.c. O_2 role in the photochemistry of $[\text{Ru}(\text{bipy})_2(\text{en})]^{+2}$ in a 0.01 M solution of TEACl in CH_2Cl_2 .

Photolysis of $[\text{Ru}(\text{bipy})_2(\text{en})]^{+2}$ with and

without the quenchers, anthracene, ferrocene, and 1,1'-dimethyl 4,4'-bipyridinium dichloride, were done. In each case, before the the photolysis was begun the emissions of the pure complex and the complex with quencher were measured. There was an attempt to correlate the quenching of the emission with the quenching of the photosubstitution reaction; although quenching of the emission was observed, no significant quenching of the photosubstitution reaction was detected. When O_2 was used as a potential quencher, an unexpected increased disappearance of the starting material was observed. Carefully, Ar, and O_2 -saturated samples were prepared and maintained in darkness in order to further study their reactivity under photolysis conditions.

2.c.1. Study of possible dark reaction of the Ar - saturated sample.

2.c.2. Study of possible thermal reaction of the O_2 - saturated sample.

In both cases, experiments 2.c.1 and 2.c.2., no thermal reaction was detected by absorption spectroscopy when samples were prepared and maintained in the dark for a period of three days.

2.c.3. Photolysis of the O₂- saturated sample.

General experimental conditions :

$[\text{Ru}(\text{bipy})_2(\text{en})]^{+2} \approx 4.9 \cdot 10^{-5} \text{ M.}$

Light intensity = $3.53 \cdot 10^{-8} \text{ einstein/sec.}$

Total irradiation time = 20 min.

Molar absorption coefficient of the starting complex (490 nm) = $10,100 \text{ M}^{-1}\text{cm}^{-1}$.

Molar absorption coefficient of one of the photoproducts (490 nm) = $4,800 \text{ M}^{-1}\text{cm}^{-1}$.

Molar absorption coefficient of other detected photoproduct (490 nm) = $8,800 \text{ M}^{-1}\text{cm}^{-1}$.

Extensive photolytic irradiation led to a final absorption spectrum in which there were maxima located at 455 and 540 nm; the maxima were assumed to correspond to two different species generated by different mechanisms.

2.c.4. Quenching of the emission by O₂.

CH₂Cl₂(pure) 0.01 M solution of TEACl in CH₂Cl₂

$I(\text{Ar})/I(\text{O}_2)$ (a) 4.32(b)

2.16(b)

(a) : Ratio of the corrected and integrated emission spectra of an Ar - saturated and an O_2 - saturated sample (20 min of bubbling the proper gas through the sample in each case) ; excitation was centered at 490 nm and the scanning was done in the 550 - 820 nm range.

(b): Average of three independent measurements.

2.c.5. Photolysis of $[\text{Ru}(\text{bipy})_2(\text{en})]^{+2}$ in 0.05 M H_2SO_4 .

General experimental conditions :

$[\text{Ru}(\text{bipy})_2(\text{en})]^{+2} \cong 4.4 \cdot 10^{-5}$ M.

Light intensity = $3.53 \cdot 10^{-8}$ einstein/sec.

Total irradiation time = 5 min.

Molar absorption coefficient of the starting complex (490 nm) = $9,000 \text{ M}^{-1}\text{cm}^{-1}$.

Molar absorption coefficient of the photoproduct (490 nm) = $8,800 \text{ M}^{-1}\text{cm}^{-1}$.

Extensive photolytic irradiation led to a final absorption spectrum with λ_{max} located at 452 nm.

2.d. Cation - assisted ligand
 photosubstitution in the photoreaction of
 $[\text{Ru}(\text{bipy})_2(\text{en})]^{+2}$ with Ag^+ in CH_3CN at 298 K.

It was reported²² that irradiation of
 $[\text{Ru}(\text{bipy})_3]^{+2}$ in the presence of Ag^+ in CH_3CN
 leads to the photosubstitution product
 $[\text{Ru}(\text{bipy})_2(\text{CH}_3\text{CN})_2]^{+2}$ by a mechanism involving
 the decay of the MLCT state via a d-d excited state to
 a ligand labilized intermediate which is intercepted by
 Ag^+ in a process which assists the substitution by
 removal of a bipy ligand.

In this work the reactivity of
 $[\text{Ru}(\text{bipy})_2(\text{en})]^{+2}$ in the presence of Ag^+ in
 CH_3CN under photolytic irradiation was investigated.
 Since the photosubstitution quantum yields observed for
 the formation of $[\text{Ru}(\text{bipy})_2(\text{CH}_3\text{CN})_2]^{+2}$ are low
 and since neither a possible pentacoordinate
 intermediate $[\text{Ru}(\text{bipy})_2(\text{en}')]^{+2}$, in which en' has
 one ammine free nor the partially solvated intermediate
 complex $[\text{Ru}(\text{bipy})_2(\text{en}')(\text{CH}_3\text{CN})]^{+2}$, can be
 isolated, the photosubstitution quantum yields were all
 evaluated only for the final observed photoproduct.

2.d.1. Quenching of emission in CH_3CN at 298 K by AgNO_3 .

Table XXXXIII. Quenching of the emission of $[\text{Ru}(\text{bipy})_2(\text{en})]^{+2}$ in CH_3CN at 298 K by AgNO_3 .

$[\text{AgNO}_3]$, M	$(I_0/I)_{\text{app}}$ (a)	$(I_0/I)_{\text{corr}}$ (b)
0.00	1.00	1.00
0.05	1.41	1.005
0.10	1.60	1.010
0.20	1.77	1.020
0.40	1.89	1.040
0.80	2.01	1.080

(a): Emission spectra corrected and integrated over the range 550 - 820 nm. Average of three runs. The excitation was centered at 490 nm .

(b): Correction made necessary due to ionic strength effects. The correction was actually an estimation that is explained later in the discussion section .

The Stern - Volmer plot for the quenching of the emission of $[\text{Ru}(\text{bipy})_2(\text{en})]^{+2}$ under these

conditions (uncorrected data) is shown in Figure 46.

2.d.2. Photolysis in a 0.40 M solution of AgNO_3 in CH_3CN .

General experimental conditions :

$[\text{Ru}(\text{bipy})_2(\text{en})]^{+2} \cong 4.1 \cdot 10^{-5} \text{ M.}$

Light intensity = $2.51 \cdot 10^{-9} \text{ einstein/sec.}$

Total irradiation time = 30 min.

Molar absorption coefficient of the starting complex (490 nm) = $9,700 \text{ M}^{-1}\text{cm}^{-1}$.

Molar absorption coefficient of the photoproduct (490 nm) = $3,300 \text{ M}^{-1}\text{cm}^{-1}$.

After extensive photolytic irradiation the final absorption spectrum had a maximum located at 425 nm.

$$I_0(\text{no Ag}^+) / I (0.4 \text{ M Ag}^+) = 2.16 \text{ (a)}$$

(a) : Ratio of the corrected and integrated emission spectra ; the excitation was centered at 490 nm and

the scanning was done in the 550 - 820 range. The emission intensities of the same samples, the one with Ag^+ and the one without the metallic cation, were measured before photolysis.

2.d.3. Photolysis in a 0.80 M solution of AgNO_3 in CH_3CN .

General experimental conditions :

$[\text{Ru}(\text{bipy})_2(\text{en})]^{+2} \cong 4.1 \cdot 10^{-5} \text{ M.}$

Light intensity = $2.51 \cdot 10^{-8} \text{ einstein/sec.}$

Total irradiation time = 30 min.

Molar absorption coefficient of the starting complex (490 nm) = $9,700 \text{ M}^{-1}\text{cm}^{-1}$.

Molar absorption coefficient of the photoproduct (490 nm) = $3,300 \text{ M}^{-1}\text{cm}^{-1}$.

After extensive photolytic irradiation the photoproduct had an absorption spectrum with λ_{max} located at 425 nm. A film of metallic Ag^0 could be observed on the walls of the cuvette, and a black precipitate was found at its bottom.

$$I_0(\text{no Ag}^+) / I(0.8 \text{ M Ag}^+) = 2.29 \text{ (a)}$$

(a) : It has the same meaning as that of (a) in experiment 2.d.2.

2.d.4. Photolysis in a 0.40 M solution of AgNO_3 in CH_3CN in the presence of methyl viologen concentration sufficient to quench > 90 % of the $[\text{Ru}(\text{bipy})_2(\text{en})]^{+2}$ excited luminescent state .

General experimental conditions :

$[\text{Ru}(\text{bipy})_2(\text{en})]^{+2} \cong 4.1 \cdot 10^{-5} \text{ M.}$

Light intensity = $2.51 \cdot 10^{-8} \text{ einstein/sec.}$

Total irradiation time = 30 min.

Molar absorption coefficient of the starting complex (490 nm) = $9,700 \text{ M}^{-1}\text{cm}^{-1}$.

Molar absorption coefficient of the photoproduct (490 nm) = $3,300 \text{ M}^{-1}\text{cm}^{-1}$.

After extensive photolytic irradiation the photoproduct still clearly showed an absorption located at λ_{max} 425 nm. Therefore, despite the efficient quenching of the triplet, the photoreaction seemed to follow the same course previously observed. A white

precipitate , presumably of AgCl could be observed (Cl⁻ was the counter ion of the MV⁺² used as the quencher of the luminescent excited state) .

$I_0(\text{no Ag}^+, \text{no MV}^{+2}) / I(0.4 \text{ M Ag}^+, \text{with MV}^{+2}) = 8.35(a)$

(a) : It has the same meaning as that of (a) in experiment 2.d.2.

3. Temperature dependence of the photosubstitution quantum yields of the complexes [Ru(bipy)₂L]⁺² in 0.01 M solution of TEACl in CH₂Cl₂ .

The quantum yields for the photosubstitution reactions of these complexes were determined over the temperature range of 274 to 305 K. In the case of [Ru(bipy)₃]⁺², the progress of the photoreaction was monitored at 450 nm; in the cases of [Ru(bipy)₂(en)]⁺² and [Ru(bipy)₂(tn)]⁺², the wavelength of monitoring was centered at 490 nm. The intensity of the exciting light was measured; the measurements were corrected for the special geometrical arrangement, including the new sample - holder and the

new filters used in these experiments. The same optical train was used in all the measurements (the excitation band was isolated by means of a combination of two Corning glass filters, CS 4 -74 and CS 3 - 70).

3.a. L = 2,2'bipyridine (bipy).

Data plotted in Figure 47.

3.b. L = ethylenediamine (en).

Data presented in Figure 47.

3.c. L = trimethylenediamine (tn).

Data presented in Figure 47.

The collected values of the quantum yields of photosubstitution for these complexes at 298 K are shown in Table XXXXIV. In the same Table XXXXIV are also reported the estimated quantum yields for LF formation. In Table XXXXV are presented the collected quantum yields of the observed photoreactions of $[\text{Ru}(\text{bipy})_2(\text{en})]^{+2}$ at 298 K, under different experimental conditions. All reported values are an average of results determined from at least three independent experiments.

Table XXXXIV. Quantum yields of photosubstitution and of the production of the higher lying LF state for bis (bipy) - methylene - linked diamine ruthenium complexes at 298 K.

Complex	0.01 M solution of TEACl in CH ₂ Cl ₂	
	$\Phi_{ph} \cdot 10^{+2} (a)$	$\Phi_{LF} (b)$
[Ru(bipy) ₃] ⁺²	4	0.93(c)
[Ru(bipy) ₂ (en)] ⁺²	0.03	1.0
[Ru(bipy) ₂ (tn)] ⁺²	0.06	1.0
	0.01 M solution of TEACl in CH ₃ CN	
	$\Phi_{ph} \cdot 10^{+2} (a)$	$\Phi_{LF} (b)$
[Ru(bipy) ₃] ⁺²	0.3(c)	0.54(c)
[Ru(bipy) ₂ (en)] ⁺²	0.08	1.0
[Ru(bipy) ₂ (tn)] ⁺²	0.14	1.0
	0.01 M solution of TEACl in H ₂ O	
	$\Phi_{ph} \cdot 10^{+2} (a)$	$\Phi_{LF} (b)$
[Ru(bipy) ₃] ⁺²	0.00(d)	0.20
[Ru(bipy) ₂ (en)] ⁺²	0.02	1.0
[Ru(bipy) ₂ (tn)] ⁺²	0.05	1.0

- (a) : Photosubstitution quantum yield.
- (b) : Quantum yield of LF formation.
- (c) : Reference⁴⁹.
- (d) : Reference⁵⁰.

Table XXXV. Quantum yields of observed photoreactions of $[\text{Ru}(\text{bipy})_2(\text{en})]^{+2}$ in different media at 298 K.

In 0.40 M solution of AgNO_3 in CH_3CN .

F $Q_{ph} \cdot 10^{+2}$

$[\text{Ru}(\text{bipy})_2(\text{CH}_3\text{CN})_2]^{+2}$ 0.04

In 0.80 M solution of AgNO_3 in CH_3CN .

F $Q_{ph} \cdot 10^{+2}$

$[\text{Ru}(\text{bipy})_2(\text{CH}_3\text{CN})_2]^{+2}$ 0.05

In 0.40 M solution of AgNO_3 in CH_3CN , in the presence of MV^{+2} , in concentration enough to quench > 90 % of the luminescent state.

F Q_{ph}

$[\text{Ru}(\text{bipy})_2(\text{CH}_3\text{CN})_2]^{+2} < 1 \cdot 10^{-5}$

In 0.01 M solution of TEACl in CH_2Cl_2 (Ar saturated).

F $Q_{ph} \cdot 10^{+2}$

$[\text{Ru}(\text{bipy})_2]\text{Cl}_2$ 0.04

In 0.01 M solution of TEACl in CH_2Cl_2 (O_2 saturated).

F

[Ru(bipy)₂]Cl₂, and [Ru(bipy)₂(dim)]²⁺ (a)In 0.05 M H₂SO₄.

F

Q_{ph}. 10⁻¹[Ru(bipy)₂(dim)]²⁺

0.98

F = observed final photoproduct, by absorption spectroscopy.

(a) : no separate evaluations of the respective quantum yields of formation of each photoproduct were made.

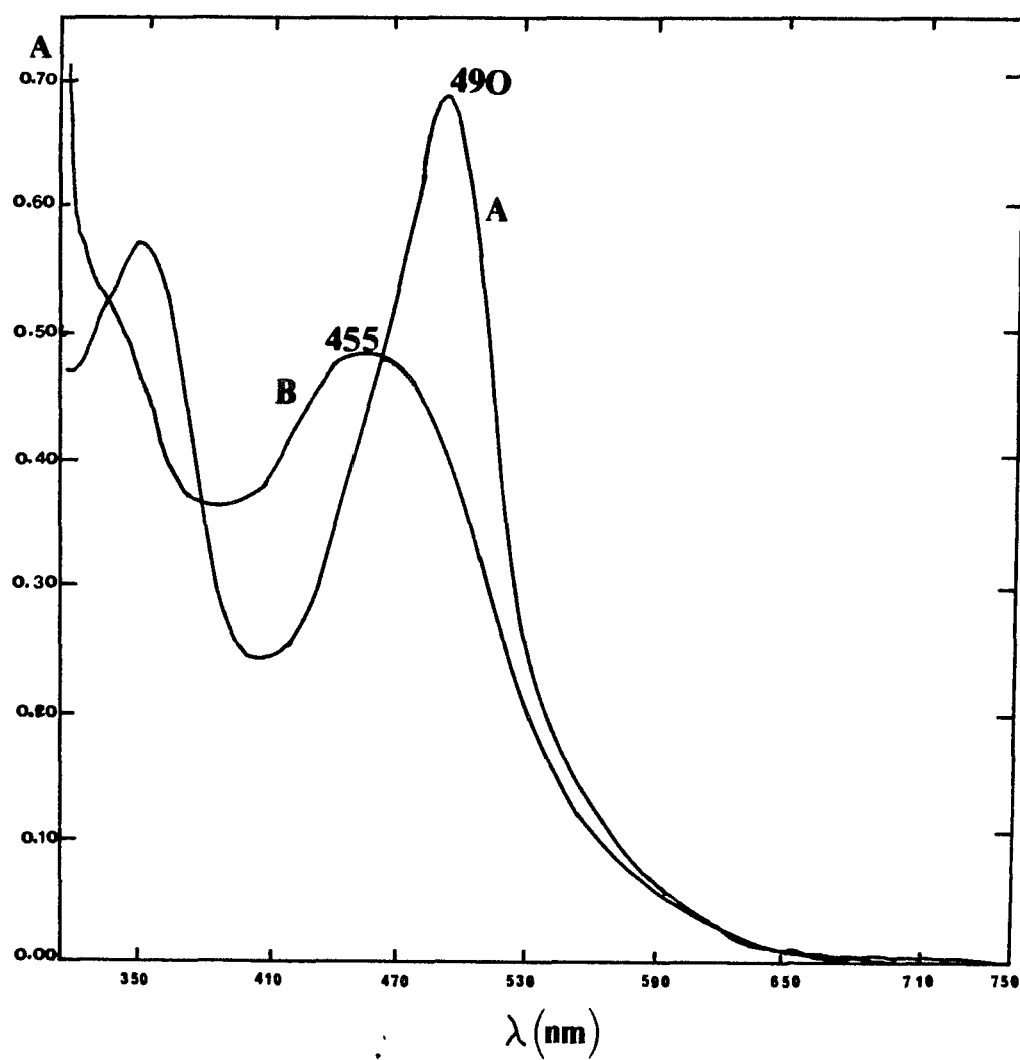


Figure 40 . Extensive photolysis of $[\text{Ru}(\text{bipy})_2(\text{en})]^{+2}$ in CH_3CN (no Cl^-). Curve A : before irradiation. Curve B : final spectrum.

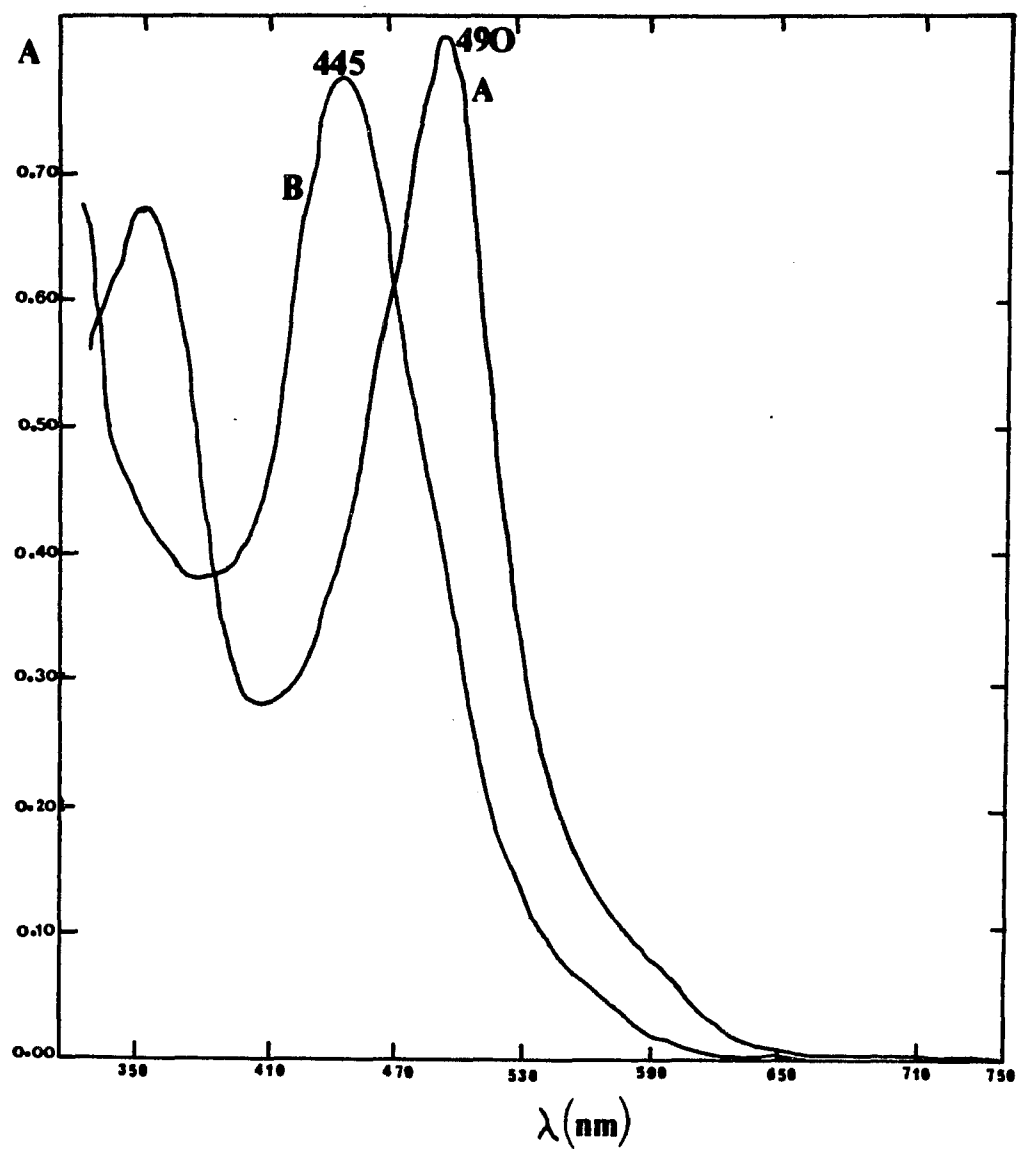


Figure 41 . Extensive photolysis of $[\text{Ru}(\text{bipy})_2(\text{en})]^{3+}$ in H_2O (no Cl^-). Curve A : before irradiation. Curve B : final spectrum.

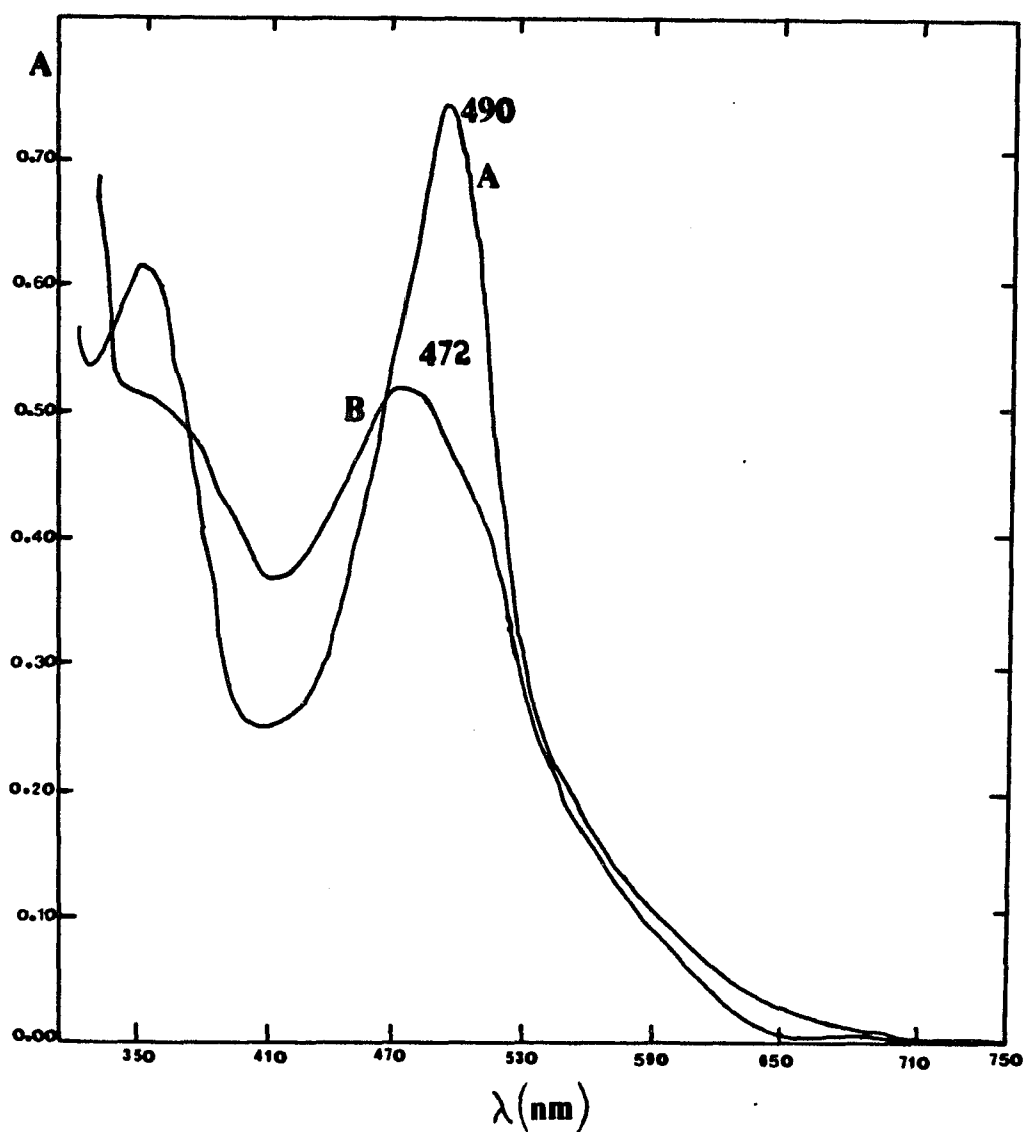


Figure 42 . Extensive photolysis of $[\text{Ru}(\text{bipy})_2(\text{en})]^{+2}$ in CH_2Cl_2 (no Cl^-). Curve A : before irradiation. Curve B : final spectrum.

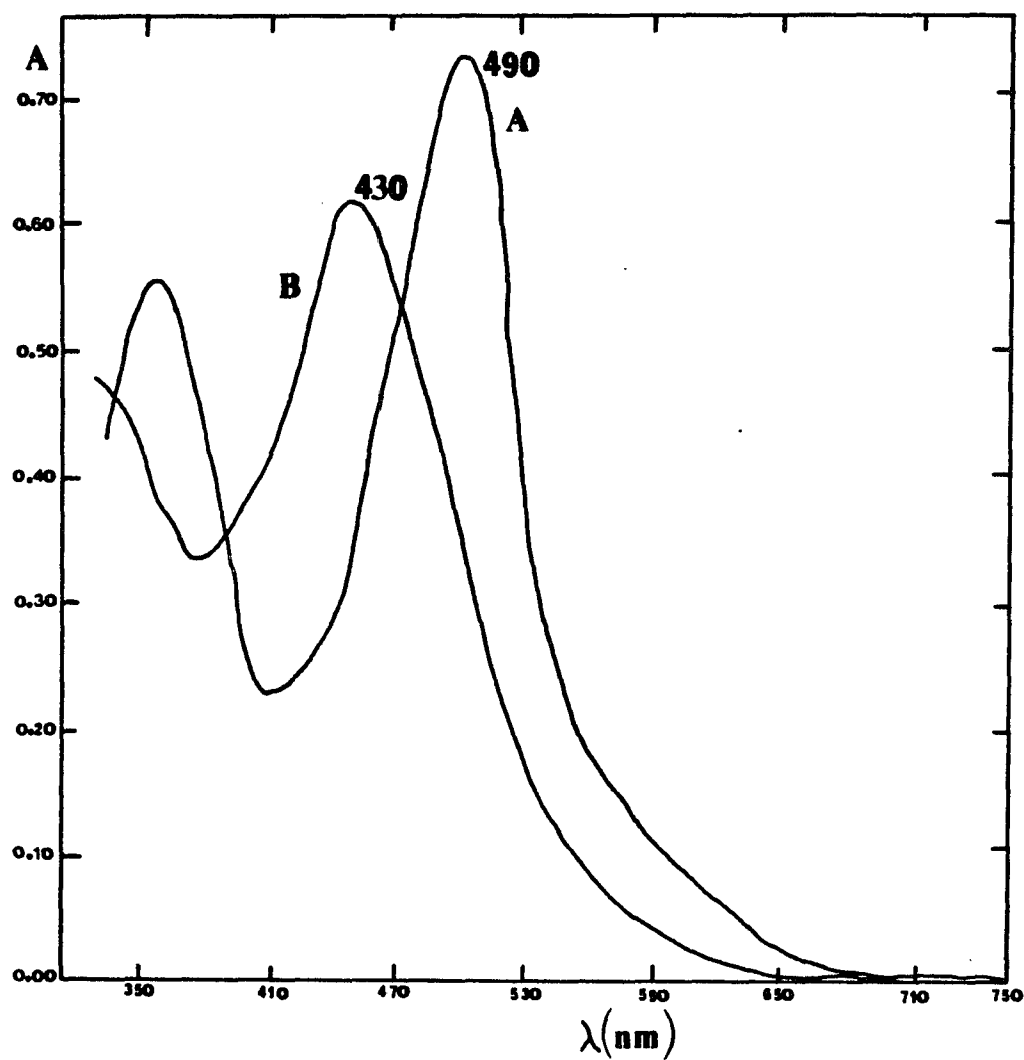


Figure 43 . Extensive photolysis of $[\text{Ru}(\text{bipy})_2(\text{tn})]^{2+}$ in CH_3CN (no Cl^-). Curve A : before irradiation. Curve B : final spectrum.

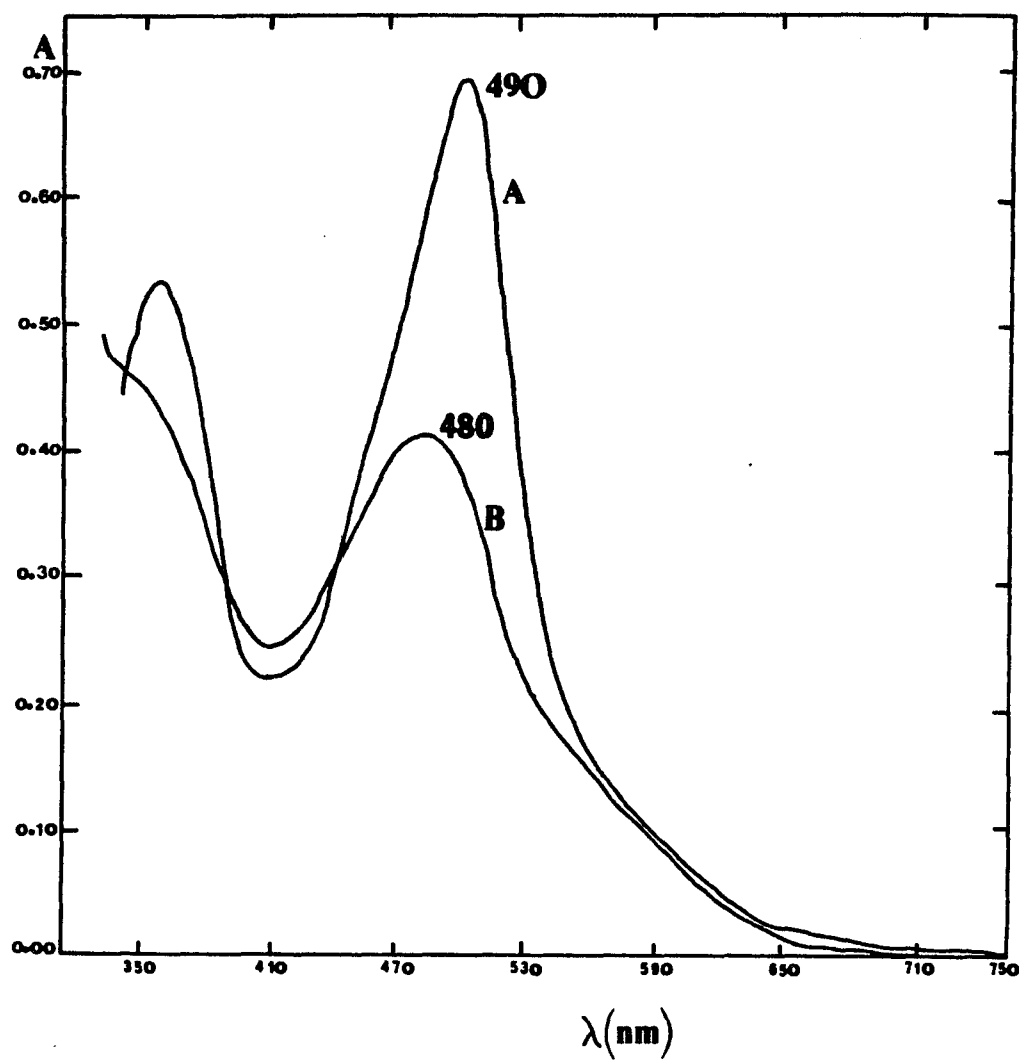


Figure 44 . Extensive photolysis of $[Ru(bipy)_2(tn)]^{+2}$ in H_2O (no Cl^-). Curve A : before irradiation. Curve B : final spectrum.

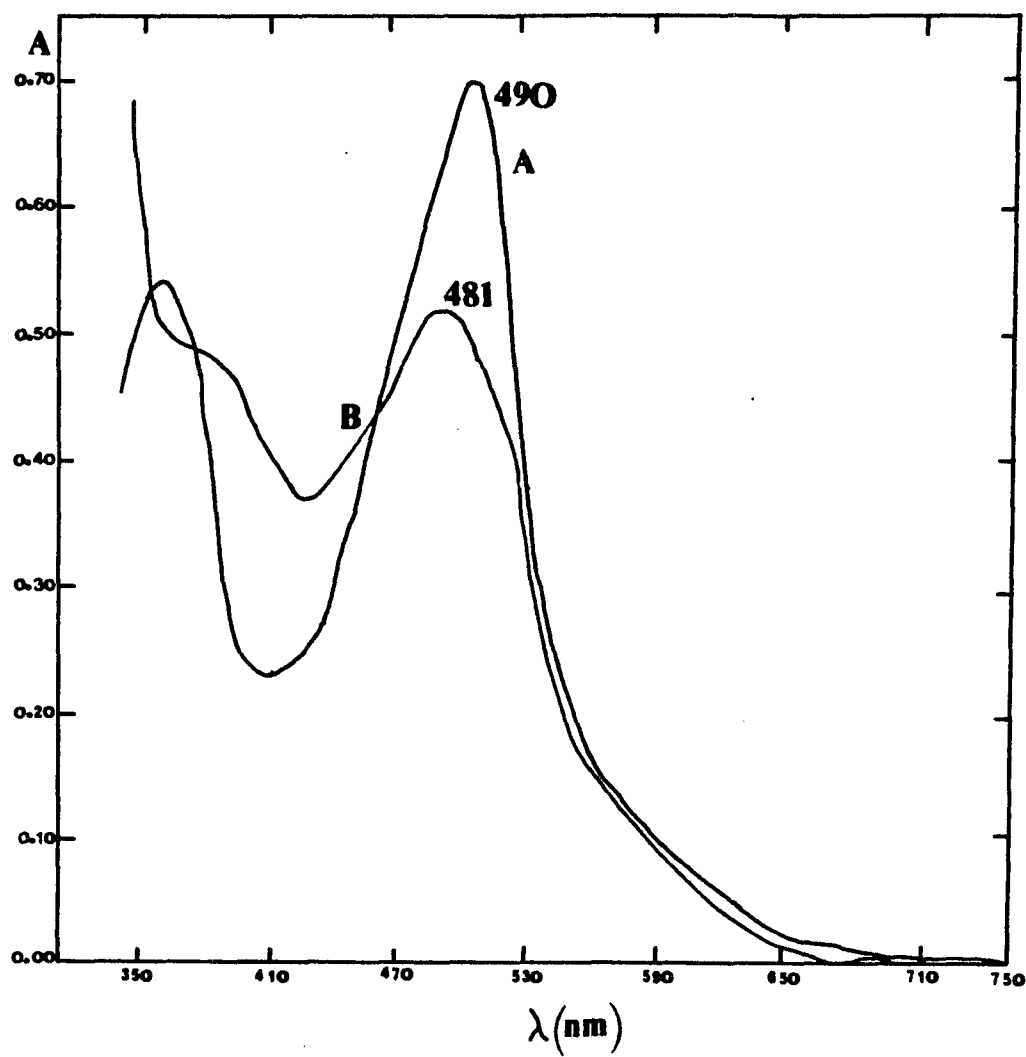


Figure 45 . Extensive photolysis of $[\text{Ru}(\text{bipy})_2(\text{tn})]^{+2}$ in CH_2Cl_2 (no Cl^-). Curve A : before irradiation. Curve B : final spectrum.

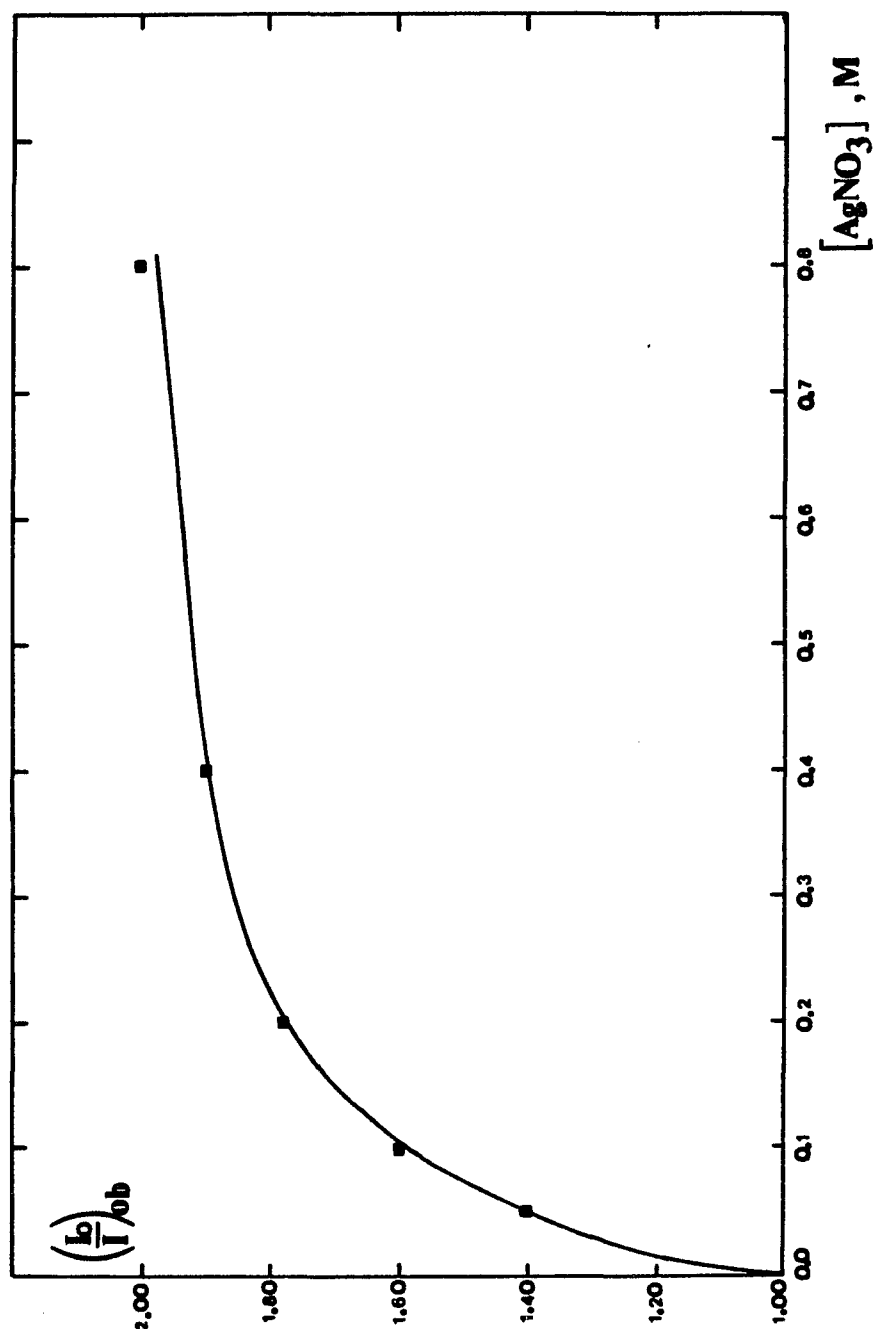


Figure 46 . Quenching of the emission of $[Ru(bipy)_2(en)]^{+2}$ in CH_3CN at 298 K by $AgNO_3$.

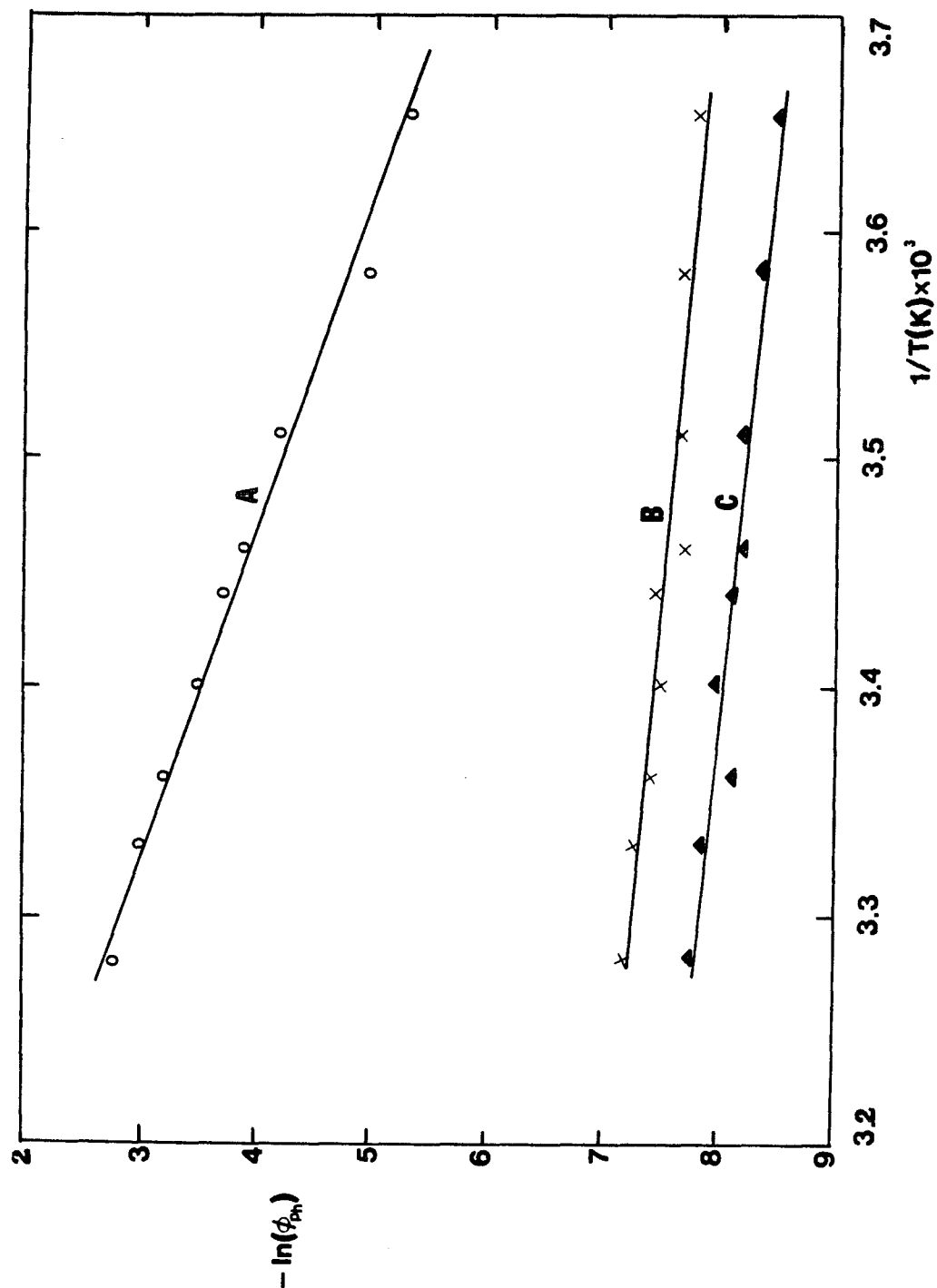


Figure 47 . Temperature dependence of the photosubstitution quantum yields of : (A) , $[\text{Ru}(\text{bipy})_3]^{+2}$; (B) , $[\text{Ru}(\text{bipy})_2(\text{tn})]^{+2}$; (C), $[\text{Ru}(\text{bipy})_2(\text{en})]^{+2}$ in a 0.01 M solution of TEACl in CH_2Cl_2 .

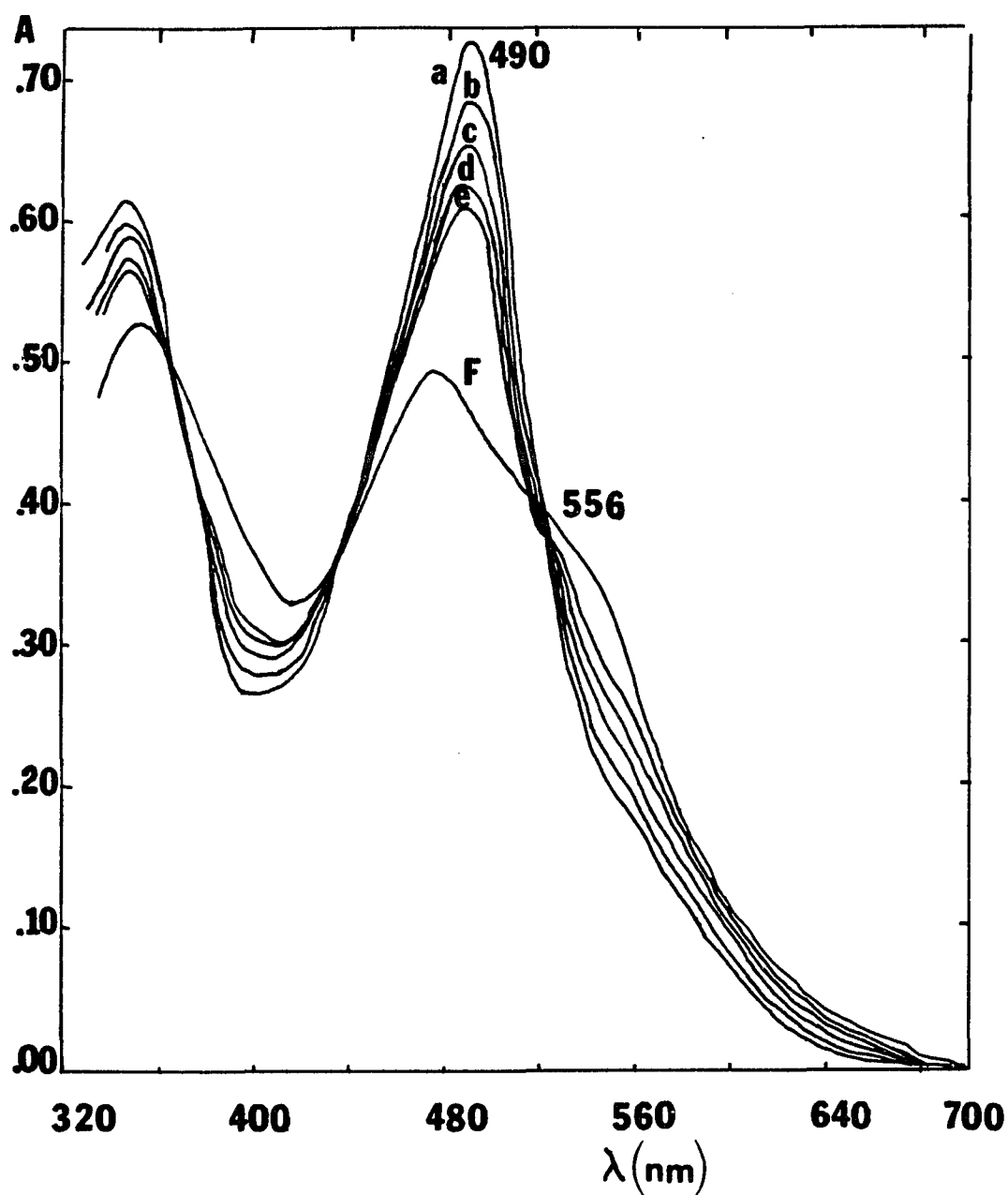


Figure 48 . Absorption spectra during the photolysis of $[Ru(bipy)_2(en)]^{+2}$ in 0.01 M TEACl in CH_3CN . The photolysis times (in min) are : curve a, 0; curve b, 10; curve c, 20; curve d, 30; curve e, 40. Curve F, 10 hours of full irradiation.

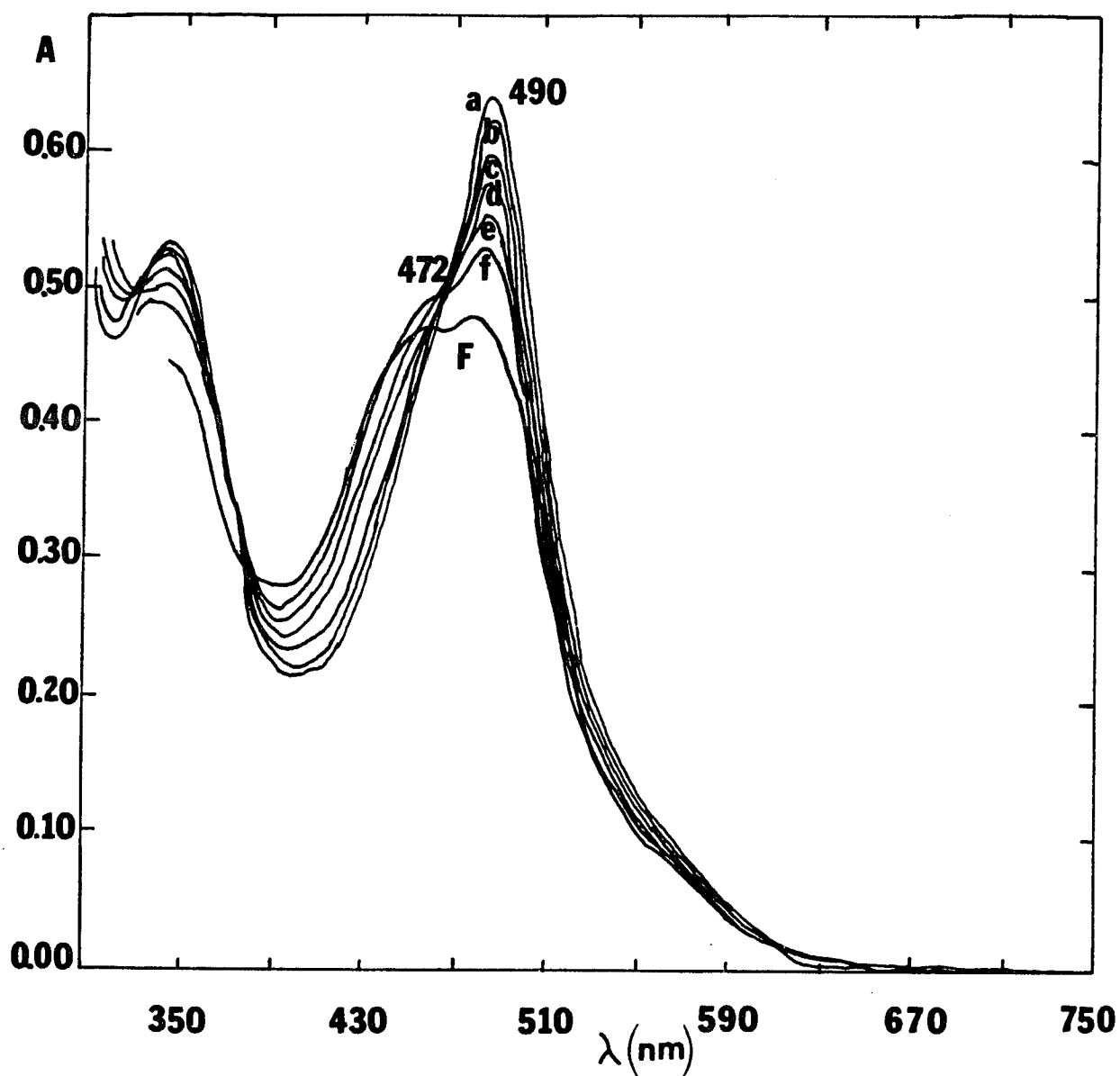


Figure 49 . Absorption spectra during the photolysis of $[\text{Ru}(\text{bipy})_2(\text{en})]^{3+}$ in 0.01 M TEACl in H_2O . The photolysis times (in min) are : curve a, 0; curve b, 20; curve c, 40; curve d, 60; curve e, 80; curve f, 100. Curve F, 10 hours of full irradiation.

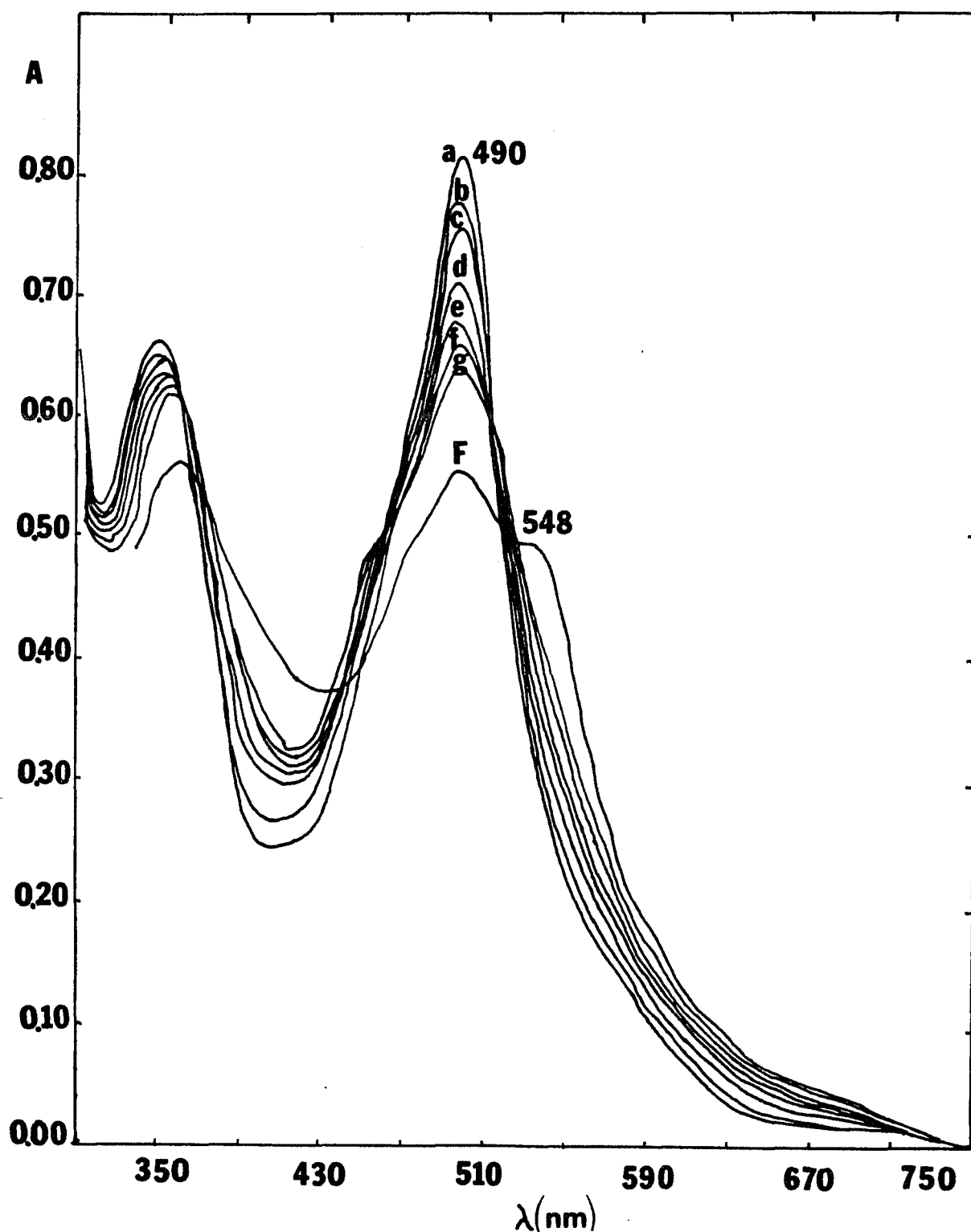


Figure 50 . Absorption spectra during the photolysis of $[\text{Ru}(\text{bipy})_2(\text{en})]^{+2}$ in 0.01 M TEACl in CH_2Cl_2 . The photolysis times (in min) are : curve a, 0; curve b, 10; curve c, 20; curve d, 30; curve e, 40; curve f, 50; curve g, 60; Curve F, 10 hours of full irradiation

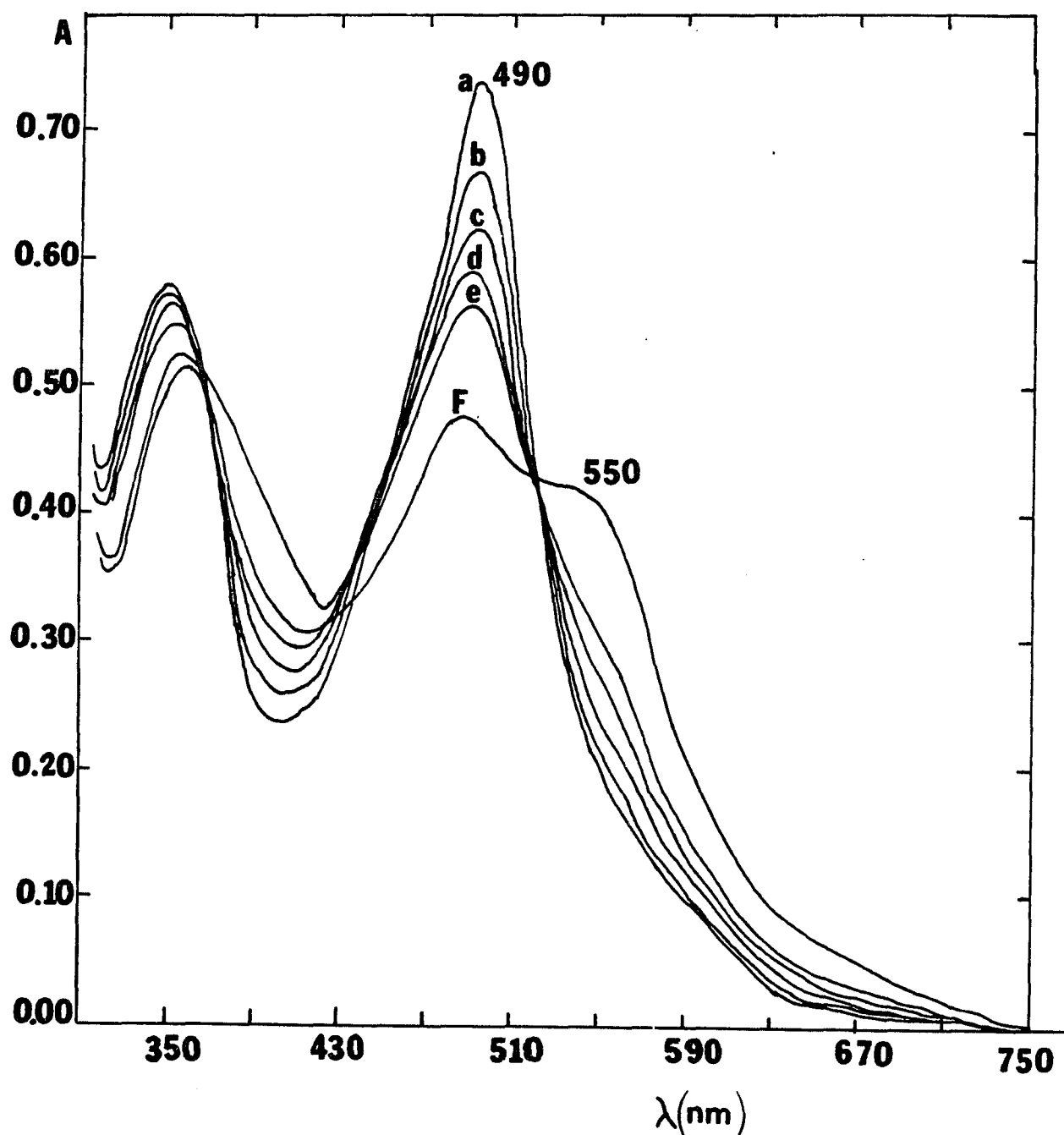


Figure 51 . Absorption spectra during the photolysis of $[\text{Ru}(\text{bipy})_2(\text{tn})]^{+2}$ in 0.01 M TEACl in CH_3CN . The photolysis times (in min) are : curve a, 0; curve b, 10; curve c, 20; curve d, 30; curve e, 40. Curve F, 10 hours of full irradiation

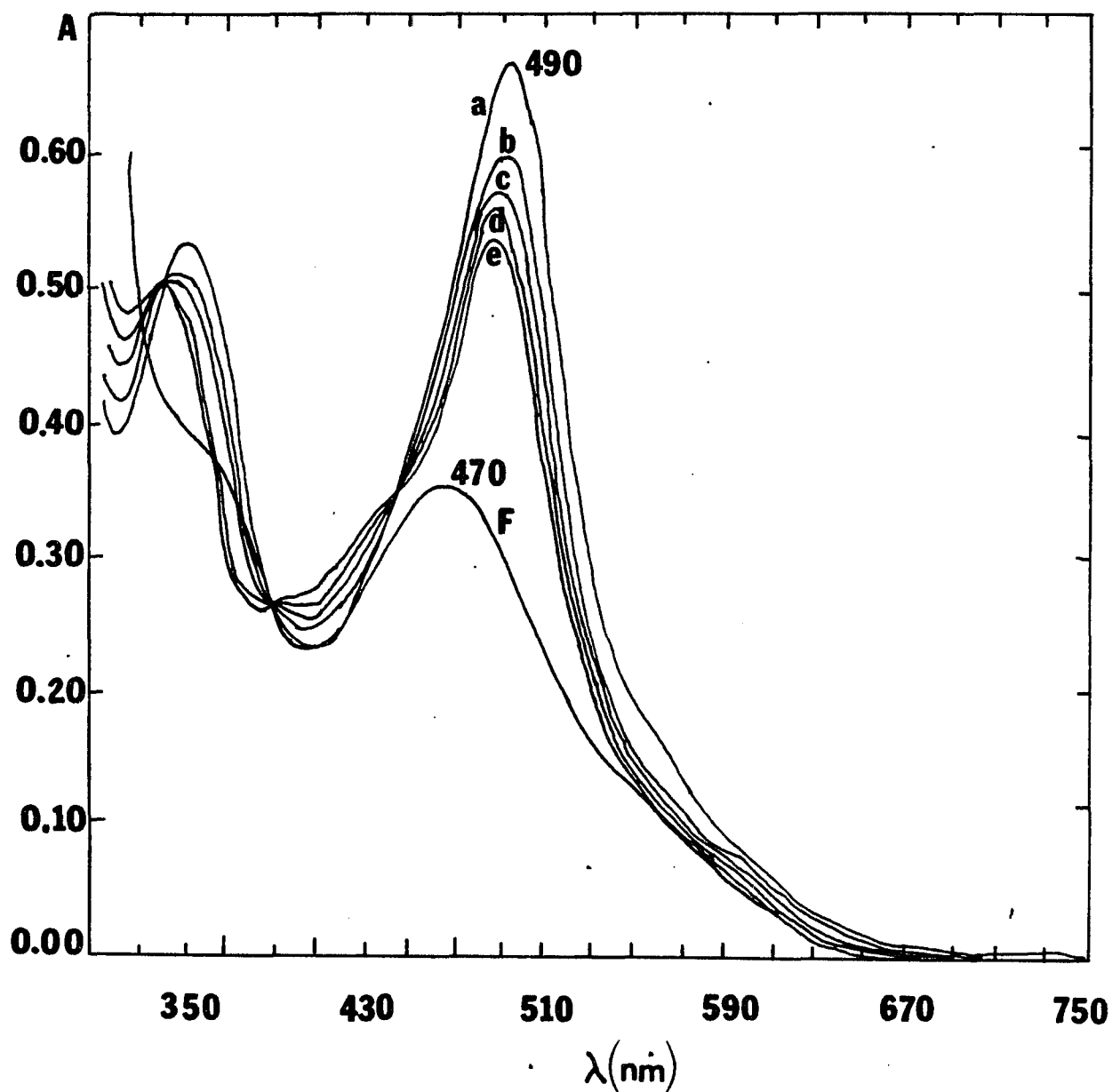


Figure 52 . Absorption spectra during the photolysis of $[\text{Ru}(\text{bipy})_2(\text{tn})]^{+2}$ in 0.01 M TEACl in H_2O . The photolysis times (in min) are : curve a, 0; curve b, 20; curve c, 40; curve d, 60; curve e, 80 . Curve F, 10 hours of full irradiation.

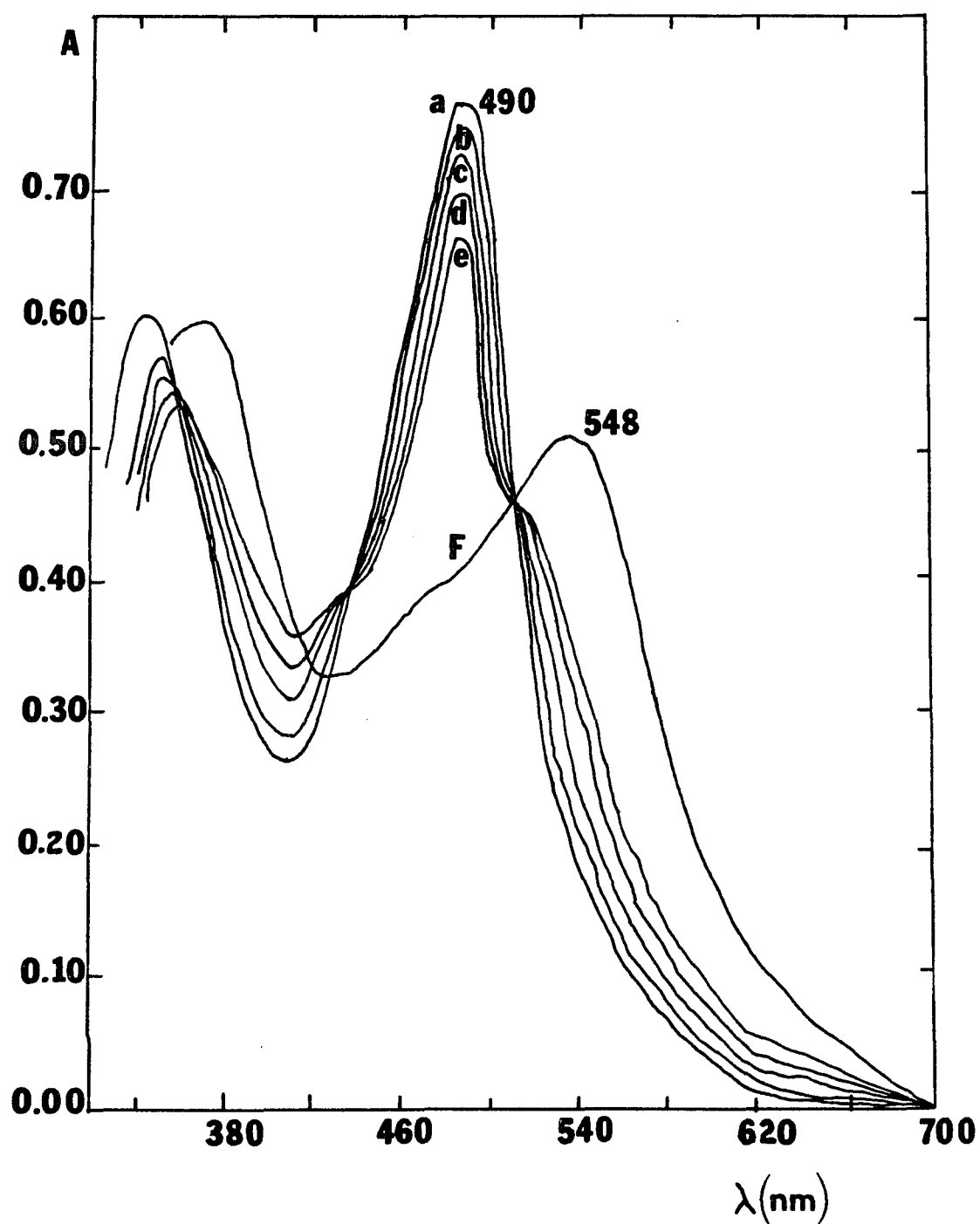


Figure 53 . Absorption spectra during the photolysis of $[\text{Ru}(\text{bipy})_2(\text{tn})]^{2+}$ in 0.01 M TEACl in CH_2Cl_2 . The photolysis times (in min) are : curve a, 0; curve b, 10; curve c, 20; curve d, 30; curve e, 40. Curve F, 10 hours of full irradiation.

CHAPTER IV. DISCUSSION OF THE EXPERIMENTAL RESULTS.

A. QUENCHING OF $[\text{Ru}(\text{bipy})_3]\text{X}_2$ ($\text{X} = \text{Cl}^-$, Br^-) EMISSION AND PHOTOSUBSTITUTION BY FERROCENE AND BY OXYGEN.

1. Introduction.

The quenching of the luminescence and of the photosubstitution reaction of tris - bipyridineruthenium(II), $[\text{Ru}(\text{bipy})_3]^{+2}$, by ferrocene and oxygen were examined. Within experimental error, the linear Stern - Volmer plots are identical for each case. This result is in conflict with that of a previous report⁴⁶ in which the Stern - Volmer plots for these two processes were different. These new results indicate that the luminescent excited state is an intermediate in the photosubstitution reaction.

Recently, the quenching of both the luminescence and the substitutional photochemistry of tris - bipyridineruthenium(II) bromide were investigated⁴⁶. The specific system examined was $[\text{Ru}(\text{bipy})_3]\text{Br}_2$ dissolved in dimethylformamide (DMF), in which 0.1 M TBABr was present. The quencher

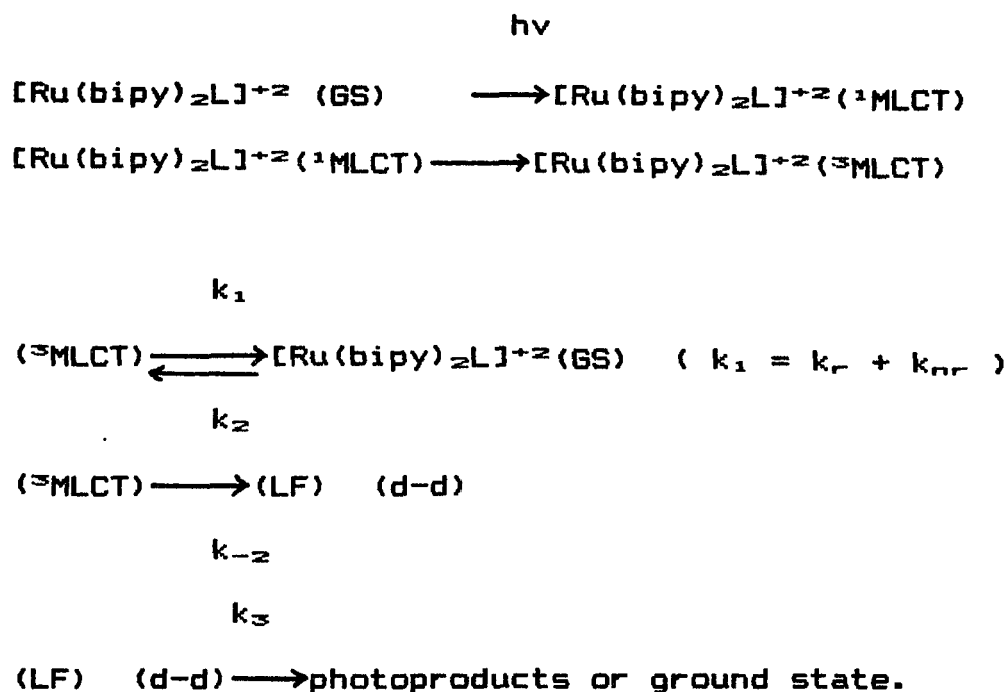
selected was ferrocene because it was neutral and thus it was unlikely to interfere with any ion - pairing equilibrium that might be involved. Although many publications had already established the occurrence of photoanation of $[\text{Ru}(\text{bipy})_3]^{+2}$ φ^0 which can be appreciable in organic solvents, the mechanism of the substitution process and the identification of the responsible excited state were not well determined. Therefore, the investigation carried out by Fasano and Hoggard⁴⁶ was a new attempt to help characterize the photochemically reactive excited state. In order to accomplish that, the quenching of the photoanation of $[\text{Ru}(\text{bipy})_3]^{+2}$ by ferrocene in DMF was examined and compared with the luminescence intensity quenching. Their results were : the Stern - Volmer plots of the quenching of luminescence intensity and of the photoanation reaction were linear; the photoanation reaction was monitored by measuring the disappearance of the absorption of $[\text{Ru}(\text{bipy})_3]\text{Br}_2$ and by following the production of $[\text{Ru}(\text{bipy})_2(\text{DMF})\text{Br}]^{+1}$, the major product that was formed in this particular quenching reaction; the Stern - Volmer plots showed a quenching rate constant 3 times greater than that of the luminescence intensity for the photosubstitution reaction. Even though this experimental evidence

suggested strongly that there was at least a partial partitioning of photosubstitution and the luminescence among separate excited states, it also argued against a model in which both excited states would be in thermal equilibrium.

Investigations have supported a kinetic model which assumes that the observed photochemical reactions occur from LF excited states which are in thermal equilibrium with the $^3\text{MLCT}$ excited states. In reference¹¹³ was studied the photochemical reaction of $[\text{Ru}(\text{bipy})_3]^{+2}$ in 0.1 M HCl at temperatures between 313 and 368 K. It was found that the photochemical reaction of $[\text{Ru}(\text{bipy})_3]^{+2}$ occurs in competition with the luminescence of the complex. Additionally, the apparent activation energies obtained from plots of $\ln(Q_{\text{ph}})$ vs. $1/T(\text{K})$ were similar in magnitude to the values obtained in the analysis of luminescence data⁹⁶. This experimental evidence was taken to be an indication that the excited state involved in the luminescence quenching might also be implicated in the photochemical reaction. A general kinetic treatment of the expected photochemical quantum yield from an equilibrium mixture of two excited states has been presented by Wagner¹¹⁴.

Meyer et al.^{74, 107} during the course of studies of the photochemistry of $[\text{Ru}(\text{bipy})_3]^{+2}$ and related complexes, of the general formulation $[\text{Ru}(\text{bipy})_2\text{L}]^{+2}$, have also analyzed their data assuming that a thermal equilibrium is involved between the excited states of the complexes.

Their simplified kinetic scheme is shown below :



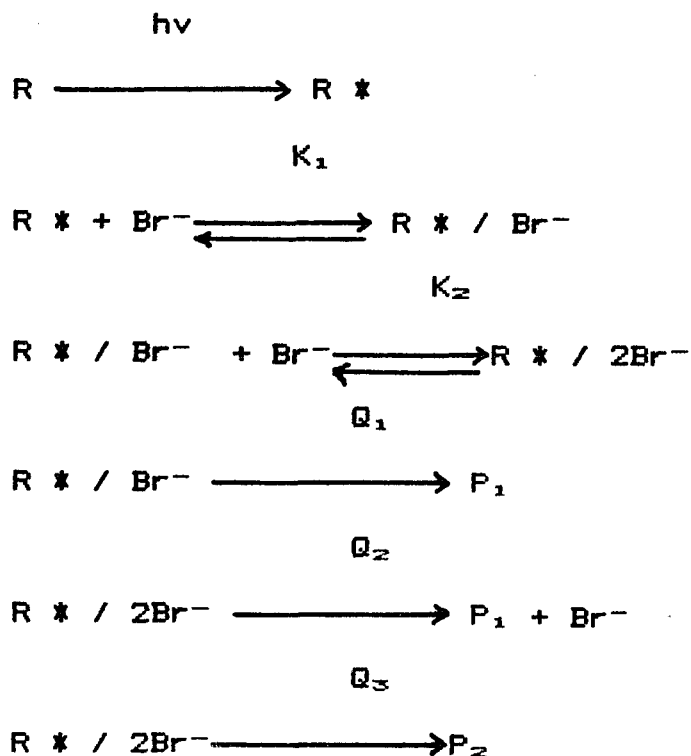
Evidence from the work of Malouf and Ford¹¹⁵ and that of Figard and Petersen¹¹⁶ also suggest that thermally equilibrated $^3\text{MLCT}$ and LF excited states can occur.

Therefore, the results presented in reference⁴⁶ were in clear conflict with the previous treatment.

From another perspective, the larger K_{av} for the photosubstitution reaction could alternatively imply a longer lifetime for the LF excited state, rather than a larger bimolecular quenching rate constant. A longer lifetime could result if the LF state were lower in energy than that of the luminescing MLCT state.

In reference¹¹² the photochemistry of $[\text{Ru}(\text{bipy})_3][\text{SCN}]_2$ dissolved in DMF was studied at different concentrations of the thiocyanate salt. The mechanisms by which the products were formed could not be conclusively established although two possible reaction schemes were proposed. The first involved a classical secondary photolysis in which one ligand X^- would coordinate to form the first photoproduct, $[\text{Ru}(\text{bipy})_2(\text{DMF})\text{X}]^{+1}$, followed by a second photoprocess in which a DMF molecule would be replaced by another ligand to form $[\text{Ru}(\text{bipy})_2\text{X}_2]$. The alternative ion - multiplet model suggested that the two products were formed from $[\text{Ru}(\text{bipy})_3]^{+2}$ in different states of ion aggregation :

$[\text{Ru}(\text{bipy})_2(\text{DMF})\text{X}]^{+1}$, P_1 , from the ion pair and $[\text{Ru}(\text{bipy})_2\text{X}_2]$, P_2 , from the ion triplet. In reference 67 the system $[\text{Ru}(\text{bipy})_3]\text{Br}_2$, R , dissolved in DMF in the presence of Br^- was studied; it was considered that the observed photochemistry could be better described by the ion - multiplet model, with one modification allowing the formation of the monosubstituted photoproduct from the ion - triplet. This scheme can be written as follows :



2. Discussion.

The above mentioned conclusions⁴⁶ did not agree well either with the currently accepted model (Figures 6 and 7) nor with some related results obtained in our laboratory. Therefore, in the present work first the equivalent chloride system was investigated.

In order to evaluate the luminescence quenching it was decided to measure the luminescent lifetimes rather than the intensities in order to avoid any inner - filter effect associated to the use of ferrocene. The corresponding Stern - Volmer plots for the ferrocene quenching of both the luminescent lifetime and photosubstitution reaction of $[\text{Ru}(\text{bipy})_3]\text{Cl}_2$ in a solution that was 0.10 M TBACl in DMF are shown in Figure 14 (experimental data are given in Table III). The lifetime quenching plot yielded a slope, K_{sv} , of $3,070 \pm 600 \text{ M}^{-1}$. An average of three separate measurements of the luminescence lifetime of the dissolved complex in the absence of the quencher gave a value of 770 nsec. Thus, the corresponding quenching rate constant was evaluated to be $4.0 \cdot 10^{+7} \text{ M}^{-1}\text{sec}^{-1}$, in relatively good agreement with the value of $5.9 \cdot 10^{+7} (\pm 10\%) \text{ M}^{-1}\text{sec}^{-1}$ reported for the same quenching

experiment, in EtOH (no salt) by Wrighton et al.⁷¹. Fasano and Hoggard noticed the peculiar fact that the k_{sv} value of the quenching of $[\text{Ru}(\text{bipy})_3]\text{Cl}_2$ emission by ferrocene in EtOH ⁷¹ had a value of 5,300 M^{-1} which was 6 times greater than that obtained by them for ferrocene in DMF, a solvent that has a lower viscosity than that of EtOH. However, it is doubtful that the comparison is worthwhile because Wrighton et al. used pure EtOH to which no Cl^- supporting electrolyte was added.

The evaluation of the slopes for the quenching of the photosubstitution process of $[\text{Ru}(\text{bipy})_3]\text{Cl}_2$ was more difficult, because the ferrocene absorbed a fraction of the incident radiation and also undergoes a photoreaction⁴⁶. No corrections were made for the generation of the two photoproducts that have been claimed to be isolatable (with quantum yields lower than $1 \cdot 10^{-3}$) after irradiation of solutions containing only ferrocene as the solute⁴⁶. Nevertheless, the measured absorption spectra, of the starting complex and those of the first photoproduct, $[\text{Ru}(\text{bipy})_2(\text{DMF})\text{Cl}]^{+1}$, which had a maximum located at 520 nm, were corrected for the partial absorption of the incident light by ferrocene.

The molar absorption coefficient of the starting complex was directly determined, while that of the second photoproduct, $[\text{Ru}(\text{bipy})_2\text{Cl}_2]$, which has a maximum located at 558 nm was experimentally evaluated by monitoring the changes in the absorption spectrum of a solution of known initial concentration of $[\text{Ru}(\text{bipy})_3]\text{Cl}_2$ under photolytic irradiation until no further modification of the spectral features was detected. A total conversion was assumed; this assumption was satisfactorily corroborated by measuring the absorption spectrum of another fresh solution of $[\text{Ru}(\text{bipy})_2\text{Cl}_2]$ that had the same concentration. The spectra and the absorbances at 558 nm, within experimental error were identical. The molar absorption coefficient for the first photoproduct was estimated like that value fitting the measured absorbance at 450 nm, after 16 min of irradiation, assuming a previously reported ⁶⁷ relative distribution of photoproducts and unreacted starting complex obtained for the system $[\text{Ru}(\text{bipy})_3]\text{Br}_2$ in DMF irradiated in the presence of TBABr. The Beer - Lambert Law of absorption was assumed in the calculation of the molar absorption coefficient of the first photoproduct, P_1 :

$$A(\lambda) = E_R(\lambda)[R] + E_{P_1}(\lambda)[P_1] + E_{P_2}(\lambda)[P_2]$$

$$\lambda = 450 \text{ nm.}$$

$$[R] + [P_1] + [P_2] = [R_0]$$

At 16 min of irradiation : $[P_1]/[R_0] = 0.24$; $[P_2]/[R_0] = 0.02$; $[R]/[R_0] = 0.74$.

After all these difficulties are considered, it appears that the difference between these two slopes ($3,070 \pm 600 \text{ M}^{-1}$, for T_{00}/T_{∞} , vs. $1,780 \pm 700 \text{ M}^{-1}$ for Q_{pho}/Q_{ph}) is probably not significant, and, more importantly, the observed trend is different from the previous result⁴⁶ in which the luminescence quenching had the smaller slope.

In order to avoid the problems associated with the use of ferrocene as a quencher, the quenching of both the luminescence and the photosubstitution by oxygen were investigated. Oxygen is a good quencher but does not absorb any of the incident radiation that is used in the experiments that were done. The selected system was $[\text{Ru}(\text{bipy})_3]\text{Cl}_2$ in a 0.10 M solution of TBACl in CH_3CN . The Stern - Volmer plots for the quenching of both processes, luminescence lifetimes and photosubstitution, were determined (Figure 15). Table

IV summarizes the experimental data. The solubilities of O_2 in the different solvents were estimated in the manner explained in the pertinent section of Experimental Results. The quenching of the photosubstitution was found to yield a Stern - Volmer plot very nearly identical to that of the quenching of the luminescence lifetime (506 ± 40 for T_{00}/T_0 vs. 470 ± 60 for Q_{ph0}/Q_{ph}). The quenching rate constant of the luminescence, evaluated from $K_{SV} = k_q T_{00}$ yielded a value of $6.8 \cdot 10^{+8} \text{ M}^{-1}\text{sec}^{-1}$, somewhat lower than the values $3.3 \cdot 10^{+9} \text{ M}^{-1}\text{sec}^{-1}$ (H_2O solvent) and $1.7 \cdot 10^{+9} \text{ M}^{-1}\text{sec}^{-1}$ (MeOH solvent) reported by Demas et al.⁷². Again, it should be noted that the Demas experiments⁷² were carried out with pure solvents.

The results obtained in the present work for the two systems already described, disagreed with the previously reported observations⁴⁶ and prompted the reinvestigation of the bromide system in DMF, in order to have equivalent conditions (i.e. supporting electrolyte) and thus to remove the vagaries of ion - pairing, which, have an importantly recognized, although not well defined role, in these systems.

Ferrocene was found to quench the $^3\text{MLCT}$ luminescence of $[\text{Ru}(\text{bipy})_3]\text{Br}_2$ in a 0.10 M TBABr solution in DMF at a nearly diffusion - controlled rate ($k_q = 3.2 \cdot 10^9 \text{ M}^{-1}\text{sec}^{-1}$). The photosubstitution was also quenched. In fact, the linear Stern - Volmer plots had slopes (Table V) that were identical within experimental error ($1,210 \pm 200$ for T_{00}/T_0 vs. $1,170 \pm 300$ for $Q_{\text{pho1}}/Q_{\text{ph1}}$; in this case, by absorption spectroscopy, the appearance of the second photoproduct was also followed, and K_{sv} for $Q_{\text{pho2}}/Q_{\text{ph2}}$ was determined to be $1,126 \pm 200$). Figure 16 displays the Stern - Volmer plots of the experiments just described. The value of these slopes agreed reasonably well with the previously reported value for the K_{sv} of the quenching of the luminescence ($826 \pm 6 \text{ M}^{-1}$)⁴⁶ but not with that of the quenching of the photosubstitution ($2,530 \pm 620$, or $2,825 \pm 580 \text{ M}^{-1}$)⁴⁶.

In order to further substantiate the collected experimental evidence, quenching by oxygen was attempted. Unfortunately, the preparation of samples, described in the experimental section, had to be modified because of the danger during the sealing of the cuvettes containing the samples dissolved in DMF;

explosions occurred, especially when the higher O_2 pressures were used. A rather modest set of experiments was carried out; just three O_2 concentrations, under conditions described in Table VI, were used. Again, the concentrations of O_2 were estimated with the use of a value for Henry's constant and the approximation given in Table VI. The K_{sv} values were practically identical (283 ± 22 for T_{00}/T_0 , 272 ± 30 for Q_{ph01}/Q_{ph1} , and 289 ± 25 for Q_{ph02}/Q_{ph2}) for all the quenching processes that were studied, although the obtained values were notoriously lower than the previous results of this work. The lower values were probably due to a different and less effective initial degassing of the samples. A certain degree of quenching occurred because some dissolved O_2 was not removed during the degassing process. In any case, the Stern - Volmer plots (Figure 17) were similar.

Finally, the quenching of both the photosubstitution and the lifetime of the luminescent state of $[Ru(bipy)_3]Br_2$ in a 0.10 M solution of TBABr in CH_2Cl_2 by ferrocene and also by oxygen were examined (experimental data in Tables VII and VIII, respectively). In each case, the corresponding linear Stern - Volmer plots had similar slopes, (4,840

$\pm 500 \text{ M}^{-1}$ for T_{obs}/T_0 and $5,070 \pm 1,200 \text{ M}^{-1}$ for $Q_{\text{pho2}}/Q_{\text{ph2}}$, when ferrocene was the quencher; $166 \pm 30 \text{ M}^{-1}$ for T_{obs}/T_0 and $147 \pm 40 \text{ M}^{-1}$ for $Q_{\text{pho2}}/Q_{\text{ph2}}$, when oxygen was the quencher). Figures 18 and 19 illustrate the Stern - Volmer plots obtained for these last two experiments.

3. Conclusions.

The quenchings of both processes, luminescence and photosubstitution, are very similar and the similarities are demonstrated by the close values of K_{SV} for each group of the different Stern - Volmer plots obtained for the systems that were investigated. The new experimental evidence gathered in the present work indicates that the excited state affected by either ferrocene or oxygen is involved in both processes. The luminescence is known to occur from the $^3\text{MLCT}$. Quenching of this excited state also results in a lesser population of the LF excited state, and consequently, a lower photosubstitution yield. The results obtained in the present work are in agreement with the postulated general model that represents the photophysical processes that take place when $[\text{Ru}(\text{bipy})_3]^{+2}$ is excited upon irradiation. However, it must be pointed out that, as long as only the

$^3\text{MLCT}$ is quenched by the additive, the excited $^3\text{MLCT}$ and LF states need not necessarily be in thermal equilibrium to show similar Stern - Volmer plots.

DISCUSSION B. CORRELATION OF LIGAND FIELD
EXCITED - STATE ENERGIES WITH LIGAND FIELD STRENGTHS IN
(POLYPYRIDINE) RUTHENIUM(II) COMPLEXES.

1. Introduction.

The temperature dependences of the emission intensities and lifetimes of the complexes tris - bipyridineruthenium(II), 4,5 - diazafluorenyl - bis - 2,2' bipyridylruthenium(II), and cis - bispyridyl - bis - 2,2' bipyridylruthenium(II), were evaluated. In the cases of the two latter complexes , $[\text{Ru}(\text{bipy})_2(\text{diaz})]^{+2}$, and $[\text{Ru}(\text{bipy})_2(\text{py})_2]^{+2}$, that have weaker ligand fields than that of $[\text{Ru}(\text{bipy})_3]^{+2}$, a dramatic decrease in both the emission intensity and lifetime occurs near 170 K; a trend to lower intensities and lower lifetimes continues at higher temperatures. This behavior is ascribed to population of a LF excited state that lies only about $2,000 \text{ cm}^{-1}$ above the lowest MLCT excited state. This $2,000 \text{ cm}^{-1}$ value is much less than that of $[\text{Ru}(\text{bipy})_3]^{+2}$, but it is consistent with the prediction of lower lying $d - d^*$ excited states for $[\text{Ru}(\text{bipy})_2(\text{diaz})]^{+2}$ and for $[\text{Ru}(\text{bipy})_2(\text{py})_2]^{+2}$.

A weak emission can be observed in the vicinity of 260 - 330 K. After a careful analysis, this weak emission was considered to come from an impurity, most likely, $[\text{Ru}(\text{bipy})_3]^{+2}$.

The data collected in this work were interpreted to fit the currently accepted model of the photophysics processes of $[\text{Ru}(\text{bipy})_2\text{L}]^{+2}$ complexes.

The good fit redemonstrated nicely that the activation energies between the MLCT and the LF excited state decrease with a decreasing average of ligand field strength, a correlation which, even when it is the expected one, had been reported not to exist in the photophysics of the complexes $[\text{Ru}(\text{bipy})_2(\text{diaz})]^{+2}$ and $[\text{Ru}(\text{bipy})_2(\text{py})_2]^{+2}$ 39,48,49.

Extensive studies on the complex tris(bipyridine)ruthenium(II), $[\text{Ru}(\text{bipy})_3]^{+2}$, have led to the model shown in Figures 6 and 7. It has been already stated that by examining either the temperature dependence of $[\text{Ru}(\text{bipy})_3]^{+2}$ luminescence lifetime or the emission intensity, Van Houten and Watts were able to evaluate the energy difference between the $^3\text{MLCT}$ and LF excited states, ΔE , to be about $3,600 \text{ cm}^{-1}$ ($[\text{Ru}(\text{bipy})_3]^{+2}$ dissolved in H_2O)⁴¹

(Fig. 8). It is normally assumed that the solvent affects only the non - radiative decay rate constant of the $^3\text{MLCT}$ excited state³⁵. Thus, population of the LF excited state becomes more efficient in nonpolar solvents, where k_{nr} is lower, and, as a result, photosubstitution also is observed to be more efficient.

Similarly, by an adequate ligand substitution, of one bipy by another chelating species, the energy of the $^3\text{MLCT}$ may be selectively perturbed and the corresponding variation in ΔE has been found to be directly correlated with the $^3\text{MLCT}$ excited state energy⁴³.

In contrast with the results and considerations described above, selective perturbation, in this case of the LF excited state of some complexes, did not seem to fit the model presented in Fig.6. For example, the observed temperature dependence of the emission intensity of $[\text{Ru}(\text{bipy})_2(\text{diaz})]^{+2}$ (temperature range 250 - 350 K) yielded a value of $3,450 \text{ cm}^{-1}$ for ΔE ⁴⁸. A similar study, over the same temperature range for $[\text{Ru}(\text{bipy})_2(\text{py})_2]^{+2}$, concluded that the value of ΔE was $3,410 \text{ cm}^{-1}$.

39.49 . Since the energy of the $^3\text{MLCT}$ excited state (relative to that of $[\text{Ru}(\text{bipy})_3]^{+2}$) is essentially constant ($E_{\text{em}}(0 - 0)$ varies by only 40 cm^{-1}) , this value of ΔE suggests little change in the energy of the presumed LF excited state .

It can be seen from these results that these E values found in the course of these studies, are very similar to that observed for $[\text{Ru}(\text{bipy})_3]^{+2}$. Nevertheless, these observations were disturbing because they seem to indicate that the energy of the presumed LF excited state does not depend upon the ligand field strength in the expected manner. It has already been stated that the ligand diazafluorene has been shown to perturb only the LF excited state while the energy of any MLCT excited state is nearly unchanged. On the other hand, pyridine is certainly lower in the spectrochemical series than bipyridine . In fact, a correct ordering of these ligands in the spectrochemical series would be $\text{bipy} > \text{py} > \text{diaz}$.

2. Discussion.

In order to attempt a rationalization of the energy changes of the LF excited state by means of ligand field theory, the temperature dependence of the

emission properties of the above mentioned complexes over an extended temperature range was reevaluated in this work, which represents a further investigation of the dynamics of the $^3\text{MLCT} - \text{LF}$ excited state transition.

The experimental procedures were those described in the Chapter II, Section C.

The relative emission intensities of the complexes $[\text{Ru}(\text{bipy})_3]^{+2}$, $[\text{Ru}(\text{bipy})_2(\text{diaz})]^{+2}$, and $[\text{Ru}(\text{bipy})_2(\text{py})_2]^{+2}$ in EtOH/MeOH(4:1, v/v) as a function of temperature are presented in Tables IX, X, and XI, respectively. These data are plotted in Figure 20. It can be observed that the emission intensity of $[\text{Ru}(\text{bipy})_2(\text{diaz})]^{+2}$ increases greatly between 160 and 140 K and that of $[\text{Ru}(\text{bipy})_2(\text{py})_2]^{+2}$ increases with a lesser slope between 230 and 150 K and with an even smaller slope between 290 and 230 K. The emission intensity of $[\text{Ru}(\text{bipy})_3]^{+2}$ increases less rapidly and with a different temperature dependence between 290 and 180 K. Similar observations of the luminescence lifetimes were made.

In Tables XII, XIII, and XIV are presented the collected experimental data for the temperature dependence of the emission quantum yield of

$[\text{Ru}(\text{bipy})_3]^{+2}$, $[\text{Ru}(\text{bipy})_2(\text{diaz})]^{+2}$, and $[\text{Ru}(\text{bipy})_2(\text{py})_2]^{+2}$, in EtOH/MeOH, respectively. The relative quantum yields were converted into absolute quantum yields by the use of $[\text{Ru}(\text{bipy})_3]^{+2}$ as the standard. The lifetime of this complex over the temperature range of 84 -330 K has been evaluated⁹² . The emission quantum yield for $[\text{Ru}(\text{bipy})_3]^{+2}$ was then determined at 140 K by the use of the calculated lifetime and its radiative rate constant ($Q_\infty = T_\infty k_r$). This procedure may introduce some systematic error so that quantitative arguments are best based upon the temperature dependence of the luminescence lifetimes . The temperature dependences of the emission quantum yields for all the three complexes are shown in Figures 21, 22, and 23, respectively. Those same figures display the resulting computer generated fit of the data (the curve - fitting parameters are presented in Table XVIII).

In Tables XV, XVI, and XVII are summarized the experimental data for the temperature dependence of the lifetimes of $[\text{Ru}(\text{bipy})_3]^{+2}$, $[\text{Ru}(\text{bipy})_2(\text{diaz})]^{+2}$, and $[\text{Ru}(\text{bipy})_2(\text{py})_2]^{+2}$ in EtOH/MeOH(4:1, v/v) . The resulting computer generated fits of the data are shown in Figures 24, 25,

and 26 respectively and the curve - fitting parameters for the treatment of those data are presented in Table XVIII.

The collected values of quantum yields of emission and of luminescence lifetimes were fit to the Equations (2) and (3), below expressed, by a nonlinear least squares routine^{39,41,49}.

$$1 / Q_{\text{e}} = [k_r + k_{nr} + k_{oe} e^{-\Delta E/RT}] / k_r \quad (2)$$

$$1 / T_{\text{e}} = k_r + k_{nr} + k_{oe} e^{-\Delta E/RT} \quad (3)$$

Clearly, these equations adequately describe the experimental data for all three complexes. Hence, no further exponential terms, suggested by Allsopp et al.⁹³, were added to describe the observed behavior in the very low - temperature region for the complexes that were investigated in this work.

The dramatic changes in the emission intensities and lifetimes of $[\text{Ru}(\text{bipy})_2(\text{diaz})]^{+2}$ and $[\text{Ru}(\text{bipy})_2(\text{py})_2]^{+2}$, observed in the low temperature region suggest possible development of rigidity of the solutions, but it should be mentioned that the solvent (EtOH/MeOH(4:1, v/v)), remains a liquid throughout this temperature range; the liquid -

glass transition occurs at ~ 95 K.

In the cases of both complexes, an additional process is apparent; a very weak emission is observed in the range 250 - 350 K. The lifetimes for these weak emissions at 250 K are approximately 2 μ sec. When the temperature is lowered to the point when the samples begin to emit strongly (~ 170 K), the lifetimes drop to about 100 nsec; this result was not expected. Furthermore, the apparent radiative rate constant in the high - temperature region is evaluated to be only 400 sec^{-1} , a value that in comparison with the usual $10^4 - 10^5 \text{ sec}^{-1}$ values ⁷⁴ is very improbable. Consideration of these observations suggested that the previously reported emission in the high - temperature region is actually due to trace impurities of some other emissive ruthenium complex (i.e., $[\text{Ru}(\text{bipy})_3]^{+2}$ and that both, $[\text{Ru}(\text{bipy})_2(\text{diaz})]^{+2}$ and $[\text{Ru}(\text{bipy})_2(\text{py})_2]^{+2}$ are essentially nonemissive above 230 K.

This finding is particularly pertinent to some reports of the photochemistry of these complexes ^{39,49}. Often, the disappearance of a starting complex is monitored by the loss of emission intensity. In the cases of $[\text{Ru}(\text{bipy})_2(\text{diaz})]^{+2}$ and

$[\text{Ru}(\text{bipy})_2(\text{py})_2]^{+2}$ at 298 K, this procedure would simply follow the disappearance of an impurity. In the work carried out in our laboratory, in the cases of both complexes the emission intensity of the luminescence detected at 298 K, that initially was thought of to come from the complexes, decreased significantly after repeated recrystallization. Although it did not completely disappear even after seven successive recrystallizations, the intensity decrease suggested that it was from an impurity.

Balzani and co-workers have reached a similar conclusion in studies of luminescence of mixed-ligand Ru(II) chelates⁷⁷. They noted that in mixed-ligand $[\text{Ru}(\text{L})_n(\text{L}')_{3-n}]^{+2}$ complexes (where L and L' are distinct diimine-type ligands and n is 1 or 2) the absorption spectra showed distinct $\text{Ru} \rightarrow \text{L}$ and $\text{Ru} \rightarrow \text{L}'$ CT bands, which were very similar to the bands of the complexes $[\text{Ru}(\text{L})_3]^{+2}$ and $[\text{Ru}(\text{L}')_3]^{+2}$, whereas the emission only occurred from the lowest-energy CT excited state; this lowest CT excited state correspond to that associated to the ligand which is easier to reduce. In contrast, Coks et al.¹¹⁸ reported that in the case of the complex $[\text{Ru}(\text{phen})_n(\text{pq})_{3-n}]^{+2}$ (phen = 1,10-phenanthroline, pq = 2-(2-pyridylquinoline))

luminescence emission from both $\text{Ru} \rightarrow \text{phen}$ and $\text{Ru} \rightarrow \text{pq}$ excited state had been observed. Also in reference ¹¹⁹ a dual emission was observed to occur from $[\text{Ru}(\text{bipy})_2(\text{NO}_2 - \text{bipy})]^{+2}$ in a rigid matrix at 77 K. Balzani and co-workers⁹⁷ found that in each of both cases there is only one true emission.

The temperature dependence of the emission intensities and lifetimes of $[\text{Ru}(\text{bipy})_3]^{+2}$, $[\text{Ru}(\text{bipy})_2(\text{diaz})]^{+2}$, and $[\text{Ru}(\text{bipy})_2(\text{py})_2]^{+2}$ were fit to Eq. (2) and Eq. (3), and the results are shown in Table XVIII. In the cases of the last two complexes, only values at or below 200 K were used in this fitting procedure. Furthermore, the absolute quantum yield of emission may contain a systematic error and only the value of ΔE would be unaffected by this possible error.

The results obtained for $[\text{Ru}(\text{bipy})_3]^{+2}$ agree with those of previous reports^{82,96,97}. Furthermore, the activation energies obtained from the temperature dependences of both the emission intensities and the lifetimes within experimental error, agree very well.

The values of the activation energy, ΔE ,

between the MLCT and LF excited states , of the complexes $[\text{Ru}(\text{bipy})_2(\text{diaz})]^{+2}$ and $[\text{Ru}(\text{bipy})_2(\text{py})_2]^{+2}$ were substantially lower than the corresponding value of $[\text{Ru}(\text{bipy})_3]^{+2}$. In both cases, these results are in agreement with the general postulates of ligand field theory. Pyridine and diazafluorene are known to be lower than bipyridine in the spectrochemical series⁴⁷. Hence, substitution of one bipy by any of these ligands would result in a decreased ligand field molecular microenvironment and , subsequently, a lower LF excited state energy. Since the $^3\text{MLCT}$ excited state is not significantly affected by this substitution, the variation in the LF excited state dictates the energy gap.

It is worthwhile to note that the redox properties for the three complexes , given in Table XX, indicate that the separation between the first oxidation and first reduction, $E_{1/2}$, is nearly the same. Based on previous correlations of electrochemical and spectroscopic data, this invariance in $E_{1/2}$ is expected because the observed emission energies are similar^{37,47} . The fact that the first oxidation potential, $E^\circ(+3/+2)$ is practically the same for the three complexes and that the emitting

state can be described as $Ru(d\pi^*)bipy(\pi^*)$ for each complex suggests that the ground state energies are nearly equivalent. As a result, since the ligand field parameter $10Dq$ decreases in the order $bipy > py > diaz$, the correlation between $10 Dq$ and ΔE is consistent with the observed trend.

The anticipated lifetime of the 3MLCT excited state at 298 K can be evaluated for both $[Ru(bipy)_2(diaz)]^{+2}$ and $[Ru(bipy)_2(py)_2]^{+2}$ with the aid of Eq.(3) and the use of the parameters reported in Table XVIII. The resulting values were 0.07 and 2.7 nsec , respectively. With these extremely short lifetimes , the 3MLCT excited state is not likely to be involved in any bimolecular process at this temperature. This expectation was confirmed during the course of the present work by the fact that no photooxidation of these two $Ru(II)$ complexes to the corresponding $Ru(III)$ complexes could be observed even in solutions containing high concentrations of persulfate .

Another interesting fact is apparent by observing Table XVIII; the activation energies for $[Ru(bipy)_2(diaz)]^{+2}$ and $[Ru(bipy)_2(py)_2]^{+2}$

obtained from emission intensity measurements are systematically lower than those obtained from lifetime measurements. On the contrary, both methods led to essentially the same value for ΔE , in the case of $[\text{Ru}(\text{bipy})_3]^{+2}$. One possible explanation would be an apparent temperature dependence of k_r ; although this hypothesis does not agree with the usual understanding that the radiative rate constant is characteristic of a molecule and not dependent of the environment conditions, such as temperature or solvent properties, this phenomenon might be induced by temperature - dependent intersystem crossing from $^1\text{MLCT}$ directly to the (presumably triplet) LF excited state. The energy lowering of the LF excited state could eventually facilitate this conversion. Nakamura has recently suggested that an apparent decrease in k_r when the ligand 3,3' - dimethyl - 2,2' bipyridine (DMB) replaces one bipyridine in the complex $[\text{Ru}(\text{bipy})_2(\text{DMB})]^{+2}$, is really connected to changes in the intersystem crossing efficiency⁵⁹. According to this interpretation, k_r could not be evaluated by the expression $k_r = Q_r/T_r$ and must be replaced by the relationship $k_r = Q_r/T_r \cdot Q_{\text{ISC}}(T)$. In this regard, at the present moment, it can be considered that, due to steric effects, the ligand DMB is

probably a weaker ligand than bipy so that the corresponding LF excited state would be lowered - as in the cases investigated in the present work - by substitution of DMB ligands, in a complex that originally contained only bipy chelating species.

$^3\text{MLCT}$ production was also determined by the method of Bolleta et al.²³. For the case of $[\text{Ru}(\text{bipy})_3]^{+2}$, the $^3\text{MLCT}$ is efficiently quenched by $\text{S}_2\text{O}_8^{2-}$ via an electron - transfer mechanism (Fig. 27). The generated species $\text{S}_2\text{O}_8^{3-}$ spontaneously dissociates so that back electron transfer is so greatly inhibited, at the extent that the process can be visualized, for all practical purposes, to be effectively irreversible. The limiting quantum yield of $[\text{Ru}(\text{bipy})_3]^{+2}$ disappearance, evaluated as a function of persulfate concentration, has been evaluated to be 2×10^{-3} , after extrapolating to infinite persulfate concentration (according with the postulated mechanism, the decomposition of each persulfate ion results in the oxidation of two equivalents of the metal complex). This result was substantiated in the present work (Table XIX, Figure 28).

In contrast, solutions of $[\text{Ru}(\text{bipy})_2(\text{diaz})]^{+2}$ were virtually unchanged upon prolonged photolytic irradiation in the presence of dissolved potassium persulfate. On the other hand, it was observed that $[\text{Ru}(\text{bipy})_2(\text{py})_2]^{+2}$ underwent a photoaquation process but not oxidation. The initial photoaquation product, $[\text{Ru}(\text{bipy})_2(\text{py})(\text{H}_2\text{O})]^{+2}$, thermally reacts, very slowly, with $\text{S}_2\text{O}_8^{2-}$. The efficiency of this photoaquation process was determined not to be affected by the presence of persulfate; no changes were observed upon irradiation.

The quantum yield of LF production can be evaluated by means of the Eq. (4).

$$Q_{\text{LF}}(T) = [k_0 e^{-\Delta E/RT}] / T_0 \quad (4)$$

$$\text{where } T_0 = k_r + k_{\text{nr}} + k_0 e^{-\Delta E/RT} \quad (5)$$

and with the aid of the fitting parameters reported in Table XVIII. These calculations can only be considered to be a qualitative approximation merely purporting to show some trend in the observed behavior of the complexes under analysis.

For instance, in the case of $[\text{Ru}(\text{bipy})_3]^{+2}$, $Q_{\text{LF}}(298 \text{ K})$ was evaluated to be

0.79 and $Q_{LF}(220\text{ K})$ was found to be 0.005. In turn, in the case of $[\text{Ru}(\text{bipy})_2(\text{diaz})]^{+2}$, the values of Q_{LF} at 298 K and that at 220 K reached both unity. Finally, in the case of $[\text{Ru}(\text{bipy})_2(\text{py})_2]^{+2}$, Q_{LF} at 298 K was unity, while the respective value at 220 K was 0.890. These calculations also agree with the trend expected from considering the relative ordering of the energies of the average ligand field strength of the different complexes.

3. Conclusions.

The model that was developed and extensively studied in many polypyridine ruthenium(II) complex seems to be valid in treating the behavior of $[\text{Ru}(\text{bipy})_2(\text{py})_2]^{+2}$ and $[\text{Ru}(\text{bipy})_2(\text{diaz})]^{+2}$. The complexes that have lower d - d excited states do have activation energies that correlate with this smaller energy gap; therefore, in the extent that the effective crystal field strength is reduced, ΔE values between the MLCT and the LF excited state are reduced as expected by theory.

C.EXPLORATORY ANALYSIS OF THE EFFECT OF ION PAIRING UPON PHOTOSUBSTITUTION QUANTUM YIELDS.

1.Introduction.

Dioxane - water mixtures have been a favorite solvent system in which to study both ion association and ionic mobilities^{101,102} because the dielectric constant can be varied over a large range. It is normally assumed that the changes in these properties that are observed as dioxane is added to water, are due to the decreasing dielectric constant rather than to a change in solvent - ion or solvent - solvent interactions. Measurements of molar conductances as a function of concentration of the dissolved investigated compound (salt, complex) have allowed investigators to deduce values of association constants for different types of electrolytes ^{98,99,100}.

In the present study, no conductance measurements were made. There was only an attempt to determine, qualitatively, the effect that the ion - pairing could have on the observed photosubstitution quantum yields of complexes subjected to photolysis. Specifically, the behavior of the complex $[\text{Ru}(\text{bipy})_2(\text{py})_2]^{+2}$, which has no chelate ring

involved in its photochemistry, was investigated.

2. Discussion.

First, (see Results C.) an estimation of the value of the molar absorption coefficient of the first monochloro intermediate generated in the photolysis of $[\text{Ru}(\text{bipy})_2(\text{py})_2]^{+2}$ was made. This estimation involved an exploratory set of experiments that were designed to test the accuracy of such an estimation. It was planned to use the same procedure in order to estimate the molar absorption coefficient of the detected intermediate in the photolysis of the complex $[\text{Ru}(\text{bipy})_2\text{DPM}]^{+2}$.

In the case of the value of the estimated molar absorption coefficient of $[\text{Ru}(\text{bipy})_2(\text{py})\text{Cl}]^{+1}$ at 450 nm there was an error of 20 % with respect to the value determined for a real sample.

Next, photolyses of $[\text{Ru}(\text{bipy})_2(\text{py})_2]^{+2}$ in different dioxane - water mixtures that contained 0.01 M TBACl, of dielectric constant in the range of 3.9 to 32.5 were carried out at 298 K. Isosbestic points were observed throughout all the photolysis experiments. The final photoproduct detected after

prolonged irradiation times was $[\text{Ru}(\text{bipy})_2]\text{Cl}_2$.

It was determined that there was a correlation between the dielectric constants of the dioxane - water mixtures used as a solvent and the evaluated photosubstitution quantum yields. The yields were significantly increased and seemed to correlate with the ability of the media to support improved ion - pair formation, that is, with the decreasing polarity of the mixtures. Larger photosubstitution quantum yields were found in those photolyses that were carried out in dioxane - water mixtures that had lower dielectric constant (Table XXIII).

In order to investigate the possible influence of the concentration of pyridine, which was the ligand being replaced by Cl^- in the photosubstitution reactions in a two stage, stepwise mechanism, photolyses of $[\text{Ru}(\text{bipy})_2(\text{py})_2]^{+2}$ dissolved in a dioxane - water mixtures 90/10 (v:v) that contained 0.01 M TBACl and different py concentrations, were carried out. No significant changes were detected (Table XXIV).

In order to study the probable influence of

the coordinating anion, photolysis of $[\text{Ru}(\text{bipy})_2(\text{py})_2]^{+2}$ dissolved in different dioxane - water mixtures that contained 0.01 M TBAClO_4 were carried out. No formation of $[\text{Ru}(\text{bipy})_2][\text{ClO}_4]_2$ was detected. These studies revealed that only one pyridine ligand is effectively lost from the starting complex, and thus, $[\text{Ru}(\text{bipy})_2(\text{py})\text{ClO}_4]^{+1}$ is generated. This complex has an absorption spectrum in which there is a maximum at 474 nm⁵¹. In the course of this work, this species was detected to be easily formed, at least, under the experimental conditions that were used. No important effect on the photosubstitution quantum yields was observed when the dissolved complex in the various dioxane - water mixtures was photolytically irradiated (Table XXV). All the determinations of photosubstitution quantum yields were made following the appearance of the first intermediate photoproduct during the initial stages of the photoreaction.

The fact that the photosubstitution reaction does not continue towards the formation of $[\text{Ru}(\text{bipy})_2][\text{ClO}_4]_2$ can be interpreted by considering the relative bulkiness of ClO_4^- relative to the size of Cl^- ; after one py ligand

becomes detached from the complex, it diffuses away, and a second ClO_4^- anion cannot enter, even in a 90/10 (v:v) dioxane - water mixture, used as a solvent system. It has been reported that photolysis of $[\text{Ru}(\text{bipy})_2(\text{py})_2]^{+2}$ in the presence of weakly coordinating anions X ($\text{X} = \text{ClO}_4^-$, NO_3^- , $\text{p} - \text{CH}_3\text{C}_6\text{H}_4\text{SO}_3^-$, or CF_3CO_2^-) result in $[\text{Ru}(\text{bipy})_2(\text{py})\text{X}]^{+1}$, even with excess of X^- and extended irradiation⁵¹.

In this work, extensive photolysis showed, qualitatively, the retention of the intermediate complex $[\text{Ru}(\text{bipy})_2(\text{py})\text{ClO}_4]^{+1}$ and also a probable partial oxidation of Ru(II) to Ru(III); this last conclusion was based on the fact that after long irradiation times, a new well defined band with a maximum located at 640 nm was apparent. The complex $[\text{Ru}(\text{bipy})_3]^{+3}$ has an absorption spectrum with a maximum located at 675 nm¹⁰³.

3. Conclusions.

In summary, these experimental results do provide qualitative but substantial proof that ion - pairing effects can modify the behavior of photosubstitution reactions of complexes that are

photolysed. The present work substantiates and complements previous observations ⁵¹. It would be desirable not only to quantify these observations but also to extend them to other interesting complexes, such as those in which a chelate ring is involved in the photosubstitution process (complexes $[\text{Ru}(\text{bipy})_2\text{L}]^{+2}$ where $\text{L} = (\text{py}) - (\text{CH}_2)_n - (\text{py})$ and $\text{H}_2\text{N} - (\text{CH}_2)_n - \text{NH}_2$).

DISCUSSION D. EFFECT OF CHELATE RING SIZE ON THE PHOTOSUBSTITUTION REACTION OF POLYPYRIDINE RUTHENIUM (II) COMPLEXES, WITH THE GENERAL FORMULATION, $[Ru(BIPY)_2L]^{+2}$.

1. Introduction.

Systematic changes in the Ru - N bonds of polypyridine ruthenium(II) complexes were made. These changes were introduced in order to modify the geometry of the complexes $[Ru(bipy)_2L]^{+2}$. It was anticipated that the changed geometry would affect the excited state processes of polypyridine ruthenium(II) complexes. In this part of the work, these changes were specifically achieved by selecting ligands, L, that would form a well ordered series of compounds. Any perturbation in the Ru - N bond overlap affects the excited state properties of polypyridine ruthenium(II) complexes; the photosubstitution process, normally attributed to involve a populated LF excited state, is one of those properties. Investigation of these kind of properties constitutes a growing field of research.

The above mentioned variation of the geometry

of the $[\text{Ru}(\text{bipy})_2\text{L}]^{+2}$ complexes was accomplished in this work by the use of two series of ligands, L. One series had two pyridines linked by methylene bridges of varying lengths (Figure 29); the other series had two ammine groups linked by methylene bridges of different lengths (Figure 36).

The perturbation, methodically forced upon the series of complexes, affected not only the size of the ring involved in the photosubstitution processes, but also the N - Ru - N chelation angle.

In this work, the photophysics of these complexes was studied at 77 K. Also investigated were the temperature dependences of the emission intensities exhibited by these complexes and, subsequently, the photochemistry of these complexes in different solvents. The quantum yields of the observed photosubstitution reactions were determined.

The data collected in this work represent only a first step in gaining a better understanding of the photosubstitution processes of polypyridine ruthenium(II) complexes. The generally postulated model of photosubstitution, described in the Introduction (Figure 9), has been used successfully to rationalize previous studies but several mechanistic aspects of

the process need clarification. Substantial data were acquired during the course of the present study; however, many more experiments need to be done. Future research should complete the gaps. The new knowledge contributed by this work combined with previously observed trends should make it possible to design further studies in order to attempt a final clarification of one principal aspect of the postulated photosubstitution model; that aspect is the role of the postulated pentacoordinated intermediate (I), a key factor in understanding the observed quantum yields of photosubstitution reactions.

2. Discussion.

2.1. Effect of chelate ring size on the photosubstitution reaction of polypyridine ruthenium(II) complexes, $[\text{Ru}(\text{bipy})_2\text{L}]^{+2}$, in which L is a polypyridine ligand that has two pyridine rings linked by methylene bridges of different lengths.

The ligands used in the present work (Figure 29) were either commercially available, (2,2' - bipyridine and 4 - picoline), or could be prepared by means of methods reported in literature.

Dipyridylmethane (DPM), and dipyridylethane (DPE) had to be synthesized. The corresponding complexes were generally prepared by heating $[\text{Ru}(\text{bipy})_2\text{Cl}_2]$ with a excess of the pertinent ligand in water - methanol mixtures for several hours. The complexes were all then precipitated as the PF_6 salt, (PF_6 is a poorly coordinating anion, and it is not expected to interfere with the photochemical behavior). Purification of the complexes was accomplished by repeated recrystallization from water - acetone or MeOH - toluene mixtures.

The photophysical and photochemical properties of these complexes were examined. It was determined that the low temperature emission (77 K) properties of the new complexes are similar to those of $[\text{Ru}(\text{bipy})_3]^{+2}$ but at higher temperature their emission intensities were observed to be significantly decreased. It was also determined that photosubstitution in organic solvents, is a very efficient processes for all the new complexes.

In the case of $[\text{Ru}(\text{bipy})_2\text{DPE}]^{+2}$, complex having a seven - membered chelate ring, the substitution of the first pyridine was found to occur thermally in solutions 0.01 M TBACl in CH_2Cl_2 so

that the photosubstitution of the second pyridine could be directly studied. Similarly in solutions of H_2SO_4 in which $[\text{Ru}(\text{bipy})_2\text{DPE}]^{+2}$ was dissolved, the first substitution was a thermal process.

In the case of the complex having a six - membered chelate ring directly connected to the processes of photoanation, $[\text{Ru}(\text{bipy})_2\text{DPM}]^{+2}$, it was found that the reclosure of the chelate ring competed significantly with the photosubstitution only in polar solvents in which the ion - pairing is not significant.

Finally, the photosubstitution of the complex which had a five membered ring ($[\text{Ru}(\text{bipy})_3]^{+2}$) was observed to be drastically different from the photoreactions of the complexes that had other ring sizes.

First, the emission quantum yields and lifetimes of the complexes at 77 K were determined. The different emission spectra of the different complexes at low temperature had no special features and displayed a well - defined vibrational fine structure similar to that of $[\text{Ru}(\text{bipy})_3]^{+2}$. Nevertheless, upon warming the solutions this fine structure in the spectra of all the complexes was lost, and a drastic decrease in the emission quantum yield

was noted, except in the case of $[\text{Ru}(\text{bipy})_3]^{+2}$. The experimental procedures that were followed in the acquisition of emission spectra at different temperatures as well as those used in order to determine lifetimes at 77 K have been described in detail in Chapter II, Section C. The excitation wavelength was 450 nm, and the range 500 - 700 nm was scanned; identical conditions were used for the acquisition of all emission spectra. The properties, in EtOH/MeOH, 4:1, v/v at 77 K are shown in Table XXVI. Absolute emission quantum yield were evaluated by the use of $[\text{Ru}(\text{bipy})_3]^{+2}$ as the reference ($Q_0 = 0.376$)¹⁰⁶.

The temperature dependence of the emission quantum yields were determined for $[\text{Ru}(\text{bipy})_2(\text{pic})_2]^{+2}$ and $[\text{Ru}(\text{bipy})_2\text{DPM}]^{+2}$ in EtOH/MeOH, 4:1, v/v over the temperature range 100 - 270 K (Figures 30 and 31, respectively).

The emission of the complex $[\text{Ru}(\text{bipy})_2\text{DPE}]^{+2}$ was so weak above the solvent glass - liquid transition (95 - 110 K) that a similar study was not attempted.

In order to evaluate the quantum yield of the LF excited state production at 298 K, the non - linear

Arrhenius plot was fitted to Eq. (2) ^{43, 62, 73, 74}. The parameters obtained by means of this fitting procedure are reported in Table XXIX.

This determination was interesting because this LF excited state is considered to be directly involved in the observed photosubstitution processes, for study of which, in the present work, solutions at ambient temperature were investigated.

Also investigated was the temperature dependence of the emission quantum yield of the complexes $[\text{Ru}(\text{bipy})_3]^{+2}$, $[\text{Ru}(\text{bipy})_2(\text{pic})_2]^{+2}$, and $[\text{Ru}(\text{bipy})_2\text{DPM}]^{+2}$ in the solvents CH_3CN , CH_2Cl_2 , and H_2O . Again, the observed emission of $[\text{Ru}(\text{bipy})_2\text{DPE}]^{+2}$ was too weak to allow accurate determinations. An attempt was made to establish activation energies, ΔE , between the $^3\text{MLCT}$ and LF excited states of the complexes in each of these solvents under conditions which were similar to those actually used in the photolysis studies which were done later. It was considered important to obtain emission quantum yield data in a temperature range in which the ambient temperature was included. It was hoped that a reasonable evaluation of the effective LF excited state population would be obtained under each

set of the experimental photolysis conditions; however, these hopes were not quite realized.

In Table XXX are reported the parameters, obtained by the standard fitting procedure used in this work, for the complexes $[\text{Ru}(\text{bipy})_3]^{+2}$, $[\text{Ru}(\text{bipy})_2(\text{pic})_2]^{+2}$, and $[\text{Ru}(\text{bipy})_2\text{DPM}]^{+2}$ dissolved in CH_3CN .

Although the curve fitting was accomplished, the values obtained were not convincing, particularly, after the values obtained for the radiative and non radiative rate constants of the complexes $[\text{Ru}(\text{bipy})_2(\text{pic})_2]^{+2}$ and $[\text{Ru}(\text{bipy})_2\text{DPM}]^{+2}$ were analyzed. At least, the analysis of those data suggested a clear trend, that showed a substantially greater population of the LF excited state in the cases of $[\text{Ru}(\text{bipy})_2(\text{pic})_2]^{+2}$ and $[\text{Ru}(\text{bipy})_2\text{DPM}]^{+2}$, than that estimated for $[\text{Ru}(\text{bipy})_3]^{+2}$. This result was reasonable since the ligands pic and DPM have a lower position in the spectrochemical series than that of the bipy ligand.

The studies of the temperature dependence of emission quantum yield, which were carried out in the present work with CH_2Cl_2 and H_2O solutions resulted in an even more frustrating experience.

Unfortunately, the experimental attempts to get better quantum yields of generation of LF excited states at 298 K were not successful. The observed variations in intensities of the emissions of the complexes $[\text{Ru}(\text{bipy})_2(\text{pic})_2]^{+2}$ and $[\text{Ru}(\text{bipy})_2\text{DPM}]^{+2}$ could not be fitted to Eq. (2); the resulting parameters lacked any possible physical meaning. The major experimental difficulty which interfered with the acquisition of these data, was that the emission intensities of those complexes at or above 298 K were too low to allow accurate determinations. Therefore, the quantum yield of LF excited state production could not be evaluated in the manner initially chosen. In Tables XXXI and XXXII are compared the emission quantum yields of $[\text{Ru}(\text{bipy})_2(\text{pic})_2]^{+2}$ and $[\text{Ru}(\text{bipy})_2\text{DPM}]^{+2}$ in CH_3CN and CH_2Cl_2 at 298 K with those of $[\text{Ru}(\text{bipy})_3]^{+2}$, in the same solvents. In each case, the emission quantum yields relative to that of $[\text{Ru}(\text{bipy})_3]^{+2}$ were determined ($Q_{\text{rel}}(298 \text{ K}) = 0.062$, in CH_3CN ; $Q_{\text{rel}}(298 \text{ K}) = 0.029$, in CH_2Cl_2 ; $Q_{\text{rel}}(298 \text{ K}) = 0.042$, in H_2O)^{106,107}.

These difficulties led to abandoning the study of the emission lifetimes as a function of temperature because lifetime determinations would not

have been feasible with the apparatus that was available at the moment this work was being done. The efficiency of LF production of the complexes $[\text{Ru}(\text{bipy})_2(\text{pic})_2]^{+2}$ and $[\text{Ru}(\text{bipy})_2\text{DPM}]^{+2}$ at 298 K in all the solvents in which their photosubstitution processes were investigated was considered to be nearly unity (Table XXXIII).

Photosubstitution quantum yields of all four complexes, $[\text{Ru}(\text{bipy})_3]^{+2}$, $[\text{Ru}(\text{bipy})_2(\text{pic})_2]^{+2}$, $[\text{Ru}(\text{bipy})_2\text{DPM}]^{+2}$, and $[\text{Ru}(\text{bipy})_2\text{DPE}]^{+2}$ in 0.50 M H_2SO_4 and in solutions that contained 0.01 M TBACl in CH_2Cl_2 and CH_3CN , respectively, at 298 K were determined. These determinations were made by means of the methods described in the experimental section. The evaluations of all the molar absorption coefficients that were necessary in order to follow the progress of the photosubstitution reactions by absorption spectroscopy have already been described in Chapter III, Section D.1.b., where a complete summary of all the experimental conditions, under which the photolysis studies were conducted, was also included.

Since the intermediate complex expected to be generated during the photolysis of $[\text{Ru}(\text{bipy})_2\text{DPM}]^{+2}$, cannot be prepared it was assumed that the ratio of the molar absorption coefficients of the initial complex and its monosubstituted photogenerated product was the same value previously determined for the complex $[\text{Ru}(\text{bipy})_2\text{DPE}]^{+2}$. This ratio was determined by

making use of the observed thermal reactions of $[\text{Ru}(\text{bipy})_2\text{DPE}]^{+2}$ that lead to a monochloro or a monoaquo - substituted intermediate; each intermediate was purposely generated under controlled conditions in CH_2Cl_2 by adding TBACl and in H_2O by means of the subsequent addition of H_2SO_4 . The ratio obtained for the complexes in CH_2Cl_2 was also assumed to be valid for CH_3CN solutions. As a way of checking on this estimation, the same procedure was applied to the complex $[\text{Ru}(\text{bipy})_2(\text{pic})_2]^{+2}$ and the molar absorption coefficients evaluated in that way contrasted with those determined directly. An error of 27 % was detected; therefore, a systematic error in the photosubstitution quantum yield of $[\text{Ru}(\text{bipy})_2\text{DPM}]^{+2}$ very probably, may be present.

All the complexes in CH_2Cl_2 and CH_3CN were found to be extremely photolabile when a strongly complexing ligand was present. Very short times of photolytic irradiation were necessary to reach approximately 10 % photosubstitution reaction. All the photosubstitution quantum yields were determined during those initial stages of the reaction while an isosbestic point was still maintained. The band at 436 nm, from a 150 W Xe - Hg lamp used as an excitation

source, was isolated by means of an interference filter.

Figures 32, 33, 34, and 35 are representative of the changes that were observed in the respective absorption spectra of the complexes, $[\text{Ru}(\text{bipy})_3]^{+2}$, $[\text{Ru}(\text{bipy})_2(\text{pic})_2]^{+2}$, $[\text{Ru}(\text{bipy})_2\text{DPM}]^{+2}$, and $[\text{Ru}(\text{bipy})_2\text{DPE}]^{+2}$ during typical photolyses.

The case of the complex $[\text{Ru}(\text{bipy})_2\text{DPE}]^{+2}$ deserves a special explanation. It was found that this complex, although stable in CH_2Cl_2 in the dark, was, nevertheless, rapidly transformed in the presence of Cl^- by a thermal reaction to a product which had an absorption maximum located at 504 nm; this thermally generated intermediate was stable in the dark for at least 1 hour. Therefore, the photolysis of this intermediate complex, rather than the photosubstitution reaction of the starting complex leading to the first photoproduct, was actually studied.

Similar results were obtained when 0.01 M solutions of TBACl in CH_3CN were used. However, in this medium, $[\text{Ru}(\text{bipy})_2\text{DPE}]^{+2}$ was stable in the dark and exhibited a photochemical behavior quite similar to that observed in the cases of the complexes $[\text{Ru}(\text{bipy})_2(\text{pic})_2]^{+2}$ and $[\text{Ru}(\text{bipy})_2\text{DPM}]^{+2}$.

In 0.50 M H_2SO_4 , $[\text{Ru}(\text{bipy})_3]^{+2}$ was found to be very photostable, while both, $[\text{Ru}(\text{bipy})_2(\text{pic})_2]^{+2}$ and $[\text{Ru}(\text{bipy})_2\text{DPM}]^{+2}$ underwent relatively efficient photoaquation processes. Just as in solutions of 0.01 M TBACl in CH_2Cl_2 , $[\text{Ru}(\text{bipy})_2\text{DPE}]^{+2}$ showed its instability in 0.50 M H_2SO_4 , in which a thermal solvolysis to the monoquo complex occurs. Once more, the process actually observed was the photolysis of the thermally generated intermediate .

In Table XXXIII, are summarized all the values of the photosubstitution quantum yields for all the complexes at 298 K that were collected during the present work ; in the same Table XXXIII are presented the estimated quantum yields of formation of the corresponding LF excited states .

It can be seen that the six and seven - membered ring ligands seem to behave almost identically to $[\text{Ru}(\text{bipy})_2(\text{py})_2]^{+2}$ in solvents in which equilibria of ion pairing can exist to some degree. However, in H_2O , the six - membered chelate ring showed a behavior similar to that of $[\text{Ru}(\text{bipy})_3]^{+2}$. The results indicated that the reclosure of the chelate

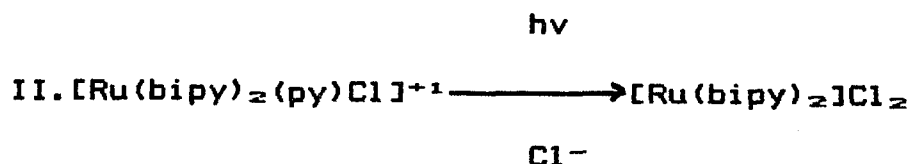
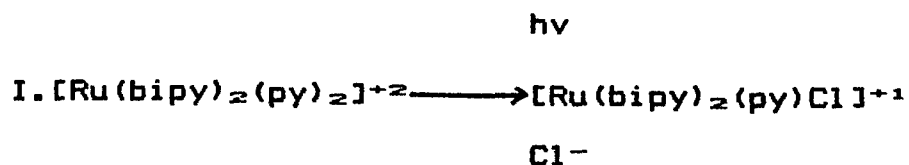
ring had become a competitive process in H_2O .

The absorption and emission spectra of the four complexes were not unusual. In all cases, the intense MLCT absorption band occurs near 450 nm. Analysis of the low temperature emission spectra revealed that $[Ru(bipy)_2DPE]^{+2}$ has an unusually low radiative rate constant. The cause of this experimental finding is at present unknown. At 298 K, the emissions of the complexes $[Ru(bipy)_2L]^{+2}$ ($L = (pic)_2$, DPM or DPE), had substantially reduced intensities; this result is commonly observed in the cases of complexes that have at least one ligand weaker than bipy in the spectrochemical series¹⁰⁸.

Population of the LF excited state is one important pathway of decay of the 3MLCT state. It has been noted previously, that the emission lifetime and the emission intensities exhibit a temperature dependence that has been ascribed to partial population of this LF excited state. In the case of $[Ru(bipy)_3]^{+2}$, reported experimental results indicate that, depending upon the solvent, 20% - 90 % of the initial population of the 3MLCT excited state is deactivated by thermal conversion to the postulated

higher - lying LF excited state¹⁰⁷. In the present work, it was estimated that in the cases of the complexes $[\text{Ru}(\text{bipy})_2(\text{pic})_2]^{+2}$ and $[\text{Ru}(\text{bipy})_2\text{DPM}]^{+2}$, essentially 100% of the excitation energy is dissipated via production of their corresponding LF excited states.

It was observed that in the early stages of photolysis of $[\text{Ru}(\text{bipy})_2(\text{pic})_2]^{+2}$ in 0.01 M solution of TBACl in CH_2Cl_2 , an isosbestic point located at 481 nm developed as the initial photoproduct which had a maximum of absorption at 508 nm accumulated (Figure 33). After a period of photolytic irradiation, a significant fraction of the exciting light began to be absorbed by this intermediate, the isosbestic point was lost, and a second species which had an absorption maximum located at 550 nm appeared. A similar behavior had been detected in previous studies of the complex $[\text{Ru}(\text{bipy})_2(\text{py})_2]^{+2}$, and the photosubstitution sequence shown by means of the reactions I and II was proposed^{51,109}. The same mechanism was assumed in order to explain the observations made in the photolysis experiment described above.



Virtually the same behavior was found during the photolysis of the complex $[\text{Ru}(\text{bipy})_2\text{DPM}]^{+2}$ in 0.01 M solution of TBACl in CH_2Cl_2 . The set of absorption spectra superimposed in Figure 34 monitor the course of the observed photosubstitution reactions; there is an initial isosbestic point which is subsequently lost when the intermediate photoproduct reached a concentration sufficiently high to absorb a substantial fraction of the incident photolytic radiation. Interestingly, the quantum yield of the photosubstitution reaction, which actually represents the quantum yield of generation of the first photosubstitution product being generated under the photolysis conditions, turned out to be as large as the corresponding value of photoproduction of the first intermediate observed when there were similar

photolysis conditions for the reaction of $[\text{Ru}(\text{bipy})_2(\text{pic})_2]^{+2}$. Apparently, with these experimental conditions this behavior indicates that the ring closure is not particularly important in the collapse of the pentacoordinated intermediate (I) postulated in the general photosubstitution model (Figure 9).

The $[\text{Ru}(\text{bipy})_2\text{DPE}]^{+2}$ complex, which was shown to be thermally unstable in 0.01 M TBACl solutions in CH_2Cl_2 , produced within a few minutes a species with an absorption maximum located at 504 nm. This product, which exhibited an absorption spectrum with features similar to those of the initially generated photoproduct observed during the photolysis of the last two complexes discussed, was assumed to have a formula in which one Cl^- anion is coordinated i.e. $[\text{Ru}(\text{bipy})_2\text{Clpy}'\text{CH}_2\text{CH}_2\text{py}]^{+1}$. The nomenclature $\text{py}'\text{CH}_2\text{CH}_2\text{py}$ was intended to symbolize the loss of one of the direct N - metal bonds. Initially both of the pyridines were coordinated, and later one pyridine ring, py' , of the ligand DPE was detached from the metal center. This intermediate thermally generated product was found to be relatively stable in the dark (no appreciable decomposition was

detected by absorption spectroscopy for about 1 hour) but it could readily undergo a photosubstitution reaction under photolysis conditions to produce $[\text{Ru}(\text{bipy})_2]\text{Cl}_2$. An isosbestic point was maintained throughout the photolysis (Figure 35); this isosbestic point conservation shows a direct relationship between the reactant, the initially thermally formed intermediate, and the product, the final complex generated by photosubstitution; in this case the product was $[\text{Ru}(\text{bipy})_2]\text{Cl}_2$. It was determined that the quantum yield for the loss of the second chelating position of the ligand DPE, which can be visualized to be the detachment of the second pyridine of the DPE ligand from the previously identified intermediate, was substantially larger than that evaluated for the similar photosubstitution process in the case of $[\text{Ru}(\text{bipy})_2\text{DPM}]^{+2}$; however, in the later case, the determined quantum yield was directly related to the detachment of the first pyridine ring, part of the structure of the ligand DPM. However, the second step in the previously presented photosubstitution scheme has been reported to have a rather low quantum yield¹⁰⁹. The different behavior observed, in the present study, may possibly result as a consequence of the increased steric strain, expected to be present in

the case of DPE.

Figure 32 shows the behavior during the photolysis of $[\text{Ru}(\text{bipy})_3]^{+2}$ in 0.01 M TBACl in CH_2Cl_2 ; an isosbestic point is maintained. The intermediate complex cannot be detected; apparently, this intermediate reverts to the starting $[\text{Ru}(\text{bipy})_3]^{+2}$, or, alternatively, proceeds via the second photosubstitution step of the mechanism, assumed to be operative in the present work, towards the generation of $[\text{Ru}(\text{bipy})_2]\text{Cl}_2$. The isosbestic point maintained throughout the photoreaction indicated that these available decay pathways are thermal and reasonably rapid. Quantitatively, this photoreaction occurred with a quantum yield substantially lower than those of the three previous complexes. The LF excited state in CH_2Cl_2 is formed very efficiently (yield, about 93 %) ¹⁰⁷. Thus the observed difference in quantum yield cannot be ascribed to variations in the population of the respective LF excited states involved in the photosubstitution processes. A second possible factor, which could be capable of explaining the low quantum yield, would be the inefficient capture of Cl^- after the postulated pentacoordinated intermediate has been produced. However, the ions are

expected to be well paired in 0.01 M solutions of TBACl in CH_2Cl_2 , and consequently, this process should be fast. In solvents of low to moderate polarity, ions are extensively associated into pairs¹¹⁰. Because the reactivity of an ion can be significantly affected by the presence of any counter-ion nearby, the ion-pairing phenomenon undoubtedly plays an important role in the chemistry of ionic species in these solvents. The existence of two distinct types of ion pairs has been established¹¹⁰; the contact ion pair, $\text{M}^+ \text{X}^-$ and the solvent separated ion pair, $\text{M}^+ // \text{X}^-$ in which a molecule of solvent is between the ions.

Therefore, considering the assumed initial favorable formation of the initially generated monosubstituted complex, $[\text{Ru}(\text{bipy})_2\text{Cl}(\text{bipy})']^{+1}$, in which $(\text{bipy})'$ denotes that bipy that has one coordination position free, it was considered that the ultimate fate of that species was responsible for the four-fold decrease observed in the photosubstitution quantum yield of $[\text{Ru}(\text{bipy})_3]^{+2}$. The conclusion was that this monosubstituted complex can rapidly reform the starting $[\text{Ru}(\text{bipy})_3]^{+2}$, a process that apparently is much less significant in the photochemistry of the other three complexes.

All four complexes were thermally stable in 0.01 M solutions of TBACl in CH_3CN but did undergo photoanation. In this solvent, the qualitative behaviors of all four complexes were similar; initially an isosbestic point occurred while an intermediate complex with an absorption maximum at 490 nm accumulated. The identity of this newly observed complex was considered to be, $[\text{Ru}(\text{bipy})_2\text{Cl}(\text{py}'-(\text{CH}_2)_n-\text{py})]^{+1}$, although $[\text{Ru}(\text{bipy})_2\text{Cl}(\text{CH}_3\text{CN})]^{+1}$ cannot be eliminated¹¹¹.

An important aspect of ion - pairing behavior is the eventual coordination of the cations of the complexes with electron - donor sites of the involved solvent. The isosbestic point was lost when the photolyses were continued and absorption due to $[\text{Ru}(\text{bipy})_2\text{Cl}_2]$ was detected. Extensive photolysis of all four complexes resulted in complete conversion to $[\text{Ru}(\text{bipy})_2\text{Cl}_2]$.

The quantum yields of the photosubstitution reactions that were investigated in this work are shown in Table XXXIII. The most dramatic decrease in this observed quantum yield was noted in the case of $[\text{Ru}(\text{bipy})_3]^{+2}$. This loss of efficiency in the photosubstitution was rationalized in terms of the expected decrease, relative to that found for

CH_2Cl_2 solutions of the degree of the ion - pairing in CH_3CN ; effective capture of the pentacoordinate intermediate by any potential ligand present in solution, such as Cl^- , as a consequence, would have been reduced and thus would directly affect the possibility of observing a more efficient photosubstitution process for that complex. In fact, this effect seemed to be operative, to a significant extent, only in the complex in which there is active participation, of a five - membered ring, that is, $[\text{Ru}(\text{bipy})_3]^{+2}$; for instance, the quantum yield of photosubstitution was still relatively high for the complex which had a six - membered ring directly involved in the photochemistry, $[\text{Ru}(\text{bipy})_2\text{DPM}]^{+2}$.

In 0.50 M H_2SO_4 , $[\text{Ru}(\text{bipy})_3]^{+2}$ was found to be photostable ($\Phi_{\text{ph}} < 1 \cdot 10^{-4}$). Under the same conditions, $[\text{Ru}(\text{bipy})_2(\text{pic})_2]^{+2}$ readily underwent a photoaquation reaction, and $[\text{Ru}(\text{bipy})_2(\text{pic})(\text{H}_2\text{O})]^{+2}$ was generated. The behavior that was observed is quantitatively similar to that previously reported for the case of $[\text{Ru}(\text{bipy})_2(\text{py})_2]^{+2}$ ¹⁰⁹. However, a different behavior was noted in this work in the case of the complex $[\text{Ru}(\text{bipy})_2\text{DPM}]^{+2}$. Photolysis of this

complex resulted in the production of a species that has an absorption spectrum identical with that of $[\text{Ru}(\text{bipy})_2(\text{H}_2\text{O})_2]^{+2}$. Furthermore, an isosbestic point, located at 476 nm was maintained throughout the photolysis. This behavior was qualitatively similar to that observed in the case of photolysis of the complex $[\text{Ru}(\text{bipy})_3]^{+2}$ in 0.01 M TBACl solutions in CH_2Cl_2 . This fact was interpreted to be evidence that would suggest that the first monoaquo photoproduct intermediate complex was not a stable intermediate, and that once formed, it rapidly underwent decay processes, either back to the starting complex or, alternatively, to a new complex that contained a second H_2O ligand. In the latter case a total detachment of the ligand allegedly involved in the photosubstitutional chemistry, in this case, DPM would occur; this last photosubstitution reaction would lead to the formation of $[\text{Ru}(\text{bipy})_2(\text{H}_2\text{O})_2]^{+2}$. Apparently, the rate of reclosure for the six - membered chelate ring is slow and this process could compete with trapping the intermediate only in solvents in which ion pairing is not extensive. Further support of this hypothesis, can be provided by the experimental observation that the photolysis reactions occurred at essentially the same rate in both media, H_2O and 0.50 M H_2SO_4 , in the

case of $[\text{Ru}(\text{bipy})_2(\text{pic})_2]^{+2}$, but the progress of the photolysis was noted to be substantially slower in the case of $[\text{Ru}(\text{bipy})_2\text{DPM}]^{+2}$ dissolved in H_2O . In short, it might be considered that the DPM ligand provided a bridge between the photochemistries occurring in the presence and the absence of a chelate ring.

Finally, $[\text{Ru}(\text{bipy})_2\text{DPE}]^{+2}$ was found to be thermally unstable in 0.50 M H_2SO_4 in which it rapidly decomposed to the monoaquo intermediate complex in less than a minute. The quantum yield of photosubstitution of this intermediate complex to $[\text{Ru}(\text{bipy})_2(\text{H}_2\text{O})_2]^{+2}$ was determined to be reasonably high. Again, this behavior contrasted with the observed reactivity of the complex $[\text{Ru}(\text{bipy})_2(\text{py})(\text{H}_2\text{O})]^{+2}$ which undergoes photosubstitution of the remaining pyridine only very slowly.

2.1.1. Conclusions.

The photosubstitution quantum yield of ruthenium(II) complexes according to the postulated photosubstitution model is determined by the competition between chelate ring reclosure and trapping the

pentacoordinate intermediate by an external ligand. The observations made in this work are consistent with that model although further studies should be designed in order to describe in a more detailed manner the photosubstitution chemistry of polypyridineruthenium(II) complexes. In the case of a complex with a five - membered chelate ring as the original chelating agent, the external ligand should be spacially close, that is, ion paired, to the complexes in order to achieve an effective competition. In contrast, the reclosure of six - membered chelate rings can be visualized to be a kinetically slower process. In this case, ring closure can compete with external ligand scavenging only when the ion pairing is not extensive. It should be pointed out that the majority of the observed effects on photosubstitution appear to be a consequence of the solvent - dependent chemistry of intermediates formed after the MLCT - LF ($d - d$) transition between those two excited states. The observations do not contradict the initial prediction that in the extent that the chelate ring involved in the photosubstitution increases, the efficiency of ring reclosure should decrease and the behavior of the pentacoordinated intermediate should converge to that expected in the case of the complex

$[\text{Ru}(\text{bipy})_2(\text{py})_2]^{+2}$.

It also is pertinent to state that, implicitly, the assumption was made that both radiative and nonradiative rate constants associated with decay pathways of the excited states of the investigated complexes were temperature (hence medium) insensitive. From another perspective, it might be argued that equating 4 - picoline with a bidentate ligand of the series presented in Figure 29, that has $n = \infty$, is misleading, because pic is a simple variation of pyridine, in which an electron - donating influence is introduced. In any case, the experimental evidence was , effectively , consistent with the $n = \infty$ interpretation.

2.2. Effect of chelate ring size on the photosubstitution reaction of polypyridine ruthenium(II) complexes, $[\text{Ru}(\text{bipy})_2\text{L}]^{+2}$, in which L indicates ligands that have two amine groups linked by methylene bridges of different lengths.

The ligands used in the present work (Figure 36) were commercially available (ethylenediamine and 1,3 - propylenediamine). The corresponding complexes were prepared by means of the procedure described in Chapter II, section B.

The photophysical and photochemical properties of these complexes were examined. It was determined that the low temperature emission (77 K) properties of these complexes were quite different from those of $[\text{Ru}(\text{bipy})_3]^{+2}$. The quantum yields of emission were found to be substantially lower, even at 77 K, than that of $[\text{Ru}(\text{bipy})_3]^{+2}$. Also, the literature value of the luminescent lifetime of the complex $[\text{Ru}(\text{bipy})_2(\text{en})]^{+2}$ at 77 K was considerably lower than that of $[\text{Ru}(\text{bipy})_3]^{+2}$. No emission characteristics of the complex $[\text{Ru}(\text{bipy})_2(\text{tn})]^{+2}$

were found during an exhaustive literature search. The shapes of the emission spectra of both, $[\text{Ru}(\text{bipy})_2(\text{en})]^{+2}$ and $[\text{Ru}(\text{bipy})_2(\text{tn})]^{+2}$, were similar to that of $[\text{Ru}(\text{bipy})_3]^{+2}$; at 77 K the typical vibrational band appeared, but a significative red - shift in the wavelength of the maxima of the respective emission spectra occurred (Table XXXIV).

At higher temperatures the previously observed vibrational band in the emission spectra of the complexes disappeared, and also their emission intensities decreased sufficiently to make the data acquisition difficult. It was then decided to attempt to improve the accuracy of the emission measurements by means of calibration curves that were deduced by the use of the emission data observed from the standard, $[\text{Ru}(\text{bipy})_3]^{+2}$. The method that was followed to evaluate the necessary correction factors for the determination of the absolute emission quantum yields has been described in the Experimental Chapter, Section C. Calibration curves for the complexes at 77 K and 298 K were determined (Tables I and II). In Table XXXIV are summarized the emission properties of the complexes at 77 K.

In Tables XXXV and XXXVI are reported the quantum yields of emission of the complexes $[\text{Ru}(\text{bipy})_2(\text{en})]^{+2}$ and $[\text{Ru}(\text{bipy})_2(\text{tn})]^{+2}$, in EtOH/MeOH, 4:1, v/v, and in H_2O , respectively.

With the aid of the correction factors deduced after the evaluation of the previously mentioned calibration curves, it was possible to study the temperature dependence of the emission quantum yields of $[\text{Ru}(\text{bipy})_2(\text{en})]^{+2}$ and $[\text{Ru}(\text{bipy})_2(\text{tn})]^{+2}$ in EtOH/MeOH, 4:1, v/v. The temperature range was 120 - 240 K. The procedure that was followed was described in the note at the end of Table XXXIV. Again, the quantum yield of emission of $[\text{Ru}(\text{bipy})_3]^{+2}$ at 140 K was used as a reference. The temperature dependence of the emission quantum yields of those two complexes is shown in Figures 37 and 38. Those same figures display the resulting computer generated fit of the experimental data (the curve fitting parameters were presented in Table XXXVII). The activation energies, ΔE , obtained in the cases of the complexes $[\text{Ru}(\text{bipy})_2(\text{en})]^{+2}$ and $[\text{Ru}(\text{bipy})_2(\text{tn})]^{+2}$, are small, in comparison with that of $[\text{Ru}(\text{bipy})_3]^{+2}$. This observation correlates well with the weaker average ligand field strength of those two complexes; the ligand field strengths for en and tn are estimated from the relative positions of the

ligands in the spectrochemical series. This present data analysis, based upon emission intensities, seemed to give better values than those similarly obtained in the previous study of the complexes $[\text{Ru}(\text{bipy})_2(\text{py})_2]^{+2}$ and $[\text{Ru}(\text{bipy})_2(\text{diaz})]^{+2}$; this fact was probably due to the new procedure (calibration curves) used to improve the data acquisition.

Determination of luminescent lifetimes of the complexes in CH_2Cl_2 and also in 0.01 M solutions of TEACl in CH_2Cl_2 at 298 K were made (Table XXXVII). These measurements gave luminescent lifetimes for both complexes of about 200 nsec in CH_2Cl_2 and a significantly reduced value of about 100 nsec for the complexes in the same solvent when it contained Cl^- as the supporting electrolyte .

The quenching of the emission of $[\text{Ru}(\text{bipy})_2(\text{en})]^{+2}$ in CH_2Cl_2 and in 0.01 M solutions of TEACl in CH_2Cl_2 at 298 K was studied. Selected quenchers were ferrocene, anthracene, methyl viologen, and 1,2,4,5, - tetracyanobenzene. In all cases, with the exemption of 1,2,4,5 - tetracyanobenzene, quenching was observed. Also, for

all the systems, linear Stern - Volmer plots were obtained. A significant decrease of the value of K_{SV} , for 0.01 M solutions of TEACl, in comparison with those values obtained for the complexes in pure CH_2Cl_2 was observed when the quenchers were ferrocene and anthracene; this result was probably due to a partial quenching of the MLCT excited state by the Cl^- anions or, alternatively, to a more effective population of the LF excited state, because of the ion pairing mechanism.

The quenching experiments conducted with the quenchers MV^{+2} and TCNB, were not considered to be satisfactory (comments in Results). In all these quenching experiments there was an attempt to correlate the quenching of the emission with that of the photosubstitution reactions. Nevertheless, no significant quenching of the photosubstitution reactions with the mentioned quenchers was detected. Photolysis carried out in the absence of the quenchers gave essentially the same results.

Oxygen was tried as a potential quencher of the photosubstitution processes. Instead of getting a decrease in the progress of the photosubstitution

reaction, an unexpected behavior was observed; this behavior is discussed later.

The photoreactivity of $[\text{Ru}(\text{bipy})_2(\text{en})]^{+2}$ in CH_3CN at 298 K in the presence of Ag^+ cation was studied.

The process by which Ag^+ quenches the luminescent state of $[\text{Ru}(\text{bipy})_3]^{+2}$ had been previously studied⁵², but the analysis of the observed kinetics indicated that most likely the observed photosubstitution reactions did not originate from that luminescent excited state. In the present study, it was considered to be worthwhile to investigate the photochemical behavior of $[\text{Ru}(\text{bipy})_2(\text{en})]^{+2}$ under similar experimental conditions in order to test the effectiveness of the assumptions involved in the models used to describe the photophysics and the photochemistry of polypyridine ruthenium(II) complexes. It was considered that the potential catalytic effect of Ag^+ in the photochemistry would be related to a decrease in the efficiency of ring closure.

Extensive photolysis of $[\text{Ru}(\text{bipy})_2(\text{en})]^{+2}$

in solutions of different concentrations of AgNO_3 in CH_3CN at 298 K led to a final absorption spectrum with a maximum located at 425 nm, and with a molar absorption coefficient ($9,300 \text{ M}^{-1}\text{cm}^{-1}$) at that wavelength ; the corresponding literature value of the molar absorption coefficient of the complex $[\text{Ru}(\text{bipy})_2(\text{CH}_3\text{CN})_2]^{+2}$ is $8,950 \text{ M}^{-1}\text{cm}^{-1}$ ¹²². Within experimental error these results characterize the complex $[\text{Ru}(\text{bipy})_2(\text{CH}_3\text{CN})_2]^{+2}$ to be the final photosubstitution product .

The extent of the quenching of the luminescent state of the complex in CH_3CN at 298 K by AgNO_3 was determined (Table XXXXIII). The Stern - Volmer plot was clearly not linear; this observation was probably related to the great changes that were induced in the ionic strength of the medium; these effects are normally discussed in accordance with modified versions of the Debye - Huckel relationship, in which the constants included in the theoretical expression are adjusted empirically¹²¹, in order to get , if there are not more phenomena involved, a linearity in the Stern - Volmer plot . These corrections were not made. There are two kinds of luminescent quenching : i) normal diffusional or dynamic quenching; ii)

associational or static quenching in which the donor and the quencher form a non - luminescent association pair which reduces the amount of excitation energy absorbed by potentially luminescent species. Normally, the fact that a particular quenching is not simply diffusional, as it is in the cases of most metal complexes, is detected by an upward curvature in the experimental Stern - Volmer plot of the uncorrected data. One of the best ways to decide if static quenching is really operative in a particular system, is to quench both the luminescent lifetime and emission intensity ; if both quenchings are observed to behave similarly, it can be demonstrated that the quenching of the emitting state occurs only by a dynamic, diffusion - controlled process, and the possibility of static quenching is ruled out because static quenching would affect only the emission intensity and not the luminescent lifetime¹²⁴. It has also been found that the value of the Stern - Volmer constant, K_{SV} , adequately corrected, shows a decrease with increasing ionic strength; this effect, reported by Fujita and Kobayashi¹²³ was taken to be evidence for static quenching, since, ionic strength influences the association constant of the ion pair¹²⁴. However, the ionic strength should also be expected to influence the

rate constant between two ionic species in the same way; therefore the mere dependence of K_{SV} on ionic strength cannot really discriminate between the static and the dynamic mechanisms.

The correction of the observed quenching of the intensity of the emission of $[Ru(bipy)_2(en)]^{+2}$ for the above mentioned ionic strength effects was not done because no lifetime measurement could be done at this time because the equipment was not available at the time these experiments were underway. In any case, no static quenching was assumed to be present.

At least, an estimation, of the observed ratios of emission intensities (I_0/I) was made; the "correction" was evaluated in the following way: K_{SV} has been determined for the quenching of the emission of $[Ru(bipy)_3]^{+2}$ in CH_3CN by $AgNO_3$; values of K_{SV} about $0.1 M^{-1}$ have been obtained¹²⁰. If the same value of K_{SV} is assumed in the case of $[Ru(bipy)_2(en)]^{+2}$, (I_0/I)_{corr} values could be obtained, from the expression,

$$(I_0/I)_{corr} = 1 + 0.1 [Ag^+]$$

These calculations were made; Table XXXXIII gives values of (I_0/I)_{corr}. Undoubtedly, although the value of K_{SV} may differ, the values calculated, if

plotted, would give a perfectly linear Stern - Volmer plot.

Photolysis of $[\text{Ru}(\text{bipy})_2(\text{en})]^{+2}$ in 0.40 and 0.80 M solutions of AgNO_3 in CH_3CN were carried out. The respective photosubstitution quantum yields that were evaluated, $0.04 \cdot 10^{-2}$ and $0.05 \cdot 10^{-2}$, were quite low. Moreover, a value of about 0.0003 has been reported for the photosubstitution quantum yield of $[\text{Ru}(\text{bipy})_3]^{+2}$ in 0.8 M AgNO_3 solution in CH_3CN ⁵².

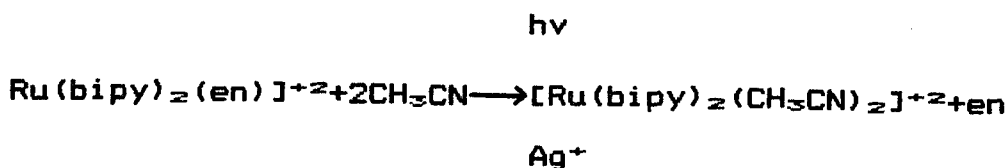
These quantum yields of photosubstitution were determined by the use of the available program described in the Experimental Section. The disappearance of $[\text{Ru}(\text{bipy})_2(\text{en})]^{+2}$ and the generation of the final photoproduct were followed by means of absorption spectroscopy (both were monitored at 490 nm). Although extensive photolytic irradiation showed that isosbestic points were maintained throughout the reaction and that, after prolonged irradiation times, the final photosubstitution occurred with high chemical yield (almost 100 %), the evaluated quantum yields were extremely low. In the absence of Ag^+ , the photolysis was found to follow a different path that led to another final photoproduct (with a

maximum in its absorption spectrum located at 455 nm).

For purposes of independent testing , emission intensities of the samples that were used in the photolysis experiments previously discussed were determined; the ratios of the intensities of samples with and without Ag^+ were evaluated and compared with the results from the already available data for the quenching of the emission of $[\text{Ru}(\text{bipy})_2(\text{en})]^{+2}$ (Table XXXXIII). However, it was then noted that the course of the photolysis with, and without Ag^+ , followed different mechanisms; thus the comparison of the quantum yields of photosubstitution that were determined by two different procedures was meaningless.

An additional photolysis experiment was conducted . $[\text{Ru}(\text{bipy})_2(\text{en})]^{+2}$, dissolved in 0.40 M AgNO_3 solution in CH_3CN which contained MV^{+2} in a concentration sufficient to quench more than 90 % of the emission from the $^3\text{MLCT}$ was subjected to photolytic irradiation. This experiment was done because Ag^+ is capable of quenching the MLCT excited state of $[\text{Ru}(\text{bipy})_3]^{+2}$ by electron - transfer, in both, aqueous and nonaqueous solutions¹²⁰. Reference¹³² states that although the electron

transfer occurs, there is a rapid back reaction between the reduced silver atom and the oxidized metal complex. As a result, the following net photosubstitution reaction

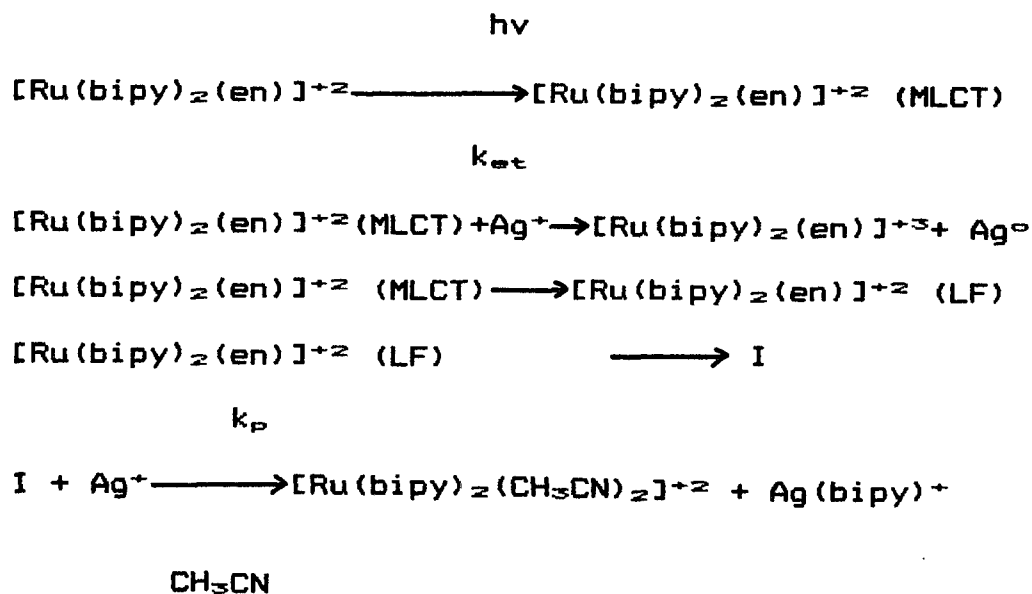


could occur by a path in which the oxidized product $[\text{Ru(bipy)}_2(\text{en})]^{+3}$ would be an intermediate. It is pertinent to recall that qualitative observations of the formation of Ag^0 during the photolysis were made; consequently, a redox process would be reasonable.

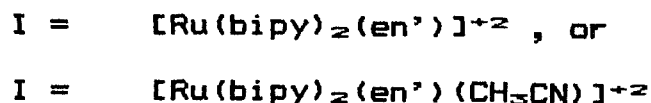
The photolysis experiment, in which MV^{+2} was present ruled out the possibility of a direct involvement of $[\text{Ru(bipy)}_2(\text{en})]^{+3}$ in the photosubstitution; however, the already observed photoproduct could still be detected (the quantum yield of photosubstitution was evaluated to be $< 1.10^{-5}$).

The experimental observations could provide a

basis for a scheme for some of the principal steps in the mechanism that is probably involved in the photosubstitution reaction. Nevertheless, further research is necessary before a final and satisfactory conclusion can be reached. The proposed scheme, is presented below.



where I, represents one or both of the species described below.



(en' has one amine free that has been dissociated from the metallic center).

Either of the species assumed to be the intermediate, I , could then revert to the ground state of the starting complex or could react with Ag^+ to obtain the complete loss of the initial en ligand.

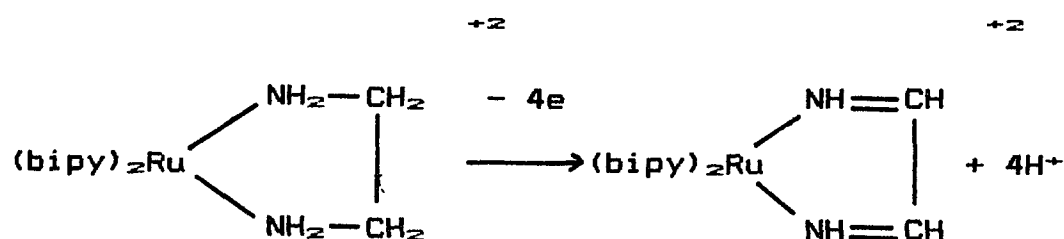
Extensive photolyses of the complexes $[\text{Ru}(\text{bipy})_2(\text{en})]^{+2}$ and $[\text{Ru}(\text{bipy})_2(\text{tn})]^{+2}$ in the absence of Cl^- in different solvents were done. Extensive photolytic irradiation of the complexes $[\text{Ru}(\text{bipy})_2(\text{en})]^{+2}$ and $[\text{Ru}(\text{bipy})_2(\text{tn})]^{+2}$, in the solvents CH_3CN , H_2O , and CH_2Cl_2 , in the absence of Cl^- , as a possible coordinating species, were also examined (Figures 40,41,42,43,44,and 45). The goal was to establish, at least qualitatively, the behaviors of those complexes in those solvents in order to detect a possible coordination of solvent molecule to the metallic center. Such a solvent coordination could interfere, if it were competitive, with the photolysis of those complexes in which there is coordination of the good coordinating anion, Cl^- .

The extensive photolysis of $[\text{Ru}(\text{bipy})_2(\text{en})]^{+2}$ in pure CH_3CN led to a final absorption spectrum with a maximum located at 425 nm, and a molar absorption coefficient of $6,500 \text{ M}^{-1}\text{cm}^{-1}$ (Figure 40). The reported absorption spectrum of the complex $[\text{Ru}(\text{bipy})_2(\text{CH}_3\text{CN})_2]^{+2}$ ¹²² has a λ_{max} at 425 nm, and a $8,590 \text{ M}^{-1}\text{cm}^{-1}$ molar absorption coefficient at that wavelength.

The four - electron oxidation of ethylenediamine to α, α' diimine (dim) has been observed in the cases of the complexes $[\text{Ru}(\text{phen})_2(\text{en})]^{+2}$ ¹³¹, tris(ethylenediamine)ruthenium(II)¹²⁹ and tetracyano - ethylenediamineferrate(II)¹³⁰. In each case the oxidized ligand remains coordinated in the metal complex.

The product of exhaustive electrolysis of acetonitrile solutions of $[\text{Ru}(\text{bipy})_2(\text{en})]^{+2}$ has been characterized by spectral and electrochemical measurements, to be $[\text{Ru}(\text{bipy})_2(\text{dim})]^{+2}$ ¹²⁵. It has been suggested that this oxidative dehydrogenation of the coordinated ethylenediamine ligand in the case of Ru complexes may be initiated by oxidation of the metal to Ru(III)¹³¹.

The net stoichiometry of the oxidation was described by the reaction :



This oxidation process was considered to consist of two sequential steps : initial oxidation of the metal to Ru(III), followed by oxidation of the

coordinated ligand.

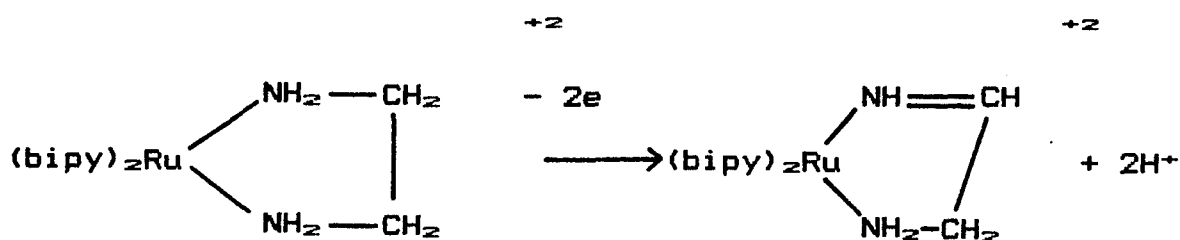
- e

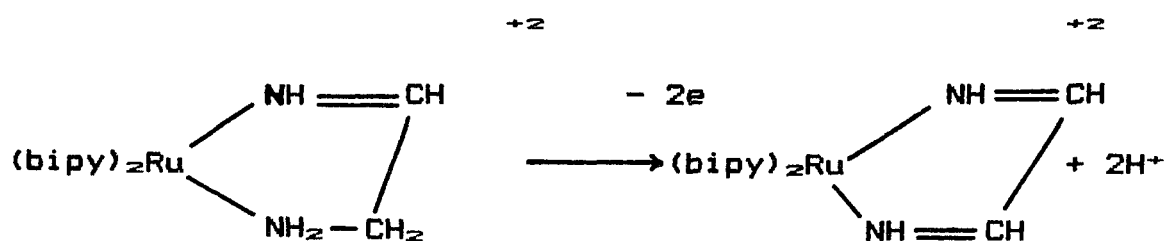


- 3 e



Spectrophotometric titrations , in which the above described dehydrogenation reactions could be followed in further detail, by means of the use of Ce(IV) which was reduced to Ce(III) during the course of the titration, have also been done¹²⁵ . These studies indicated that the net stoichiometry of the oxidation could be further broken down in two stepwise processes that are shown below . The first step involves the oxidation to a monoimine intermediate, and the second step involves the oxidation of the monoimine to the final, stable, α - α' diimine.





The absorption spectrum of this complex, $[\text{Ru}(\text{bipy})_2(\text{dim})]^{+2}$, dissolved in CH_3CN has a maximum located at 454 nm, and a molar absorption coefficient of $14,000 \text{ M}^{-1}\text{cm}^{-1}$ ¹²⁵. Further experiments should be done to properly characterize the product photogenerated in this work. This product could be $[\text{Ru}(\text{bipy})_2(\text{dim})]^{+2}$ which was produced with a low chemical yield.

The extensive photolysis of $[\text{Ru}(\text{bipy})_2(\text{en})]^{+2}$ in H_2O (Figure 41), seems to rule out the formation of $[\text{Ru}(\text{bipy})_2(\text{H}_2\text{O})_2]^{+2}$ as a final photosubstitution product, because this last complex has a λ_{max} located at 480 nm¹³⁶. However, the formation of a species with an absorption spectrum in which a maximum occurs at 445 nm was apparent. This final product could probably be $[\text{Ru}(\text{bipy})_2(\text{dim})]^{+2}$, or, alternatively, $[\text{Ru}(\text{bipy})_2(\text{en}')(\text{H}_2\text{O})]^{+2}$, the first product of the photosubstitution reaction.

The extensive photolysis of $[\text{Ru}(\text{bipy})_2(\text{en})]^{+2}$ in pure CH_2Cl_2 (Figure 42) produced a reaction of the starting complex, even when it was dissolved in this recognized non-coordinating solvent. Qualitatively, a maximum in the absorbance of this species was determined to be located at 472 nm. No explanation is currently available for this observed reaction, although the oxidation of the ligand, en, via an electron-transfer photochemical reaction cannot be eliminated. Such an intramolecular photo-redox process would eventually involve the reduction of the metal center to Ru(I) by a LMCT transition. An interesting fact is that for a configuration d^7 metal ion, the number of luminescence studies thus far completed is small, and very few reports of emission of complexes of d^7 metal ions in solution exist. This result is different than that for complexes having a metal with a configuration d^6 for which many emissions are reported. Reported emission of some complexes of Co(II), doped into MgF_2 , or ZnF_2 ^{133, 135} were unique contributions; the emissions were lost in solution. Later, luminescence for $[\text{CoCl}_6]^{-4}$ and $[\text{Co}(\text{H}_2\text{O})_6]^{+2}$ were observed¹³⁴ but for an emission to occur, it was stated that there must be electron-hole recombination process in order

to explain such an unusual behavior.

In the present study, measurements of the emission intensity of a sample subjected to photolysis, $[\text{Ru}(\text{bipy})_2(\text{en})]^{+2}$ dissolved in CH_2Cl_2 , were periodically made and were compared with the emission of the sample before the beginning of the photolytic irradiation. Qualitatively, a continuous decrease in the emission intensity was found as the photolysis advanced. No change in the shape of the original spectrum was detected. There was no shifts in the maximum of emission and no appearance of new transitions; only a progressive apparent quenching of the intensity of the emission was observed.

The extensive photolysis of $[\text{Ru}(\text{bipy})_2(\text{tn})]^{+2}$ dissolved in CH_3CN led to a final photoproduct with an absorption spectrum exhibiting a maximum located at 430 nm. Its molar absorption coefficient agreed, within experimental error, with that of the complex $[\text{Ru}(\text{bipy})_2(\text{CH}_3\text{CN})_2]^{+2}$. Therefore, the formation of this final complex was assumed.

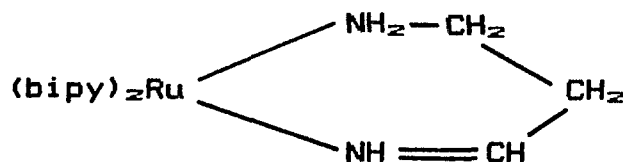
The extensive photolysis of $[\text{Ru}(\text{bipy})_2(\text{tn})]^{+2}$ in pure H_2O (Figure 44) led to

a final photoproduct with an absorption maximum located at 480 nm ; this result is characteristic of the maximum absorption of $[\text{Ru}(\text{bipy})_2(\text{H}_2\text{O})_2]^{+2}$.

Perhaps, a full conversion was not achieved even after 10 hours of photolytic irradiation. The reported molar absorption coefficient of that complex is $8,500 \text{ M}^{-1}\text{cm}^{-1}$; this value is substantially higher than that calculated with the assumption of a 100 % chemical yield. The final photoproduct was probably $[\text{Ru}(\text{bipy})_2(\text{H}_2\text{O})_2]^{+2}$ that was generated in low chemical yield.

The extensive photolysis of $[\text{Ru}(\text{bipy})_2(\text{tn})]^{+2}$ in pure CH_2Cl_2 , showed, again unexpectedly, the occurrence of some photodegradation of the starting complex. Qualitatively, a species with a maximum of absorption at 481 nm was observed to be formed. Once more, some partial oxidation of the ligand, tn , probably occurred . However, although the oxidation of the ligand to give the first imine intermediate ,

+2



might be probable, this species has been reported to be unstable with respect to further oxidation at the imine site¹²⁵; $[\text{Ru}(\text{bipy})_2(\text{tn})]^{+2}$, does not give, as a consequence, a stable final $\alpha - \alpha'$ diimine oxidation product.

At this point, it becomes pertinent to recall that extensive photolysis of O_2 saturated samples of $[\text{Ru}(\text{bipy})_2(\text{en})]^{+2}$ in a 0.01 M TEACl solution in CH_2Cl_2 led to the detection of two species, one of which has an absorption maximum at 455 nm (probably $[\text{Ru}(\text{bipy})_2(\text{dim})]^{+2}$), and the other has a maximum at 540 nm (very likely, $[\text{Ru}(\text{bipy})_2]\text{Cl}_2$).

Additionally, a photolysis of $[\text{Ru}(\text{bipy})_2(\text{en})]^{+2}$, dissolved in the oxidizing medium, 0.05 M H_2SO_4 , led to a final photoproduct with a final absorption spectrum that had a maximum located at 452 nm; that is, once more there exists the possibility of partial generation of a complex with an oxidized ligand. Something similar to $[\text{Ru}(\text{bipy})_2(\text{dim})]^{+2}$ seemed feasible. In both cases, the reactions were not thermally induced; Ar - degassed samples of the dissolved complex in each medium were kept in darkness for three days, and no change in

their initial absorption spectra was detected.

Recently, a correlation between the quantum yield for the photosubstitution reactions observed from several $[\text{Ru}(\text{bipy})_2\text{L}]^{+2}$ complexes and the energy of the low - temperature (0 - 0) emission (77 K, in 1:1, MeOH/EtOH, glass) was reported¹²⁶. That correlation was found to be linear and appeared to be consistent with the excited state model initially proposed by Watts and co-workers¹²⁷. The variations in photosubstitution quantum yields were interpreted merely in terms of changes in the energy difference, ΔE between the emitting MLCT and the thermally populated LF (d - d) excited states. Later, a new set of experimental results seemed to suggest that the description proposed previously, in the case of $[\text{Ru}(\text{bipy})_2\text{L}]^{+2}$ complexes, was inadequate, or at least, incomplete in its treatment of photosubstitution reactions¹²⁸. Specifically, the temperature dependence of the quantum yield of the photosubstitution processes of the complexes $[\text{Ru}(\text{bipy})_2(\text{py})_2]^{+2}$ and $[\text{Ru}(\text{bipy})_2(\text{CH}_3\text{CN})_2]^{+2}$ as well as the temperature dependencies exhibited by the luminescent lifetimes were examined. Different temperature dependencies between the luminescent lifetimes

and the photosubstitution quantum yields of those complexes were observed in each case. Therefore, it was concluded that the observed photosubstitution reactions of $[\text{Ru}(\text{bipy})_2\text{L}]^{+2}$ complexes were not a simple result of thermal population of a LF excited state. The probable involvement of some LF excited state was still accepted. It was speculated that the real excited state associated with the photosubstitution processes should be different from that directly associated with the luminescent state that provides one available energy degradation pathway. What was even more important, was the idea that there could be direct population of the photoreactive, LF excited state that would be competitive with the population of the emitting MLCT excited state ¹²⁸. However, no considerations of the generation and further behavior of the pentacoordinate intermediate complex, (I), postulated to be formed, in accord with the general model of photosubstitution of polypyridine ruthenium(II) complexes was made. No analysis of possible effects associated with reclosure of the chelate ring was suggested.

In the present work, many observations of the effect of chelate ring size on the progress of the photosubstitution reactions of $[\text{Ru}(\text{bipy})_2\text{L}]^{+2}$ complexes were made, and many speculations about the behavior of the postulated pentacoordinate intermediate (I) of several complexes have been made.

Next, the results observed during the photolysis of the complexes $[\text{Ru}(\text{bipy})_2(\text{en})]^{+2}$ and $[\text{Ru}(\text{bipy})_2(\text{tn})]^{+2}$ are discussed. The photochemical studies of these two complexes were similar in the sense that the first photosubstitution product could not be observed.

The molar absorption coefficients of the final photoproducts were used in the evaluation of the photosubstitution quantum yields.

The molar absorption coefficients at 490 nm of all the different photoproducts that were generated and that were used in the evaluation of the photosubstitution quantum yields, were determined from the literature information and from experimental determinations. These photoproducts were $[\text{Ru}(\text{bipy})_2]\text{Cl}_2$, $[\text{Ru}(\text{bipy})_2(\text{H}_2\text{O})_2]^{+2}$, $[\text{Ru}(\text{bipy})_2(\text{dim})]^{+2}$, and $[\text{Ru}(\text{bipy})_2(\text{CH}_3\text{CN})_2]^{+2}$

54, 122, 125, 136 .

Photolysis of the complexes $[\text{Ru}(\text{bipy})_2(\text{en})]^{+2}$ and $[\text{Ru}(\text{bipy})_2(\text{tn})]^{+2}$ in 0.01 M TEACl solutions in CH_3CN , H_2O , and CH_2Cl_2 were examined. Additionally, the temperature dependence of the photosubstitution quantum yields of the complexes $[\text{Ru}(\text{bipy})_3]^{+2}$, $[\text{Ru}(\text{bipy})_2(\text{en})]^{+2}$, and $[\text{Ru}(\text{bipy})_2(\text{tn})]^{+2}$ was investigated over the temperature range of 274 to 305 K.

Table XXXIV summarizes the data related to the photosubstitution quantum yields and to the production of LF excited states in all the molecules at 298 K. Table XXXV gives the values of the quantum yields of the detected photoreactions of $[\text{Ru}(\text{bipy})_2(\text{en})]^{+2}$ dissolved in different media. Figure 47 shows the temperature dependence of the photosubstitution quantum yields of the complexes in 0.01 M TEACl solution in CH_2Cl_2 .

The photolysis of $[\text{Ru}(\text{bipy})_2(\text{en})]^{+2}$ in 0.01M TEACl solution in CH_3CN showed that isosbestic points were maintained throughout the initial stages of the slow photosubstitution reaction. However, no clear appearance of a first photoproduct was noticed; probably the absorbance of the first photoproduct was

masked by that of the starting $[\text{Ru}(\text{bipy})_2(\text{en})]^{+2}$. Nevertheless, the monitoring did detect a slow increase in the absorbance at 556 nm that is attributed to the formation of $[\text{Ru}(\text{bipy})_2]\text{Cl}_2$ (Figure 48).

The photolysis of $[\text{Ru}(\text{bipy})_2(\text{en})]^{+2}$ in 0.01 M TEACl solution in CH_2Cl_2 showed features similar to those exhibited when CH_3CN was the solvent. Again, isosbestic points were maintained throughout the initial stages of the reaction (about 10 % of decrease in initial absorption at 490 nm). Generation of $[\text{Ru}(\text{bipy})_2]\text{Cl}_2$ could be presumed on the basis of the observed increase in absorption at 548 nm. No intermediate, first photosubstitution product could be followed by absorption spectroscopy (Figure 50).

The photolysis of $[\text{Ru}(\text{bipy})_2(\text{en})]^{+2}$ in 0.01 M TEACl solution in H_2O led , once more , to no apparent first photoproduct; only after prolonged irradiation was the formation of a species with a maximum of its absorbance located at 472 nm apparent. This final photoproduct was considered to be $[\text{Ru}(\text{bipy})_2(\text{H}_2\text{O})_2]^{+2}$; this assignment was made by means of an analysis of the final absorption spectrum.

Photolysis of $[\text{Ru}(\text{bipy})_2(\text{tn})]^{+2}$ in 0.01 M TEACl solution in CH_3CN , was found to be comparatively more efficient than that observed, under similar conditions, in the case of $[\text{Ru}(\text{bipy})_2(\text{en})]^{+2}$. Again, isosbestic points were maintained throughout the reaction although no first intermediate could be detected. The generation of a final photoproduct absorbing at 550 nm was apparent; this species was assumed to be $[\text{Ru}(\text{bipy})_2]\text{Cl}_2$ (Figure 51).

Photolysis of $[\text{Ru}(\text{bipy})_2(\text{tn})]^{+2}$ in 0.01 M TEACl solution in CH_2Cl_2 displayed similar changes. Retention of isosbestic points throughout the initial periods of photoreaction, no detection of a first photosubstitution intermediate product, and apparent generation of $[\text{Ru}(\text{bipy})_2]\text{Cl}_2$, the final photosubstitution product absorbing at 548 nm (Figure 53), were the characteristics.

Photolysis of $[\text{Ru}(\text{bipy})_2(\text{tn})]^{+2}$ in 0.01 M TEACl solution in H_2O showed a behavior similar to that observed in the case of $[\text{Ru}(\text{bipy})_2(\text{en})]^{+2}$ under the same experimental conditions. In this case, a slow photosubstitution reaction was detected and a final absorption spectrum with a maximum located at 470 nm

was observed. This final photoproduct was considered to be $[\text{Ru}(\text{bipy})_2(\text{H}_2\text{O})_2]^{+2}$; this assignment was based on the observed absorption characteristics (Figure 52).

The photosubstitution quantum yield can be postulated to be given by the following relationship :

$$Q_{ph} = (Q_{LF})(Q_I)(Q_{L1})(Q_{L2})$$

in which Q_{LF} , Q_I , Q_{L1} , and Q_{L2} are respectively, the quantum yields, (Q_{LF}) for LF formation from the excited state $^3\text{MLCT}$, (Q_I) for pentacoordinated intermediate formation from LF, (Q_{L1}) for monosubstituted product formation from the intermediate, the species which could be formulated to be $[\text{Ru}(\text{bipy})_2\text{L}'\text{X}]^{+1}$, in which L' represents the ligand originally bonded to the starting complex en or tn, that has one chelating position free, and X is the new entering ligand, and (Q_{L2}) for the specific process leading to the final observed photosubstitution product. This final process proceeds by loss of the previously gained chelate X , or by total detachment of the initial ligand L and simultaneous gain of a second chelate species X .

Both Q_{LF} and Q_I are temperature

dependent, and unraveling the two activation energies is a difficult task. In the cases of the complexes $[\text{Ru}(\text{bipy})_2(\text{en})]^{+2}$ and $[\text{Ru}(\text{bipy})_2(\text{tn})]^{+2}$, the activation energies related to the quantum yield of population of the LF excited state, Q_{LF} were determined to be rather low; consequently, the Q_{LF} of both complexes in all solvents in which their photosubstitution processes were investigated were assumed to be unity. Thus, any observed temperature dependence of the photosubstitution quantum yield should be related to either Q_1 , Q_{L1} , or Q_{L2} . Since no important dependence was noted (Figure 47), it was concluded that the LF excited state undergoes photosubstitution processes that have moderately small activation energies. Linear plots with very small slopes were obtained in Figure 47 ($\ln(1/Q_{\text{ph}})$ vs. $1/T(\text{K})$). Therefore, both Q_1 , Q_{L1} , and Q_{L2} must have small activation energies.

Further information on the dynamics of the respective LF excited states in the cases of the complexes $[\text{Ru}(\text{bipy})_2(\text{en})]^{+2}$ and $[\text{Ru}(\text{bipy})_2(\text{tn})]^{+2}$ were obtained from the quenching experiments with Ferr, An, and MV^{+2} . The photosubstitution quantum yields were unaffected,

although quenching of the luminescence was noted. Both complexes exhibited identical behaviors. This similarity was considered to be a strong reason to suggest that the lifetimes of the LF excited state were sufficiently short to make any detection of deactivation by means of a bimolecular processes unreasonable. Decay of the LF excited state by the route of formation of a pentacoordinated intermediate and a rapid radiationless decay are available to the LF excited state. Additionally, the ring closure, reforming the chelate ring, can be competitive with an effective trapping of an external ligand, ion, or solvent molecule; both processes directly affect Q_L .

During the photochemical studies carried out with these complexes, photosubstitution quantum yields of the final products of the photoreaction were determined. It was impossible to detect the intermediates. Figures 48 - 53 show the course of photolyses; all are very sluggish, in comparison with those complexes in which L ligands were pyridine groups linked by methylene bridges. The complex $[\text{Ru}(\text{bipy})_2(\text{tn})]^{+2}$ always showed a photosubstitution quantum yield larger than that of $[\text{Ru}(\text{bipy})_2(\text{en})]^{+2}$. The results collected in Table

XXXXIV also show the low values observed for the photosubstitution reactions.

2.2.1. Conclusions.

The complex which had a five - membered ring, directly related to the photosubstitutional chemistry, $[\text{Ru}(\text{bipy})_2(\text{en})]^{+2}$, exhibited a very different behavior from that of the previously discussed series of complexes, $[\text{Ru}(\text{bipy})_3]^{+2}$. However, no direct comparison can be made, because one of the series involved a chelating N that was part of an aromatic ring, while the other had a chelating N that was merely bonded to a methylene chain. Therefore, a very important effect seemed to be operative, and the reactivity towards the photosubstitution for both series was different.

It can be seen that the photosubstitution quantum yields cannot be easily correlated with the polarity of the solvent since the observed photosubstitution quantum yields in the case of the complexes was higher in CH_3CN than in CH_2Cl_2 and in H_2O . Also the data reported in Table XXXV, about the photolysis of $[\text{Ru}(\text{bipy})_2(\text{en})]^{+2}$ dissolved in CH_3CN in the presence of Ag^+ show an increase in the photosubstitution quantum yield; therefore, Ag^+

really seems to have a catalytic effect on the photochemistry.

Perhaps the tendency of the ring in these complexes to re - chelate is much more significant than of the previously studied series of complexes. Tendency towards re - chelation would justify the significantly different photosubstitutional behavior of both series of complexes. A comparison of the observed photosubstitution quantum yields of $[\text{Ru}(\text{bipy})_2(\text{en})]^{+2}$ and $[\text{Ru}(\text{bipy})_2(\text{tn})]^{+2}$, seems to demonstrate a more efficient population of the LF excited state of $[\text{Ru}(\text{bipy})_2(\text{tn})]^{+2}$ and, consequently, a relatively more efficient final photosubstitution quantum yield.

The complex that involved a six - membered ring in its photochemistry, $[\text{Ru}(\text{bipy})_2(\text{tn})]^{+2}$, showed a behavior completely different from that of $[\text{Ru}(\text{bipy})_2\text{DPM}]^{+2}$.

Only in H_2O , all three complexes exhibit a barely detectable photosubstitution; this observation probably demonstrates the lack of adequate ion - pairing equilibria in aqueous systems. Nevertheless, it

seems that other processes are operative in the photochemical behavior of $[\text{Ru}(\text{bipy})_2(\text{en})]^{+2}$ and $[\text{Ru}(\text{bipy})_2(\text{tn})]^{+2}$.

CHAPTER V. GENERAL CONCLUSIONS AND
SUGGESTIONS FOR FUTURE RESEARCH.

It had been reported that the quenching of the emission intensity and that of the photosubstitution reaction were very different in the complex tris - 2,2'bipyridylruthenium(II)⁴⁶. The reinvestigation of the photophysical and photochemical behavior of tris - 2,2'bipyridylruthenium(II) under different conditions, by means of the quenching of both the luminescent lifetime and the photosubstitution reaction with ferrocene and oxygen allowed to determine that the quenching of the luminescence and the quenching of the photochemistry are very similar. Therefore the results here obtained support the idea that the excited state affected by a quencher is involved in the two processes that were studied. The results obtained in this work are in agreement with the postulated general model that represents the photophysics of tris - 2,2'bipyridylruthenium(II) and related polypyridineruthenium(II) complexes.

It had been reported^{39,48,49} that the activation energies between the ³MLCT and the LF

excited states were very similar in the cases of the complexes $\text{cis} - \text{bispyridylbis}2,2'\text{bipyridylruthenium(II)}$ and $4,5 \text{ diazafluorenyl bis}2,2'\text{bipyridylruthenium(II)}$ to the ΔE value evaluated in the case of $[\text{Ru}(\text{bipy})_3]^{+2}$, although they have a lesser average ligand field strength in comparison to the $\text{tris} - 2,2'\text{bipyridylruthenium(II)}$ complex. The reinvestigation of the temperature dependence of the emission intensities and lifetimes of those complexes allowed us to evaluate the energy difference between the $^3\text{MLCT}$ and LF excited states. In good agreement with the generally observed trends of the photophysics of polypyridine ruthenium(II) complexes, the results obtained in this work permit to conclude that the ligand field excited state energies are well correlated with the ligand field strength; lesser average ligand field strengths make more accessible thermal population of LF excited states from $^3\text{MLCT}$ states.

The determination of the photochemistry of the complex $\text{cis} - \text{bispyridylbis} - 2,2'\text{bipyridylruthenium(II)}$ in mixtures dioxane - water provided information that substantiates the generally observed effects that solvents have in photochemical

reactions. The photosubstitution quantum yields were larger and well correlated with the decreasing polarity of the mixtures in which exist a better support for the ion - pair formation.

Investigation of the effect that the chelate ring size has on the photochemistry of several polypyridine ruthenium(II) complexes with the general formulation $[\text{Ru}(\text{bipy})_2\text{L}]^{+2}$ was accomplished in this work by the use of two series of ligands L.

The photochemistry of the series in which L has two pyridine rings linked by methylene bridges of varying lengths seem to indicate that in the extent that the chelate ring increases, the process of ring reclosure - recoordination of the postulated pentacoordinated intermediate - that regenerates the starting complex, becomes less efficient. The photosubstitution quantum yields were found to be larger in solvents of decreased polarity; all the complexes of this series are more photoactive than $[\text{Ru}(\text{bipy})_3]^{+2}$.

The photochemistry of the series in which L has two amine groups linked by methylene bridges was found to be completely different; this different

behavior is considered to be explained by considering that different kinds of chelating N - Ru metal center bonds are involved in this case in which the N atoms are bonded to an aliphatic chain instead of being part of an aromatic ring. Sluggish photosubstitution reactions in comparison with the previous series were observed. Complexes with a larger chelate rings still have larger quantum yields of photosubstitution, fact indicative of a less efficient process of ring reclosure; nevertheless, no clear correlation can be found with the effect that the solvent has in the photochemical behavior.

New reactions probably involving the oxidation of the ligands ethylenediamine and 1,3 - propylenediamine were detected to occur. Temperature dependence studies of the photosubstitution reactions indicated low apparent activation energies for the complexes of this series.

Silver cation has a catalytic effect upon the photosubstitution of the complex ethylenediamine bis 2,2'-bipyridyl ruthenium(II) .

The temperature dependence of the lifetimes of both series of complexes should be evaluated in order

to achieve a more complete description of the dynamics of the $^3\text{MLCT}$ and LF excited states. These observations should be correlated with the chelate ring size, aromaticity of the N donor ligand, and the chelation angle; the chelation angle should be evaluated by crystallographic studies.

Then the photosubstitution quantum yields of these complexes in different solvents should be evaluated at different Cl^- concentrations. This would allow us to correlate the photochemistry with the $[\text{Cl}^-]$ by means of the Eq.(1). If a linear plot of $Q(P)^{-1}$ vs. $[\text{Cl}^-]^{-1}$ were obtained, the intercept would give the efficiency of the generation of the postulated pentacoordinated intermediate from the LF excited state. Additionally, the relative importance that the process of ring reclosure has in all the different complexes could be estimated from the slope/intercept ratio of the expected linear plot. The evaluation of this parameter would be a substantial experimental evidence contributing to a further understanding of the photochemistry of polypyridineruthenium(II) complexes.

Photolysis of $[\text{Ru}(\text{bipy})_2(\text{en})]^{+2}$ dissolved in CH_3CN in the presence of Ag^+ led to the

generation of $[\text{Ru}(\text{bipy})_2(\text{CH}_3\text{CN})_2]^{+2}$. This observation was rationalized by the assumption that the postulated pentacoordinate intermediate is complexed by Ag^+ ; this process would reduce the efficiency of ring reclosure and subsequently enhance the formation of photosubstitution product. It would be desirable to extend this investigation to all the complexes $[\text{Ru}(\text{bipy})_2\text{L}]^{+2}$ that were included in the two series that were studied in this work ($\text{L} = \text{py} - (\text{CH}_2)_n - \text{py}$ and $\text{L} = \text{H}_2\text{N} - (\text{CH}_2)_n - \text{NH}_2$).

The temperature dependence of the photosubstitution quantum yields of the complexes in which L's are $\text{py} - (\text{CH}_2)_n - \text{py}$ should be evaluated and contrasted with the temperature dependence of the photochemistry of the complexes $[\text{Ru}(\text{bipy})_2(\text{en})]^{+2}$ and $[\text{Ru}(\text{bipy})_2(\text{tn})]^{+2}$.

The next intermediate after the LF state has been hypothesized to be a pentacoordinated intermediate. Results obtained in the case of some carbonyl complexes¹³⁷ indicate that the rate constant of the trapping of either a solvent molecule or an external ligand by this intermediate will be diffusion controlled.

It is suggested to examine the behavior of this pentacoordinate intermediate with flash photolysis experiments. Previous studies of this nature with the complex $[\text{Ru}(\text{bipy})_3]^{+2}$ have resulted in the determination of the absorption spectrum of the $^3\text{MLCT}$ excited state¹³⁸. Nevertheless, the pentacoordinate intermediate originated from this complex could not be formed in significant yields due to the large thermal activation energy required for initial population of the LF excited state and the subsequent production of the pentacoordinated intermediate. The lifetime of the LF excited state of the complex $[\text{Ru}(\text{bipy})_2(\text{diaz})]^{+2}$ at 298 K has been estimated to be $< 100 \text{ psec}^{69}$. Flash photolysis experiments should be carried out with $[\text{Ru}(\text{bipy})_2(\text{diaz})]^{+2}$, $[\text{Ru}(\text{bipy})_2\text{DPM}]^{+2}$, and $[\text{Ru}(\text{bipy})_2(\text{en})]^{+2}$, as a first step before extending similar studies to the rest of the complexes of the two series that were studied in this work. The solvent should be CH_2Cl_2 and the counterion PF_6^- in order to enhance conditions for the lifetime of the pentacoordinate intermediate and allow its observation. Next, Cl^- should be gradually added and the rate of disappearance of the intermediate evaluated. The same procedure should be followed at several temperatures in order to evaluate Arrhenius equations for the ring

reclosure and Cl^- trapping processes.

APPENDIX A.1. REMOVAL OF INNER FILTER EFFECT
PRODUCED BY QUENCHER ABSORPTION FROM APPARENT QUENCHING
EMISSION MEASUREMENTS.

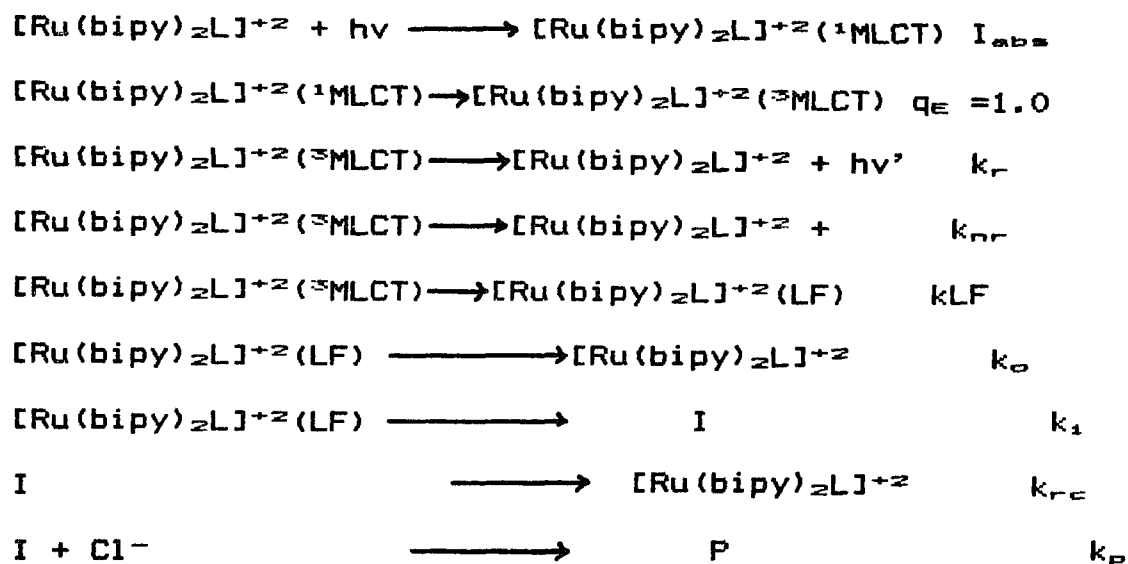
The equation below expressed was used in order to correct the experimental data reported in Table XXXX. In Figure 39 there is an anomalous curvature in the Stern - Volmer plot. Therefore, the emission intensities were corrected for absorption of the incident light by ferrocene, by means of the following equation¹⁰⁴.

$$(I_0/I)_{\text{corr}} = (I_0/I)_{\text{app}} \{ [1 - 10^{-A_D + A_Q}] / [1 - 10^{-A_D}] \} \{ A_D / [A_D + A_Q] \}$$

in which $(I_0/I)_{\text{app}}$ is the observed ratio of emission intensity from an unquenched sample to that from a quenched one, and A_D and A_Q are the absorbances per centimeter at the exciting wavelength (490 nm) of the complex $[\text{Ru}(\text{bipy})_2(\text{en})]^{+2}$, (donor, D), and ferrocene, (quencher, Q), used in that particular set of experiments. The correction was 25 % for the highest concentration of ferrocene that was used. The absorption by ferrocene at the concentrations used at the wavelengths of the emission was negligible.

APPENDIX A.2. DEPENDENCY OF THE QUANTUM YIELD
OF PHOTOSUBSTITUTION UPON $[Cl^-]$ CONCENTRATION .

The photosubstitution reaction sequence is assumed to be that shown below. In this scheme, I is the pentacoordinated intermediate formed by loss of a single ligand.



Furthermore, once the unidentate, six - coordinate species (P) is formed, there is no regeneration of the starting material. This has been discussed in the cases of the complexes $[Ru(bipy)_2L]^{+2}$ and $[Ru(bipy)_2(py)_2]^{+2}$ in reference⁴⁹.

$$d(P) / dt = [I][Cl^-]$$

Assuming a steady state for both excited states of the complex $[Ru(bipy)_2L]^{+2}$ (3MLCT) and $[Ru(bipy)_2L]^{+2}$ (LF) leads to the following formation rate expression :

$$d(P)/dt = Q(LF) \cdot Q(I) \cdot \{ k_p [Cl^-] / (k_{rc} + k_p [Cl^-]) \} \cdot I_{abs}$$

where $Q(LF) = k_{LF} / (k_r + k_{nr} + k_{LF})$ and

$$Q(I) = k_1 / (k_0 + k_1)$$

Thus, the quantum yield of product formation is :

$$Q(P) = Q(LF) \cdot Q(I) \cdot \{ k_p [Cl^-] / (k_{rc} + k_p [Cl^-]) \}$$

A simple rearrangement yields to the expression :

$$1/Q(P) = 1/Q(LF) \cdot Q(I) + \{ k_{rc} / Q(LF) \cdot Q(I) \cdot k_p \} \{ 1/[Cl^-] \}$$

and, since $Q(LF) = k_{LF} \cdot T_{\infty}$

$$1 / Q(P) = 1 / [T_{\infty} \cdot Q(I) \cdot k_{LF}] + \{ 1 / [T_{\infty} \cdot Q(I) \cdot k_{LF}] \} \{ k_{rc} / k_p \} \{ 1 / [Cl^-] \}$$

REFERENCES.

- (1) Seddon, K.R. *Coord. Chem. Revs.* 1982, 41, 79; Ford, P.C. *Rev. Chem. Intermediates*, 1979, 2, 267; Balzani, V.; Bolletta, F.; Gandolfi M. T.; Maestri M. *Topics Curr. Chem.* 1978, 75, 1; Crosby, G.A. *Accts. Chem. Res.* 1975, 8, 231; Watts, R.J. *J. Chem. Ed.* 1983, 60, 834.
- (2) Creutz, C. *Inorg. Chem.* 1978, 17, 1046; Meyer, T.J. *Israel J. Chem.* 1978, 17, 1046; Meyer, T.J. *Accts. Chem. Res.* 1978, 11, 94; Creutz, C.; Keller, A.; Sutin, N.; Zipp, P. *J. Am. Chem. Soc.* 1982, 104, 3618; Sutin, N. *J. Photochem.* 1979, 10, 19; Bock, C. R.; Connor, J. A.; Gutierrez, A. R.; Meyer, T.J.; Whitten, D.G.; Sullivan, B.P.; Nagle, J.K. *J. Am. Chem. Soc.* 1978, 101, 4815.
- (3) Tfouni, E.; Ford, P.C. *Inorg. Chem.* 1980, 19, 72; Malouf, G.; Ford, P.C. *J. Am. Chem. Soc.* 1974, 96, 601; *ibid*, 1977, 99, 7213.
- (4) Juris, A.; Manfrin, M.F.; Maestri, M.; Serpone, N. *Inorg. Chem.* 1978, 17, 2258; Brown, M.G.; Sutin, N. *J. Am. Chem. Soc.* 1979, 101, 883; Sutin, N.J. *J. Photochem.* 1979, 10, 19; Creutz, C.; Sutin, N. *Inorg. Chem.* 1976, 15, 496; Chou, M.; Creutz, C.; Sutin, N. *J. Am. Chem. Soc.* 1977, 99, 5615

- (5) Bock, C.R.; Connor, J.A.; Gutierrez, A.R.; Meyer, T.J.; Whitten, D.G.; Sullivan, B.P.; Nagle, J.K. J. Am. Chem. Soc. 1979, 101, 4815.
- (6) Marcus, R.A. Discuss. Faraday Soc. 1960, 29, 21; Hush, N.S. Trans. Faraday Soc. 1961, 57, 557.
- (7) For a review see : Harriman, A.; West, M.A., " Photogeneration of Hydrogen", Academic Press, New York, 1982.
- (8) Lytle, F.E.; Hercules, D.M. J. Am. Chem. Soc. 1969, 91, 253.
- (9) Crosby, G.A.; Perkins, W.G.; Klassen, D.M. J. Chem. Phys. 1965, 43, 1498.
- (10) Klassen, D.M.; Crosby, G.A. J. Chem. Phys. 1968, 48, 1853.
- (11) Harrigan, R.W.; Crosby, G.A. Chem. Phys. Lett. 1973, 21, 487.
- (12) Baker, D.C.; Crosby, G.A. Chem. Phys. 1974, 4, 428.
- (13) Harrigan, R.W.; Crosby, G.A. J. Chem. Phys. 1973, 59, 3468.
- (14) Hager, G.D.; Crosby, G.A. J. Am. Chem. Soc. 1975, 97, 7031.
- (15) Hager, G.D.; Watts, R.J.; Crosby, G.A. J. Am. Chem. Soc. 1975, 97, 7037.
- (16) Hipps, K.W.; Crosby, G.A. J. Am. Chem. Soc. 1975,

97, 7042.

(17) Felix, F.; Ferguson, J.; Gudel, H.U.; Ludi, A. Chem.Phys.Lett. 1979, 62, 153.

(18) Felix, F.; Ferguson, J.; Gudel, H.U.; Ludi, A. J. Am. Chem. Soc. 1980, 102, 4096.

(19) Demas, J.N.; Crosby, G.A. J. Am. Chem. Soc. 1971, 93, 2841.

(20) Demas, J.N.; Taylor, D.G. Inorg. Chem. 1979, 18, 3177.

(21) Mandal, K.; Pearson, T.D.L.; Krug, W.P.; Demas, J.N. J. Am. Chem. Soc. 1983, 105, 701.

(22) Calvert, J.M.; Meyer, T.J. Inorg. Chem. 1982, 21, 3978.

(23) Ferguson, J.; Krausz, E.R. Chem.Phys.Lett. 1982, 93, 21; Ferguson, J.; Herren, F. Chem. Phys. 1983, 76, 45.

(24) Wrighton, M.S.; Smothers, W.K. J. Am. Chem. Soc. 1983, 105, 1067; Bradley, P.G.; Kress, N.; Hornberger, B.A.; Dallinger, R.F.; Woodruff, W.H. J. Am. Chem. Soc. 1981, 103, 7441; Carlin, C.M.; DeArmond, M.K. Chem.Phys.Lett. 1982, 89, 297; Ferguson, J.; Herren, F. Chem.Phys.Lett. 1982, 89, 371.

(25) For a review see : DeArmond, M.K.; Carlin, C.M. Coord. Chem. Revs. 1981, 36, 325.

(26) Yersin, H.; Gallhumber, E. J. Am. Chem. Soc. 1984,

106, 6583.

(27) Felix, F.; Ferguson, J.; Gudel, H.U.; Ludi, A. Chem.Phys.Lett. 1979, 62, 153; Felix, F.; Ferguson, J.; Gudel, H.U.; Ludi, A. J. Am. Chem. Soc. 1980, 102, 4096; Decurtins, S.; Felix, F.; Ferguson, J.; Gudel, H.U.; Ludi, A. J. Am. Chem. Soc. 1980, 102, 4102.

(28) Hipps, K.W. Inorg. Chem. 1980, 19, 1390; Fujita, I.; Kobayashi, H. Inorg. Chem. 1973, 12, 2758.

(29) Carlin, C.M.; DeArmond, M.K. Chem.Phys.Lett. 1982, 89, 297; Carlin, C.M.; DeArmond, M.K. J. Am. Chem. Soc. 1985, 107, 53.

(30) Dallinger, R.F.; Woodruff, W.H. J. Am. Chem. Soc. 1979, 101, 4391; Bradley, P.G.; Kress, N.; Hornberger, B.A.; Dallinger, R.F.; Woodruff, W.H. J. Am. Chem. Soc. 1981, 103, 7441.

(31) Forster, M.; Hester, R.E. Chem.Phys.Lett. 1981, 81, 42.

(32) Smothers, W.K.; Wrighton, M.S. J. Am. Chem. Soc. 1983, 105, 1067.

(33) McClanahan, S.; Hayes, T.; Kincaid, J. J. Am. Chem. Soc. 1983, 105, 4486.

(34) Caspar, J.V.; Westermoreland, T.D.; Allen, G.H.; Bradley, P.G.; Meyer, T.J. ; Woodruff, W.H. J. Am. Chem. Soc. 1984, 106, 3492.

(35) Sutin, N.; Creutz, C. Adv. Chem. Ser. 1978, 168,

- 1; Lachish, U.; Infelta, P.; Gratzel, M. Chem.Phys.Lett. 1979, 62, 317; Bensasson, R.V.; Salet, C.; Balzani, V. C. R. Acad. Sci. Ser. B. 1979, 289, 41.
- (36) Braterman, P.S.; Harriman, A.; Heath, G.A.; Yellowlees, L.J. J. Chem. Soc. Dalton Trans. 1983, 1801.
- (37) Demas, J.N.; Crosby, G.A. J. Am. Chem. Soc. 1971, 93, 2841.
- (38) Englman, R.; Jortner, J. Mol. Phys. 1970, 18, 145; Freed, K.F.; Jortner, J. J.Chem.Phys. 1970, 52, 6272.
- (39) Caspar, J.V.; Meyer, T.J. Inorg. Chem. 1983, 22, 2444.
- (40) Kober, E.M.; Sullivan, B.P.; Dressick, W.J.; Caspar, J.V.; Meyer, T.J. J. Am. Chem. Soc. 1980, 102, 7383; Caspar, J.V.; Kober, E.M.; Sullivan, B.P.; Meyer, T.J. J. Am. Chem. Soc. 1982, 104, 630; Caspar, J.V.; Meyer, T.J. J. Phys. Chem. 1983, 87, 952.
- (41) Van Houten, J.; Watts, R.J. J. Am. Chem. Soc. 1976, 97, 3843; *ibid*, 1976, 98, 4853.
- (42) Nakamura, K. Bull.Chem. Soc. Jpn. 1982, 55, 1639.
- (43) Cherry, W.R.; Henderson, L.J. Inorg. Chem. 1984, 23, 983.
- (44) Demas, J.N.; Adamson, A.W. J. Am. Chem. Soc. 1973, 95, 5159; Van Houten, J.; Watts, R.J. Inorg. Chem. 1978, 17, 3381; Xu, J.; Porter, G.B. Can. J. Chem.

1982, 60, 2856.

(45) Caspar, J.V.; Meyer, T.J. J. Am. Chem. Soc. 1983, 105, 5583.

(46) Fasano, R.; Hoggard, P.E. Inorg. Chem. 1983, 22, 566.

(47) Henderson, L.J.; Fronczek, F.R.; Cherry, W.R. J. Am. Chem. Soc. 1984, 106, 5876.

(48) Henderson, L.J.; Cherry, W.R. unpublished results.

(49) Durham, B.; Caspar, J.V.; Nagle, J.K.; Meyer, T.J. J. Am. Chem. Soc. 1982, 104, 4803.

(50) Hoggard, P.E.; Porter, G.B. J. Am. Chem. Soc. 1978, 100, 1457; Gleria, M.; Minto, F.; Beggiato, G.; Bortolus, P. J. Chem. Soc. Chem. Commun. 1978, 285.

(51) Durham, B.; Walsh, J.L.; Carter, C.L.; Meyer, T.J. Inorg. Chem. 1980, 19, 860.

(52) Foreman, T.K.; Bonilha, J.B.S.; Whitten, D.G. J. Phys. Chem. 1982, 86, 3436.

(53) Gordon, A.J.; Ford, R.A. "The Chemist's Companion", Wiley Interscience Pub, New York, 1972.

(54) Kalyanasundaram, K. Coord. Chem. Revs. 1982, 46, 159.

(55) Fabian, R.H.; Klassen, D.M.; Sanntag, R.W. Inorg. Chem. 1980, 19, 1977; *ibid*, 1977, 19, 80.

(56) Sullivan, B.P.; Salmon, D.J.; Meyer, T.J. Inorg. Chem. 1978, 17, 3334.

- (57) Sprintschnik, G.; Sprintschnik, H.W.; Kirsh, P.P.; Whitten, D.G. *J. Am. Chem. Soc.* 1977, 99, 4947.
- (58) Perrin, D.D.; Armarego, W.L.F.; Perrin, D.R., "Purification of Laboratory Chemicals", Pergamon Press, New York, 1980.
- (59) Nakamaru, K. *Bull. Chem. Soc. Jpn.* 1982, 55, 2697.
- (60) Iwata, S.; Tanaka, J.; Nagakura, S. *J. Am. Chem. Soc.* 1966, 88, 894.
- (61) Lawton, E.A.; McRitchie, D.D. *J. Org. Chem.* 1959, 24, 26.
- (62) Scott, D.R.; Becker, R.S. *The J. of Chem. Phys.* 1961, 35, 516.
- (63) Newkome, G.R.; Gupta, V.K.; Taylor, H.C.R.; Fronczek, F.R. *Organomet. Chem.* 1984, 3, 1549.
- (64) Kloc, K.; Mlochowsky, J.; Szule, Z. *Heterocycles* 1978, 9, 849.
- (65) Newkome, G.R.; Koppersmith, D.L. *J. Org. Chem.* 1973, 38, 4461.
- (66) Dwyer, F.P.; Goodwin, H.A.; Gyarfas, E.C. *Aust. J. Chem.* 1963, 16, 544.
- (67) Sullivan, B.P.; Salmon, D.J.; Meyer, T.J.; Peedin, J. *Inorg. Chem.* 1979, 18, 3369.
- (68) Krause, R.A. *Inorg. Chim. Acta* 1977, 22, 209.
- (69) Wallace, W.M.; Hoggard, P.E. *Inorg. Chem.* 1980, 19, 2141.

- (70) Brown, G.M.; Weaver, T.R.; Keene, F.R.; Meyer, T.J. Inorg. Chem. 1976, 15, 190.
- (71) Kobayashi, H.; Kaizu, Y. Coord. Chem. Revs. 1985, 64, 53.
- (72) Hatchard, C.G.; Parker, C.A. Proc. Roy. Soc. London 1956, A235, 518.
- (73) Murov, S.L. " Handbook of Photochemistry ", M. Dekker; New York, 1973.
- (74) Omega Temperature Measurement Handbook and Encyclopedia, T - 41, 1984.
- (75) "Conversion Tables for Thermocouples", booklet o77989, issue2; Leeds&Northrup Company.
- (76) Calvert, J.G.; Pitts, J.N. " Photochemistry "; John Wiley & Sons, New York, 1966.
- (77) Demas, J.N.; Crosby, G.A. J. Phys. Chem. 1971, 75, 991.
- (78) Lakowicz, J.R. " Principles of Fluorescence Spectroscopy"; Plenum Press, New York, 1983.
- (79) Ware, W. " Creation and Detection of the Excited State" ;Dekker, New York, 1971.
- (80) Demas, J.N. " Excited State Lifetime Measurements "; Academic Press, New York, 1983.
- (81) Osburn, J.O.; Markovic, P.L. Chem. Eng. 1969, Aug. 105 .
- (82) Borigelleti, F.; Juris, A.; Balzani, V.; Belser,

- P.; von Zellwsky, A. *Inorg. Chem.* 1983, 22, 3335.
- (83) Bolleta, F.; Juris, A.; Maestri, M.; Sandrini, D. *Inorg. Chim. Acta* 1980, 44, L175.
- (84) Kunze, R.W.; Fuoss, R.M. *J. Phys. Chem.* 1963, 67, 911.
- (85) Ricci, J.E.; Nesse, G.N. *J. Phys. Chem.* 1942, 64, 2305.
- (86) Demas, J.N.; Crosby, G.A. *J. Am. Chem. Soc.* 1971, 93, 2841.
- (87) Cook, M.J.; Lewis, A.P.; McAuliffe, G.S.G.; Skarda, V.; Thompson, A.J. *J. Chem. Soc. Perkins Trans.II* 1984, 1293.
- (88) Turro, N. J. "Modern Molecular Photochemistry"; Benjamin/Cummings, California, 1978.
- (89) Henderson, L.J.; Cherry, W.R. *Chem.Phys.Lett.* 1985, 114, 553.
- (90) Hoggard, P.E.; Porter, G.B. *J. Am. Chem. Soc.* 1978, 100, 1457; Van Houten, J.; Watts, R.J. *Inorg. Chem.* 1978, 17, 3381; Wallace, W.M.; Hoggard, P.E. *Inorg. Chem.* 1980, 19, 2141.
- (91) Wrighton, M.S.; Pdungsap, L.; Morse, D.L. *J.Phys.Chem.* 1975, 79, 66.
- (92) Demas, J.N.; Diemente, D.; Harris, E.W. *J. Am. Chem. Soc.* 1973, 95, 6864.
- (93) Allsopp, S.R.; Cox, A.; Kemp, T.J.; Reed, W.J.

J.Chem.Soc.Faraday Trans.I 1978, 5, 1275.

(94) Caspar, J.V.; Meyer, T.J.; Inorg. Chem. 1983, 22, 2444; Durham, B.; Caspar, J.V.; Nagle, J.K.; Meyer, T.J. J. Am. Chem. Soc. 1982, 104, 4803; Van Houten, J.; Watts, R.J. J. Am. Chem. Soc. 1976, 98, 4853; Caspar, J.V.; Meyer, T.J. J. Am. Chem. Soc. 1983, 105, 5583.

(95) Caspar, J.V.; Meyer, T.J. J. Am. Chem. Soc. 1983, 105, 5583.

(96) Van Houten, J.; Watts, R.J. J. Am. Chem. Soc. 1976, 98, 4853.

(97) Belser, P.; von ZeKewsky, A.; Juris, A.; Barigelletti, F.; Balzani, V. Chem. Phys. Lett. 1984, 104, 100.

(98) Hanna, E.M.; Pethybridge, A.D.; Prue, J.E. Electrochimica Acta 1971, 16, 677.

(99) Newman, D.S.; Blinn, E.; Carlson, B.L. The J. of Phys.Chem. 1979, 83, 676; Iwamoto, E.; Monya, S.; Yamamoto, Y.; J.Chem.Soc.Faraday Trans. I, 1983, 79, 625; Iwamoto, E.; Imai, K.; Yamamoto, Y. Inorg. Chem. 1984, 23, 986.

(100) Atkinson, G.; Hallada, C.J. J. Am. Chem. Soc. 1962, 84, 721.

(101) Fuoss, R.M.; Kraus, C.A. J. Am. Chem. Soc. 1933, 55, 2307.

- (102) Fabry, T.L.; Fuoss, R.M. *J. Phys. Chem.* 1964, 68, 971.
- (103) Creutz, C.; Sutin, N. *Proc. Nat. Acad. Sci. USA* 1975, 72, 2858.
- (104) Demas, J.N.; Adamson, A.W. *J. Am. Chem. Soc.* 1973, 95, 5159; Navon, G.; Sutin, N. *Inorg. Chem.* 1974, 13, 2159.
- (105) Weast, R.C. " *Handbook of Chemistry and Physics* ", 51st. ed.; Chemical Rubber Co.; Cleveland, Ohio, 1970.
- (106) Demas, J.N.; Crosby, G.A. *J. Am. Chem. Soc.* 1971, 93, 2841; Fujita, I.; Kobayashi, H. *Inorg. Chem.* 1973, 17, 2758.
- (107) Durham, B.; Caspar, J.V.; Nagle, J.K.; Meyer, T.J. *J. Am. Chem. Soc.* 1982, 104, 4803; Caspar, J.V.; Meyer, T.J. *op. cit.* 1983, 105, 5583.
- (108) Wacholtz, W.M.; Auerbach, R.A.; Schmehl, R.H.; Ollino, M.; Cherry, W.R. *Inorg. Chem.* 1985, 24, 1758.
- (109) Pinnik, D.V.; Durham, B. *Inorg. Chem.* 1984, 23, 1440.
- (110) Szwark, M. " *Ions and Ions Pairs in Organic Reactions* ", Wiley, New York, v1, 1972, v2, 1974.
- (111) Jones, R.F.; Cole - Hamilton, D.J. *Inorg. Chim. Acta* 1981, 53, L3; Adeyemi, S.A.; Miller, F.J.; Meyer, T.J. *Inorg. Chem.* 1972, 11, 994.

- (112) Hoggard, P.E.; Porter, G.B. J. Am. Chem. Soc. 1978, 100, 1457.
- (113) Van Houten, J.; Watts, R.J. Inorg. Chem. 1978, 17, 3381.
- (114) Wagner, P.J. " Creation and Detection of the Excited State "v1, part A. A.A. Lamola, Ed. Marcel Dekker, New York, 1971.
- (115) Malouf, G.; Ford, P.C. J. Am. Chem. Soc. 1977, 99, 7213.
- (116) Figard, J.E.; Petersen, J.D. Inorg. Chem. 1978, 17, 1059.
- (117) Rillema, D.P.; Allen, G.H.; Meyer, T.J., manuscript in preparation.
- (118) Cocks, A.T.; Wright, R.; seddon, K.R. Chem. Phys. Lett. 1982, 85, 369.
- (119) Juris, A.; Barigelletti, F.; Balzani, V.; Belser, P.; Zelewsky, A. von Israel J. Chem. 1982, 22, 87.
- (120) Chandrasekaran, K.; Foreman, T.K.; Whitten, D.G. Nouv. J. Chim. 1981, 5, 275; Foreman, T.K.; Giannotti, C.; Whitten, D.G. J. Am. Chem. Soc. 1980, 102, 1170.
- (121) Gaines, G.L. The J. of Phys. Chem. 1979, 83, 3038; Demas, J.N.; Addington, J.W. J. Am. Chem. Soc. 1976, 98, 5800; Bolleta, F.; Maestri, M.; Moggi, L.; Balzani, V. J. Am. Chem. Soc. 1973, 95, 7864; Lavalley, C.; Lavalley, D.K.; Deutsch, E.A. Inorg. Chem. 1978, 17, 2217.

- (122) Brown, G.M.; Callahan, R.W.; Meyer, T.J. *Inorg.Chem.* 1975, 14, 1915.
- (123) Fujita, I.; Kobayashi, H. *Ber. Bursenges. Phys.Chem.* 1972, 76, 115.
- (124) Bolleta, F.; Maestri, M.; Moggi, L. *The J.of Phys.Chem.* 1973, 77, 861.
- (125) Brown, G.M.; Weaver, T.R.; Keene, F.R.; Meyer, T.J. *Inorg.Chem.* 1976, 15, 190.
- (126) Pinnick, D.V.; Durham, B. *Inorg.Chem.* 1984, 23, 1440.
- (127) Van Houten, J.; Watts, R.J. *Inorg.Chem.* 1978, 17, 3381.
- (128) Pinnick, D.V.; Durham, B. *Inorg.Chem.* 1984, 23, 3841.
- (129) Lane, B.C.; Lester, J.E.; Basolo, F. *Chem. Commun.* 1971, 1618.
- (130) Goedken, V.L. *J.Am.Chem.Soc. Commun.* 1972, 207.
- (131) Mahoney, D.F.; Beattie, E. *Inorg.Chem.* 1973, 2561.
- (132) Kinnaird, G.M.; Whitten, D.G. *Chem. Phys.Lett.* 1982, 88, 275.
- (133) Johnson, L.F.; Dietz, R.E.; Guggenheim, H.J. *Appl. Phys.Lett.* 1964, 5, 21.
- (134) Trutic, A.; Bohun, A. *Czech. J. Phys.* 1963, 13, 45.

(135) Dubenskii, K.K.; Karis, Ya.E.; Ryskin, A.I.; Feofilov, P.P.; Khilko, Opt. Spectrosk. 1965, 19, 353; Gumlich, H.E.; Schulz, H.J. J.Phys.Chem.Solids 1966, 27, 187; Reynolds, M.L.; Garlick, G.F.J. Infrared Phys. 1967, 7, 151.

(136) Durham, B.; Wilson, S.R.; Hodgson, D.J.; Meyer, T.J. J.Am.Chem. Soc. 1980, 102, 600.

(137) Church, S.P.; Horman, H.; Grevels, F.W.; Schaffner, K. J.Chem. Soc.Chem.Comm. 1984, 78; Hughey, L.; Anderson, C.D.; Meyer, T.J. J.Organomet. Chem. 1978, 100, 4095; Waltz, W.L.; Hacklerberg, O.; Dorfman, L.M.; Wociki, A. J.Am.Chem.Soc. 1978, 100, 7259.

(138) Braterman, P.S.; Harriman, A.; Heath, G.A.; Yellowless, L.J. J.Chem.Soc.Dalton Trans. 1983, 1801; Sutin, N.; Creutz, C. Adv.Chem.Ser. 1978, 1681; Lachisch, V.; Infelta, P.P.; Gratzel, M. Che.Phys.Lett. 1979, 62, 317; Bensasson, R.V.; Salet, C.; Balzani, V. C.R.Acas. Sci. Ser.B 1979, 289, 41.

(139) McKenzie, E.D. Coord.Chem. Rev. 1971, 6, 187.

VITA

Mario A. Ollino was born on December 8, 1951 in Valparaiso, Chile. He received his elementary education at Colegio Agustin Edwards, Valparaiso. He received his secondary education at Colegio La Salle, Valparaiso, where he graduated in 1968. In 1969 he entered Universidad Tecnica Federico Santa Maria in Valparaiso, where he obtained a teaching assistantship in 1971 in general chemistry; he performed these duties until 1974 when he was appointed to be an instructor in the Chemistry Department in Universidad Santa Maria. There he finished the coursework conducing to his degree in 1977 and received his Bachelors in Chemical Engineering in 1981. His thesis was entitled " Design and Study of Economic Feasibility of a Plant for the Exploitation of Low - Grade National Pyrolusite Ores ".

He was coauthor of several editions of Freshman General Chemistry Manuals. In 1979, he presented the lecture " Utilization of National Pyrolusite Ores " at the 5th Chilean Convention of Chemical Engineering. On several occasions he was sent by the Extension Academic Department of Santa Maria University to carry out activities designed to improve the efficiency of technical personnel at the Empresa

Nacional del Petroleo and at the Empresa Cuprifera El Teniente (Rancagua). He was a participant in academic administrative activities and was appointed in 1981 to be teaching coordinator of the Chemistry Department, Science Faculty, of Universidad Santa Maria. Between 1979 and 1982 he took several post - graduate courses in the fields of Physical Chemistry and Inorganic Chemistry for a total of 24 credits.

In August 1982 he obtained a study leave from Universidad Santa Maria to pursue a higher degree ; at the same time he was also awarded a study fellowship by the Oficina de Planificacion Nacional, Chile, and he became a graduate student in the Department of Chemistry at LSU University at Baton Rouge where he is presently a candidate for the degree of Doctor of Philosophy.

From his research three papers have already been published : Inorg. Chem., 1985, 24, 1417, entitled " Quenching of Photosubstitution in Ruthenium Polypyridine Complexes ", Inorg. Chem., 1985, 24, 1758, entitled " Correlation of Ligand Field Excited Strength in (Polypyridine) Ruthenium (II) Complexes ", J. of Phot., 1985, 31, 199, entitled " Effect of Chelate Ring Size on the Photoanation Reactions of Polypyridine Ruthenium Complexes ".

DOCTORAL EXAMINATION AND DISSERTATION REPORT

Candidate: Mario A. Ollino

Major Field: Chemistry

Title of Dissertation: Photophysics and Photochemical Studies of
Polypyridine Ruthenium (II) Complexes

Approved:

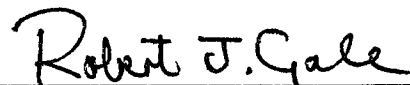


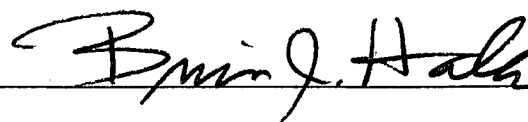
Major Professor and Chairman

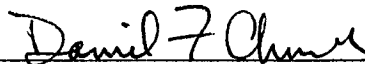


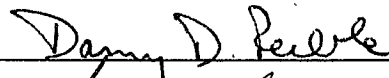
Dean of the Graduate School

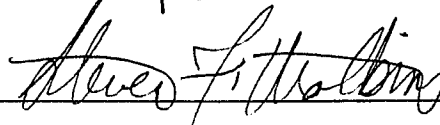
EXAMINING COMMITTEE:











Date of Examination:

October 31, 1986